Observatório Nacional

Ministério da Ciência, Tecnologia e Inovação

THE NEOPROTEROZOIC-EARLY PALEOZOIC TECTONIC EVOLUTION OF THE NORTHEAST OF BRAZIL: AN INTEGRATED GEOLOGICAL-GEOPHYSICAL ANALYSIS OF THE PRE-SILUIAN BASEMENT OF PARNAÍBA BASIN.

Amanda Lira Porto

Tese de Doutorado apresentada ao Programa de Pós-graduação em Geofísica do Observatório Nacional/MCTI, como parte dos requisitos necessários à obtenção do Título de Doutor em Ciências.

Orientador: Emanuele F. La Terra

Co-orientadores Sergio Luiz Fontes

Rio de Janeiro

Junho de 2021

THE NEOPROTEROZOIC-EARLY PALEOZOIC TECTONIC EVOLUTION OF THE NORTHEAST OF BRAZIL:
AN INTEGRATED GEOLOGICAL-GEOPHYSICAL ANALYSIS OF THE PRE-SILURIAN BASEMENT OF PARNAÍBA BASIN.

Amanda Lira Porto

TESE SUBMETIDA AO PROGRAMA DE PÓS-GRADUAÇÃO EM GEOFÍSICA DO OBSERVATÓRIO NACIONAL/MCTI COMO PARTE DOS REQUISITOS NECESSÁRIOS PARA À OBTENÇÃO DO TÍTULO DE DOUTOR EM CIÊNCIAS EM GEOFÍSICA.

Examinada por:

Prof. Reinhardt Adolfo Fuck, D.Sc.

Prof. David de Castro, D.Sc.

Prof[a]. Monica da Costa Pereira Lavalle Heilbron, D.Sc.

Prof. Daniel Franco, D.Sc

Dr. Claudio Lima (Suplente)

Prof. Cosme P. Neto, D.Sc (Suplente)

RIO DE JANEIRO, RJ – BRASIL

JUNHO DE 2021

Porto, Amanda

/Amanda Porto. – Rio de Janeiro: ON/MCTI, 2021.

XII, XX p.: 177.; xxx cm.

Orientador: Emanuele La Terra

Co-orientadores: Sergio L. Fontes

Tese (doutorado) – ON/MCTI/Programa de Pós-graduação em Geofísica, 2021.

Referências Bibliográficas: p. 146 – 163.

1. Parnaíba Basin. 2. Neoproteorozic 3. West Gondwana. I. La Terra, Emanuele Oo-orientador *et al.* II. Observatório Nacional/MCTI, Programa de Pós-graduação em Geofísica. III. THE NEOPROTEROZOIC-EARLY PALEOZOIC TECTONIC EVOLUTION OF THE NORTHEAST OF BRAZIL:

AN INTEGRATED GEOLOGICAL-GEOPHYSICAL ANALYSIS OF THE PRE-SILURIAN BASEMENT OF PARNAÍBA BASIN.

"A criatividade é o catalisador por excelência das aproximações de opostos."
Nise da Silveira

"Tenho tão nítido o Brasil que pode ser, e há de ser, que me dói o Brasil que é."
Darcy Ribeiro

Agradecimentos

Agradeço às mulheres da minha vida.
À minha mãe, que torce, vibra e faz tanto por mim, minha grande fã, minha ídola.
À minha avó Nininha, a avó mais sagaz que alguém pode ter, pelas acolhidas.
À minha tia Paula e sua linda trupe da Fazenda do Serrote, que tornaram meus momentos de pesquisa muito mais criativos, com suas belas paisagens.
Vó Edeilda, Barbara, Renata, Ana... todas as mulheres da minha família.
Agradeço ao meu pai e aos meus primos-irmãos pelos conselhos de toda sorte.
Agradeço imensamente ao Jimmy, meu parceiro tão amado, que atravessa comigo essa pandemia de mãos dadas e passos calmos.
Agradeço ao meu orientador Emanuele e co-orientador Sergio, por sempre confiarem no meu trabalho e viabilizarem ideias e parcerias.
Agradeço a toda equipe do Observatório Nacional, instituição de brio e de brilho.
Agradeço ao projeto PABIP e à sua equipe, que viabilizaram meu mestrado e meu doutorado na bacia do Parnaíba e à ANP pela cocessão dos dados
Agradeço ao Claudio Lima, grande pessoa, grande geólogo, com quem tive trocas riquíssimas e generosas sobre a bacia do Parnaíba e seus desdobramentos.
Agradeço ao André Assis, amigo de geologia, de campo e de música.
Agradeço ao Caxito e ao Ciro, que ajudaram a desatar os nós tectônicos por aqui.
Agradeço à magnífica Monica, inspiração pulsante para a formação de qualquer geóloga da minha querida UERJ.
Agradeço à UERJ e ao Professor Egberto, pelo pontapé inicial em minha história com o Parnaíba.
Agradeço aos “amigos-colegas”: Mariana, Larissa, Professora Carol, Rose, Henrique, Victor Schuback, Isis, Luana... “tamo” juntos!

Valeu, gente! Viva a ciência brasileira! Viva o SUS! Vacina para todos!

Abstract of Thesis presented to Observatório Nacional/MCTI as a partial fulfillment of the requirements for the degree of Doctor of Science (D.Sc.)

THE NEOPROTEROZOIC-EARLY PALEOZOIC TECTONIC EVOLUTION OF THE NORTHEAST OF BRAZIL: AN INTEGRATED GEOLOGICAL-GEOPHYSICAL ANALYSIS OF THE PRE-SILURIAN BASEMENT OF PARNAÍBA BASIN.

Amanda Lira Porto

June /2021

Advisor: Emanuele Francesco La Terra

Co-advisors: Sergio Luiz Fontes

Department: Geophysics

The Phanerozoic sedimentary sequences of Parnaíba basin (PB) occupy at least 600.000 km^2 of the NE region of Brazil. A regional Pre-Silurian unconformity marks the erosive planar base of the PB, and indistinctly cuts key tectonic units for the understanding of the Neoproterozoic evolution of western Gondwana (WG) in this region. The PB also preserves one of the largest Ordovician-Silurian sedimentary records of WG, represented by the Serra Grande Group. A comparative analysis of geophysical and geological datasets is presented here supporting a new proposal for the tectonic configuration of the pre-Silurian basement of PB, as well as presenting some insights related to the tectono-sedimentary controls of PB during the Early Paleozoic. Using integrated seismic interpretation and gravity modelling, constrained by an updated grid of the Moho depth, well data and a compilation of recent geophysical studies, two main basement blocks in the center of the basin were identified. They represent pre-Brasiliano inliers, surrounded by Brasiliano mobile belts, and assigned to two major crustal building blocks of western Gondwana. The Grajaú block belongs to the Amazonian-West Africa block, and is characterized by

low gravity anomaly, thicker crust (41-45km), transparent seismic pattern of the basement and a high velocity lower crust. The Teresina block belongs to the Central African block and is characterized by slightly thinner crust (39-41km), higher values of gravity and magnetic anomalies and by the presence of a mid-crustal reflectivity (MCR), observed in seven seismic lines and here interpreted as a remnant of a paleosuture zone between both blocks. Along a NE-SW 500-km seismic and gravity profile, the MCR was interpreted as crustal-scale thrust faults verging westwards and also defined the Barra do Corda mobile belt, which was formed by the closure of the Goiás-Pharusian ocean, in between the Grajaú and Teresina blocks. This belt deforms the eastern margin of the Ediacaran Riachão foreland basin (RB), observed in seismic and well data beneath the SW portion of PB. The western margin of RB is bounded by eastwards verging thrust faults, interpreted as a zone of back-thrusts and thinned crust (~36km) in the eastern prolongation of the Araguaia belt beneath PB. To the east, the limit between the Teresina block and the Borborema Province is marked by the NE-SW Transbrasiliano Fault Zone (TBFZ), along which Neoproterozoic mylonites were recovered from wellbores, and a system of narrow pull-apart basins is interpreted in the seismic data, possibly during the Cambro-Ordovician. Field observations in the NE portion of PB described conglomerates in a scarp-related alluvial fan system composing the basal Ordovician-Sulurian sequence of PB (Ipu Formation). As also suggested in the seismic data, these deposits were possibly controlled by tectonic reactivations along the TBFZ. Finally, the isopach maps of the Paleozoic sequences of PB indicate that the basement configuration played a role in the basin tectono-stratigraphy. The depocenter of PB from Early Paleozoic to Early Mesozoic lied upon the Teresina Block and then, during the Mesozoic, it migrated to the west, towards the Grajaú block.

Resumo da Tese apresentada ao Programa de Pós-graduação em Geofísica do Observatório Nacional/MCTI como parte dos requisitos necessários para a obtenção do título de Doutor em Ciências (D.Sc.).

EVOLUÇÃO TECTÔNICA DA REGIÃO NORDESTE DO BRASIL DURANTE O NEOPROTEROZOICO ATÉ O PALEOZÓICO INFERIOR: UMA ANÁLISE GEOLÓGICA E GEOFÍSICA INTEGRADA DO EMBASAMENTO PRÉ-SILURIANO DA BACIA DO PARNAÍBA.

Amanda Lira Porto

Junho /2021

Orientador: Emanuele Francesco La Terra

Co-orientador: Sergio Luiz Fontes

Departmento: Geofísica

As sequências sedimentares fanerozóicas da Bacia do Parnaíba (BP) recobrem pelo menos 600.000 km^2 da região nordeste brasileira. Uma discordância regional pré-Siluriana marca a base erosiva desta bacia, truncando indistintivamente unidades geotectônicas do embasamento, importantes para o entendimento da evolução Neoproterozóica da região oeste to paleocontinente Gondwana (OG). A BP também preserva um dos maiores registros da sedimentação Ordovicio-Siluriana do OG, representado pelo Grupo Serra Grande. Uma análise comparativa de dados geofísicos e geológicos é apresentada aqui, embasando uma nova proposição para o arcabouço tectônico do embasamento pré-Siluriano da BP, bem como apresentando novas idéias relacionadas ao controle tectono-estratigráfico da bacia durante o Paleozóico Inferior. Utilizando interpretações sísmicas integradas a modelagens gravitacionais diretas e a um mapa atualizado da profundidade da Moho, além de dados de poços e da compilação de recentes estudos geofísicos na área, foi possível identificar dois blocos do embasamento sob a porção central da bacia. Eles representam blocos pre-Brasilianos, circunscritos por faixas móveis

Brasilianas e assinalados a dois blocos crustais maiores que compuseram a porção oeste do paleocontinente Gondwana. O bloco Grajaú, a oeste, pertence ao bloco Amazônico-Oeste Africano e é caracterizado por uma baixa anomalia gravimétrica, crosta espessa (41-45 km), padrão sísmico transparente do embasamento, onde uma anomalia de alta velocidade é observada na crosta inferior. O bloco Teresina, a leste, pertence ao bloco Central Africano e é caracterizado por uma crosta mais afinada (39-41 km), valores maiores de anomalia gravimétrica e pela presença de uma reflexão na crosta intermediária (MCR), observada em sete linhas sísmicas e aqui interpretada como uma zona de paleosutura remanescente preservada entre ambos os blocos. Ao longo de um perfil símico e gravimétrico de direção NE-SO e 500 km de comprimento, foi possivel interpretar o MCR associado a falhas de empurrões de escalas crustais, com vergências para oeste, definindo assim a faixa móvel Barra do Corda, formada através do fechamento do oceano Goiás, que separava os blocos Grajaú e Teresina. Esta faixa móvel limita e deforma a borda leste da bacia Ediacarana do Riachão (RB), do tipo *foreland* e observada sob a porção sudoeste da BP. A borda oeste da Bacia do Riachão, por sua vez, é limitada por falhas de empurrão com vergência para leste, interpretadas como uma zona de retro-empurrão associada ao prolongamento a leste da Faixa Araguaia sob a BP, onde também se observa um afinamento crustal (~36 km). O limite entre o bloco Teresina e a Província Borborema é dado pela zona de falhas do Transbrasiliano (TBFZ), com orientação NE-SO, e ao logo da qual ocorrem milonitos Neoproterozóicos amostrados em poços, e um sistema de estreitas bacias to tipo “pull-apart” interpretadas no dado sísmico e possivelmente formadas durante o Cambro-Ordoviciano. Dados de campo da porção NE da bacia descrevem conglomerados típicos de leques aluviais em borda de falha compondo a sequência basal da BP (Formação Ipu; Ordovicio-Siluriano). Como também sugerido no dado sísmico, esses depósitos foram possivelmente formados por reativações tectônicas da TBFZ. Finalmente, mapas de isópacas das sequências Paleozóicas da BP indicam a importância da configuração de seu embasamento para sua evolução tectôno-estratigráfica. Seu depocentro durante o Paleozóico até o início do Mesozóico estava localizado sobre o bloco Teresina, enquanto que durante o Mesozóico, migra para oeste, sobre o bloco Grajaú.

Contents

List of Figures

List of Tables

Chaper 1

Introduction

At least one third of the continental extension of the northeastern region of Brazil is covered by the Phanerozoic sediments of the Parnaíba basin, which occupies approximately 670.000 (e.g., Cordani et al., 1984) of the states of Ceará, Piauí, Maranhão and Bahia, as well as part of the Pará and Tocantins states, in the northern region of Brazil. The two thirds left are mainly represented by the Precambrian rocks of the Borborema Province (Almeida *et al*. 1981;Caxito et al., 2020), located in the easternmost portion of the NE region, and by the northern margin of the São Francisco craton (Heilbron et al., 2017), to the south, in the state of Bahia. These pre-Cambrian rocks compose the eastern basement of the Parnaíba basin. To the west/northwest, the basin is bordered by pre-Cambrian rocks of the northern region of Brazil, named as the Araguaia belt (Hasui et al., 1977; Herz et al., 1989)and the Gurupi belt (Klein et al., 2017), that in turn encompasses the marginal terranes of the Amazonian and São Luis-West Africa cratons, respectively. The metamorphic and magmatic rocks prevailing in these basement units were formed or reworked during the Neoproterozoic Era (~1.0 Ga – 540 Ma), when the massive Gondwana paleocontinent was formed after a series of diachronic processes of oceanic consumption and continental collisions (Torsvik and Cocks, 2013; Schmitt et al., 2018).

A schematic reconstruction of the western portion of the Gondwana paleocontinent is presented in Fig. 2.1, just before it was broken-up at ca. 180 Ma, giving birth to the South Atlantic Ocean (Schmitt et al.,2016; Schmitt et al., 2018). Since the stabilization of this massive paleocontinent and even after its break-up, the Parnaíba basin (PB; e.g. Vaz et al., 2007) resists as a sedimentary basin unit, preserving palogeographic hints for the evolution of the planet in the last ~450Ma (Late Ordovician-Silurian times), when the first sedimentary rocks were deposited.

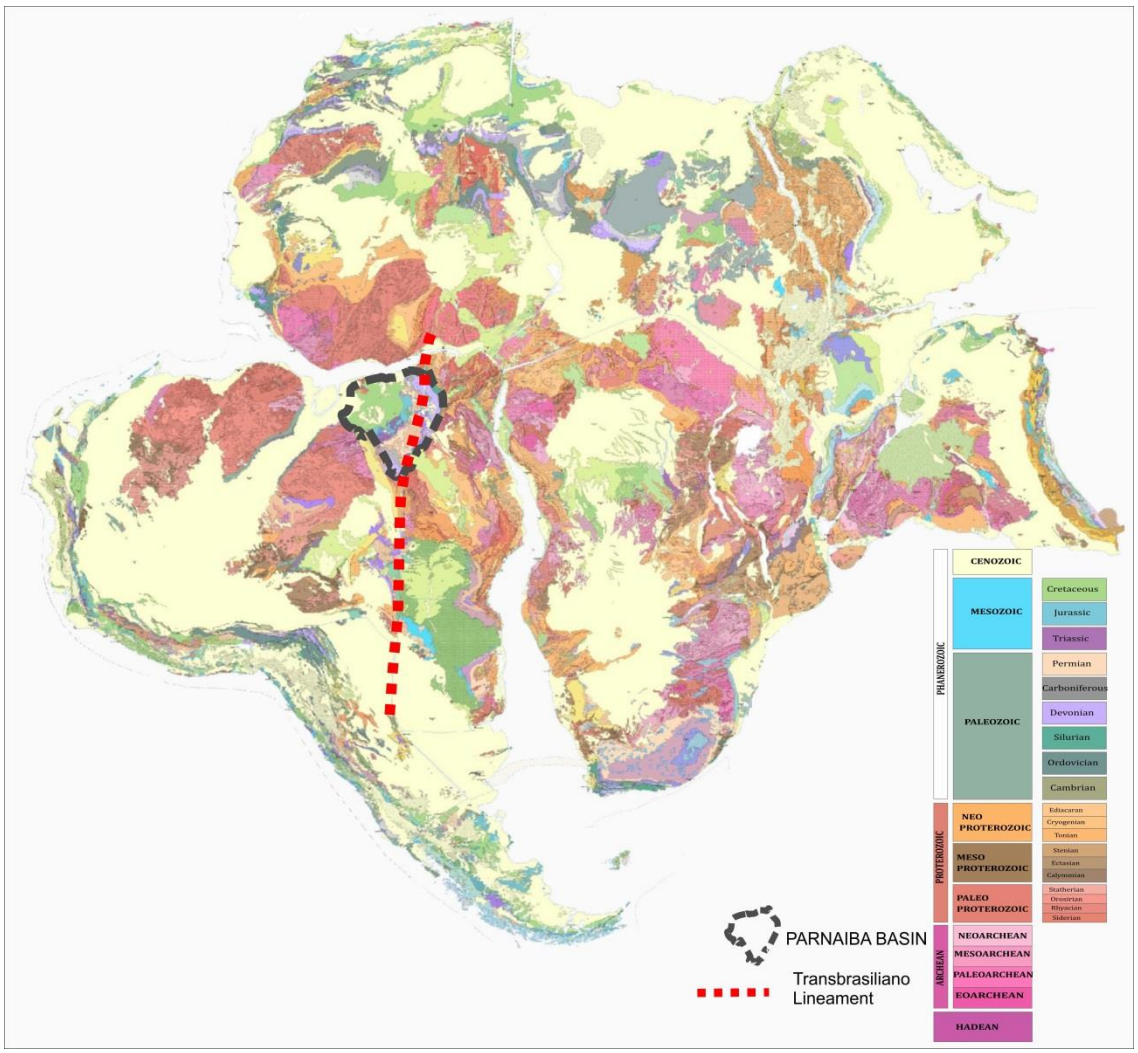

Fig. 1.1 Location of the Parnaíba basin upon the western portion of the Gondwana paleocontinent. The map is modified after the Gondwana Project Map (Schmitt et al.,2016; Schmitt et al., 2018), which was built using GPlates software and re-assembled continental fragments at 183 Ma. The colors indicate the geochronological information of the geological units based on International Chronostratigraphic Chart (IUGS/ICS - v. 2016/12).

The PB is classified as a “cratonic” sedimentary basin (Allen & Armitage, 2012) and along with some other similar long-lived cratonic basins in South America and Africa (such as Solimões, Amazonianas, Paraná, Taoudenni and Congo basins), hides key information of the so-called Brasiliano-Pan African orogenic collage (e.g. Brito Neves et al., 2014), which represents the main tectonic event that affected the Neoproterozoic basement of these basins, during the consolidation of the western portion of Gondwana (Fig.1.1).

There are plenty of uncertainties during the exercise of plate reconstruction. In the specific case of the NE of Brazil and western Gondwana, one of the matters of debate in the scientific community is regarding the nature of the “internal” orogens

observed along the Borborema Province, Araguaia and Gurupi belts. Broadly speaking, two main theories represent the end members of this discussion (e.g. Schmitt et al., 2018). They are related to whether there were different large oceans separating faraway paleocontinents (e.g., Clymene Ocean, Tohver et al. 2012) or if these belts were the product of intracontinental rifting and basin inversion of continental fragments that were close to each other and part of the same block (e.g., Araguaia Belt, Cordani et al. 2013a; Gurupi belt, Klein et al., 2017)

This second idea is debated in Cordani et al. (2013a) and Ganade de Araujo et al. (2014). For them, the western Gondwana was formed by the convergence of two groups of blocks: Amazonian-West African cratons and Central African blocks (Saharan, São Francisco-Congo, Kalahari and Rio de La Plata), due to the consequent closure of the Goais-Pharusian Ocean, between 630 and 580 Ma. This huge orogeny was developed along a corridor of continental scale and roughly NE-SW, called as the Transbrasiliano-Kandi shear zone. This “tectonic entity” crosses the eastern portion of Parnaíba basin and played an important role during its development (Brito Neves et al., 1984; Cunha, 1986; De Castro et al., 2014; Assis et al; 2019).

On the other hand, Tohver et al. (2012) and Trindade et al. (2006) assume the closure of the Clymene Ocean, which would be located to the western margin of Parnaíba basin. According to these authors, this ocean went through a long phase of subduction resulting in the formation of the Araguaia and Rockelides (in Africa) belts, suturing the Amazonian craton in the last stages (Ediacaran-Cambrian) of the western Gondwana amalgamation. For this assumption, they argue the presence of a magmatic arc hidden beneath Parnaíba basin. The sutures along the closure of both oceanic domains advocated by both theories discussed here for the western Gondwana, as well as the geographic position of the Parnaíba basin are illustrated in Fig.1.2.

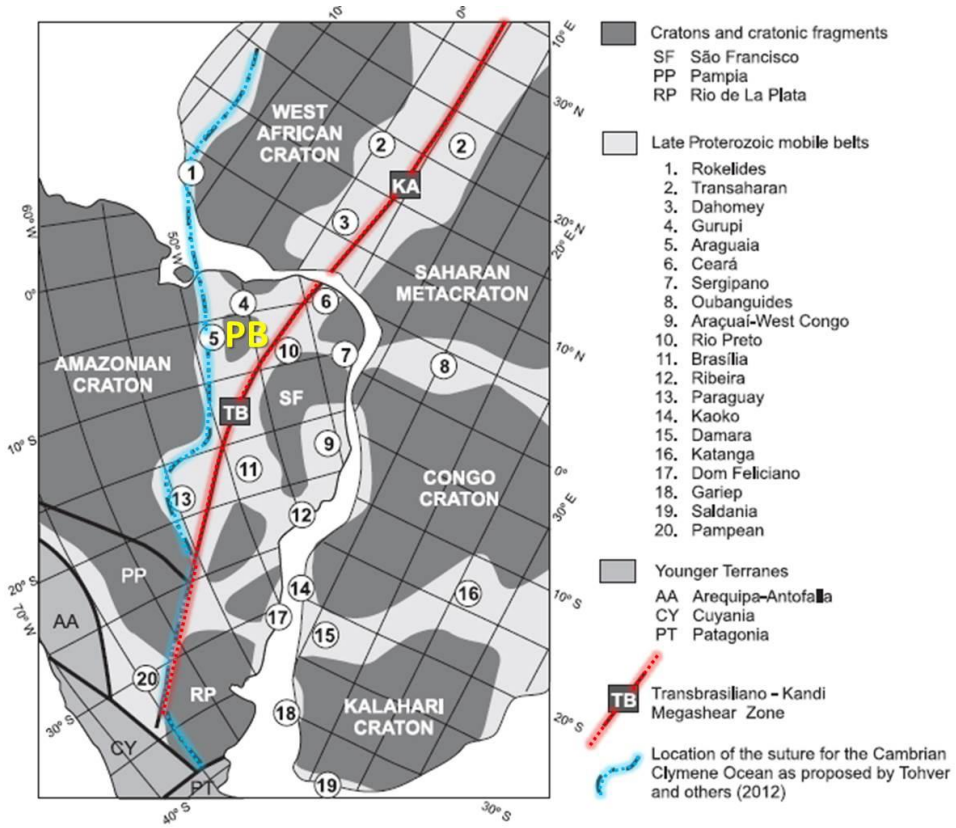

Fig. 1.2. Location and outline of the Transbrasiliano-Kandi mega-shear zone and of the suture of the Cambrian Clymene ocean in a schematic paleoreconstruction of South America and Africa, before the Gondwana break-up. In yellow, “PB” locates the Parnaíba basin. Modified after Cordani et al. (2013b).

Given the complexity of the debate proposed in the previous paragraphs, it is clear that the Phanerozoic sedimentary cover of Parnaíba basin hides key elements to support a more precise paleoreconstruction of Gondwana. Therefore, it is very important to better understand the subsurface geology of this area, and the geophysical investigation encompasses the most powerful tools to accomplish this.

Recently, there were big advances in this direction and the Parnaíba basin (PB) became one of the most studied cratonic basins in the world (Mckenzie and Tribaldos, 2018). Part of these results is compiled in the Special Publication of the Geological Society of London (eg. Daly et al., 2018), following a series of geophysical acquisitions and analyses along the W-E Deep Regional Profile (DRP), shown in Fig.1.3. These new results revealed a much more complex tectonic framework for the PB basement, and evidenced the prolongation of such crustal-scale Neoproterozoic suture zones (see Fig.2.2), beneath the western and eastern portions of the basin.

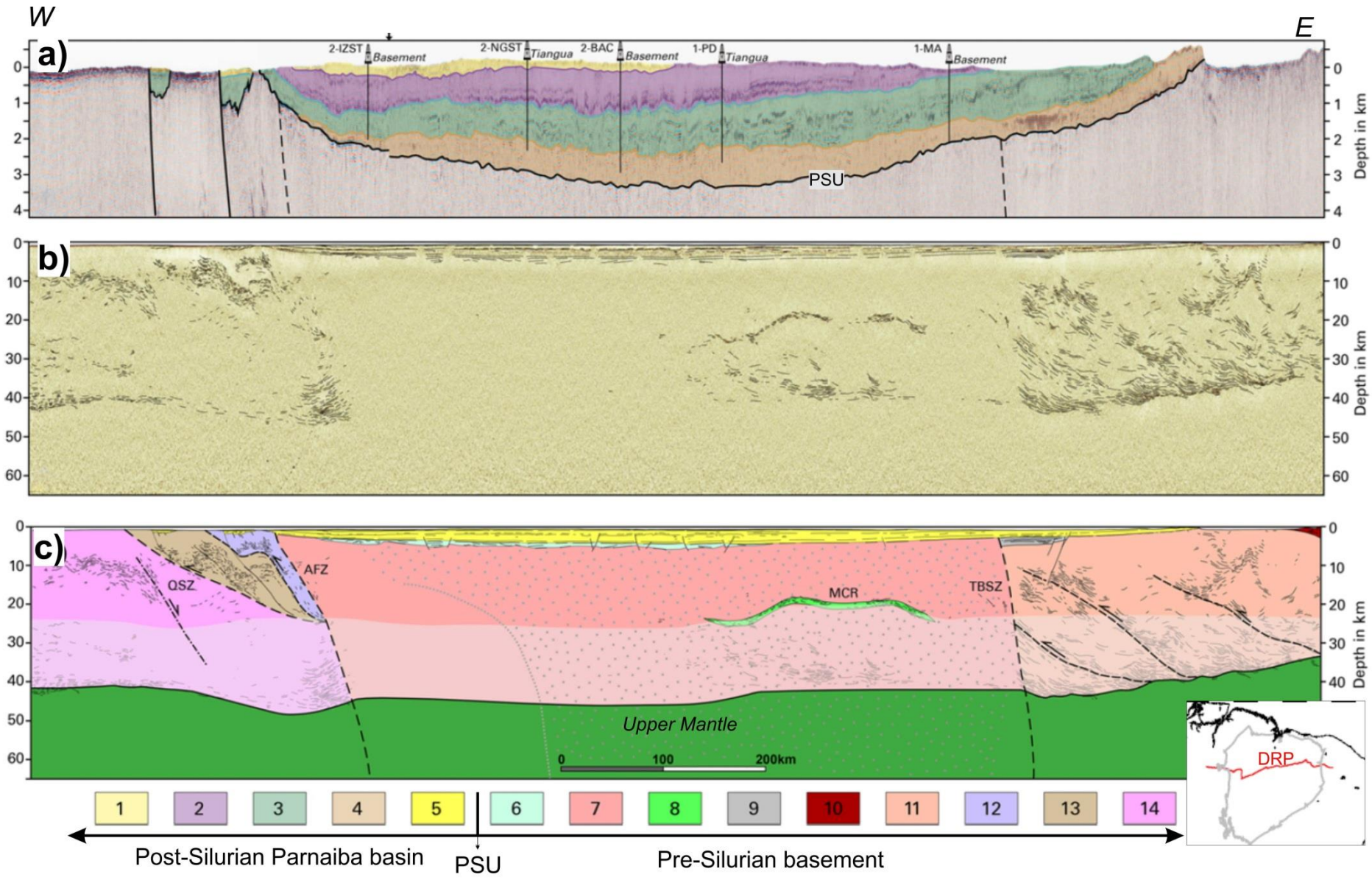
W
E
a)
2-IZST
Basement
2-NGST
Tiangua
2-BAC
Basement
1-PD
Tiangua
1-MA
Basement
PSU
Depth in km
b)
Depth in km
c)
QSZ
AFZ
MCR
TBSZ
Upper Mantle
0
100
200km
DRP
Depth in km
1
2
3
4
5
6
7
8
9
10
11
12
13
14
Post-Silurian Parnaiba basin
PSU
Pre-Silurian basement

Fig. 1.3 (previous page) Seismic interpretation along the Deep Regional Seismic Profile (DRP; modified after Daly et al., 2018 and Daly et al. 2014): (a) Zoom to the Phanerozoic section of Parnaíba basin along DRP(1:30 vertical exaggeration), showing the cratonic basin megasequences (1) Cretaceous Grajaú Group, (2) Late Carboniferous–Middle Triassic Balsas Group, (3) Lower Devonian–Late Carboniferous Canindé Group, (4) Late Ordovician–Lower Devonian Serra Grande Group, "PSU" stays for the Pre-Silurian unconformity; (b) Line interpretation of the Parnaíba deep seismic reflection profile; (c) and the respective geological interpretation, in which (5) Early Silurian–Triassic cratonic basin megasequence; (6) Late Neoproterozoic and Cambrian sedimentary remnants of the Riachão Basin; (7) Parnaíba Block crystalline basement; (8) mid-crustal reflectivity (MCR); (9) Cambrian volcanics and sediments of the Campo Maior graben; (10) Neoproterozoic Cruzeta Complex of the Borborema Province; (11) Neoproterozoic granitic gneisses of the Borborema Province; (12) Neoproterozoic schists of the Estrondo Group; (13) Neoproterozic phyllites of the Tocantins Group; (14) Paleoproterozoic Amazonian Craton; "QSZ" stays for Quatipuru suture zone, "AFZ",Araguaína Fault zone (both in Araguaia belt) and "TBFZ" is the Transbrasiliano Fault Zone.

Daly *et al.* (2014; Fig.1.3) have assumed the presence of a cratonic block called as the Parnaíba block, observing the seismic character and seismic Moho depth of the central Parnaíba basin along DRP. These authors also recognized a mid-crustal reflectivity (MCR) in the easter-central portion of Parnaíba block. The seismological studies of Coelho et al. (2018) and Soares et al (2018), and the magneto-telluric profile of Solon et al. (2018), all constrained along this E-W regional profile, pointed out geophysical differences (crustal thickness, velocity anomalies and resistivity patterns) between the eastern and western portions of the central Parnaíba basin. These new results challenge the idea of a unique cratonic nucleus beneath PB, especially if brought to the broader collisional context of western Gondwana (Cordani et al., 2013a and b; Ganade de Araujo et al., 2014; Caxito et al., 2020).

The present PhD research aims to shed more light on the hidden substract of Parnaíba basin, broaden the constrained study area along the 2D DRP profile by adding new geophysical and geological data to the discussion. Indeed, most of the recent paleotectonic maps of the pre-Silurian Parnaíba basin basement were either older than the recent geophysical discoveries or have not taken into consideration the regional context of Neoproterozoic western Gondwana amalgamation. This thesis addresses these gaps, complementing regional tectonic maps of Gondwana in NE Brazil. This is covered mainly in Chapter 3 of the present thesis.

Another relevant outcome of Daly et al. (2018) is the wide recognition of a remarkable regional unconformity in the base of Parnaíba basin that indistinctly cuts the Brasiliano tectonic units of the basement. This was called as the "Pre-Silurian

unconformity" in Porto et al. (2018), "PSU" in Fig.2.3, and represents a geological hiatus between the end of the Brasiliano Orogeny (~480Ma; Late Cambrian, Cordani et al., 2013b) and the initial deposition of Parnaíba basin, in the transition of the Late Ordovician and Early Silurian (~450 Ma), that is also observed in other cratonic basins across Gondwana (e.g. Linol et al., 2016a,b and Assis et al., 2019). Due to the non-fossiliferous content and limited areal exposures, the first sedimentary sequences of these Gondwanan "cratonic" basins, and consequently, the basal unconformities beneath them, are yet poorly dated and understood in terms of paleogeographic and paleotectonic conditions (e.g. Assis et al., 2019). In Chapter 4 of the present thesis, new surface and subsurface data of the NE portion of Parnaíba basin will be presented and discussed.

The understanding of the Neoproterozoic evolution of the basement of Parnaíba basin, in NE of Brazil, added to the understanding of the initial deposition of such basins in western Gondwana, supports the formulation of another topic of debate in the geoscientific community: *"how do cratonic basins form?"* (Allen & Armitage, 2012; Daly et al., 2019). The scope of this thesis is far from covering this complex topic, but aims to give some new information to converge into a model that encompasses the complexity and variety of such basin types, linked to the heterogeneities derived from the tectonic processes that affect old continental crusts.

Chapter 2

Thesis structure, Dataset and Methods

2.1 Thesis structure

In order to understand the tectonic evolution of the Parnaíba Basin and adjacent areas of the NE of Brazil, we have subdivided the results of this thesis into two main chapters: 3 and 4. Their disposal follows the geochronological order of events: first, the Neoproterozoic/Early Paleozoic configuration of the basement, then the Ordovician-Silurian installation of PB and some possible links between its subsequent Paleozoic evolution and the basement configuration proposed here. Each chapter is composed of an introductory topic presenting the general outline, followed by the results, and the final remarks. The results are presented in the layout of scientific papers, already submitted along the PhD research timeline, followed by a topic called as “Additional information”, where related results not encompassed in the scopes of the respective papers are presented.

Chapter 3 is considered the denser topic of this thesis in terms of research dedication. It is entitled as “The Neoproterozoic/ Early Paleozoic basement of Parnaíba Basin in West Gondwana amalgamation context” and presents a compilation of recent literature added to reinterpretations and new interpretations of different geophysical datasets of the pre-Silurian basement of Parnaíba basin, including the analysis of the lithosphere, lower crust and upper crust. In the “Scientific paper 1” (item 3.2), a new tectonic configuration for the NE of Brazil in the regional context of West Gondwana amalgamation is proposed, including the “hidden” basement of Parnaíba basin.

In chapter 4, entitled as “The initial Ordovician-Silurian subsidence and Paleozoic tectonic evolution of Parnaíba Basin: links with the basement configuration”, the results of field observations and seismic interpretation in the NE of Parnaíba basin are presented and they are mainly related to the characterization of the first lithostratigraphic group of Parnaíba basin, the Serra Grande group (Ordovician-Silurian). These results were published in the “Scientific paper 2”, which

was actually prior to the submission of “Scientific paper 1” (Chapter 3). One additional topic shows new examples of the basal regional unconformity of Parnaíba basin, the Pre-Silurian unconformity. The other is composed by well data analysis showing the Phanerozoic evolution of Parnaíba basin in terms of depocenter migration and regional unconformities. In the Appendix 3, a “Conference Paper” is attached as part of the efforts related to this theme.

2.2 Dataset

In Figure 2.1, we display the available dataset used during the PhD research, as well as the location of the surface geological data collected during the field trip to the NE of Parnaíba basin, in February/2018, better explained in Chapter 4. The details of the seismic reflection and potential field surveys are presented in Table 1. They are all public data, released and granted by the Brazilian National Petroleum Agency (ANP), except for the Deep Regional Seismic Profile (DRP in Fig.2.1), granted by BP Energy do Brasil as part of the “Parnaíba Basin Analysis Project”(PBAP, see Daly et al., 2018).

We also display the location of the 89 seismographic stations (Fig.2.1) compiled from the literature and used to build the updated crustal thickness map of Parnaíba basin, presented in Chapter 1. The full information of the geographic coordinates, station names, Moho depth estimations, and references are detailed in Appendix I. The specific dataset of the “Scientific paper 1”, in Chapter 3, is displayed in item 3.3.1, with the respective applicability in the study.

We have analyzed 51 public wellbores, which were also granted by ANP. The complete well list is available in the Appendix II, where we also display the available geological well tops, used as inputs for the isopach grids of Parnaíba basin. Only 20 wells have penetrated the pre-Silurian basement, and their geological details are available in Appendix II, which is equivalent to the Supplementary Material 2 of the “Scientific Paper 1”.

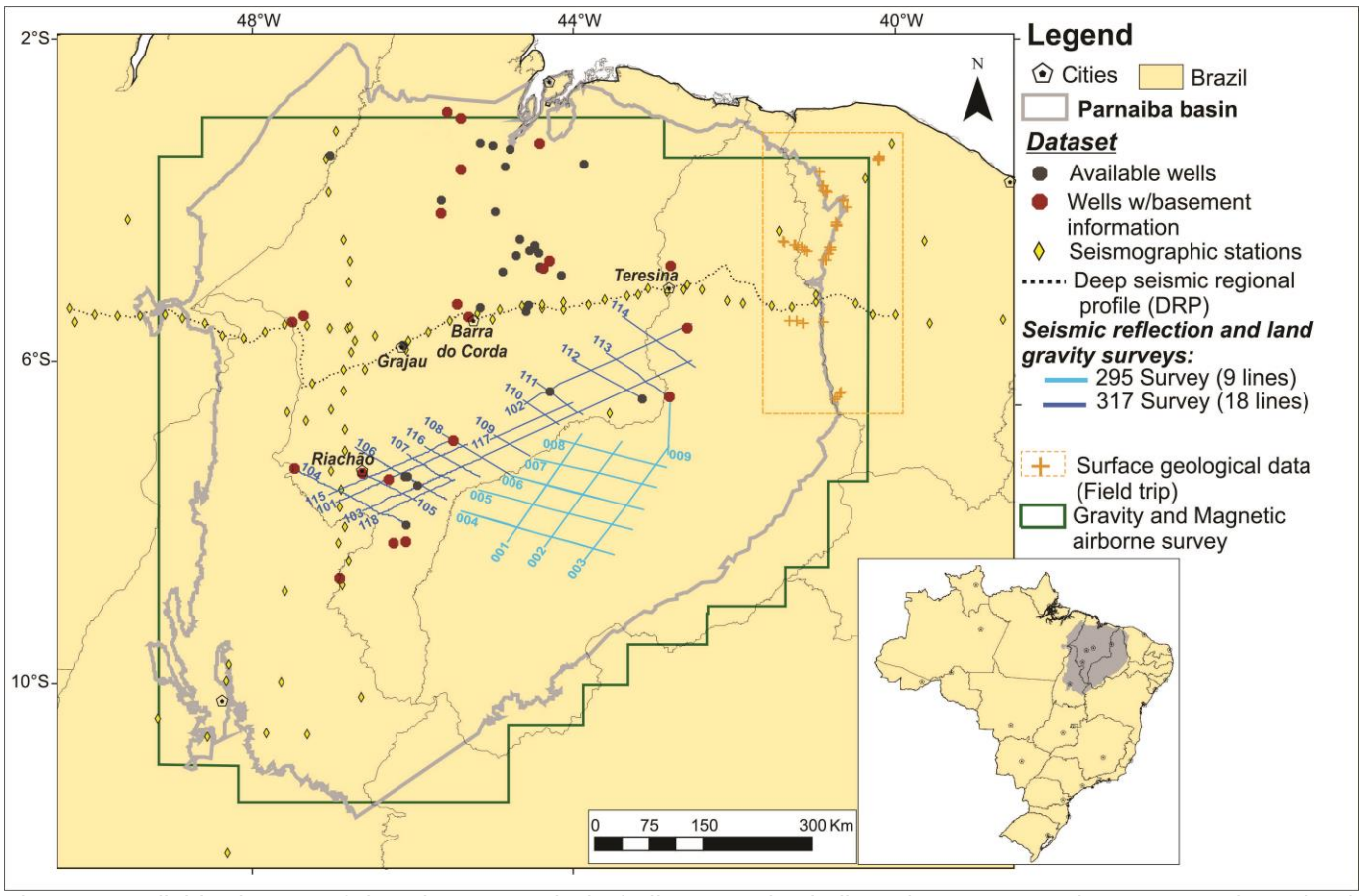

Fig. 2.1: Available dataset of the PhD research, including 20 seismic lines (DRP, 295 and 317 surveys); 27 land gravity profiles (295 and 317 surveys) , 51 wellbores, of which only 20 reached the pre-Silurian basement, one airborne magnetic and gravimetric survey. The field trip area is located in the NE of Parnaíba basin.

Data Type	Survey	No. of Profiles	Year	Operator	Aquisition/Processing information
2D Seismic Reflection	0031_PARNAIBA_45	1	1977	Petrobras	PSTM (prestack time-migrated)
	0295_ANP_2D_PARNAIBA	9	2009	ANP	PSTM (prestack time-migrated)
	0317_2D_ANP_BACIA_DO_ PARNAIBA	18	2013	ANP	PSTM (prestack time-migrated)
	Deep Seismic Reflection Profile (DRP)	1	2012	BP/ Global Geophysical Services Inc.	PSDM (poststack depth-migrated)
Gravity and Magnetic Airborne Survey	0050_GRAVIMAG002_ANP	-	2005 /2006	ANP	Survey Area: 748,612.4 km2. Flight lines: E-W 6 km spaced Tie lines: N-S 24 km-spaced.
Land Gravity Profiles	0317_GRAV_ANP_BACIA_DO _PARNAIBA	18	2013	ANP	Sample Interval: 200 m No. gravity stations : 13125
	0295_GRAV_ANP_PARNAIBA	9	2009	ANP	Sample Interval: 200 m No. gravity stations : 7942

Table 2.1: Details of the available geophysical dataset

2.3 Methods

In the flowchart below (Fig.2.2), we present the steps of the PhD research following the activities timeline. As it is shown, the field trip and the publication of the "Scientific Paper 2", presented here in Chapter 4, were done before the conclusion of "Scientific Paper 1" and the results of Chapter 3.

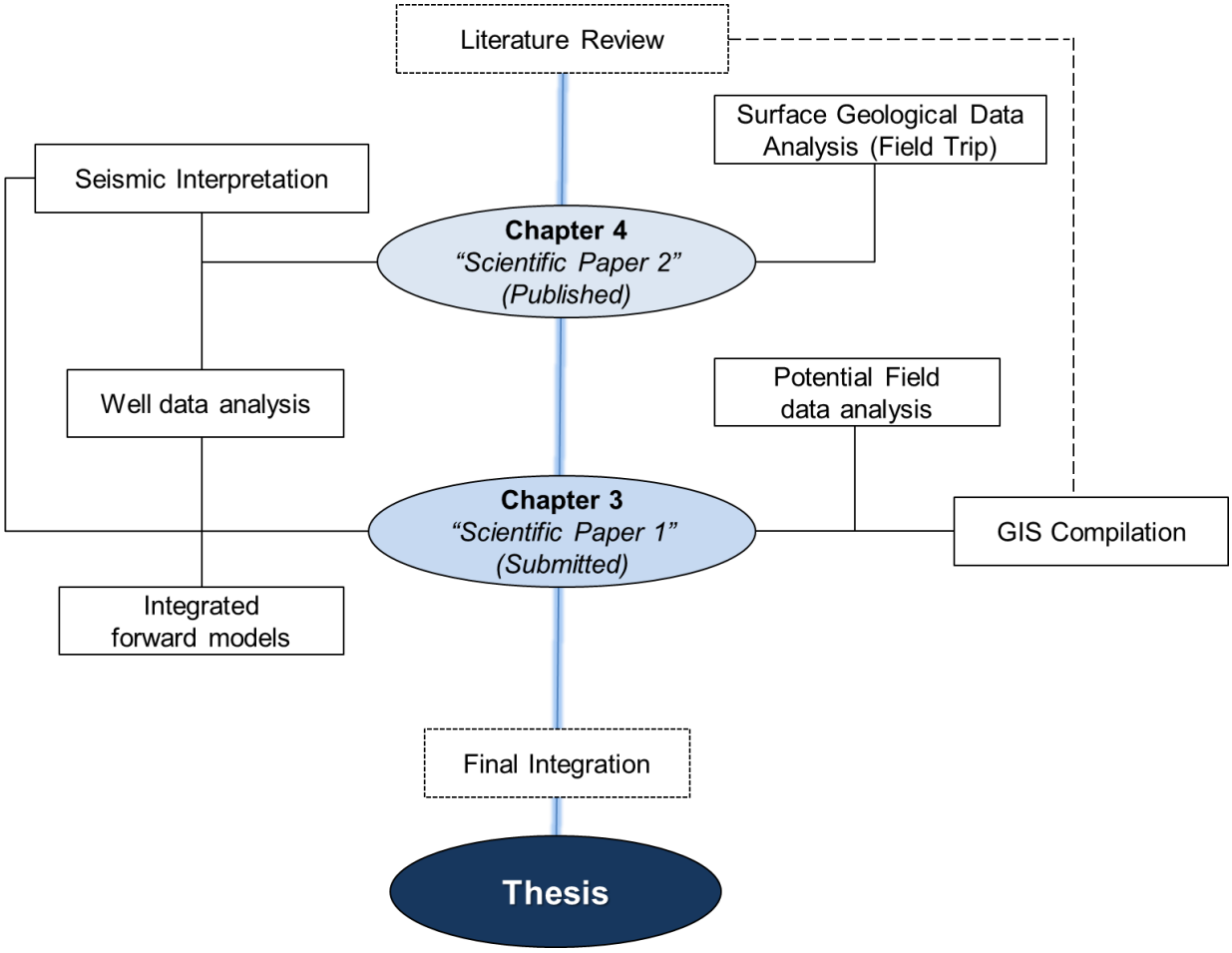

Fig. 2.2: Flowchart with the main activities performed during the PhD research and the respective chapters and publications in which the related results are presented.

Four main methodologies of work were applied during the PhD research and they are explained in the following topics.

- ***Literature Review and GIS compilation***

As expected in most of the scientific researches, literature review is a basic start to understand the state of the art of the object of study and this was not different here. In Chapter 3, it was a fundamental step to achieve the results, including: (1) the

review of the most updated regional tectonic studies about the western portion of the Gondwana paleocontinent (see item 3.2.1); (2) the evolution of available paleo reconstructions of the hidden basement beneath the Parnaíba basin (see item 3.2.2); and (3) the integration of recent geophysical studies in this area (see items 3.2.4, 3.3.1, 3.3.2 in Chapter 3).

The recently published geophysical datasets were evaluated in a common GIS database, in which it was possible to cross-correlate different types of anomalies related to the lithosphere, lower and upper crust, together with the main structural lineaments and the limits of outcropping geological units. This step supported the definition of preliminary tectonic domains beneath Parnaíba basin, later tested in the integrated forward model along L103, discussed in Chapter 3. The integration of the Moho depths estimated from 89 seismographic stations available in the literature allowed the creation of an updated crustal thickness map beneath PB, presented in item 3.2.5. The table 2.2 below presents the main details of the different geophysical surveys used during this compilation.

Data Type	Dataset or survey name	Source	Amount	Data processing	Application in the study	Item of the present Thesis
Seismology data	Seismographic stations, earthquakes and raypaths	Feng et al., 2007	N/A	Rayleigh wave tomograph	S wave velocity variations to estimate Lithsopheric thickness. Lithsopheric thickness for Pangea paleoreconstruction.	Item 3.3.1
		McKenzie & Rodriguez Tribaldos, 2018				
	Seismographic stations	Assumpção et al., 2013	3 stations	Receiver function method and H-k stacking approach	Crustal Thickness (Moho depth).	Item 3.2.5 and Appendix I
		Trindade,2014	5 stations			
		Luz et al.,2015	7 stations			
		Albuquerque et al., 2017	5 stations			
		Coelho et al., 2018	9 stations			
		Araujo, 2019	38 stations			
		Queiroz, 2019	21 stations			
Seismic Refraction Data	Wide-angle Reflection–Refraction data (WARR)	Soares et al., 2018	1 profile (parallel to DRP)	Ray tracing velocity model	Comparative analysis. Velocity anomalies within the upper mantle and lower crust.	Item 3.2.4
Electromagnetic data	Magnetotelluric (MT) stations	Rocha et al., 2019	72 stations (1 profile)	3D resistivity inversion model	Comparative analysis. Crustal distribution of electromagnetic resistivity.	Items 3.2.4 and 3.3.2
		Solon et al., 2018	39 stations (along DRP)			
	Geomagnetic Deep Sounding (GDS) stations	Arora et al., 1999	29 stations	Thin-sheet inversion model	Crustal distribution of electromagnetic conductance.	Items 3.3.2
Gravity data	E-W Deep Regional Profile (DRP)	Tozer, 2018	1 profile (along DRP)	Complete Bouguer correction	Comparative analysis and input for the 2D Forward Modelling.	Item 3.2.4
	Sampled from airborne surveys: 0050_GRAVIMAG002_ANP + Earth Gravitational Model 2008	De Castro et al., 2014	1 profile	Complete Bouguer correction	Comparative analysis and input for the 2D Forward Modelling.	Item 3.2.4
Magnetic data	Sampled from airborne surveys: 0050_GRAVIMAG002_ANP + 13 surveys of Brazilian Geological Survey (CPRM)	De Castro et al., 2014	1 profile	Reduced-to-pole correction	Comparative analysis.	Item 3.2.4

Table 2.2 Details of the geophysical datasets used in the GIS compilation of this thesis

- ***Seismic Interpretation***

The seismic reflection data interpretation of 295 and 317 surveys (Table 2.1 and Fig. 2.1) is being performed by the PhD candidate since 2014, during her Undergraduate major project (Porto, 2014) and Master thesis (Porto, 2017). The details of these activities are described in both aforementioned studies and a summary of the main steps are listed below and exemplified in Fig.2.3.

  - **1st) Identification of Key Seismic Sequences:** it consists of a qualitative analysis of the 2D seismic profiles, in two-way travel time domain, in order to identify the main seismic patterns. It followed four main criteria: the frequency and the amplitude of the seismic signal and the continuity and geometry of the reflections.

  - **2nd) Well-Seismic Data Calibration:** it consists of matching the synthetic seismogram extracted from well logs to the real seismograms extracted from the seismic profiles. The available sonic logs were used to generate the synthetic density and the synthetic checkshot curves, as well as the acoustic impedance curves (product of density and P-wave seismic velocity). Then, the reflection coefficient (RC) was calculated and a Ricker type wavelet (zero-phase, 25Hz) was convolved in order to simulate the effect of a seismic wavelet moving downwards. Finally, the resulted synthetic trace is correlated to the original seismic traces in the vicinity of the wellbore location, in order to find the best fit between them, also comparing the horizons interpreted during the qualitative analysis with the stratigraphic well tops. We have used 8 wells to calibrate six lines in the southern portion of 317 surveys, where the Riachão basin (Porto, 2017; Figs.2.3 and 2.4) is located, and only one well was available for the 295 survey (Porto, 2014; Figs.2.3 and 2.4).

  - **3rd) Velocity Model and Depth Conversion:** In a cube (XYZ; Fig.2.3), five interpreted horizons were gridded in time domain. They are from base to top: top of Basement, Pre-Silurian Unconformity, top of Jaicós Formation, top of Pimenteiras Formation, and Permian Anhydrite layer. Using the velocity values from the time vs. depth tables from the eight wells, the velocity variation gradient was calculated for each well and

interpolated in between them to build a preliminary velocity cube. The grids of the seismic horizons were added to the cube and, following their geometries and the tendency of the velocities variations from the wells, a final velocity cube was calculated for the area. Using the velocity values from the cube, the seismic profiles were converted from two-way travel time to depth domain.

- As a final step, the geological horizons are reinterpreted in the depth converted seismic lines, as well as the main faults. The well-seismic calibration and the velocity model were done in *SeisWorks software* (*Halliburton*), and the seismic interpretation and associated horizons grids were performed using the *Petrel software (Schlumberger).*

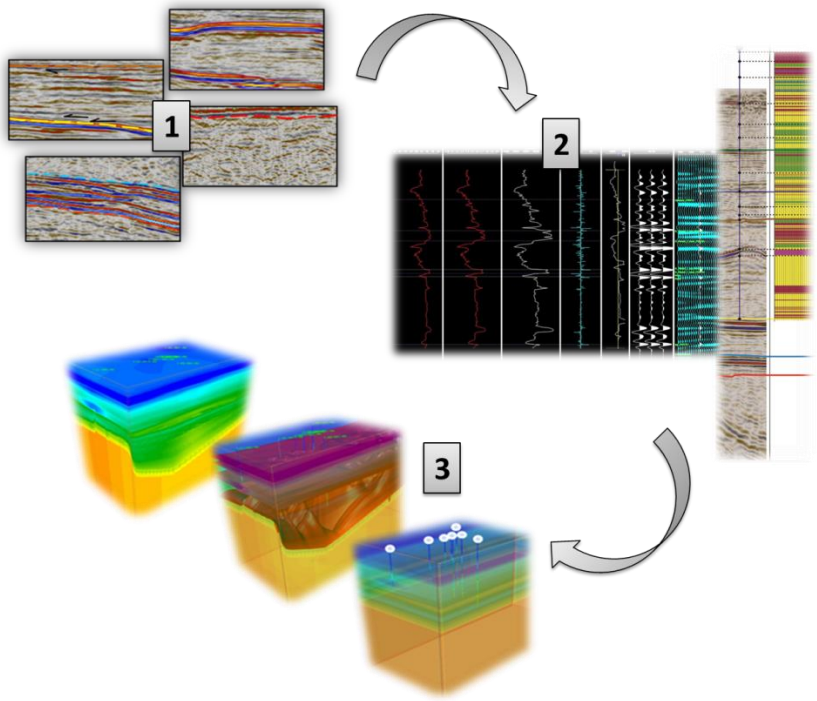

Fig.2.3: Illustrative examples of the three main steps of seismic interpretation described in the text. The images are compiled from previous studies of the PhD candidate in the Parnaíba basin (Porto, 2014 and 2017).

The main points of attention during the seismic interpretation for this thesis are listed below and also located in the map of Fig.2.4, where there is also the location of the nine wells calibrated to the seismic profiles, and of the velocity cube used to convert some of the lines to depth.

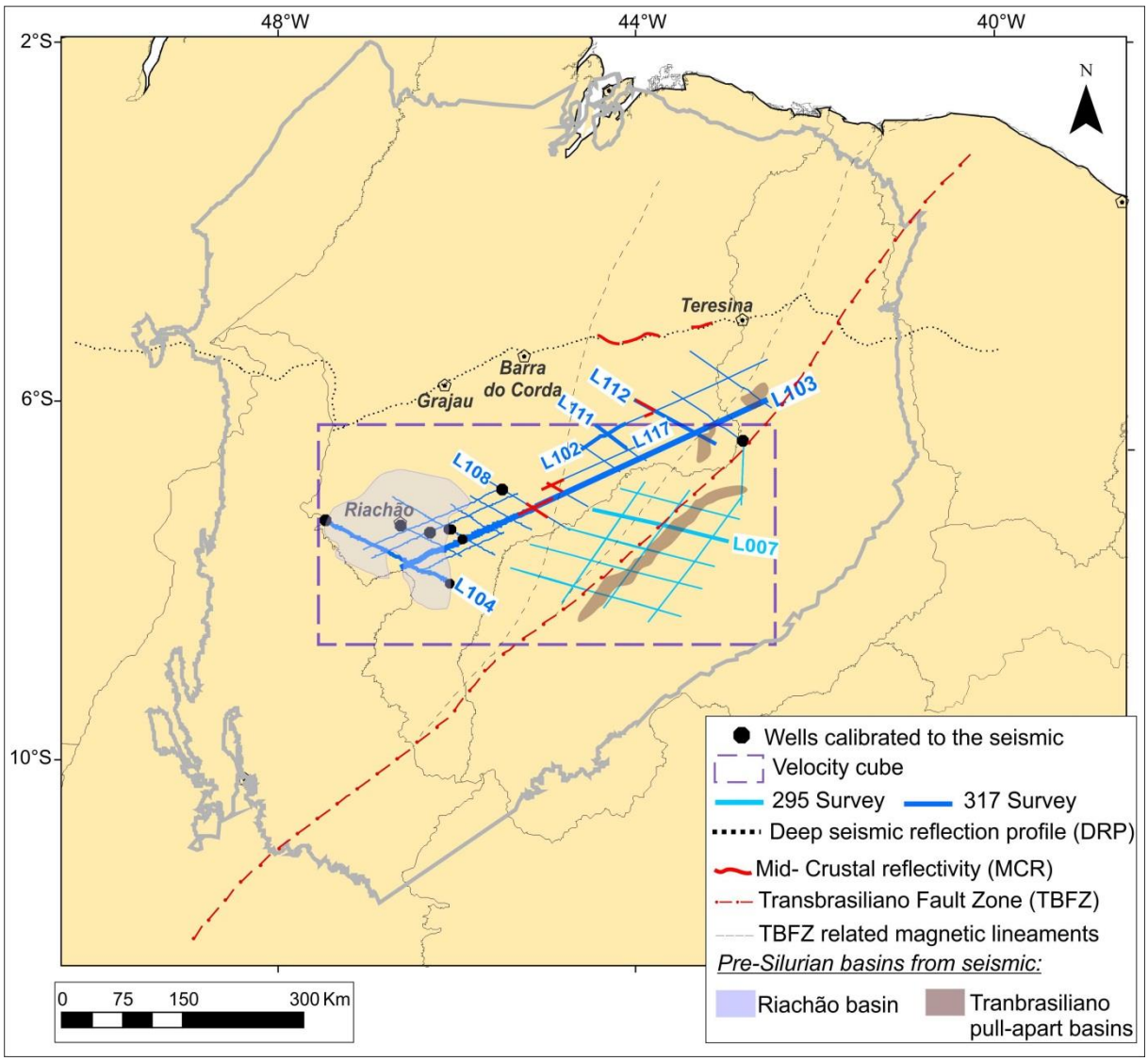

Fig. 2.4 Location of the wells used for the seismic-well tie and the limits of the velocity cube, used for depth conversion of some of the seismic lines. The labeled lines are the ones presented in the thesis. In red, we show the location of the MCR, presented along the DRP, and L103, L108, L117, L112, in Chapter 3. In item 3.2.8, L104 and L007 illustrate the Pre-Silurian basins beneath Parnaíba basin. In Chapter 4, L102, part of L103, L111 are also interpreted. In the north, L212 is presented in Chapter 5 to illustrate a regional Cretaceous unconformity.

- *The mid-crustal reflectivity (MCR)*: it refers to seismic anomalies located in the mid-portion of the crust within the basement of Parnaíba basin. It was first defined by Daly et al. (2014) along the DRP (Fig.2.4). It is presented in six different seismic lines, including the DRP, and also in a grid map in two-way travel time (see item 3.2.7).

- *Pre-Silurian basins beneath Parnaíba basin*: they include the Riachão basin and a system of narrow grabens along the Transbrasiliano Fault Zone, here called as the Transbrasiliano Pull-Apart Basin System (see items 3.2.8, 4.2 and 4.3).

- *The pre-Silurian unconformity (PSU):* it is represented by the regional unconformity in the base of the Parnaíba basin, presented in different examples and in a grid in two-way time in Chapter 4.
- *Unconformities, faults and folds:* They are presented as isolated examples along the following chapters of the thesis, located within the basement or in the Parnaíba basin (see item 4.4).

- ***Integrated 2D Gravity Forward Models along L103***

The integrated two-dimension gravity forward model was performed along the 500-km-long "317_103" profile (L103; see location in Fig.2.4) using the GM-SYS tool in the Oasis Montaj software (Geosoft). The main purpose was to test the interpretation of the basement configuration beneath Parnaíba basin. As described by Blakely (1995), the forward method considers an initial model of the sources based on geological and geophysical information. The model's anomaly is calculated and compared with the observed anomaly. The initial parameters of the model are then adjusted several times in order to generate the best fit between both observed and calculated anomalies.

In the case of the gravity forward model along L103, the observed complete Bouguer anomaly is compared to the total calculated gravitational attraction of an interpreted geological model. The root-mean square (RMS) error of this fit is then calculated and needs to be diminished as close as possible to the error floor (given by the observed measurement errors), in order to have a reasonable final adjustment. For the Bouguer correction, the typical crustal density of 2670 $kg.m^{-3}$ was used for the Bouguer slab (Blakely, 1995). For the interpreted geological model along L103, two parameters were inferred: (1) the shape (lateral extension, thickness and depth) of the geological units in subsurface; and (2) the average density values of these geological units.

According to Saltus & Blakely (2011), even though gravity anomalies interpretations are mathematically non-unique due to the multiple theoretical possible solutions, it does not mean that there is not a single interpretation to fit into a better geological scenario. For these authors, additional information provided in the real world allows a more reasonable decision on, for example, the more likely depth of a

geological body, regardless of the fact that an infinite number of mathematic solutions could also fit to the observed data. Following this idea, it is proposed here to integrate different types of prior information to constrain the interpreted geological model along L103. These constraints include information of previous published models in Parnaíba basin, seismological hints of the crustal thickness, the seismic interpretation along L103 and density values available in well data.

The deepest density contrast considered for the model is defined by the crust-mantle boundary (Moho discontinuity), at approximately 40km depth. The shape of this boundary was based on the sampled profile along L103, extracted from the new grid of Moho depth in Parnaíba basin, which was based on seismological data (see items 3.2.9 of Chapter 3). For the shallower portions of the crust, the interpretation of the seismic reflection profile along L103 (see Fig. 3.10 in Chapter 3) was considered. The still poorly described mid-crustal reflectivity observed in L103 (see Fig. 3.7 in Chapter 3) was tested using two different geological interpretations available in the literature. The best solution was picked based on the smallest calculated RMS error and then, included in the full model of L103. This step is described in item 3.3.3, of Chapter 3.

Finally, the constant density values of the geological layers were chosen based mainly on the literature studies of De Castro et al. (2014) and Tozer et al. (2017), who also applied forward modelling to unravel the hidden basement beneath Parnaíba basin. For the Riachão basin, the values were based on the forward model of Porto et al. (2018). One of the basement density values was based on whole rock density measurement available in well folder (1-MS-1-MA well). The details are available in the table 2.3 below:

Literaure Tectonic Domains (Tozer et al.,2017 and De Castro et al., 2014)	Depth Domain	Lithology/ Geological Unit	Density Values			Equivalent codes in Table 3.2 / Fig.3.10
			Tozer et al., 2017	De Castro et al., 2014	This Thesis	
Araguaia Belt	Shallow / Upper Crust	Supracrustal Metasedimentary Sequence (Estrondo Group)	2780	2700	2780	7
		Metamorphic/Igneous Basement (Tocantins Group)	2890	2810	2810	8
		Goias Magmatic Arc -NW Block	2870	2810	NA	NA
		Goias Magmatic Arc -SE Block	2870	2710	NA	NA
	Middle Crust	Mafic Rocks		2810	2850	3
		Ultramafic Rocks (Quatipuru Suture Zone?)	3125	2900		3
		Lower Crust	2900	3000	3000	2
Parnaiba Block	Shallow Crust	Mesozoic Igneous Sills/Dykes	2900	2900	2900	22
		Parnaiba Basin Sedimentary Sequences	2460	2450	2450	21
		Pre-Silurian Sedimentary Sequences (Cambrian Rifts/Riachao Basin)	2460	2550	2510	19
		Undifferendiated Metasedimentary Sequences	NA	2690	2740*	15
		Upper Crust	2810	2810	2790 and 2820	4 and 9
		Middle Crust	2985 (MCR)	2870	2850	3
		Lower Crust	2985 (MCR)	3000	3000	2
Borborema Province	Shallow Crust	Supracrustal Metasedimentary Sequence	NA	2750	NA	NA
		Upper Crust	2870	2750	2840	6
		Middle Crust	NA	2870	2850	3
		Lower Crust	2900	3000	3000	2
		Upper Mantle	3100	3200	3150	1

**Density value available in 1-MS-1-MA well*

Table 2.3: Comparison between literature density values interpreted for geological units beneath Parnaíba basin, available in the studies of De Castro et al. (2014) and Tozer et al. (2017) and the ones used in this thesis (see Chapter 3). The locations of the profiles modelled by both aforementioned studies are shown in Fig. 3.3. "NA" means not applicable or not available.

- ***Well Data Analysis***

The 51 wellbores available in this study (Fig.2.1; see Appendix II) were mainly used: (1) to constrain the seismic interpretation, as previously described, (2) to analyze the lithological information of the pre-Silurian basement, available in the well reports, cuttings or core descriptions, supporting the final tectonic interpretation of Chapter 3; and (3) as input for the isopach maps of the Phanerozoic sequences of Parnaíba basin, presented in Chapter 4.

Chapter 3

The Neoproterozoic/ Early Paleozoic basement of Parnaíba Basin in West Gondwana amalgamation context

3.1 General Outlines

In Chapter 3, a compilation of published and new geophysical datasets is presented and interpreted under the light of the recent geotectonic studies of the western portion of the Gondwana paleocontinent during the Brasiliano orogeny (Neoproterozoic/ Early Paleozoic), in the area equivalent to the Parnaíba basin and marginal terranes in North and NE Brazil.

The chapter is subdivided into two main topics. Item 3.2 consists of the "Scientific Paper 1", entitled as ***"The Neoproterozoic basement of the Phanerozoic Parnaíba Basin (NE Brazil) from combined geophysical-geological analysis: a missing piece of the western Gondwana puzzle",*** in which the present PhD candidate is the first author. In the following item 3.3, additional information not encompassed in the scope of the "Scientific Paper 1" is presented to complement the results of item 3.2. Finally, item 3.3, called as "Final Remarks", summarizes the results of Chapter 3.

The introductory topics, including dataset details and the geological context of the study area are available in items 3.2.1, 3.2.2 and 3.2.3. The results of GIS literature compilation and geotectonic reinterpretation of the basement units beneath the Parnaíba basin are presented in items 3.2.4 and 3.2.5, and complemented by the additional items 3.3.1 and 3.3.2. Airborne gravity and magnetic maps of Parnaíba basement are analyzed in topic 3.2.6. Seismic interpretations of the deep and shallow basement, supported by wellbore information, are presented in items 3.2.7 and 3.2.8. Integrated 2D forward models are presented in items 3.2.9 and 3.3.3. Finally, the new proposal of the tectonic map of the basement of Parnaíba basin is presented in item 3.2.10, as well as a sketch of its Neoproterozoic evolution.

3.2 Scientific Paper 1

[Submitted to "Precambrian Research" on 25th May 2021. Current status: Under Review. Figures, tables, and topics numbering is adapted to the present Thesis layout]

THE NEOPROTEROZOIC BASEMENT OF THE PHANEROZOIC PARNAÍBA BASIN (NE BRAZIL) FROM COMBINED GEOPHYSICAL-GEOLOGICAL ANALYSIS: A MISSING PIECE OF THE WESTERN GONDWANA PUZZLE.

Amanda Porto[1*]; Ciro Carvalho[2]; Claudio Lima[3]; Monica Heilbron[4]; Fabricio Caxito[5], Emanuele La Terra[1] & Sergio Luiz Fontes[1]

*[1] Observatório Nacional, COGEO, Rua General José Cristino, 77, 20941-400, Rio de Janeiro, RJ, Brazil; [2] Geological Survey of Brazil (SGB/CPRM), Av. Brasil 1731, 30140-002, Belo Horizonte, MG, Brazil; [3]LIMAGEO, Rua Coelho Neto 20/503, 22231-110, Rio de Janeiro, RJ, Brazil (Independent Researcher); [4]TEKTOs, Universidade do Estado do Rio de Janeiro, Rua São Francisco Xavier 524 4th floor, 20550-012, Rio de Janeiro, RJ, Brazil; [5] Centro de Pesquisa Manoel Teixeira da Costa, Instituto de Geociências, Universidade Federal de Minas Gerais (CPMTC-IGC-UFMG), Campus Pampulha, Av. Antônio Carlos 6627, CEP 31270-901,Belo Horizonte, MG, Brazil; *Corresponding author (e-mail: amandaliraporto@gmail.com)*

Abstract

A regional Pre-Silurian unconformity marks the erosive planar base of the Phanerozoic Parnaíba basin (PB), and indistinctly cuts key tectonic units for the understating of the Neoproterozoic evolution of western Gondwana in the NE of Brazil. We present a comparative analysis of geophysical and geological datasets in the PB, and propose a new tectonic configuration for its pre-Silurian basement, composed of different terranes amalgamated during the Brasiliano orogeny. Using integrated seismic interpretation and gravity modelling, constrained by an updated grid of the Moho depth, well data and a compilation of recent geophysical studies, we have identified two main blocks in the center of the basin, representing pre-Brasiliano inliers, surrounded by Brasiliano mobile belts, and assigned to two major crustal building blocks of western Gondwana: the Amazonian-West Africa (AWB; to the west/north) and the Central African blocks (CAB; to the east/northeast). The Grajaú

block belongs to the AWB and is characterized by low gravity anomaly, thicker crust (41-45km), transparent seismic character of the basement and a high velocity lower crust. The Teresina block belongs to the CAB and is characterized by slightly thinner crust (39-41km), higher values of gravity and magnetic anomalies and by the presence of a mid-crustal reflectivity (MCR), observed in seven seismic lines and here interpreted as a remnant of paleosuture zone between both blocks. Along a NE-SW 500-km seismic and gravity profile, we interpreted the MCR as crustal-scale thrust faults verging westwards and also defined the Barra do Corda mobile belt, which was formed by the closure of the Goiás-Pharusian ocean along the Transbrasiliano-Kandi corridor and subsequent collision of the Grajaú and Teresina blocks. This belt is found between the Grajaú and Teresina blocks and deforms the eastern margin of the Ediacaran Riachão foreland basin (RB), observed in seismic and well data beneath the SW portion of PB and overlying the southern Grajaú block. The western margin of RB is bounded by eastwards verging thrust faults, interpreted as a zone of back-thrusts and thinned crust (~36km) in the eastern prolongation of the Araguaia belt beneath PB. To the east, the limit between the Teresina block and the Borborema Province is marked by the NE-SW Transbrasiliano Fault Zone, along which Neoproterozoic mylonites were recovered from wellbores, and a system of narrow pull-apart basins is interpreted in the seismic data, triggered by Early Paleozoic transtensional reactivations of the TBFZ, prior to the deposition of the basal Ordovician-Silurian sequence of PB. This complex collisional tectonic setting of PB basement jeopardizes the idea of a stable cratonic block beneath it, inciting new formation models that account for the observed crustal and lithospheric heterogeneities.

3.2.1. Introduction

According to different authors (i.e. Cordani et al., 2013a; Cordani et al., 2013b; Brito Neves and Fuck, 2014; Caxito et al., 2020, 2021), two main tectonic blocks make up the western portion of the Gondwana paleocontinent at the end of the Neoproterozoic: the Amazonian-West African block, to NW, and the Central African block, to the east (Fig.3.1). They were amalgamated during the Brasiliano-Pan African orogenic cycle, by the closure of the Pharusian-Goiás ocean, along which the transcontinental NE-SW Transbrasiliano-Kandi Fault Zone (TBFZ) has been established, from the terminal continental collision (c.a. 615–610 Ma) to post-collisional (580–500 Ma) stages.

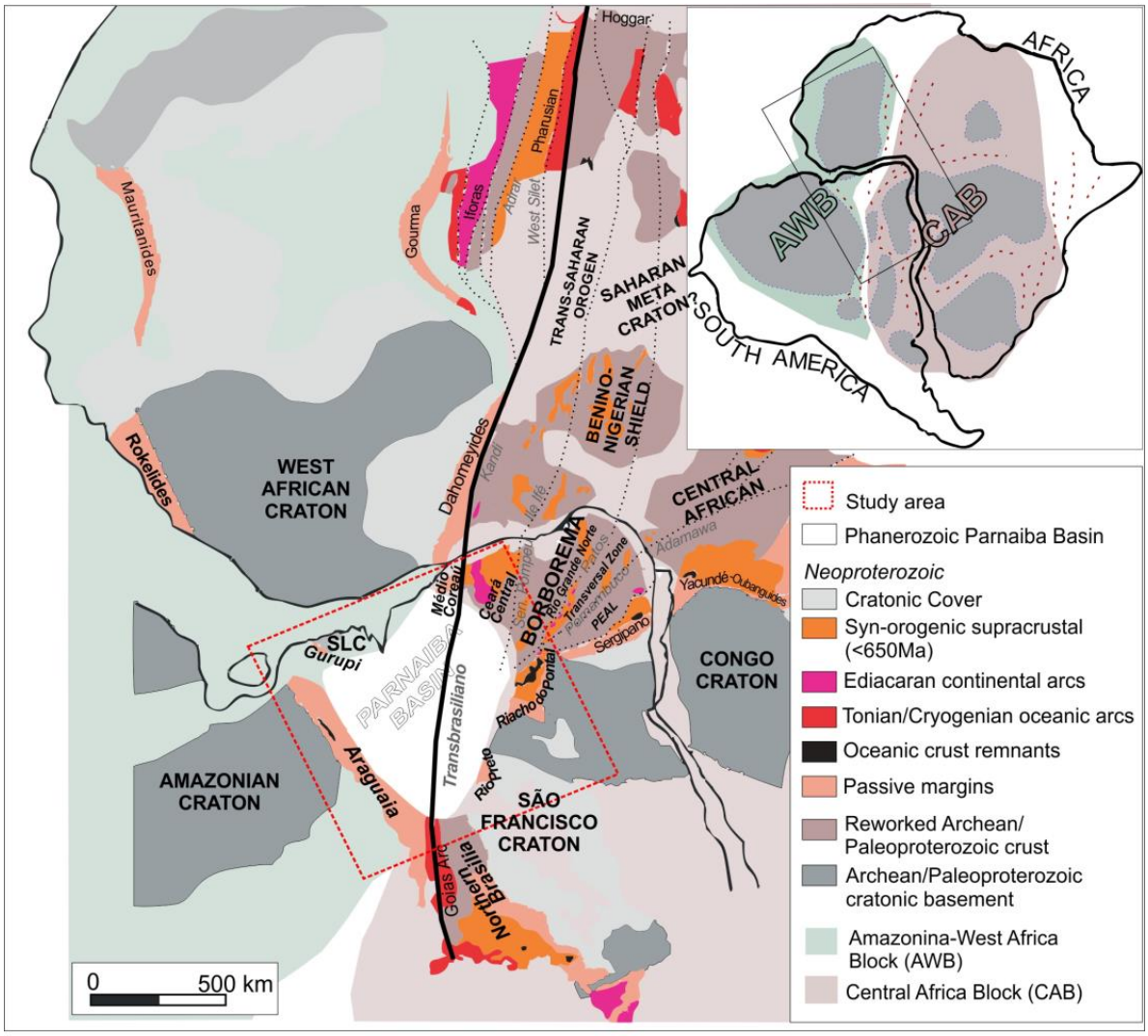

Fig.3.1: Main geotectonic elements of NE Brazil and NW Africa, during the stabilization of the western Gondwana paleocontinent. Note the current position of the Phanerozoic Parnaíba Basin in relation to the two main crustal building blocks: Amazonian-West African Block, to the NW, and the Central African block, to the east, as well as the location of the intercontinental Transbrasiliano Lineament. Modified after Caxito et al. (2020).

After orogenic stabilization and erosion, large cratonic sedimentary basins (such as Solimões, Amazonianas, Parnaíba, Paraná, Chaco, Taoudenni and Congo basins) were installed, occupying large areas of Gondwana and prevailing even after the Pangea consolidation (Permo-Carboniferous). The driven subsidence mechanism for their origin and further long evolution of such basins is still uncertain in the literature. Daly et al. (2019) recently reinforced the temporal connection between the installation of such basins and the final stages of continental collisional events, when large masses of continents were formed. Most of the so-far proposed cratonic basin formation theories (e.g. Tozer, 2017; Daly et al., 2019) imply causative links with their

basement configuration, or with deep crustal and mantle anomalies, indicating the importance of integrated subsurface analysis in order to improve the knowledge on such tectonic settings.

Recently, the Parnaíba basin (PB), in NE of Brazil, became one of the most studied cratonic basins in the world (Mckenzie and Tribaldos, 2018) due to prospective activities conducted by the petroleum industry and general scientific efforts (Daly et al., 2019). The almost undeformed subhorizontal sedimentary sequences were deposited upon a flat erosive peneplane, termed the Pre-Silurian Unconformity (PSU; Porto et al., 2018; Daly et al., 2014). This regional unconformity indiscriminately cross-cuts distinct Brasiliano blocks (Daly et al. 2014, 2018) and possibly truncates a major suture zone along the NE-SW Transbrasiliano lineament (Caxito et al., 2020; Fig.3.1), representing a key element for the western Gondwana tectonic history.

A comprehensive compilation of recent literature data and new geophysical datasets (see table 3.1) of the Parnaíba Basin are presented here in order to investigate the hidden pre-Silurian basement of the NE of Brazil, constrained by geotectonic reconstructions of western Gondwana. A similar approach was published by Daly et al. (2018), although these authors were focused mainly along a W-E Deep Regional Profile (DRP), which crosses the entire center of the Parnaíba basin and adjacent edges. Here we broaden this study area and add new geophysical data to constrain the Moho depth and crustal structure under the PB. Indeed, most of the recent paleotectonic maps of the pre-Silurian Parnaíba basin basement were either older than the recent geophysical discoveries or have not taken into consideration the regional context of Neoproterozoic western Gondwana amalgamation. This paper addresses these gaps to present a new tectonic framework for the underlying basement of the Parnaíba Basin, complementing regional tectonic maps of Gondwana in NE of Brazil.

3.2.2 Geological Context

Neoproterozoic belts around PB and the West Gondwana amalgamation

Several orogenic belts are located in the surrounding margins of Parnaíba basin (PB): Gurupi, Araguaia, Northern Brasília, Rio Preto, Riacho do Pontal belts besides smaller reworked terranes and crustal scale shear zones within the

Borborema Province (Fig.3.1). They were developed during the Neoproterozoic Era, as the result of the subduction and closure of a major oceanic domain, the Goiás-Pharusian Ocean, extending from NE Africa to Central Brazil, and followed by the development of several accretionary and collisional processes (Cordani et al., 2013a; Caxito et al., 2020). These complex tectonic processes are part of the Brasiliano-Pan African collage, resulting in the formation of the Gondwana paleocontinent (Torsvik and Cocks, 2013).

Understanding the configuration of the western portion of Gondwana, where the Parnaíba basin and the NE Brazilian belts are located, requires an integrated view of the complex diachronic processes involving continental masses of different ages and scales, in which collisional fronts of distinct paleogeography are coeval to extensional processes in other areas (Brito Neves et al., 2014). Ganade de Araujo et al. (2014) tentatively grouped these distinct belts as part of one single West Gondwana (WG) Orogen. This proposal is based on the compartmentation of WG assembly into two crustal building blocks (Cordani et al., 2013a), shown in Fig.3.1. To the west, the Amazonian-West Africa block (AWB) encompasses the major Amazonian and São Luis-West African cratons, as well as a continental fragment beneath the Parnaíba basin. To the east, the Central African block (CAB), includes the Saharan metacraton, the Borborema Province, São Francisco-Congo, Kalahari and Rio de la Plata cratons, and, to the south, the Paranápanema, Goiás Massif and Luiz Alves fragments (not shown in Fig. 3.1).

Brito Neves et al. (2014) defined the configuration of the South American Platform, considering it as a stable part of WG since the Late Neoproterozoic, and proposed a similar tectonic subdivision to the one aforementioned (Cordani et al., 2013b), naming two domains: the pre-Brasiliano Amazonian domain (N-NW) and the Neoproterozoic Brasiliano domain (central-eastern). For these authors, they are separated by weakness zones, associated to the N-S and NE-SW structural trends of the Araguaia-Rokelides suture and to the Transbrasiliano lineament, respectively. For Cordani et al. (2013a, 2013b), the main suture zones are only well-constrained to the Transbrasiliano-Kandi tectonic corridor (NE-SW), along which occurred the closure of the Goiás-Pharusian Ocean. In this proposal, the Araguaia belt is interpreted as an intracontinental thrust belt (reactivated aulacogen?), formed during the final stages of the Brasiliano orogeny, with the main vergence towards the Amazonian craton (Cordani et al., 2016). In both paleoreconstructions of western Gondwana, the hidden

basement beneath the Parnaíba basin remains a fundamental piece to unravel the Neoproterozoic puzzle of the NE sector of Brazil (Fig.3.1).

The long-lived Brasiliano orogeny in this region started at ca. 900-850 Ma, with intra-oceanic arc collisions, followed by the continental collision main episode ca. 615-600 Ma, and finally, post-collisional granitoids and foreland basins developed in the 580-500Ma interval (Ganade de Araujo et al., 2014). Just by the Middle Cambrian, the West Gondwana was already consolidated (Cordani et al., 2013b). The diachronic evolution of these events is detailed in the next paragraphs, according to the recent publications and focusing on the surrounding terranes of PB.

The Goiás Ocean, located to the south of PB, was consumed from ca. 900Ma to 600Ma, due to the convergence between the Amazonian and São Francisco cratons, involving also the Archean Goiás Massif microcontinent and the formation of the Goiás Magmatic Arc (GMA) and the Brasília belt (Fig.3.1). GMA records at least three phases of magmatism pulses: juvenile (ca. 900-800 Ma) and younger (ca. 650-630 Ma) island arcs and associated volcano-sedimentary sequences and late- to post-orogenic (~ 600 Ma) granites (Cordani et al., 2013b).

Synchronously, in the NE of PB, the Pharusian ocean consumption resulted from the West African Craton and the Saharan Metacraton convergence, including the Northern Borborema Province (Médio Coreaú, Ceará Central and possibly part of the Rio Grande do Norte domains in Fig.3.1; e.g. Caxito et al., 2020). Due to the presence of high pressure and ultra-high pressure metamorphosed mafic and ultramafic rocks in NE Brazil and NW Africa (ca. 620-608 Ma), this region is interpreted as a typical Himalayan-scale mountain belt during the Ediacaran (Ganade De Araujo et al., 2014).

To the SE sector of Parnaíba basin, the Transversal Zone and adjacent domains in the southern Borborema Province (Fig.3.1) were formed after a series of transpressional accretionary collisions, as a result of dextral strike-slip movements along the Transbrasiliano-Kandi corridor, in the terminal stages of Northern Borborema and the West African Craton orogeny (Ganade et al., 2021). According to Caxito et al. (2020), this kynematic resulted from the closure of longitudinal branches of the Goiás-Pharusian ocean, such as the Transnordestino-Central African ocean, involving also the northern margin of the São Francisco craton (Riacho do Pontal and Rio Preto belts in Fig.3.1)

At the northern and western boundaries of PB, the Gurupi and Araguaia belts, respectively, are the results of the terminal events of the of West Gondwana amalgamation, involving the São Luís-West African, Amazonian cratons and the suggested Parnaíba block. For Klein et al. (2017), the Gurupi belt represents an inverted aborted rift, during an Ediacaran intracontinental orogeny, without any or with very little oceanization. A similar hypothesis is argued for the Araguaia belt (Kotschoubey et al., 2005). Recent geochemical analysis of the ophiolitic units (~750 Ma) in this region supports that they are remnants of exhumed lithospheric mantle, being the Araguaia belt the result of a fossil Neoproterozoic hyper-extended margin (Hodel et al., 2019). No magmatic arc is described for both belts, and the aforementioned authors believe that their respective suture zones are covered by Phanerozoic PB sediments.

The Parnaíba Block – a cratonic nucleus beneath Parnaíba basin?

The prolongation of Neoproterozoic Brasiliano structures beneath the Phanerozoic sedimentary sequences of the Parnaíba basin (PB) was already a consensus in the first paleoreconstruction maps proposed for its basement. According to Brito Neves et al. (1984), the increase of metamorphic grade towards the basin interior observed in the northern (Gurupi belt) and western (Araguaia belt) margins of PB was a strong indication for the presence of the internal zones of these belts, juxtaposed to the margins of a cratonic nucleus beneath its center (red contour in Fig.3.2). These authors have also pointed out the importance of the Transbrasiliano fault zone (TBFZ), as a NE-SW cataclastic zone cross-cutting the PB and defining the eastern boundary of the proposed cratonic nucleus. Cunha (1986), who also proposed a cratonic nucleus beneath PB (orange contour in Fig. 3.2) using sparse wellbore data, has noticed the thickening of the Early Paleozoic sedimentary sequences of PB along the NE-SW TBFZ trend and along the perpendicular NW-SE Picos-Santa Inês trend (parallel to the Gurupi belt; Fig. 3.2). Góes et al. (1990) presented similar observations, adding sparse seismic profiles interpretation and defining sets of grabens, surrounding a narrower cratonic nucleus limit (yellow contour in Fig.3.2).

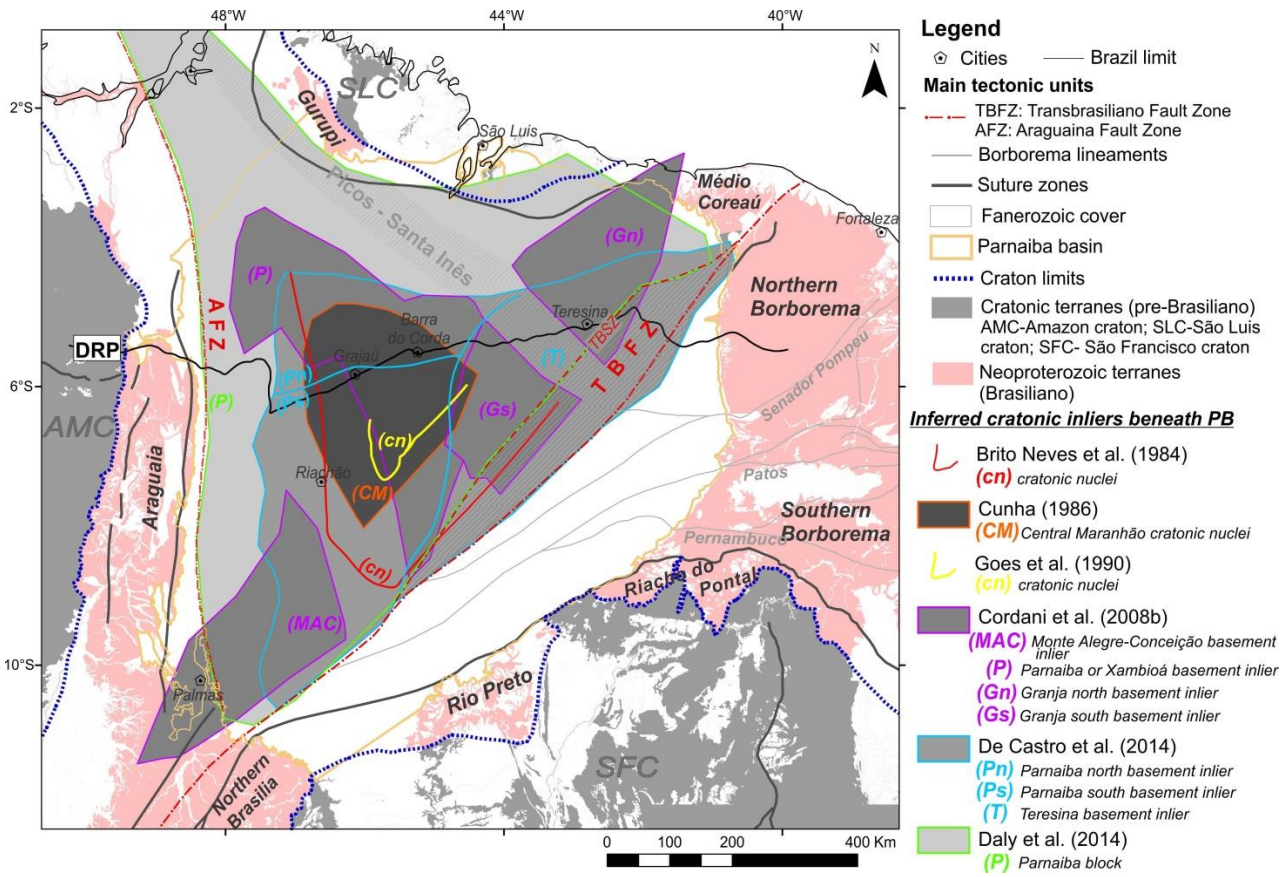

Fig.3.2: Seven different interpretations of basement inliers beneath the Phanerozoic Parnaíba basin. The main tectonic limits are derived from the GIS database available in the "Tectonic map of South America" (Cordani et al., 2016), with the exception to the Araguaína Fault Zone (AFZ) and the Transbrasiliano Shear Zone (TBSZ), interpreted by Daly et al. (2014).

Later, in the 90s, the advances from new acquisitions of gravity and magnetic surveys, as well as more detailed fieldworks in the vicinities of the basin lead to the definition of four different cratonic inliers beneath the basin. Cordani et al. (2008b) have interpreted three pre-Brasiliano massifs composed of medium to high-grade metamorphic rocks of Early Paleoproterozoic age: Granja north, Granja south, and Monte Alegre de Goiás-Conceição do Tocantins blocks (purple contours in Fig.3.2). Juxtaposed to the western limit of the Granja north block, close to the cities of Barra do Corda and Grajaú, these authors have speculated about the presence of a fourth basement block, named as Parnaíba massif, showing a NW-SE elongation, entirely concealed by PB sediments. These blocks could be the result of a major paleocontinent break-up at ca. 900Ma, while the intervenient belts possibly resulted from the later Brasiliano orogeny (Cordani et al., 2008b). The above mentioned authors have also interpreted a pronounced NNW-SSE graben, identified as a lower Bouguer anomaly, close to the Riachão city, in the SW portion of PB, where Brito Neves et al. (1984) first defined a molassic basin, registered in four wells by clastic

pre-Silurian sediments. Recent seismic interpretations (Porto, 2017; Porto et al., 2018) redefined this graben as an Ediacaran foreland basin, named as the Riachão basin, further discussed along the paper.

De Castro et al. (2014), in an integrated analysis of potential field data, have proposed an alternative subdivision of the basement inliers presented so far (blue contours in Fig.3.2). For these authors, the basement of PB was severely affected by two extensional phases prior to the basin installation (pre-Silurian times), forming a dense array of rifts imprinted as NNW-SSE (1st rifting phase) and NE-SW (2nd rifting phase) magnetic and gravimetric lineaments. This interpretation was not confirmed by subsequent studies using seismic reflection data (Daly et al., 2014; Castro et al., 2016; Porto et al., 2018).

More recently, Daly et al (2014) defined a 500-km-wide crustal block, named as the Parnaíba block (green color in Fig.3.2) along the W-E Deep Seismic Reflection Profile (DRP, Fig.3.2). As proposed by these authors, this block comprises two entities due to differences in the seismic character of the crust. To the west of Barra do Corda, comprising ca. 60% of the Parnaíba block, the crust shows a transparent seismic pattern, without any evidence of the Moho reflection. In contrast, to the east, they have observed a subhorizontal high amplitude mid-crustal reflectivity above some moderate amplitude events, interpreted as the Moho signal. The seismic limits of the Parnaíba block were defined by an abrupt vertical fault (Araguaína fault zone in Fig.3.2), to the west, associated to the Araguaia belt suture, and to the east of the Transbrasiliano Shear Zone (TBSZ in Fig.3.2), by eastward dipping events, related to the Neoproterozoic thrust belts of the Borborema Province.

In the vicinity of Teresina, there is an offset of approximately 90 to 100km between the TBSZ interpreted by Daly et al. (2014) and the Transbrasiliano lineament adopted here (Fig.3.2), based on the South American Tectonic map of Cordani et al. (2016), and also interpreted by De Castro et al. (2014). Within this offset, Daly et al. (2014) interpreted a narrow (~40km width) NE-SW-elongated rift structure in the seismic data, called the Campo Maior trough. They interpreted this structure as coeval to the Cambro-Ordovician Jaibaras trough (Oliveira and Mohriak, 2003), that outcrops in the NE of PB. These rift basins seem to connect further south to other graben-like structures already observed in seismic data by several authors

(e.g. Porto, 2014; Morais Neto et al., 2013; Abelha et al., 2018; Schuback, 2019). Here we call this region as the Transbrasiliano Fault Zone (TBFZ in Fig.3.2).

In 2018, as the result of the studies sponsored by the petroleum industry and the Brazilian National Petroleum Agency (ANP), published in the Special Publication of the Geological Society of London (eg. Daly et al, 2018), the Parnaíba basin became one of the most studied cratonic basins in the world (Mckenzie and Tribaldos, 2018). Following a series of geophysical acquisitions and analysis along the W-E Deep Regional Profile (DRP in Fig.3.2), further discussed in the next topic, the distinction between the western and eastern portions of the Parnaíba block, first suggested by Daly et al. (2014), became clear. These new results revealed a much more complex tectonic framework for the PB basement, challenging the idea of a single cratonic nucleus beneath it.

3.2.3 Dataset and Methods

To investigate the tectonic framework of Parnaíba Basin basement, first we will present a comprehensive compilation of the recent geophysical studies carried out in the basin, shown in item 3.2.4. Using a GIS database, we compiled, analyzed and merged the key results of these studies, presented in map view and in 2D sections (Figs. 3.3 and 3.4, respectively), coming up with a proposal for the tectonic compartmentation of the buried basement of PB. This envisaged framework is analyzed and refined under the light of the new results of this paper, presented in the subsequent topics.

Table 3.1 summarizes the available datasets used in topics 3.2.5 to 3.2.9, including their application in the present study. We produce a new crustal thickness map, based on information of 89 seismographic stations available in the literature (item 3.2.5; Fig.3.5 and the “Supplementary Material 1”). Afterwards, we compare this map with literature compilation (item 3.2.4) and present an update of the proposed crustal domains. In the following item 3.2.6, we perform a qualitative analysis of the aerogravity and magnetic maps, defining tectonic lineaments and refining the crustal domains configuration, under the light of the results of item 3.2.5.

Data Type	Dataset or survey name	Source	Amount	Data processing	Application in the study
Seismology data	Seismographic stations See Supplementary Data II	Assumpção et al., 2013 Trindade,2014 Luz et al.,2015 Albuquerque et al., 2017 Coelho et al., 2018 Araujo, 2019 Queiroz, 2019	3 stations 5 stations 7 stations 5 stations 9 stations 38 stations 21 stations	Receiver function method and H-stacking approach	Crustal Thickness Map (Moho depth). (See Fig.3.5)
2D Seismic Reflection Data	0295_ANP_2D_PARNAÍBA	BDEP/ANP public data	01 profile (L007)	PSTM (pre-stack time-migrated) converted to depth	Interpretation of Pre-Silurian basement. (See Fig.3.9)
	0317_2D_ANP_BACIA_DO_PARNAÍBA		01 profile (L104)		
			05 profiles (L103,L108,L112,L117)	PSTM (pre-stack time-migrated)	Interpretation of the Mid-Crustal Reflectivity (See Fig.3.7) and Pre-Silurian basement (See Fig. 3.10)
Gravity and Magnetic Airborne Surveys	0050_GRAVIMAG002_ANP	BDEP/ANP public data	Survey Area: 748,612.4 km2; Flight lines: E-W 6 km spaced; Tie lines: N-S 24 km-spaced.	Gravity data: Bouguer correction, Residual Bouguer. Magnetic data: Total magnetic intensity (TMI), First Vertical Derivative.	Interpretation of main gravity and magnetic lineaments and domains (See Fig.3.6)
Land Gravity	0295_GRAV_ANP_BACIA_DO_PARNAÍBA	BDEP/ANP public data	01 profile (L007);	Complete Bouguer correction	Qualitative analysis (See Fig.3.9)
	0317_GRAV_ANP_BACIA_DO_PARNAÍBA	BDEP/ANP public data	05 profiles (L104, L108,L112,L117)	Complete Bouguer correction	Qualitative analysis (See Figs.3.7 and 3.9)
			01 profile (L103); 500km long w/approx. 2500 gravity stations.	Complete Bouguer correction	2D Forward Modelling (See Fig.3.10)
Well data	See Supplementary Data II	BDEP/ANP public data	20	N/A	Lithological analysis of the Pre-Silurian basement, as well as geocronological control, when absolute ages are available (See Fig.3.8)

Table 3.1 Details of the available datasets used for the present study. The full information about the Seismographic stations and well data are available in the supplementary materials.

The next step presents the interpretation of four seismic lines (see Fig.3.7), where mid-crustal reflectivities were identified, and compared with the Bouguer response of equivalent land gravity profiles (item 3.2.7). Updated seismic interpretations (L104 and L007 in Fig.3.8) of the shallow basement underlying the PB are presented in item 3.2.8, constrained by well data (see Supplementary Material 2 and Fig.3.8). Finally, we have also conducted a two-dimensional forward model along a semi-regional scale gravity profile in the center of PB (L103; item 3.2.9), seeking to adjust the Bouguer anomaly to the crustal blocks identified along the equivalent seismic line and the estimated Moho depth relief from our crustal thickness map.

All the pertinent information, including literature compilation, crustal thickness variations derived from seismological data, gravity and magnetic anomalies, seismic interpretations and wellbore data, were then accounted to propose a new tectonic map for the basement in the Parnaíba basin area. This is presented in item 3.2.10, along with a proposal for the tectonic evolution for the region during the western Gondwana amalgamation, supported by the most updated and available paleoreconstructions.

3.2.4 A tectonic compartmentation of the Parnaíba basement based on recent geophysical studies

In this topic we discuss the evolution of the geophysical studies recently published focusing on the interpretation of the basement of the Parnaíba basin. The main results were compiled in the GIS base map presented in Fig. 3.3 and also in four crustal-scale sections: A-A', B-B', C-C' and D-D' (Figs. 3.3 and 3.4), summarized in seven different geophysical profiles (Figs. 3.4a to g). We also describe the main distinctive geophysical features of the crustal domains here adopted for the basement of PB. Upon the profiles (Fig.3.4) and in the map (Fig.3.3), these domains are also represented, in order to illustrate their geographic distribution.

The first relevant study using a broad geophysical dataset to investigate the basement of the Parnaíba basin was published by De Castro et al. (2014). These authors combined airborne and satellite gravity and magnetic surveys covering the entire basin area and margins, applying different filters and numerical models to define several geophysical domains within the basement. The profiles of Figs. 3.4a

and 3.4b represent, respectively, the reduce-to-pole magnetic and the Bouguer gravity anomalies from De Castro et al. (2014), along a NW-SE ~1190km-long profile (A-A' in Fig.3.3). The lateral contacts between the basement domains interpreted by these authors are also displayed in Fig.3.4a (black vertical lines), based on analytic signal solutions of the magnetic and gravity datasets.

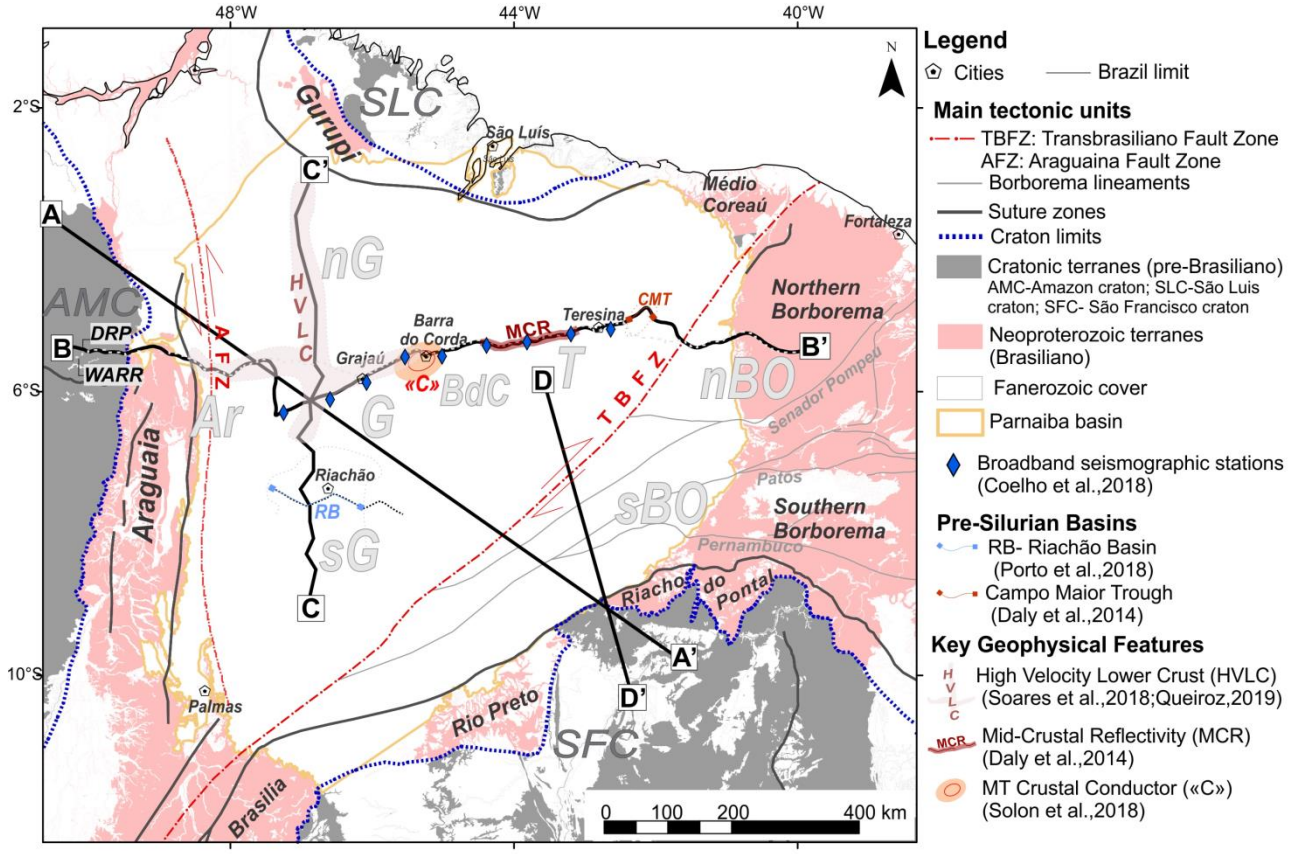

Fig.3.3: Literature compilation map with the location of the main geophysical features observed in the basement of Parnaíba basin. The black profiles are presented in Fig.3.4 and represent: A-A': gravity and magnetic anomalies (De Castro et al.,2014); B-B': Deep Regional Profile, compiled in Daly et al. (2019) and WARR data interpreted by Soares et al.(2018), Araujo (2019) and Schiffer et al.(2021); C-C': N-S transect of Queiroz (2019); and D-D': Deep MT profile of Rocha et al.(2019). The abbreviations of the proposed crustal domains refer to: Ar: Araguaia belt domain; G: Grajaú domain; nG: Northern Grajaú subdomain; sG: Southern Grajaú subdomain; BdC: Barra do Corda transitional domain; T: Teresina domain; nBO: Northern Borborema subdomain; sBO: Southern Borborema subdomain (including the Transversa. Zone and southern domains of Boborema Province), these last two are part of the Borborema Province.

After 2014, several studies along or in the vicinities of the ~1400km-long W-E Deep Regional Profile (DRP in Fig.3.2), crossing the center of PB, brought new perspectives for the interpretation of the basement. They have included a deep seismic reflection profile (DSRP, Daly et al., 2014), down to 14s (~ 60km depth); 823 terrestrial gravity measurements analyzed by Tozer (2017; Fig.3.4c) and Tozer et al.

(2017), 39 broadband magnetotelluric stations (Solon et al., 2018), 9 broadband seismographic stations (blue symbols in Fig.3.3; Coelho et al., 2018), and the wide-angle reflection and refraction profile (WARR; Soares et al., 2018).

A representative summary diagram of a typical cratonic basin was proposed by Daly et al. (2019), using as starting point the DSRP and all the additional studies along DRP. They have pointed out key observations of the lithosphere, lower crust, upper crust and shallow covers. These authors have also superimposed to this diagram the schematic configuration of the pre-Silurian Riachão basin (RB in Fig.3.3), interpreted by Porto et al. (2018). We modified this sketch (Fig.3.4d) adding some crustal features from the WARR profile from Soares et al. (2018), and from the 3D inversion MT model of Solon et al. (2018). We have also included in this profile the lithosphere-asthenosphere boundary (LAB) proposed for the basin area in Agurto-Detzel et al. (2017).

More recently, the contributions of De Lima et al. (2019), Araújo (2019) and Schiffer et al. (2021) added new information to the WARR profile of Soares et al. (2018), combining useful information from the DSRP of Daly et al. (2014). These authors reinforced the differentiation between the western and eastern portions of central Parnaíba basement. In the profile of Fig.3.4e, we compiled the results of the 2D tomography inversion model for the S-wave (Araujo, 2019) together with the final Vp/Vs ratios obtained by Schiffer et al. (2021).

Furthermore, two semi-regional scale profiles located in the western and southeastern margins of PB (C-C’ and D-D’ in Fig.3.3, respectively) were analyzed. The first profile refers to the S-N transect of Queiroz (2019) based on receiver function analysis and common conversion point (CCP) migrations of 26 seismographic stations. This author calculated the Vp/Vs ratios of the crust and the Moho depth based on H–κ stacking approach (e.g. Zhu & Kanamori, 2000), presented in Fig.3.4e. In Fig.3.4f, we present the final 3D vertical inversion resistivity model along the NNW-SSE 470km–long profile of Rocha et al. (2019). They have used magnetotelluric (MT) data from 49 broadband and 23 long period stations, crossing the SE margin of Parnaíba basin and part of the southern Borborema Province and northern São Francisco craton. Both electrical anomalies observed by Solon et al. (2018) and Rocha et al. (2019) are presented in the same color scale, in Figs.3.4d and 3.4f, respectively.

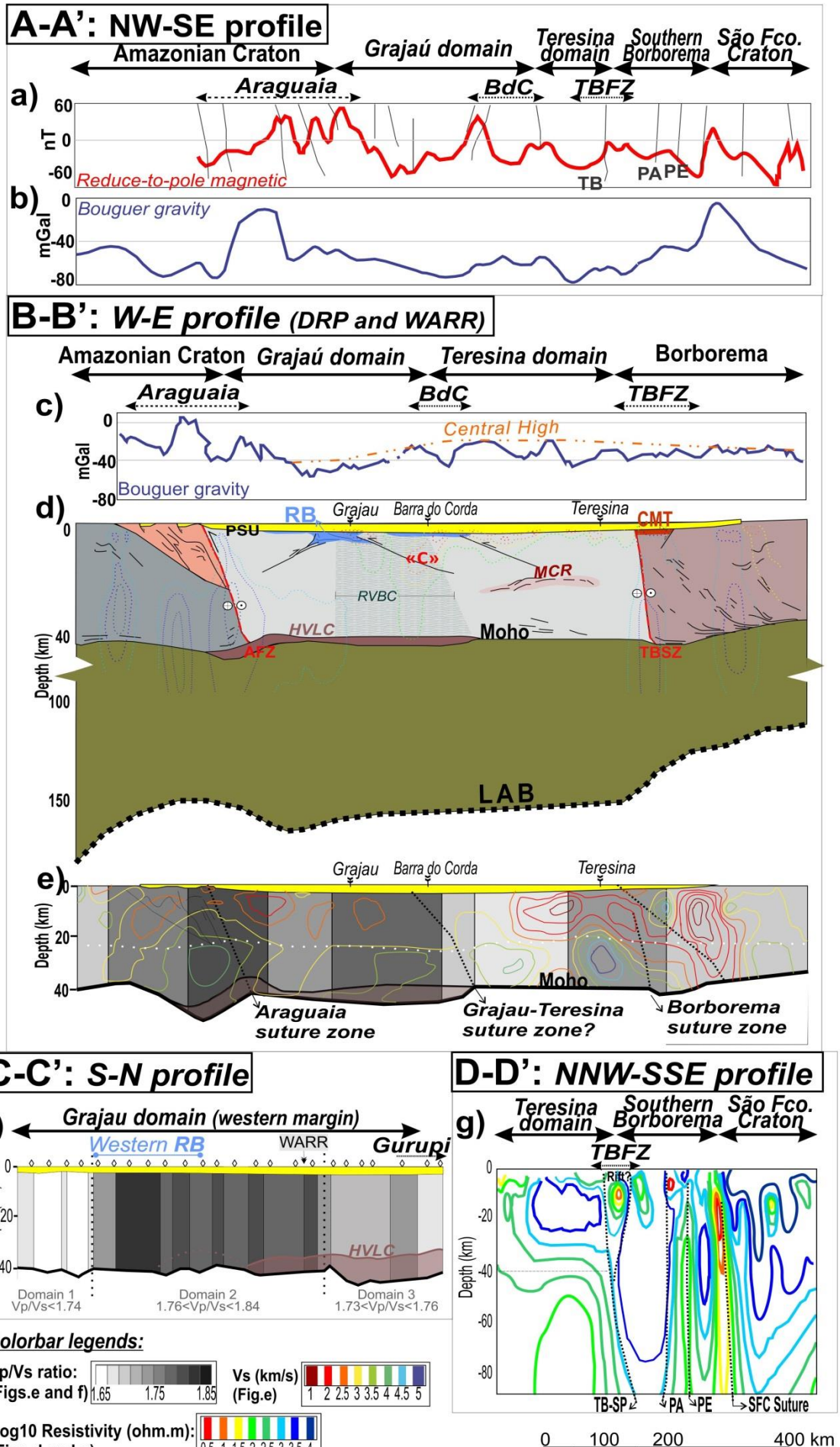
A-A': NW-SE profile
Amazonian Craton
Grajaú domain
Teresina domain
Southern Borborema
São Fco. Craton
a)
Araguaia
BdC
TBFZ
60
0
-60
nT
Reduce-to-pole magnetic
TB
PA
PE
b)
0
-40
-80
mGal
Bouguer gravity
B-B': W-E profile (DRP and WARR)
Amazonian Craton
Grajaú domain
Teresina domain
Borborema
Araguaia
BdC
TBFZ
c)
0
-40
-80
mGal
Central High
Bouguer gravity
d)
RB
Grajau
Barra do Corda
Teresina
CMT
PSU
«C»
MCR
RVBC
HVLC
Moho
AFZ
TBSZ
Depth (km)
0
40
100
150
LAB
e)
Grajau
Barra do Corda
Teresina
0
20
40
Depth (km)
Moho
Araguaia suture zone
Grajau-Teresina suture zone?
Borborema suture zone
C-C': S-N profile
f)
Grajau domain (western margin)
Western RB
WARR
Gurupi
0
20
40
Depth (km)
HVLC
Domain 1
Vp/Vs<1.74
Domain 2
1.76<Vp/Vs<1.84
Domain 3
1.73<Vp/Vs<1.76
D-D': NNW-SSE profile
g)
Teresina domain
Southern Borborema
São Fco. Craton
TBFZ
Rift?
0
-20
-40
-60
-80
Depth (km)
TB-SP
PA
PE
SFC Suture
0
100
200
400 km
Colorbar legends:
Vp/Vs ratio:
(Figs.e and f)
1.65
1.75
1.85
Vs (km/s)
(Fig.e)
1
2
2.5
3
3.5
4
4.5
5
Log10 Resistivity (ohm.m):
(Figs.d and g)
0.5
1
1.5
2
2.5
3
3.5
4

(PREVIOUS PAGE) **Fig.3.4:** Seven 2D profiles compiled and combined from the literature, presented in the same vertical and horizontal scales. Profiles location on Fig. 3.: A-A' is the NW-SE profile of De Castro et al. (2014): (a) Reduce-to-pole magnetic anomaly and the main boundaries (black lines) derived from analytical solutions); (b) the Bouguer anomaly. B-B' represents a E-W profile where several studies were merged: (c) Bouguer anomaly (with regional component removal) from Tozer (2017); (d) schematic geological compilation modified after Daly et al.(2019), with resistive anomalies from Solon et al. (2018) and seismic features of Soares et al.(2018) overlaid, as well as the lithosphere-asthenosphere boundary modelled by Agurto-Detzel et al. (2017), and (e) the crustal S-wave velocities and Vp/Vs ratios modelled by Araujo (2019) and Schiffer et al.(2021), respectively, along the WARR profile from Soares et al.(2018). C-C' is the S-N transect of Queiroz (2019), with Vp/Vs ratios and the Moho depth. And D-D´ is the NNW-SSE MT profile of Rocha et al. (2019). The tectonic domains and abbreviations of specific features are explained in the text.

Looking to the summary profile of Fig.3.4d along the DRP (B-B' in Fig.3.3), it is possible to observe that the continental lithospheric thickness below the Parnaíba basin is greater than 150km (Daly et al., 2019). McKenzie and Rodriguez Tribaldos (2018) obtained a range of 170-180 km for lithospheric thickness in the NW portion of PB, indicating a possible prolongation of the Amazonian craton "core" in this region. Eastwards, in the Borborema Province, these authors have observed a lithospheric thinning (140-110 km). The study of Agurto-Detzel et al. (2017), based on seismological data, indicates a lithospheric thinning to east in Borborema Province, and also in the SW margin of PB, beneath the southeastern portion of the Araguaia belt, as represented by the lithosphere-asthenosphere boundary (LAB) in Fig.3.4d.

The average continental crust beneath the Parnaíba basin is approximately 40km thick, according to the seismic interpretation of the DSRP in Daly et al., 2014. As previously discussed, these authors have identified a transparent seismic pattern for the crust within the so-called Parnaíba block, especially to the west. In the eastern Parnaíba block, between the cities of Barra do Corda and Teresina, a high-amplitude, mid-crustal reflectivity (MCR in Fig. 3 and Fig.3.4d), was observed at depths of 15-20km and the seismic Moho was recovered at 38km depth. In the following item 3.2.6, we will discuss in detail this particular MCR feature, with additional examples. These authors did not interpret the tectonic nature of the Parnaíba block, indicating that it could comprise two entities due to seismic-acoustic differences, even though these differences could be also associated to losses of seismic signal caused by the presence of shallow igneous rocks in the basin.

Further seismic studies shed light on distinctive anomalies within the Parnaíba block. Under the western portion of PB, close to Grajaú city (Fig. 3), Coelho et al. (2018) and Soares *et al*. (2018) recovered slightly thicker crust (~44km) besides high P and S-wave velocities. Soares et al. (2018) defined this area as the **Grajaú domain** (G in Fig. 3), in which they observed a 5 km-thick high-velocity (Vp=7.1-7.3 km/s) layer in the lower crust (HVLC in Figs. 3.3 and 3.4), extending from the Araguaia belt to the center of PB. A high S-wave velocity in the lower crust was also recovered in one station of Coelho et al. (2018), close to the Grajaú (blue symbol in Fig.3.3), also in agreement with the Vs values recovered by Araujo (2019; Fig.3.4e). To the NW of the Grajaú domain, along the S-N transect (C-C' in Fig. 3 and Fig.3.4f; Queiroz, 2019), the crust is also thicker. This author also observed a duplicated and discontinuous character of the base of the crust in the CCP stacking model, and interpreted it as a magmatic underplated body that correlates with the extension of the HVLC observed in the WARR profile. A reverberatory effect was described to the west of Barra do Corda city (RVBC in Fig.3.4d; Soares et al., 2018), within both the upper and lower crustal layers, coinciding with the region where Schiffer et al. (2021) observed a high Vp/Vs ratio (1.79; Fig.3.4e). The set of seismic features was interpreted as an indication of pervasive mafic intrusions within the crust and concentrated within the lower crust (underplating).

In the eastern portion of PB, to the east of Barra do Corda city, Soares et *al*. (2018) interpreted the **Teresina domain** ("T" in Fig.3.3), following the same proposal of De Castro et al. (2014; Fig.3.2). The Moho transition recovered from the WARR data in this domain is flat and sharp, at ~39km depth. The same signature was observed by Coelho et al. (2018) in three stations to the east of Teresina city (blue symbols in Fig.3.3). According to Soares et al. (2018), the upper crustal Vp gradient is smoother in Teresina, in contrast to the steep gradient within the Grajaú domain. The upper mantle velocity is also slightly higher (Vp>8,4 km/s) in this domain. In the mid-western portion of the Teresina domain, the 200km-long MCR was observed in the seismic data (Daly et al., 2014), although no Vp or Vs increase was observed in the WARR data. According to Schiffer et al. (2021), the Vp/Vs ratios of the crust are lower in the Teresina domain, varying from 1.73, in the west, to 1.76 in the eastern portion. This possibly indicates an absence of the pervasive mafic intrusions interpreted for the adjacent Grajaú domain. The S-wave velocity values in the upper crust of the Teresina domain are low (2.0 km/s) and two zones of high velocity

anomalies in the lower crust are observed, dipping eastwards, one in the vicinities of Barra do Corda city, and the other, more pronounced, close to Teresina (Fig.3.4e).

Between the Grajaú and Teresina domains, we defined a new domain, called the Barra do Corda transitional domain ("**BdC**" in Fig.3.3). Solon et al. (2018) observed a cylindrical shape crustal conductor ("C"), down to 30km, dipping slightly westwards in the same location of Barra do Corda. According to these authors, this feature might correlate to the concentration of graphite along crustal-scale faults, marking a paleosuture hidden in the basement of PB. Regionally, they have also observed a distinction between a western resistive crust, encompassing the western portion of the Grajaú domain, and a central and eastern moderate to conductive crust, encompassing the BdC transition zone, Teresina domain and the TBFZ. Rocha et al. (2019) observed the same electrical resistivity values for the SE portion of the Teresina domain (Fig.3.4g, D-D' in Fig.3.3). Schiffer et al. (2021) have also correlated the limit between "G" and "T" domains to a possible Neoproterozoic suture zone, observed by subtle eastward dipping anomalies in the crustal CCP staking section. Additionally, Araujo (2019) observed a high S-wave velocity anomaly within the lower crust (3.1 km/s) in vicinities of BdC (Fig.3.4e).

In the potential field data interpretations of De Castro et al. (2014), three distinct geophysical domains within the Parnaíba central basement were proposed, as already presented in Fig.3.2 (blue contours). These domains are named as the Parnaíba North (Pn) and Parnaíba South (Ps) to the west, and the Teresina (T), to the east. They were defined based on distinctive gravity and magnetic anomalies, discussed later in item 3.2.8. According to our compilation, we believe that they roughly correlate to the proposed Grajaú and Teresina domains of Soares et al. (2018). Upon the magnetic and gravity NW-SE profiles of Fig.3.4a and 3.4b, respectively (A-A' in Fig.3.3), we propose our tectonic subdivision (black arrows). It is possible to notice that the central portion of PB, encompassing Grajaú and Teresina domains, is represented by a low Bouguer anomaly (~-40mGal; Fig.3.4b), in contrast to the positive anomalies in the marginal tectonic domains: Araguaia belt (NW) and northern São Francisco craton (SE). The lowest gravity value of the profile (~70mGal) is located in the western portion, where we interpreted the Grajaú domain (Parnaíba South for De Castro et al., 2014). To the east, where we interpreted the Barra do Corda/Teresina domains, a residual positive anomaly (~50mGal) is observed.

Fig.3.4c shows the Bouguer gravity anomaly in the DRP, with the long wavelength component removed (Tozer, 2017). As well as De Castro et al. (2014; Fig.3.4b), Tozer (2017) noticed a basin-wide gravity low characterizing the Parnaíba area, contrasting with its margins. When correcting the gravitational effect of the sedimentary sequences of PB, Tozer (2017) observed a residual gravity anomaly in the central portion of the basin, to the east of Barra do Corda city, upon the MCR location. This mass excess (~175 kg/m^3) was interpreted as caused by a high-density lower crust, as a result of basaltic intrusions or granulite metamorphism. However, this central high is equivalent to the Teresina domain, where no evidence of high velocity lower crust was observed (Soares et al., 2018; Coelho et al., 2018). The Grajaú domain, presented in both Bouguer profiles of Figs.3.4b and 3.4c, is characterized by a negative gravimetric anomaly. In the NW-SE profiles (A-A´ in Fig.3.3; Figs. 3.4a and b), the transition between "**T**" and "**G**" domains is marked by a positive magnetic anomaly (Fig.3.4a), where De Castro et al. (2014) have found an alignment of the magnetic and gravimetric analytic signal solutions (black vertical lines in Fig.3.4a), possibly indicating a geological contact. It is worth saying that in this profile, the Teresina domain is much narrower, following the overall shape of this domain indicated by De Castro et al. (2014) in the map of Fig.3.2.

Steep crustal-scale faults mark the eastern limit of the Teresina domain and the western limit of the Grajaú domain (Fig.3.4d; Daly et al., 2019). Beneath the **Araguaia belt** (AR in Fig.3.3), the Moho bends downwards, reaching 51km depth (Soares et al., 2018). In the upper crust, down to 15km, curved and high amplitude reflections were interpreted by Daly et al. (2014) as the ophiolitic units of the Araguaia belt, thrusted towards the Amazonian craton and bounded to the east by Araguaína sinistral strike-slip fault (AFZ in Fig.3.4d). In the Bouguer profiles (Fig.3.4b and c), this region is characterized by a positive-negative contrast. On the other hand, at the opposite eastern edge of the DRP, the Moho depth varies from 41km beneath the dextral Transbrasiliano shear zone (**TBSZ** in Fig.3.3 and 4d) to 35km under the Borborema Province. Daly et al. (2014) described an undulatory Moho with anastomosed eastward dipping mid-crustal seismic reflections, interpreted as the Neoproterozoic shear zones of Borborema. According to Schiffer et al. (2021) and Araujo (2019), high Vp/Vs ratios (1.81 and 1.76) and the high Vs values in the lower crust (3.6 km/s and 3.4 km/s) under the Araguaia belt and TBFZ, respectively, indicate the presence of suture zones. De Castro et al. (2014) have also observed a

strong alignment of the sources derived from analytic signal depth analysis based on gravity and magnetic data in this region. They are represented in Fig.3.4a by black vertical lines, marking the main suture zones in the Araguaia and Southern Borborema domains. In the MT profile of Solon et al. (2018), both AR and BO domains (Fig.3.3) are characterized by narrow and vertical resistive anomaly zones (Fig.3.4d), crossing the upper crust down to the upper mantle. To the SE, Rocha et al. (2019) observed a similar crustal electrical pattern (Fig.3.4g), inferring the prolongation of the main suture zones of southern Borborema beneath PB.

A remarkable planar unconformity is demonstrated by the seismic image of the DSRP marking the base of the Phanerozoic Parnaíba basin. It represents a profound erosive peneplane (Daly et al., 2014, 2018), here called as the Pre-Silurian Unconformity (PSU in Fig.3.4d). Beneath the PSU, remnant basins were observed in the seismic data and in few wells. In Figs. 3.3 and 3.4d, they are represented by the Campo Maior trough (CMT; Daly et al., 2014), and the Riachão basin (RB; Porto et al., 2018). As previously described, the CMT is located within the limits of the TBFZ (Figs. 3.2 and 3.3) and the RB was observed in the SW of the Parnaíba basin, approximately ~120km apart from the DRP (Fig.3.3), upon the southern prolongation of the Grajaú domain. The pre-Silurian basins will be better described in the next topics, along with new interpretations.

In terms of crustal geophysical anomalies recovered under these basins, Soares et al. (2018) observed low velocities within the upper crust close to the TBFZ, possibly related to the presence of a Cambrian rift, in agreement to the interpretation of CMT. Solon et al. (2018) have recovered a high to moderate resistive upper crust in the same region (Fig.3.4d). To the SE, a high resistive body within TBFZ was identified in the shallow crust (Fig.3.4g), interpreted as a rift basin by Rocha et al. (2019). Additionally, Romero et al. (2019), using broad-band MT data along the SE border of Parnaíba, also described resistive graben-like structures, down to ~2 km depth.

The S-N transect of Queiroz (2019; C-C’ in Fig3) crosses the western portion of the foreland Riachão basin (RB), where Porto et al. (2018) observed a highly reflective upper crust in the seismic data, interpreted as the eastward verging thrusted margin of RB. In this portion, Queiroz (2019) has observed the highest Vp/Vs ratios of the profile (~1.83 in Fig.3.4f) and associated them either to a mafic

composition of the crust or to the presence of basaltic intrusions. Here, we have assigned this region as the southern portion of the Grajaú domain. Northwards in the C-C' profile (Fig.3.4f), close to the crossing point with the DRP and WARR profiles, the crust is thicker and the Vp/Vs ratios are slightly lower, decreasing towards the Gurupi belt. This signature of a thicker crust conveys with the interpretation of an underplate (HVLC in Figs. 3.3, 3.4e and 3.4f). The opposite southernmost portion of the S-N transect presents very low Vp/Vs ratios (<1.70), interpreted by Queiroz (2019) as a felsic crust, possibly without the igneous intrusions observed in the central PB.

Finally, after compiling and reinterpreting the several geophysical datasets, we could propose a comprehensive subdivision of the main crustal domains partially or entirely hidden by the sediments of the Parnaíba basin. These seven proposed domains, presented below from west to east, will be refined and tectonically interpreted along the text. They are:

- **Araguaia belt domain (AR),** encompassing the western margin of PB and interpreted as the eastward prolongation of the outcropping Araguaia belt beneath PB;
- **Grajaú domain (G)**, located in the mid-western portion of PB and that can be divided into two subdomains: *Southern "G",* where the pre-Silurian Riachão basin was described, and *Northern "G",* where the crust is thicker (~43-44km) and a high-velocity lower crust was observed;
- **Barra do Corda transitional domain (BdC),** located in the vicinities of the homonymous city in between the "G" and "T" domains, defined mainly due to the remarkable conductive crustal anomaly observed by Solon et al. (2018) and after the analysis along the WARR data made by Schiffer et al. (2021), suggesting the presence of a suture zone in this region;
- **Teresina Domain (T):** located in the mid-eastern portion of PB, where the MCR was first described and where the crust is slightly thinner (~38-39km). It is bounded to the east by the Transbrasiliano Fault Zone;
- **Transbrasiliano Fault Zone (TBFZ):** located along the NE-SW homonymous tectonic lineament, and where the Campo Maior trough was described, under a slightly thicker crust than the adjacent "T" and

Borborema domains, in the DRP;

- **Borborema domain (BO):** encompassing the eastern and southeastern portions of PB and interpreted as the westward prolongation of the outcropping structural domains of the Borborema Province beneath the PB and truncated by the TBFZ. Following the recent tectonic study of Caxito et al. (2020), it is here subdivided into *Northern* BO and *Southern BO* subdomains.

3.2.5 Crustal Thickness Map of the Parnaíba basin

Until very recently, most of the maps showing estimations for the Moho depth (crust/mantle boundary) based on seismic datasets (e.g. Feng et al., 2007; Lloyd et al., 2010; Chulick et al., 2013), satellite gravity surveys (e.g. Van der Meijde et al., 2013) or a combination of both (e.g. Assumpção et al., 2013; Uieda and Barbosa, 2017) were restricted to continental scale of the South American plate, with low resolution within the Parnaíba basin area. According to Chulick et al. (2013), the average thickness of the continental crust of South America is 38.17 km (+/- 8.7 km), which is approximately 1 km thinner than the global average. In Brazil, Assumpção et al. (2013) showed an average crust thickness of 39km (+/- 5km), without any clear discrepancy between different tectonic settings, such as intracratonic basins or Neoproterozoic fold belts, except to the thinned crust found in the Borborema Province (30-35km) and within the Tocantins Province (Araguaia belt). Both anomalies are located respectively in the eastern and western margins of the Parnaíba basin. Within the Parnaíba basin area, Feng et al. (2007) and Lloyd et al. (2010) have shown a thicker crust (40-45km) in the central part, slightly shifted to the west, while in the other maps this region is less precise.

The studies carried out by Coelho et al. (2018), and more recently by Araujo (2019) and Queiroz (2019) brought information of at least 68 seismographic stations along both the E-W Deep Regional Profile and the N-S transect (B-B’ and C-C’ in Fig.3.3). Added to 21 seismographic stations available in the surrounding margins of PB, from Assumpção et al. (2013), Trindade (2014), Luz et al. (2015) and Albuquerque et al. (2017), we were able to update the Moho depth contour map of the Parnaíba basin area, compiling the crustal thickness estimates from 89 stations

(see full information in the Supplementary Material 1). The results are shown in Fig.3.5.

The compiled studies used receiver functions to estimate the crustal thickness by the H–κ stacking approach (e.g. Zhu & Kanamori, 2000). We interpolated the average H–κ stacking of the Moho depth (crust-mantle boundary) values using a geostatistical algorithm available in the ESRI ArcMap 10.0 software, which applies an ordinary krigging interpolation method with spherical semivariogram model fit. In the interpolation, only the central values of the measurements were considered (i.e. the measurements errors were not taken into account). Despite the considerable number of stations, their spatial distribution remains irregular within the entire basin extent, implying higher uncertainties especially in the northern and southeastern portions of the basin.

The crustal thickness contour map of Fig.3.5 shows a first order crustal thinning from about 50km to the west, in the Araguaia domain to ca. 30km to the east, in the Borborema domain, a pattern that accompanies the lithospheric thinning determined by Agurto-Detzel et al. (2017; Fig.3.4d). The average value calculated from the sum of the Moho depth estimates from the 89 stations yielded 40.7km in the study area. There is a clear difference between the western (thicker crust, >41km) and the eastern (thinner crust, <39km) portions of the central Parnaíba basin, reinforcing the observations along the DRP (Coelho et al., 2018; Soares et al.,2018; Araujo, 2019; De Lima et al., 2019; Schiffer et al., 2021) and the separation between the Grajaú and Teresina domains, respectively. This boundary is marked by the 40km Moho depth contour line in the vicinities of Barra do Corda city.

The most striking observations of this map are related to the crustal thickness variations observed in the western portion of the Parnaíba basin, in the Araguaia and Grajaú domains, where there is a better spatial distribution of the dataset. The northern and southern portions of the Araguaia belt (respectively, “nAr” and “sAr” subdomains in Fig.3.5) present the highest crustal thickness values of the map: 49km and 53km, respectively, while in the central portion of the Araguaia domain, beneath the PB, the thickness values are at least 17km lower. Three stations compiled from the study of Albuquerque et al. (2017; green stations in Fig.3.5) recovered values of 31.6 to 36km for the Moho depth in this region. This “indentation” of thinner crust was also observed by these authors westwards, within the Carajás Province in the

Amazonian Craton. To the east, the stations of Queiroz (2019) along the N-S transect (yellow stations in Fig.3.5) have presented higher crustal thickness estimates, varying from 40 to 43km. In our study, we propose to individualize this portion of thinner crust within the Araguaia domain as the Eastern Araguaia subdomain ("eAr" in Fig.3.5). The "eAr" encompasses the western margin of the Riachão basin, where westwards dipping reflections were interpreted in the shallow basement as the back

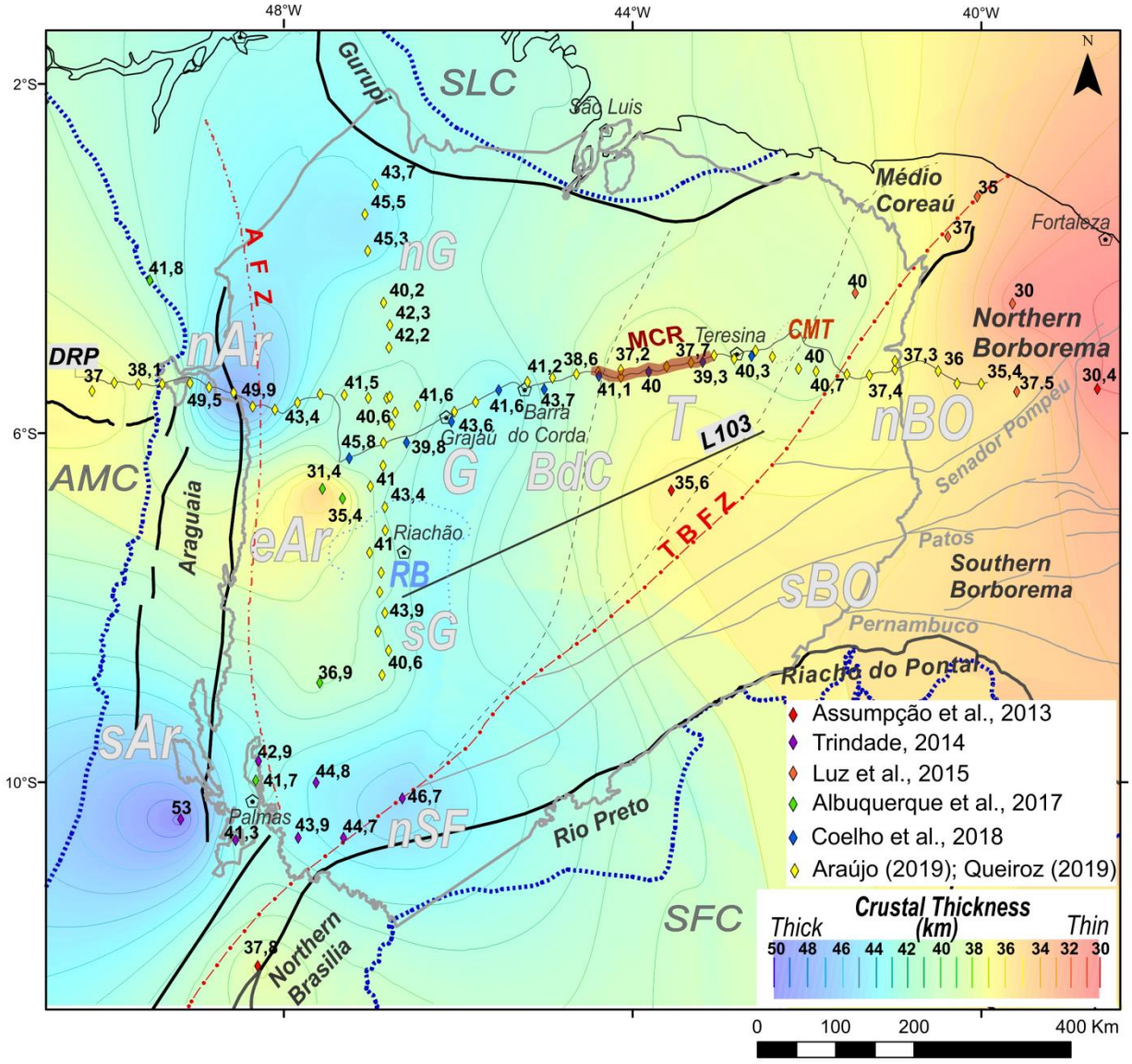

thrusts related with the evolution of the Araguaia belt (Porto et al., 2018). This domain also coincides with the region of thinned lithosphere observed by Agurto-Detzel et al. (2017).

Fig. 3.5 Crustal thickness map of the Parnaíba Basin and surroundings, based on 89 seismographic stations (H–κ stacking approach) from recent literature compilation. Some average crustal thickness values are displayed close to the respective station (see full information in Supplementary Material 1).

The location of the seismic profiles L103 and the DRP are represented by gray lines. The abbreviations of the proposed crustal domains refer to: nAr: Northern Araguaia belt subdomain; sAr: Southern Araguaia belt subdomain; eAr: Eastern Araguaia belt subdomain; G: Grajaú domain; nG: Northern Grajaú subdomain; sG: Southern Grajaú subdomain; BdC: Barra do Corda transitional domain; T: Teresina domain; nBO: Northern Borborema subdomain; sBO: Southern Borborema subdomain; nSF: Northern São Francisco domain. RB stays for the pre-Silurian Riachão basin; CMT is the Campo Maior Trough; MCR, the mid-crustal reflectivity along the DRP. AFZ and TBFZ are Araguaína and Transbrasiliano fault zones, respectively.

To the east, within the Grajaú domain (G in Fig.3.5), we also observe subtle thickness variations of the crust. In the northernmost portion, close to the limit with the Gurupi belt, the crust reaches 45.5km thick, decreasing to approximately 42km thick close to the DRP. This region is defined as the Northern Grajaú subdomain ("nG" in Fig.3.5 and Fig.3.3). Southwards, the crustal thickness decreases to ~40km, beneath the eastern portion of the Riachão basin, here assigned to the Southern Grajaú subdomain ("sG" in Fig.3.5).

In the southernmost portion of the Parnaíba basin, close to the Transbrasiliano Fault Zone (TBFZ in Fig.3.5), the crust reaches a maximum thickness of 46.7 km, with an average value of 44km (purple stations in Fig.3.5). According to the tectonic map of South America of Cordani et al. (2016), this region coincides with the suture zone of the northern São Francisco craton (SFC in Fig.3.5). Here we identified this region as the Northern São Francisco domain ("nSF" in Fig.3.5). Following the NE-SW trend of the TBFZ towards the NE, the crust is much thinner than in the SW, presenting values equal or lower than 40km thick. No abrupt crustal thickness variation is observed between the Teresina domain ("T" in Fig.3.5) and this portion of the TBFZ domain. A slightly thicker (40-41km) crust is observed beneath the TBFZ in the DRP and possibly extends northwards. In the eastern prolongation of DRP, the northern Borborema subdomain ("nBo" in Fig.3.5) presents a continuous crustal thinning towards offshore Brazil, varying from approximately 37.5 to 30km thick. The Southern Borborema subdomain and the southern prolongation of the Teresina domain are not well represented in the map, due to the lack of data. Only one station, close to the seismic profile L103, recovered a 35.6km thick crust (red station in Fig.3.5; Assumpção et al., 2013), suggesting that possibly the Teresina domain presents a thinner crust southwards.

3.2.6 Interpretations of Gravity and Magnetic Anomalies

The aerogravity and magnetic public maps (see details in Table 3.1) are presented in figure 3.6, including the complete Bouguer anomaly map (Fig.3.6a), the residual filtered Bouguer map (wavelength < 95km; Fig.3.6c), the total magnetic intensity map (TMI; Fig.3.6b) and the first vertical derivative filter of the TMI map (Fig.3.6d). In Figures 6e and 6f, we present the interpreted gravity and magnetic lineaments, respectively, superimposed on the crustal thickness map of Fig.3.5, as well as the abbreviations of the proposed basement domains. We also locate in Fig.3.6a the “A-A’” NW-SE profile of De Castro et al. (2014) and the Deep Regional Profile (DRP), both already presented in Figs. 3.3 and 3.4, respectively. The L103 profile is also located in Fig.3.6, as it will be discussed further in the text during the 2D gravity model (item 3.2.9).

Only a small part of the outcropping Araguaia belt is covered by the available surveys. In the gravity maps (Figs. 3.6a and 3.6c), this mobile belt is represented by N-S elongated negative and positive stripes, following the N-S structural trends of geological contacts and faults. In the complete Bouguer map (Fig.3.6a), a striking N-S elongated negative anomaly is noticed in the western portion, outside the basin limits, towards Amazonian craton. Along this negative Bouguer anomaly, the crust thickness map shows two regions of thicker crust to the north and to the south, separated by a central region of thinner crust, which extends from the AMC to the PB. Here we assign these regions to three subdomains: the northern, southern and eastern Araguaia belt subdomains (nAr, sAr and eAr in Fig.3.6e, f). The low residual gravity anomaly (Fig.3.6c) also observed in this region possibly reflects the low density metasedimentary units of the Estrondo and Tocantins groups, part of the external domain of the Araguaia belt , as corroborated by the interpretation along the DRP (Fig.3.4d; Daly et al., 2014). To the east, beneath the western basin margin, the gravity anomaly is characterized by N-S-trending positive stripes (Figs. 3.6a and 3.6c). De Castro et al. (2014) interpreted this positive anomaly as the prolongation of the Goiás Magmatic Arc in this region. Our preferred interpretation is that the positive stripes reflect the presence of higher-grade metamorphic rocks in the hidden internal zone of the Araguaia belt, covered by PB. Moreover, these stripes could be associated to basement highs, uplifted during Mesozoic episodes of tectonic inversion along the Araguaína Fault Zone (AFZ in Fig.3.5), as argued by Daly et al.

(2014). These authors, using structural restoration, showed a basement uplift of ca. 2km in this region, which resulted in folding the Pre-Silurian Unconformity (PSU) and in the consequent partial erosion of the Paleozoic sediments.

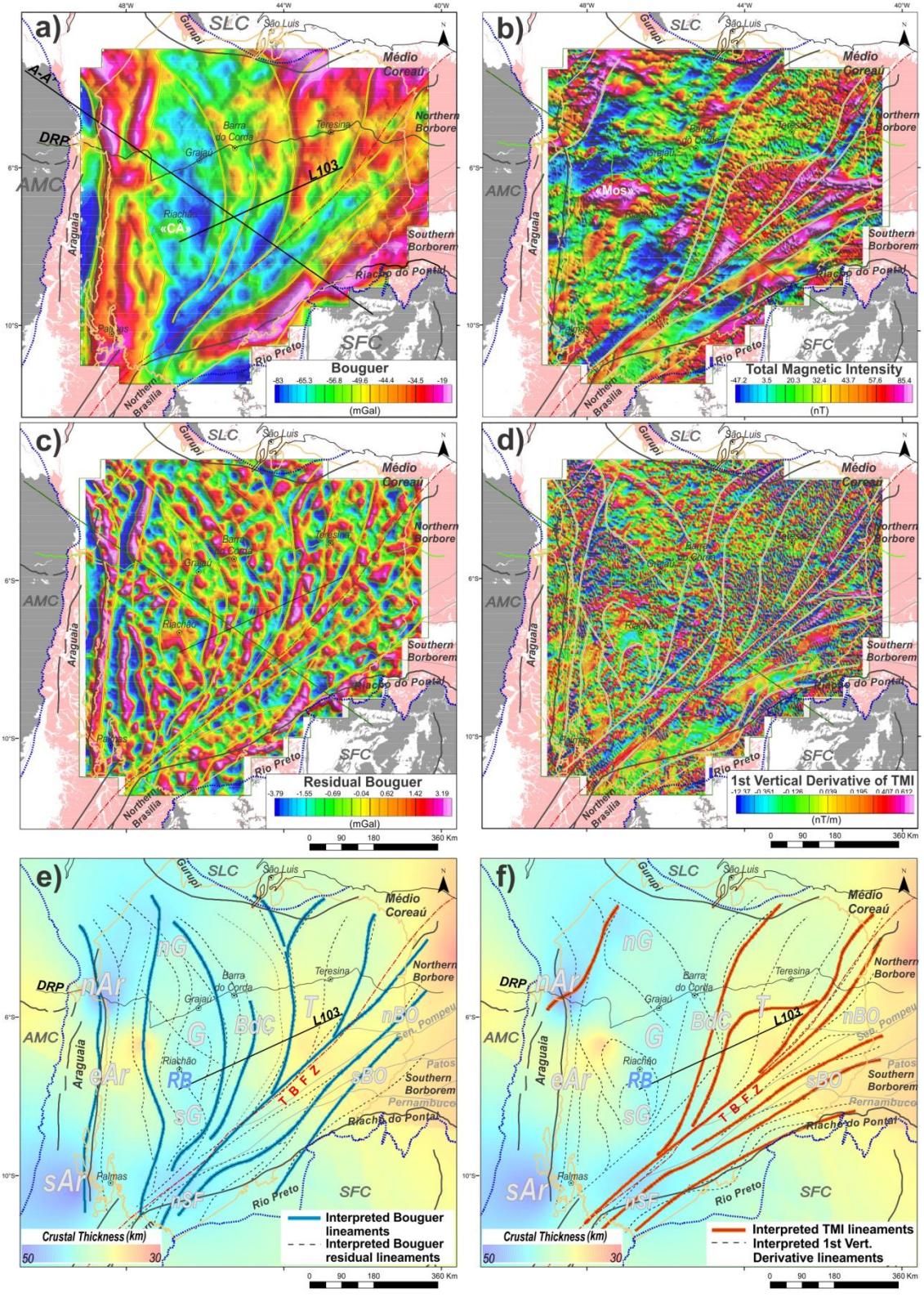

Fig.3.6 (a)Complete Bouguer anomaly; (b) Total Magnetic Anomaly Intensity (TMI) map; (c) residual filter of the Bouguer anomaly map; (d) 1st Vertical Derivative of the TMI map. The interpreted

lineaments are displayed upon the maps, as well as the locations of A-A' profile (De Castro et al., 2014), the DRP and L103 profile. In (e) and (f) we present the interpreted gravity and magnetic lineaments, respectively, upon the crustal thickness map of Fig.3.5, as well as the locations of the proposed tectonic domains.

In contrast to the gravity anomaly pattern, in the magnetic maps (Fig.3.6b and 6d), the Araguaia belt domain is characterized mainly by ENE-SSW lineaments, not showing any compatibility with the N-S structural trend of the outcropping belt. This internal fabric prevails towards the Grajaú domain, located eastwards, and it was also observed by De Castro et al. (2014), westwards, in the Amazonian craton. This magnetic pattern can either reflect the inherited pre-Brasiliano structural trends of the Amazonian Craton beneath the Araguaia belt and Parnaíba basin or the imprint of a later tectonic event, such as the emplacement of Mesozoic mafic magmatic rocks and associated extensional stresses during Gondwana break-up (e.g. Mocitaiba et al., 2017). One example of how the shallow magmatic rocks can mask the basement response in the magnetic maps is observed in Fig.3.6b, where a remarkable positive magnetic anomaly is located in the vicinities of Riachão city and is coincident with the outcrops of the Mesozoic Mosquito basalts ("Mo" in Fig.3.6b). De Castro et al. (2018) interpreted this region as the E-W elongated North Mosquito Magnetic Domain.

The mid-western portion of the Parnaíba basin, called here as the Grajaú domain, is characterized by low values of TMI anomalies (Fig.3.6b) and by a broad N-S elongated Bouguer low (Fig.3.6a). The negative anomaly was also observed in the regional gravity map of De Castro et al. (2014) and possibly correlates to the deeper values of the Moho depth (Fig.3.6e and 3.6f). In the Bouguer residual map (Fig.3.6c), we have interpreted curved lineaments within the central portion of the Grajaú domain (Fig.3.6e), bounded to the south by the NE-SW TBFZ and to the north by WNW-ESE trends, possibly indicating an imprint of the Gurupi belt structures in the northern Grajaú subdomain. In the southern Grajaú subdomain, a low magnetic anomaly in the TMI map (Fig.3.6b) and curved lineaments were interpreted in the first derivative map (Fig.3.6d) and are possibly related to the presence of the pre-Silurian Riachão basin (RB). According to Porto et al. (2018), the basin lies upon a NNW-SSE-elongated low Bouguer anomaly, centered to the east, where the eastern depocenter is located (~4km thick). To the western portion of the RB, here assigned to the eastern Araguaia domain ("eAr" in Fig.3.6e), the Bouguer values increase and are correlated with the highly reflective pre-Riachão basement and with the central

basement high (“CA” in Fig.3.6a), also observed in the seismic data, as discussed ahead.

Likewise De Castro et al. (2014), we have observed the high frequency magnetic pattern that individualizes the Teresina domain (“T” in Figs. 3.6e and 3.6f), in the eastern part of PB. In the TMI map, it is noticeable the contrast of the higher values of magnetic anomalies in this eastern-northeastern portion of the basin in relation to the western portion. In the Bouguer map (Fig.3.6a), the gravity anomalies, especially in the NE of PB, are also very high when compared to the rest of the basin area. Remarkable positive gravimetric and magnetic signatures were also observed by Pedrosa Jr. et al. (2014) within the outcropping Médio Coreaú domain (Borborema Province), mainly related to the high-grade metamorphic rocks of the Paleoproterozoic Granja complex. The similarity between the potential field data signatures of the Médio Coreaú and Teresina domains suggest a connection between both domains in the NE Parnaíba basin limit. The external shape of the Teresina domain resembles a “balloon”, wider in the NE and narrowing southwards, where the NE-SW lineaments of the Transbrasiliano Fault Zone (TBFZ) are superimposed (Figs. 3.6a.and 3.6b). Internally, we observe sigmoidal residual Bouguer lineaments (Figs.3.6c), and NE-SW elongated magnetic lineaments (Figs.3.6b and 3.6d). This sigmoidal shape resembles a typical “S-C fabric”, normally microscopically observed in shear zones, and it was observed in the magnetic maps of Pedrosa Jr. et al. (2014) in the Médio Coreaú Domain, correlated to the dextral shear along the Sobral-Pedro II fault, a subsidiary fault of the TBFZ, during the Ediacaran/Early Cambrian.

Between the Grajaú and the Teresina domains, in the vicinities of Barra do Corda, in the central Parnaíba, the sigmoidal shape of the residual Bouguer anomalies persists. Linear positive and negative gravity anomalies with an overall N-S trend, curve to the east towards the Teresina domain. They terminate parallel to the NE-SW Médio Coreaú domain, in NE, and to the southern prolongation of the TBFZ, in the Northern Brasília belt. De Castro et al. (2014) interpreted these low linear gravity residual anomalies as an array of buried grabens beneath PB, formed during an extensional phase between the Neoproterozoic and Eopaleozoic, although they did not discard the possibility that these lighter sources could be caused by granitic rocks or low-grade metasedimentary sequences within the basement, fitting with the interpretation of a Neoproterozoic belt. Since the seismic data (Daly et al.,

2014 and Porto, 2017) did not confirm the presence of such rifts in the central Parnaíba basin, we prefer the second interpretation for the Barra do Corda transitional domain ("BdC" in Figs.3.6e and 3.6f), with agreement to the suggestion of Schiffer et al. (2021) of a buried suture zone in this region.

To the southeast of the Parnaíba basin, in the southern segment of TBFZ, the trends of the gravity and magnetic signatures are mainly NE-SW oriented. A striking positive NE-SW Bouguer anomaly (Fig.3.6a) marks the limit with the northern margin of the São Francisco Craton. It is noticeable the NE-SW bend of the E-W shear zones within the Southern Borborema subdomain beneath the Parnaíba basin, reinforcing the tectonic interpretation of Late Neoproterozoic/ Early Paleozoic right-lateral displacements along the TBFZ (e.g. Brito Neves & Fuck, 2013). In between the Northern and Southern Borborema subdomains ("nBo" and "sBo", respectively in Fig.3.6f), a very strong E-W positive magnetic anomaly seems to connect to the NE-SW Senador Pompeu shear zone and is truncated by the TBFZ.

3.2.7 Mid-Crustal Reflectivity in central Parnaíba basin basement.

The Mid-Crustal Reflectivity (MCR) in the Parnaíba basin was first described by Daly et al. (2014) along the staked deep seismic reflection profile (DRP-MCR; Fig.3.7a). They have observed a subhorizontal layer of high amplitude curved reflectors, up to 3km thick, in the eastern Parnaíba block (here, Teresina domain). This reflectivity terminates laterally into an acoustically featureless seismic pattern and, beneath it, subhorizontal, moderate amplitude events define the Moho at 38 km depth. Here we use the denomination of DRP-MCR. Tozer et al. (2017), in order to better assess the spatial extent of the DRP-MCR, the nature of the lower crust and the Moho reflectivity, have analyzed unmigrated CDP reflection stacked from five wide-angle split-spread receiver gathers near the center of the basin. They have traced the MCR laterally for approximately 250km at depths ranging from 17 to 25km (~ 8.5s-13s in TWTT), with average P-wave velocity of 6.75–7.0 km/s.

We bring here new observations of similar mid-crustal reflectivities in a different 2D seismic reflection survey (Table 3.1) within the central Parnaíba basin, approximately 80 km southwards from the DRP-MCR, in the region here assigned as the Barra do Corda transitional domain (BdC). The map of Fig.7a shows the location of the new interpreted top of the MCR seismic horizon and respective contour map in

two-way travel time (excluding the DRP-MCR). Raw and interpreted versions of four seismic reflection profiles, with the equivalent Bouguer anomaly data are displayed in Figs.3.7b to 3.7e.

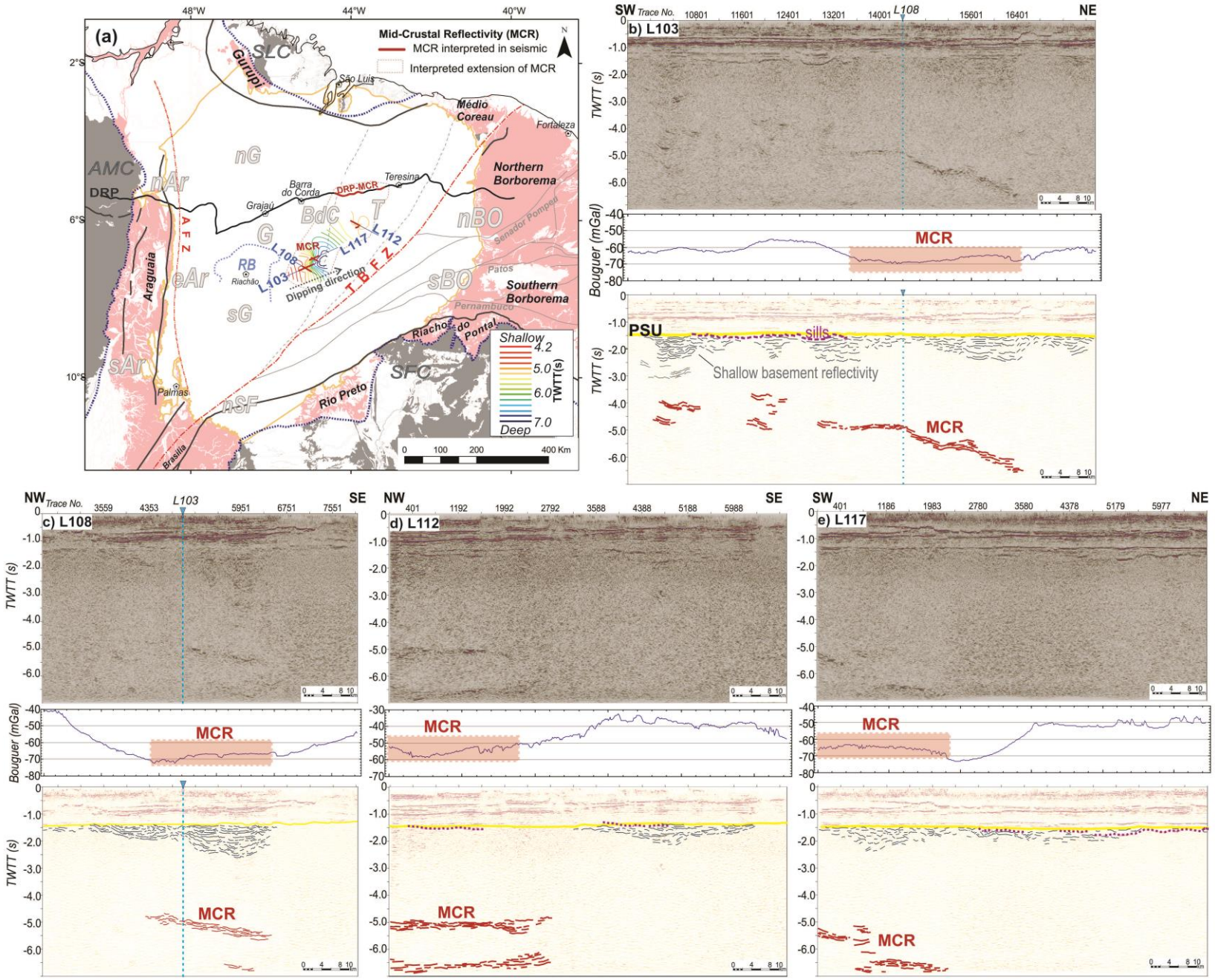
(a)
Mid-Crustal Reflectivity (MCR)
MCR interpreted in seismic
Interpreted extension of MCR
48°W
44°W
40°W
2°S
6°S
10°S
SLC
Gurupi
São Luis
Médio Coreau
Fortaleza
AMC
DRP
nAr
nG
Barra do Corda
DRP-MCR
Teresina
Northern Borborema
Grajaú
BdC
T
nBO
Senador Pompeu
AFZ
G
L108
MCR
L117
L112
TBFZ
Araguaia
RB
Riachão
L103
Dipping direction
eAr
sBO
Patos
Southern Borborema
Pernambuco
sG
Riachão do Poço
Portal
Shallow
4.2
5.0
6.0
7.0
Deep
TWTT(s)
sAr
SFC
Palmas
nSF
Rio Preto
Brasília
0 100 200 400 Km
SW
Trace No.
10801 11601 12401 13201 14001 L108 15601 16401
NE
b) L103
TWTT (s)
Bouguer (mGal)
MCR
PSU
sills
Shallow basement reflectivity
NW
SE
c) L108
L103
3559 4353 5951 6751 7551
d) L112
401 1192 1992 2792 3588 4388 5188 5988
e) L117
401 1186 1983 2780 3580 4378 5179 5977

(PREVIOUS PAGE) Fig.3.7 (a) Map showing the spatial distribution of the Mid-Crustal Reflectivity and the new MCR contour map relief in two-way travel time (TWTT). (b), (c), (d), (e) show the raw and interpreted seismic sections in time domain, with the associated gravity Bouguer anomalies, highlighting the presence of the new observed MCRs.

Likewise the DRP-MCR, the new proposed MCR presents the same internal seismic facies described by Daly et al. (2014), however, there are some striking differences: it is much shorter, varying from 7 to 48km long, and also shallower, varying from 4.0 to 7.0s depth (TWTT). Regarding the Bouguer anomaly, the new MCRs occur in low anomaly zones, with an average value of -60 to -70 mGal, with exception to L112 (Fig.3.7d), in which the range is a bit higher (-50 to -60 mGal). The Bouguer anomaly along the DRP-MCR, however, is much higher, varying from approximately -20 to -40 mGal, as observed in the profile of Tozer (2017), in figure 4c, coincident to the location of the interpreted “Central High".

In the southern seismic profiles (L103, L108 and L117 in Figs.3.7b, 3.7c and 3.7e respectively), the new MCRs are dipping NE, as shown by the contour map of Fig.3.7a. This is best displayed in part of L103, where the MCR presents a peculiar shape of “steps”, intercalating inclined and horizontal segments, varying from 7.0 s (in the base of the profile, to NE) to approximately 4.2s depth. To the SW of L103, the MCR is not clear, but scattered highly reflective events within the basement seem to connect it up to shallower depths within the basement, in the eastern thrusted margin of the Riachão basin (Porto et al., 2018). This interpretation is further discussed in item 3.2.9 of the paper. To the north, however, the new MCR seems to get horizontal (L112 Fig.3.7d), similar to the DRP-MCR shape, characterized by two high amplitude parallel levels of reflectivity, one at approximately 4.8s and the basal one down to 7.0 s.

Another interesting observation in all four seismic sections (Fig.3.6b to 3.6e) is the presence of a chaotic seismic pattern with moderate amplitude in the shallow basement of the Parnaíba basin, beneath the flat Pre-Silurian Unconformity (PSU). This shallow basement reflectivity (Fig.3.6b) presents an undulated to triangular basal limit and a lateral extension that seems to correlate with the extension of the MCR in lines L103, L108 and L117. More studies are required to better investigate the nature of this seismic pattern.

It is relevant to emphasize that there are also many differences in terms of acquisition and seismic processing parameters between the ANP seismic data, presented here (see table 3.1), and the MCR-DRP (Daly et al. 2014; Tozer et al., 2017), what might compromise a fair comparison of the MCR in both datasets. Besides that, no further investigation of the seismic processing steps, or even post-processing filters, was here applied in order to mitigate any non-geological noise that might have interfered the proper imaging of new MCR and the deep Parnaíba basin basement in general.

In terms of possible interpretations, Tozer et al. (2017) interpreted the DRP-MCR as the top of a fast, high density lower crustal body that occupies the entire Parnaíba basin area. These authors accounted the basin subsidence to the load caused by the anomalous dense lower crust, testing this hypothesis in flexural models. The subsequent seismic studies (Soares et al., 2018; Coelho et al., 2018, De Lima et al., 2019), although, did not confirm the presence of a high velocity lower crust in this region of the DRP. In fact, they have observed it to the west, within the Grajaú domain (HVLC in Figs.3.3 and 3.4). According to Manenti et al. (2018), the DRP-MCR could be interpreted as a magmatic intrusive subhorizontal layer confined to the middle continental crust (laccolith or sill?). De Castro et al. (2018) have observed the MCR along L103 (Fig.3.7b) and have interpreted it as a deep intra-basement intrusive feature, dipping northeastward from 9 to 12.5km depth, characterized by a positive long-wavelength deep magnetic anomaly. They correlated this region to the DRP-MCR described by Daly et al. (2014) and Tozer et al. (2017) and interpreted these features as feeder zones for the magmatic rocks observed in the Parnaíba basin.

Here, due to the spatial distribution of the MCR after the new observations (Fig.3.7a), it is interpreted as a tectonic crustal discontinuity related to the limit between the Teresina and Grajaú domains, within the Barra do Corda transitional zone. As already proposed by Solon et al. (2018; “C” crustal conductor in Fig.3.3 and 4d) and Schiffer et al. (2021; Fig.3.4e), it possibly highlights the presence of a paleosuture zone in this area. In L103, we will test this hypothesis in a 2D gravity forward model (see item 3.2.9), connecting the MCR to a crustal scale thrust fault inserted in a Neoproterozoic thrust belt that separates both crustal domains. Nevertheless, the possibility of igneous intrusions allocated within the MCR crustal

discontinuity during the Mesozoic magmatic event that affected the Parnaíba basin is not discarded.

3.2.8 The shallow basement from well data and seismic interpretation

We present here the analysis of the shallow basement of the Parnaíba basin based on available wellbores and seismic reflection data. We define shallow basement as the geological sequences immediately beneath the Pre-Silurian Unconformity (PSU), which limits the base of the first sedimentary sequence of PB, the Serra Grande Group (Orodovician-Silurian). The PSU, named after Porto (2017), was first identified along the DRP by Daly et al. (2014) as a pronounced flat seismic horizon (yellow in Fig.3.7) that represents an erosional and angular unconformity crosscutting Early Paleozoic and Proterozoic basement units, possibly as a result of a peneplanation stage after the Neoproterozoic Brasiliano orogeny and before PB installation. Assis et al. (2019) have also recognized the PSU in field works along the NE margin of PB.

The map of Fig 3.8 shows the basement information available in 20 wellbores in the Parnaíba basin, of which only 7 have absolute age information, either published in the study of Cordani et al. (2008a) or mentioned in their own well reports. The detailed basement lithological description of these wells can be found in the Supplementary Material 2. The surface and subsurface geological units of Fig.3.8 are colored according to geochronological information and the symbols of the wells are classified by the basement lithological description: sedimentary/volcano sedimentary (circles), metamorphic (triangles) and metamorphic rocks with mylonitic texture (stars). We also present the location of the profiles L104, L007 (Fig.3.9) and L103 (Fig.3.10), as well as the limits and main related structures of the pre-Silurian basins observed in the seismic data. These basins will be here described in detail and they are named as the Ediacaran Riachão basin (light blue in Fig.3.8) and the Cambro-Ordovician Transbrasiliano pull-apart basins (TBPAB; light brown in Fig.3.8).

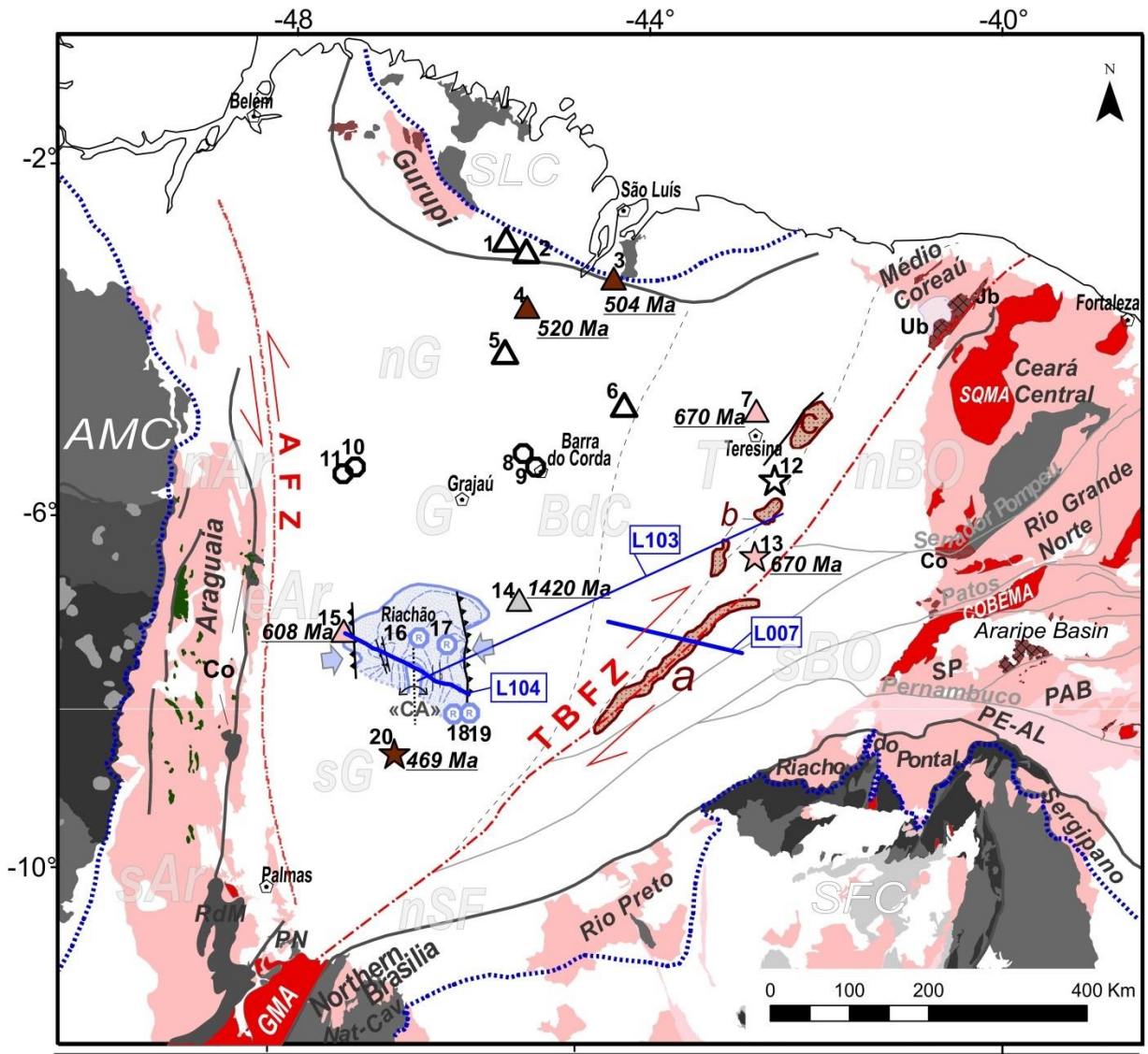

Legend

Cities — Seismic Lines

TBFZ: Transbrasiliano Fault Zone
AFZ: Araguaína Fault Zone

Suture zones — Craton limits

Borborema lineaments — Magnetic lineaments

Pre-Silurian surface geology

- Cambro-Ordovician Basins
  Jb- Jaibaras Group
- *Cambrian Igneous Units*
- Late Neoproterozoic Units
- Ediacaran Basins
  Ub - Ubajara Basin
- Early Neoproterozoic Units
- Neoproterozoic Granitoids
- Mafic/Ultramafic units (Ophiolite ?)
- Mesoproterozoic Units
- Paleoproterozoic Units
- Late Archean Units
- Early Archean Units

Pre-Silurian subsurface geology

Undifferentiated Pre-Silurian rocks :

8, 9, 10, 11 Clastic sedimentary/ volcano-sedimentary rock

1, 2, 5, 6 Metamorphic rock

12 Mylonitc Rock

Cambro-Ordovician units

Transbrasiliano Pull-Apart Basins (TBPAB)

20 *Mylonitic Syenite* 469 ± 11 Ma (K/Ar)

3 *Quartzite* 504 ± 15 Ma (K-Ar)

4 *Schist* 520 Ma (Rb-Sr)

Neoproterozoic units

Ediacaran Riachão Basin(RB)

16, 17, 18, 19 Riachão III sequence (clastic sedimentary rocks)

Thrust faults — «CA»: Central High — Tectonic transport direction

15 Diorite gneiss 608 ± 21 Ma (K-Ar)

7 Gneiss 670 Ma (Rb-Sr)

13 Cataclastic phillyte 670 Ma (Rb-Sr)

Mesoproterozoic (or older?) unit :

14 Quartz-mica schist 1420 Ma (Rb-Sr)

(PREVIOUS PAGE) Fig.3.8 Map showing the outcropping units and subsurface units beneath the Parnaíba basin and surrounding areas. The Phanerozoic covers, including the Parnaíba basin, are shown in white. The symbols represent the available wellbores with basement information (see Supplementary Material 2) and the contours of the pre-Silurian basins are derived from seismic studies. In blue the seismic lines presented in Figs.3.9 and 3.10. The outcropping Neoproterozoic magmatic arcs are: Santa Quitéria-Tamboril Magmatic arc (SQMA); Conceição and Betânia Magmatic arcs (COBEMA) and Goiás Magmatic Arc (GMA). "RdM" stands for Rio dos Mangues complex; "PN", for Porto Nacional and "Nat-Cav", for Natividade Cavalcante block, Paleoproterozoic units in southern Parnaíba basin. "Co" is the Archean Colmeia complex within the Araguaia belt. The subdomains of Northern and Southern Borborema are represented, "SP" is São Pedro; "PAB", Piancó-Alto Brígida, and "PE-AL", Pernambuco-Alagoas. In light gray, the abbreviations of the proposed tectonic domains of the paper in white color (AR, Araguaia; BdC, Barra do Corda; Bo, Borborema; G, Grajaú; SFC, São Francisco Craton; SLC, São Luis Craton; T, Teresina. Letters n and s in the labels stand for north and south, respectively.

In the map of Fig.3.8 the presence of Neoproterozoic terranes or Neoproterozoic reworked terranes, assigned to the Brasiliano mobile belts, outcropping around the PB (light pink) is remarkable. Adjacent to them, we can find in grey (Fig.3.8), the pre-Brasiliano basement cratons and inliers (Mesoproterozoic, Paleoproterozoic and Archean units), including the Amazonian (AMC), São Luís (SLC) and São Francisco (SFC) cratons. Along the TBFZ, in the northeastern and southeastern edges of PB, we can find in red (Fig.3.8), the Tamboril/Santa Quitéria (SQMA) and Goiás (GMA) magmatic arcs, respectively (e.g. Caixito et al., 2020). To the south of the E-W Patos Lineament, within the Borborema Province, there is the Conceição and Betânia magmatic arcs (COBEMA; e.g. Caixito et al., 2020), separating the Northern and Southern Borborema (including the Transversal Zone) subdomains. These Neoproterozoic magmatic arcs are indications of the subduction of oceanic realms followed by continental collision (e.g. Cordani et al., 2013a; Caxito et al., 2020). Neoproterozoic metamorphic and mylonitic rocks recovered from wells (7 and 13 wells in Fig.3.8) in the Teresina and TBFZ domains are strong indications that the Brasiliano orogeny also affected the eastern portion of the Parnaíba basin basement (Cordani et al., 2008a).

To the west, within the Araguaia belt, we represent in dark green (Fig.3.8) the mafic and ultramafic bodies, already interpreted as ophiolites (e.g. Paixão et al., 2008), suggestive for the presence of a suture zone to the west of PB, although no outcropping magmatic arc is described associated to these units. To the east of these bodies, there are minor Archean and Paleoproterozoic units, such as the Colmeia

complex (Co), the Rio dos Mangues (RdM) and Porto Nacional (PN) complexes, exposed in the western and southwestern edges of PB (Fig.3.8), respectively. These blocks can be interpreted as reworked portions of the Amazonian craton during the Neoproterozoic (e.g. Hodel et al., 2019; Assis et al., 2021), and, due to the geographic position, they possibly extend beneath the western portion of PB. The occurrence of a Neoproterozoic gneiss, reached by the well “15” (Figs. 3.8 and 3.9a), in the western margin of the Riachão basin, suggests the prolongation of Araguaia belt related units underlying PB (Cordani et al., 2008a), in this work named the eastern Araguaia belt domain (eAr).

Interestingly, within the central portion of the Grajaú domain, some sedimentary and volcano-sedimentary units were sampled under PB. We suggest that these rocks might correlate with the Riachão basin, although no basin was identified before along the deep regional seismic reflection profile (DRSP in Fig. 3.3; Daly et al., 2014), located in the vicinities of these wells. These rocks could also be related to the presence of small Early Paleozoic grabens in this region, or even to a much older sedimentary cover of Proterozoic age. In the northern portion of the Grajaú domain, getting closer to the limit with the Neoproterozoic Gurupi belt, low-grade metamorphic rocks are observed (1, 2, 3, 4 and 5 in Fig. 3.8), suggesting the prolongation of this belt in this region. According to Cordani et al. (2009a), the Cambro-Ordovician K-Ar dating of these rocks might indicate the age of the post-orogenic regional cooling. To the south, in the limit between Grajaú and Barra do Corda domains, one well (14 in Fig.3.8) recovered a Mesoproterozoic schist (Rb-Sr dating). Cordani et al. (2009a) have interpreted it either as a pre-Brasiliano cratonic inlier or a reworked pre-Brasiliano unit inside a mobile belt. Here we prefer the second option, indicating the reworked margin between the Grajaú and Barra do Corda domains, as further discussed in the next topic.

The interpretation of L104 and L007 seismic reflection profiles (see Table 3.1) are presented in Figures 9a and 9b, respectively. Above them we present also the non-interpreted versions of the seismic profiles, which were converted to depth, down to 7km. The details of the velocity model are available in Porto (2017, 2014). Both interpretations focused on showing the different signatures within the PB basement domains, and more importantly, the differences between both pre-Silurian basins systems already recognized beneath PB: the Ediacaran Riachão basin (RB), in L104 and the Cambro-Ordovician Transbrasiliano pull-apart basins (TBPAB), in L007. The

SW-NE 500km-long L103 profile, located in Fig.3.8, crosses both RB and TBPAB, and also the Mid-Crustal Reflectivity, representing a regional view of the central portion of PB basement, and it will be discussed together with the 2D forward model, in the next topic.

- *The Riachão basin (L104)*

The pre-Silurian Riachão basin (Fig.3.8 and 9a) was first described by Porto et al. (2018) as a remnant of a 120km wide N-S strike foreland basin beneath the SW portion of the Parnaíba Basin. It is composed of three seismoestratigraphic sequences (Riachão I, II and III) reaching approximately 4 km of maximum thickness, with thrusted margins of opposite vergencies and a central basement high (central arch “CA” in Fig.3.8) separating two depocenters. Miranda (2017) also interpreted the same dataset with similar results, with exception to the alternative interpretation of normal faults controlling the eastern depocenter (equivalent to Riachão III), during a later phase of extensional reactivation. Porto et al. (2018) tentatively dated RB sedimentation from Late Neoproterozoic (Ediacaran) to Early Paleozoic (Cambrian), correlating the basal Riachão I unit to the Ediacaran platform carbonates, also present in the Bambuí (São Francisco Basin, to the south of PB) and Ubajara (Ub in Fig.3.8, NE margin of PB) groups, due to its high amplitude and high frequency seismic character, internally composed of layered parallel events.

In L104 (Fig.3.9a), we can see the Riachão basin (in blue), extending laterally about 140km and with maximum ~4.5km depth, eroded on top by the flat Pre-Silurian Unconformity (in yellow), upon which lie the subhorizontal sequences of the Parnaíba basin. RB is divided into three sequences, as proposed by Porto et al. (2018): the basal Riachão I sequence (in blue), the Riachão II sequence (in pale pink) and the Riachão III sequence (in orange), the only one reached by well data (16, 17, 18 and 19 in Fig.3.8), composed of clastic sediments.

Underneath the western Riachão Basin, along 2/3 of the entire extension of L104 (Fig.3.9a), a remarkable highly reflective upper crust, characterized by short and curved westwards dipping events, indicates thrusted and folded metamorphic units of the pre-Riachão basement. This region is considered as part of the Eastern Araguaia subdomain (pink in Fig.3.9a). In the western tip of L104, the Carolina well (15 in Fig.3.8) reached Quartz-diorite gneiss of approx. 608 Ma (K-Ar) at 1170m depth,

according to Cordani et al. (2008a). This rock is interpreted as the Neoproterozoic Carolina gneiss (Fig.3.9a) and is thrusted upon the highly reflective upper crust. In this well, the basal formations of the Serra Grande Group (Ipu and Tianguá formations) are absent.

Some seismic events rooted in the highly reflective upper crust are interpreted as eastward verging thrust faults deforming the western margin of the Riachão basin. This is the case of a ramp anticline structure deforming the Riachão I sequence, also recognized in Porto et al. (2018) and Miranda (2017). Above it, the depocenter of the Riachão II sequence is located. This sequence thickens westwards and is thinning towards the eroded basement structural high, named as the “Central Arch”, represented by the gray arrows in L104 (Fig.3.9a). Here we interpreted on top some normal faults caused possibly by the gravitational collapse of the arch, filled up with sediments of the Riachão III sequence. This interpretation is similar to the one proposed by Miranda (2017). According to both aforementioned studies, the compressive phase of western RB is related to backthrusts of the Neoproterozoic Araguaia belt upon an undeformed block beneath the Parnaíba basin, to the east. This undeformed block is here considered to be part of the Southern Grajaú subdomain (grayish green in Fig.3.9a) and is characterized by a seismic transparent pattern.

Overlying the Southern Grajaú basement block, to the east of L104 (Fig.3.9a), we interpreted the eastern depocenter of the Riachão basin, where the Riachão III sequence reaches approximately 4km thick. Both Riachão I and III sequences, as well as the top of the pre-Riachão basement are dipping eastwards in this portion, bounded by west verging thrust faults. This structural interpretation for the eastern margin in RB is compatible with Porto et al. (2018), but differs of what Miranda (2017) has proposed, as these faults would be inverted normal faults. In both cases, the configuration of the eastern RB would involve a compressional phase, which, from our perspective, was caused by the collision between basement inliers within the Grajaú and Teresina domains, along the Barra do Corda transitional zone, here interpreted as a mobile belt. This structural context is more clearly explained by observing the L103 profile (Fig.3.10, next topic).

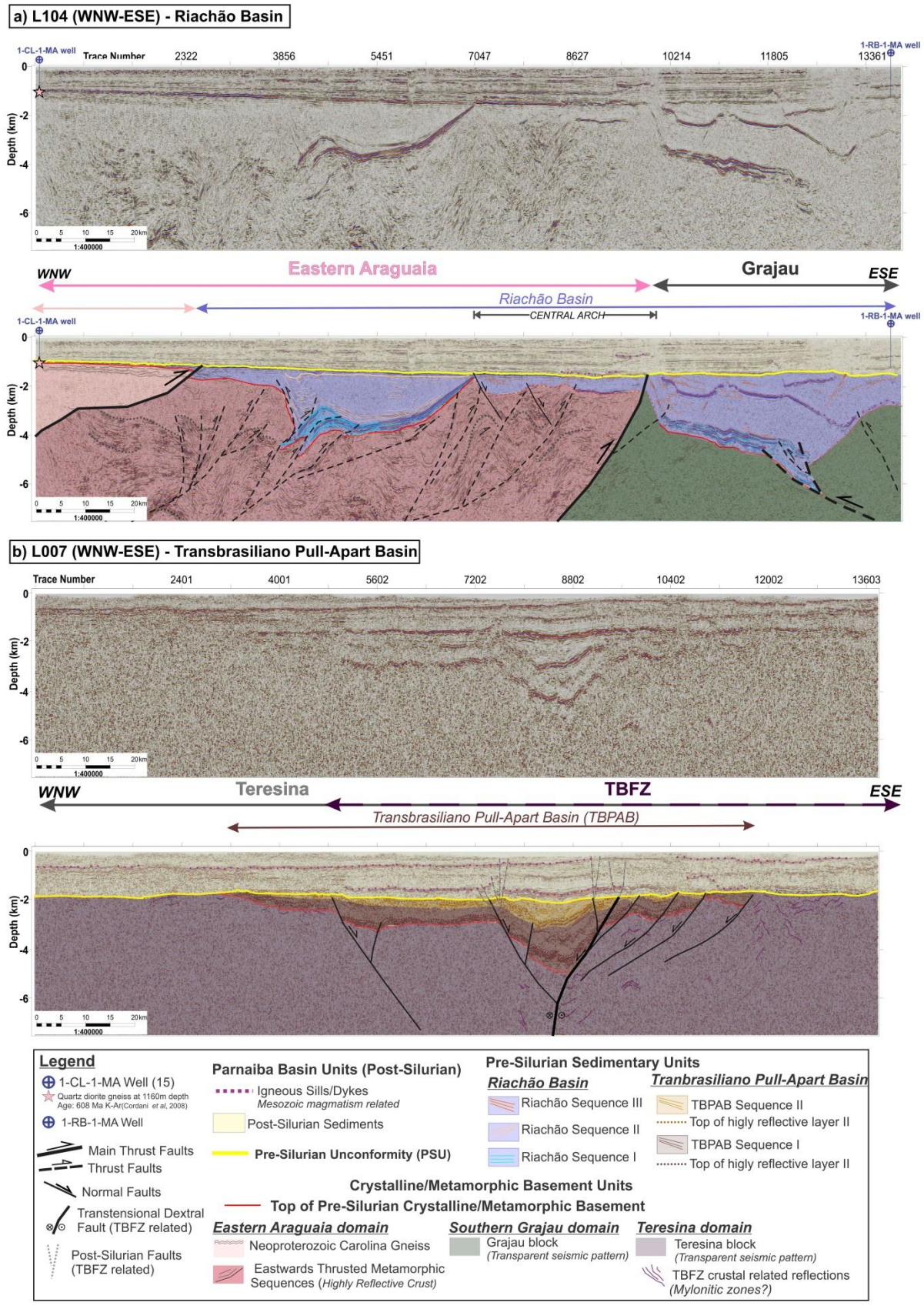

Fig.3.9 Seismic reflection lines converted to depth (above) with the equivalent geological interpretations in (a) L104 and (b) L007, highlighting the main pre-Silurian basins beneath the

Parnaíba Basin: Riachão and Transbrasiliano pull-apart basins, respectively, and the shallow basement units. Their locations are displayed in the map of Fig.3.8.

A remarkable characteristic of the eastern depocenter of the Riachão basin is the presence of saucer-shaped igneous sills intruding the Riachão III sequence (purple dotted line in Fig.3.9a). In some lines (e.g. Porto, 2017; Porto et al., 2018), these bodies cross the PSU and connects to shallower sills in PB, indicating a probable Mesozoic age for them. The presence of igneous sills in this region might be one of the causes for the transparent seismic pattern of the Grajaú block, due to seismic signal losses.

Finally, a simplified representation of the structural framework of RB is displayed in the map of Fig.3.8, based on the seismic mapping of Porto et al. (2018). It is possible to notice the N-S elongation of the Central Arch ("CA"), separating both western and eastern depocenters of the Riachão basin, bounded by N-S thrust faults of opposite polarity. According to the tectonic subdivision proposed here (Figs.3.8, 3.9a), each one of these depocenters lies upon different basement units, part of the Eastern Araguaia subdomain (eAr) and Southern Grajaú subdomain (sG), respectively. Here, we agree with the interpretation that the RB is a Late Neoproterozoic (Ediacaran) foreland basin and we believe that the basin extension beneath the western PB is much larger than it is represented in the available maps, once the seismic and wellbores dataset is limited in this area. It is also worth noting that RB was severely eroded before the PB installation, due to the presence of remarkable angular unconformities in the seismic data.

- *Transbrasiliano pull-apart basin (L007)*

The most updated stratigraphic chart of the Parnaíba basin (e.g. Vaz et al., 2007) describes a pre-Silurian (Cambro-Ordovician) sedimentary sequence filling up graben-like structures in the eastern PB, attributed to the Jaibaras Group (e.g. Oliveira & Mohriak, 2003). Later, many other authors identified such types of graben-like structures along the NE-SW Transbrasiliano Fault Zone, using 2D seismic reflection data (e.g. Morais Neto et al., 2013; Porto, 2014; Daly et al. 2014; De Castro et al., 2016; Abelha et al., 2018; Schuback, 2019). These studies agree that such basins were installed as a result of brittle dextral reactivations along the Neoproterozoic suture zones, during the Early Paleozoic. Morais Neto et al. (2013) recognized at least two phases of reactivations along the NE-SW TBFZ related faults:

first, a dextral transtensional one, causing the installation of the Cambro-Ordovician basin, and a later transpressional phase, inverting these structures and affecting also the post-Silurian sediments of the Parnaíba basin, possibly related to Mesozoic reactivations.

In L007 (Fig.3.9b), we have interpreted this graben-like structure with a maximum width of approximately 110km, composed of a narrow (~25km of width) and deep (~4.5km) central trough. The limits of this NE-SW-elongated trough and other graben-like structures are displayed in the map of Fig.3.8, based on the studies of Schuback (2019), Assis et al. (2019) and Daly et al. (2014), labeled as “a”, “b” and “c”, respectively. Together with the Jaibaras basin (Jb), in the NE margin of PB, this set of narrow NE-SW elongated grabens composes the here defined Transbrasiliano Pull-Apart Basins (TBAPB).

Similar to what Schuback (2019) proposed, here we have interpreted two Cambro-Ordovician seismic sequences filling up the pull-apart basin, called as the basal TBPAB sequence I (brown in Fig.3.9b) and above the TBPAB sequence II (light brown in Fig.3.9b). The limit between these two sequences is represented by high amplitude reflectors, which separate low amplitude seismic patterns, above and below it. Morais Neto et al. (2013), Porto (2014) and Abelha et al. (2018) interpreted these events as Mesozoic igneous sills, although here we believe that the thickness, frequency and amplitude characters of these events differ from the “peak-and-trough” typical signature of the sills in the basin.

Another remarkable high amplitude event is located at the base of TBPAB sequence I. Schuback (2019) interpreted it as a pre-rift sequence, since it does not show any thickening along the rift faults, while Morais Neto et al. (2013) interpreted the same layer as the top of the crystalline basement. Assis et al. (2019), analyzing the graben-like structures further north (such as the one in L103, Fig.3.10), suggested that these events could represent the carbonate sequences of the Late Neoproterozoic Ubajara Group (Ub, in Fig.3.8), correlated to the Riachão I sequence (Porto et al., 2018).

The interpretation presented here is analogous to what Oliveira & Mohriak, (2003) proposed for the Jaibaras basin, which seems to be the most reasonable one in terms of lithostratigraphic correlation, once there are not any available wellbore data penetrating the TBAPB in the Parnaíba basin so far. They proposed the

following tectonostratigraphic evolution: (1) Coreaú Dike Swarm intruding the Neoproterozoic Ubajara Group, prior to the first extensional tectonic pulse, which reactivated NE-SW shear zones and was responsible for the Mucambo pluton emplacement (2), followed by the deposition of the Massapê and Parapuí formations and associated Parapuí volcano-sedimentary rocks (here taken as coeval to the TBPAB sequence I). Then a second pulse (3) is responsible for the emplacement of the Meruoca pluton and by the deposition of the alluvial fans of the Aprazível Formation (here taken as coeval to the TBPAB sequence II) along the same discontinuities.

According to the tectonic compartmentation proposed here, the TBPAB lies upon the Transbrasiliano Fault Zone, at the limit between the Teresina and Borborema domains. In Fig.3.8, we display two wells close to the TBFZ that have reached metamorphic rocks with mylonitic texture (12 and 13 in Fig.3.8). One of these wells recovered a cataclastic phyllite beneath the basin sediments, at 2374m depth and yielded an absolute age of 670 +/- 21 Ma (K-Ar, Cordani et al., 2009). This information is an indication for the presence of a fault zone (TBFZ) in this region, possibly active prior to the installation of the Early Paleozoic TBPAB, reworking the margins of the Teresina domain, during the Neoproterozoic.

Comparing the RB and TBPAB pre-Silurian basins (Fig.3.9), many differences can be pointed out. Besides overlying different tectonic units of the basement (Fig.3.8), as proposed here, they differ in size, internal seismic character, overall external geometry, structural configuration and possibly in age, too. Also, the Pre-Silurian unconformity (PSU in Fig.3.9) is represented as a much more pronounced angular erosional unconformity in the Riachão basin region than in the TBPAB basins. In fact, according to Assis et al. (2019), there is a thickening of the basal Ordovician-Silurian Ipu Formation (Serra Grande Group of the Parnaíba basin) upon these grabens (“b” in Fig.3.8). This is also suggested in the seismic interpretation of Abelha et al. (2018). Assis et al. (2019) indicate that the first sequences of the Serra Grande Group filled up paleodepressions caused by transtensional reactivations along the TBFZ. The isopach maps of Early Paleozoic sequences of PB (Tozer, 2017; Daly et al., 2019) reinforce this observation, showing thickening upon the northeastern Teresina domain and TBFZ, while to the west, close to the Riachão basin, these sequences are thinner or even absent, as confirmed in the Carolina well (15 in Fig.3.8).

3.2.9 2D Forward Model

The SW-NE 500km-long seismic reflection profile of L103 (Fig.3.10d) crosses both Riachão and Transbrasiliano Pull-Apart pre-Silurian basins, as well as the Mid-Crustal Reflectivity (Fig.3.7), representing a regional view of the central portion of the Parnaíba basin shallow basement. Along L103, there is also a land gravity survey (see Table 3.1), presented in the Bouguer anomaly profile (blue line) in Fig.3.10c. We also sampled the Moho relief profile (Fig.3.10a), based on the seismological information map of Fig.3.5, using the control points of the gravity stations along L103. This way, we were able to perform an integrated 2D gravity forward model (sketch of Fig 10c), down to the base of the crust and up to the shallow basement, including supracrustal units.

The first step of L103 forward modelling was the fit between crustal thicknesses, derived from the seismology compilation, and the complete Bouguer observed anomaly. We started with a very simple model of uniform continental crust (2.67 g/cm3) and lithospheric mantle (3.15 g/cm3), using the sampled Moho relief (Fig.3.10a) as a boundary between both. The calculated gravity anomaly of the Moho is displayed in Fig.3.10b as the black curve; the observed complete Bouguer data is displayed in dotted blue line. The blue curve (Fig.3.10b) is the 3rd polynomial fit of the complete Bouguer data, calculated using least-squares fitting for the 3rd order trend of the input data, and that is an approximation for the regional response of the gravity data, caused by deep sources such as the crust-mantle contrast (e.g. Beltrão et al., 1991). It is possible to notice a reasonable fit between the 3rd polynomial fit and the calculated Moho anomaly, following the same trend of low gravity anomaly/deep crust to the west in contrast to high gravity anomaly/shallower crust to NE. However, when compared to the complete Bouguer observed anomaly, the error of the fit is much larger (RMS error=21.5 mGal), possibly due to density contrasts within the continental crust, caused by geological heterogeneities.

The second step was to adjust the seismic interpretation along L103 (Fig.3.10d) to the full interpretative crustal model in order to achieve the best fit with the observed Bouguer gravity profile. The seismic line is displayed in two-way travel time domain, down to 7s. A raw and non-interpreted version of L103 is presented above a full geoseismic interpreted version, with the respective tectonic domains assigned above by the colored arrows. Using approximations of the depth conversion

velocity model of Porto (2017) for the SW half of L103, we have fit the seismic interpretation down to 14km. The density values of the supracrustal sedimentary units were the same used in Porto et al. (2018) for the 2D forward model of the Riachão basin. For the crystalline and metamorphic basement units, we compiled the density values used in the forward models of De Castro et al. (2014), along the profile A-A' in Figs.3.3 and 3.4b, and of Tozer et al. (2017), along the DRP (Fig.3.4c), calculating average values of both in some cases. The density of the MCR was taken from this second study. For the deeper portions of the crust (>14km), we have used values that increase with depth, from 2.82-2.84 g/cm3 in the deep upper crust to 3.0 g/cm3 at the base of the lower crust. The full discrimination of the density values is available in Table 3.2, with the respective identification codes of the geological units of Fig.3.10c. This table also presents the regional tectonic interpretation of these units assigned to the western Gondwana paleocontinent, discussed later in item 3.2.10.

We have achieved a satisfactory fit (RMS error = 2.1 mGal) between the final model and the observed Bouguer anomaly, even though we have considered constant density values for the Upper Lithospheric Mantle and for the shallow sequences of the Parnaíba basin, not taking into account, for instance, the shallow diabase sills. We describe bellow each crustal domain of the basement of the Parnaíba basin, interpreted along L103 (Fig. 3.10 and Table 3.2), and supported by the previous results (Figs. 3.3, 3.5, 3.6, 3.8 and 3.9).

- *Eastern Araguaia belt subdomain (eAr):* Only a small part of this domain is observed in the SW tip of L103 (Fig.3.10d), which is better displayed in L104 (Fig. 3.9a), characterized by a highly reflective crust in the seismic data. The eAr is assigned to the Araguaia belt domain, and is here related to the eastwards verging thrusts that deform the western border of the Riachão basin, upon the Grajaú block (Fig.3.9b). At the SW tip of L103, the Moho is found at ~ 43km; nevertheless, it is worth noting that thin crust is found westward within the "eAr" domain (see Fig.3.5). To better fit the Bouguer anomaly variation of approximately -70 to -60 mGal, we have interpreted two metasedimentary units (8 and 7 in Fig.3.10c and Table 3.2), juxtaposed by high angle reverse faults, dipping to southwest.

Western Gondwana Crustal Building Blocks	Crustal Domains	Geological Unit	L103 2D Gravity Model (Fig.3.10) Density Code	(kg/m3)
Phanerozoic Covers	Parnaíba Basin	Mesozoic Diabase Sills (Mosquito or Sardinha Fms.)	22	2900
		Phanerozoic Sedimentary Sequences	21	2450
	Transbrasiliano Pull Apart Basins	Cambro-Ordovician volcano-sedimentary sequences (e.g .Jaibaras Group)	19	2510
Amazonian-West African Block (AWB)	Riachão Basin (Ediacaran Foreland Basin)	Riachão III Sequence (Clastic sediments)	18a	2510
		Riachão I Sequence (Carbonate Plattform)	18b	2710
	Grajaú Block (pre-Brasiliano inlier)	Undifferentiated metamorphic basement (transparent seismic character)	9	2790
	Eastern Araguaia belt subdomain (Eastward backthrusted units)	Metasedimentary Unit I (Highly Reflective Upper Crust)	7	2780
		Metasedimentary Unit II (Highly Reflective Upper Crust)	8	2810
	Deep Upper Crust (Araguaia Belt/Grajaú Domains)		4	2820
	Barra do Corda belt (Westwards thrusted Supracrustal units/ External Zone)	Undifferentiated Metasedimentary Cover	15	2740
		Metamorphic Rocks I (Low grade?)	10	2760
		Metamorphic Rocks II (Medium to Low grade?)	11	2805
		Syn-collisional Granitoids I	14a	2740
	Barra do Corda belt (Internal zone)	Metamorphic Rock III (High grade?)	12	2780
		Metamorphic Rock IV (High grade?)	13	2810
		Syn-collisional Granitoids II	14b	2765
Central Africa Block (CAB)	Mid-Crustal Reflectivity (Dettachment fault,suture zone?)		20	2985
	Deep Upper Crust (Barra do Corda belt basement)		5	2830
	Teresina Block (pre-Brasiliano inlier)	Archean/Paleproterozoic reworked rocks (?)	16	2820
	Transbrasiliano Fault Zone (TBFZ)	Metamorphic Rock VI (Mylonite?)	17	2790
	Deep Upper Crust (Teresina domain)		6	2840
	Middle Crust		3	2850
	Lower Crust		2	3000
	Mantle		1	3150

Table 3.2 Tectonic domains, geological units and density values used in the 2D model of Fig.3.10.

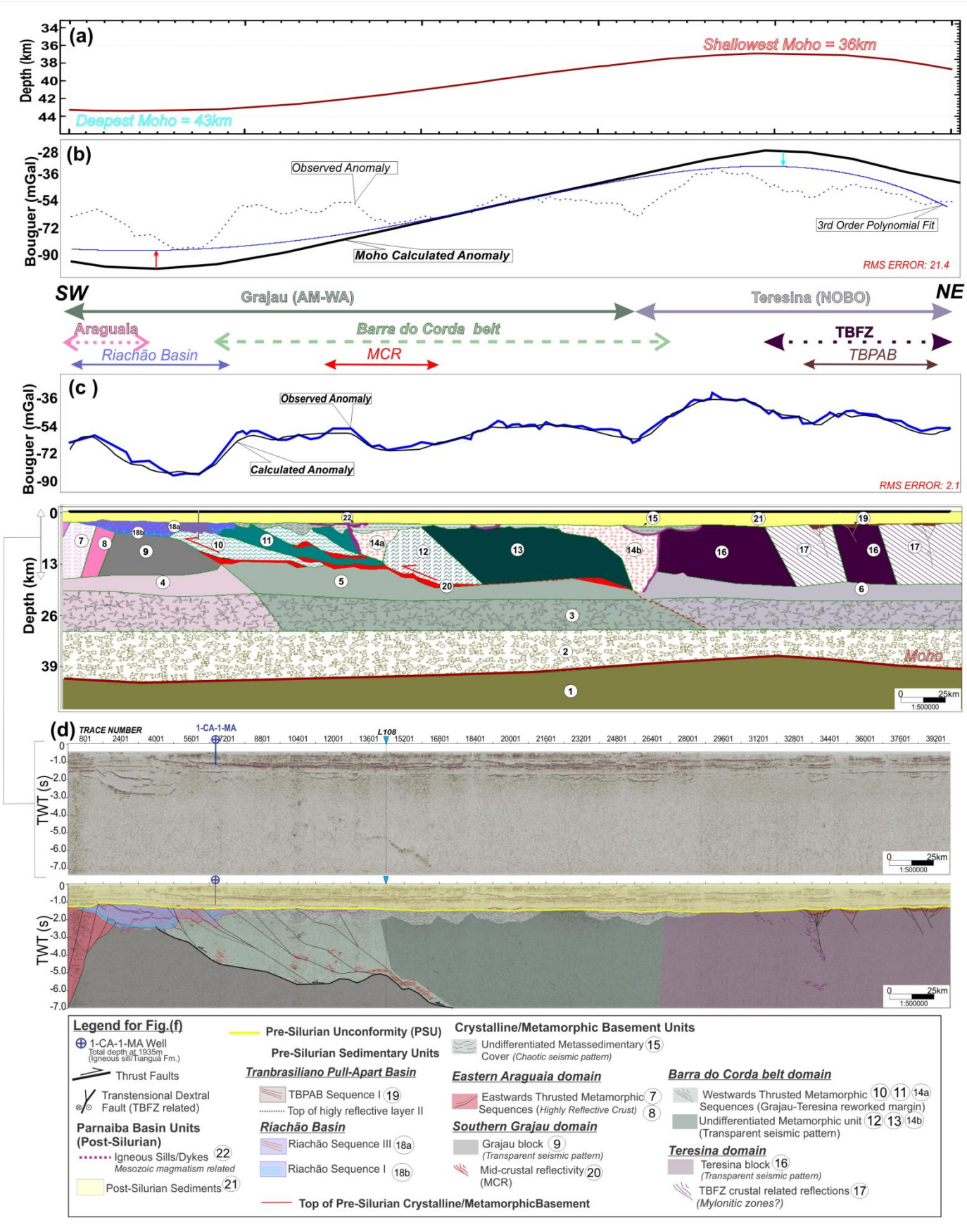

Fig.3.10 (a) Moho depth along L103, sampled from the map of Fig.3.5; (b) Forward model of the continental crust-mantle boundary in relation to the Bouguer gravity anomaly (land survey) and the 3rd polynomial filter; (c) the full forward model of L103 in relation to the Bouguer gravity anomaly. The shallow crust (down to 14km) is based on the geological interpretation of the seismic reflection data of L103, displayed in TWTT in (d), raw (above) and interpreted (below) versions.

- *Grajaú block in the Southern Grajaú subdomain (sG):* It is characterized by a transparent seismic pattern (see L104, Fig.3.9; and L103, Fig.3.10) and a Bouguer gravity low (Fig.3.10c), which is represented by a step of -20 to -25 mGal in relation to the adjacent tectonic units. Certainly, this low anomaly is also also due to the sedimentary deposits of the Riachão basin (approximately 3km thick) located upon it and the thick crustal values from the seismology (~43km). We have interpreted this block as an undifferentiated pre-Brasiliano basement inlier (9 in Fig.3.10c and Table 3.2).

- *Riachão basin (RB):* Differently from L104 (Fig.3.9a and 9c), where it is possible to see the two depocenters of RB, each side of the N-S central arch, including the three Riachão sequences, in L103 we have only Riachão I and III sequences, representing the eastern depocenter of the basin (18a and 18b, respectively in Fig.3.10c and Table 3.2). Within Riachão III sequence, it is possible to notice the igneous sills crossing the Pre-Silurian Unconformity (PSU), here interpreted as Mesozoic diabase sills (22 in Fig.3.10c and Table 3.2). To the east, the seismic events of the Riachao I and III sequences disappear, turning into a chaotic seismic pattern, which we interpreted, likewise Porto et al. (2018), as the deformed eastern margin of RB, affected by the westward verging thrust faults of the Barra do Corda belt. This region coincides with the lowest Bouguer anomaly value of L103.

- *Barra do Corda belt (BdC):* In the seismic data (Fig.3.10d), the eastern margin of the Riachão basin, between traces 5601 and 12001, is marked by a chaotic seismic pattern with sparse short events of moderate to high amplitude, that seem to connect with the Mid-Crustal Reflectivity (MCR, Fig.3.6), between traces 12001 and 16801. Here, we proposed a series of subhorizontal westverging thrust faults forming a nappe style tectonic regime, alternating low grade with medium grade metamorphic overthrusted units (10 and 11 in Fig.3.10c and Table 3.2) and occupying approximately 100km of lateral extent along L103. In this context, the MCR would be related to a detachment fault down to the upper/lower crust boundary, along which possibly igneous intrusions or hydrothermal fluids have penetrated, causing the high acoustic impedance character observed in the seismic line and interpreted as a high

density value in the forward model (20 in Fig.3.10c and Table 3.2). The Bouguer anomaly of this region is represented by high to moderate values and a residual undulated anomaly (Fig 10c). Here we interpret this region as the external zone of BdC mobile belt, upon the eastern portion of the Grajaú block. To the east, this pattern of the Bouguer profile is interrupted by a low gravity anomaly, here interpreted as a syn-orogenic granitic intrusion (14a in Fig.3.10c and Table 3.2). Adjacent to it, the gravity values increase, and we interpreted two units of high-grade metamorphic rocks (12 and 13), with transparent seismic character, representing a possible internal zone of the BdC belt. Finally, a narrow trough in the Bouguer profile (-65mGal) is observed close to traces 24801-26801 in Fig10d, followed by a great positive increase. We interpreted this trough as a sin-orogenic granite (14b), marking the transition to the Teresina block.

- *Teresina block in the Teresina domain (T):* As well as the internal zone of the Barra do Corda belt, the Teresina block is represented by a transparent seismic pattern in Fig.3.10d.Therefore, we have interpreted it mainly based on the Bouguer anomaly profile (Fig10c) and the compilation of the other geophysical datasets already discussed here, such as the seismological Moho depth, that reaches 36km in Fig.3.10a and the distinctive magnetic anomaly (Fig.3.6b and 6d). Regarding the gravity anomaly, this region is characterized by the highest values (>-35mGal) of L103, leading to the interpretation of a dense crustal unit, here taken as Archean/Paleoproterozoic reworked rocks (16 in Fig10 and Table 3.2), representing a pre-Brasiliano basement inlier.

- *TBFZ and TBAPB:* As testified by well data (12 and 13 in Fig.3.8), to the north and to the south of L103, Neoproterozoic (?) mylonitic rocks occur along the NE portion of the dextral Transbrasiliano Fault zone. Therefore, we have considered such units in the final model of (17 in Fig.3.10c and Table 3.2), with a slightly lower density than the adjacent units of the Teresina block. In the seismic basement, very subtle vertically aligned short events of moderate amplitude might correlate to this fault zone. In the shallow basement, we have interpreted the Early Ordovician pull-apart basins (19), constrained by basement faults and equivalent to the TBPAB sequence I, better detailed in L007(Fig.3.9b). The locations of these basins are displayed in Fig.3.9c. as

proposed by Assis et al. (2019).

- *The "unknown" Undifferentiated Metasedimentary Cover:* In the central portion of L103, the shallow basement, right beneath the PSU, down to 2.5s, presents a moderate penetrative reflectivity of short and curved events, resembling deformed low grade foliated metamorphic rocks. This was also observed in the other lines of figure 3.7 and we have called it as the Undifferentiated Metasedimentary Cover (15 in Fig.3.10c and Table 3.2). Fifty-kilometers apart L103, Porto et al. (2018) described the same pattern and associated it to the schist recovered by the 1-MS-1-MA well, dated by Rb-Sr of Mesoproterozoic age (14 in Fig.3.8, Cordani et al., 2008a). Another possible explanation for such anomalies is related to sparse grabens of Early Paleozoic age present in a larger area beneath the Parnaíba basin, some of them perhaps reactivating shear zones within the Barra do Corda belt, as already suggested in the potential field data analysis of De Castro et al. (2014). It is also important to consider that these patterns could be seismic artifacts caused by the absorption of the seismic signal or even by internal multiples, due to the presence of great volumes of high impedance igneous rocks in the Parnaíba basin or even within the metamorphic shallow basement, such as some bodies interpreted along L103 (22 in Fig.3.10c).

3.2.10 Discussions

The new Paleotectonic map of the Parnaíba basin basement

Several orogenic belts, smaller reworked terranes and shear zones are found in the surrounding margins of the Parnaíba basin. They were developed during the Brasiliano orogeny as the result of the subduction and closure of a major oceanic domain, the Goiás-Pharusian Ocean, followed by the development of several accretionary and collisional processes (Cordani et al., 2013a; Caxito et al., 2020). In this context, the hidden basement beneath the Parnaíba basin remains a fundamental piece to unravel the Neoproterozoic puzzle in the NE of Brazil. Is there a stable cratonic nucleus beneath the Parnaíba basin, the so-called Parnaíba block (Fig.3.2; Daly et al, 2014 and 2018)? Or is the configuration of the Parnaíba basement much more related to a continental collisional tectonic setting?

The first paleoreconstructions, mostly on the basis of rocks sampled by wells and gravity studies, suggested that the hidden basement beneath the Parnaíba basin comprises Pre-Brasiliano massifs composed of medium to high-grade metamorphic rocks of Early Paleoproterozoic age – possibly produced by a major paleocontinent break-up at ca. 900Ma, while the intervenient belts possibly resulted from the later Brasiliano orogeny (Cordani et al., 2008b). Weakness zones, associated to the N-S and NE-SW structural trends of the Araguaia-Rokelides suture and to the Transbrasiliano lineament, respectively, have been recognized as been fundamental structures during the long lived Brasiliano orogeny (Cordani et al., 2013a, 2013b; Brito Neves et al., 2014; Ganade de Araujo et al., 2014; Caxito et al., 2020 and 2021). Recent geophysical studies greatly improved the individualization of crustal blocks under PB, mainly along the Deep Regional Profile (Figs. 3.3 and 3.4; Daly et al., 2018; Soares et al., 2018; Solon et al., 2018; Coelho et al., 2018; De Lima et al.; 2019; Araujo, 2019; Schiffer et al., 2021). On the other hand, these studies usually have not focused on the causative processes justifying the juxtaposition of geophysical distinct blocks in the central portion of the PB.

Building up on these studies, on recent models of western Gondwana amalgamation (Caxito et al., 2020 and 2021) and on the analysis of the data we produced and reported in the previous topics, we came up with the Paleotectonic map of the Pre-Silurian basement of the Parnaíba basin and surrounding areas (Fig.3.11) and with a sketch for its Neoproterozoic evolution (Fig.3.12).

According to our interpretation, the Precambrian basement units of the Parnaíba basin, here assigned to crustal domains, explained in the previous topics, are divided into two larger crustal building blocks involved in western Gondwana amalgamation: the Amazonian-West Africa and the Central African blocks (Fig.1), following the studies of Cordani et al. (2013a). They are listed below, as well as represented in the legend of Fig.3.11a and in Table 3.2.

- **Amazonian-West Africa block (AWB)**, including the Amazonian and São Luis-West Africa cratons and minor pre-Brasiliano inliers, such as the hidden Grajaú block, as well as the associated Neoproterozoic Gurupi and Araguaia belts.
- **Central African block (CAB)**, including the Northern Borborema Province (nBo), composed of the hidden Teresina domain and the

outcropping Médio Coreaú, Ceará Central and Rio Grande do Norte domains; the Barra do Corda belt, interpreted as a Brasiliano belt along the Transbrasiliano-Kandi corridor (e.g. Cordani et al., 2013); to SE, the Southern Borborema Province (sBo), composed of the São Pedro, Piancó-Alto Brígida, Alto Pajeú and Pernambuco-Alagoas domains (Caixito et al., 2020) and finally, to the south, the Northern São Francisco margin (nSF), including the Natividade-Cavalcante and Cristalândia blocks, and associated Northern Brasília, Rio Preto and Riacho do Pontal belts.

In Fig.3.11a, besides the crustal domains and subdomains of the Proterozoic basement (Paleoproterozoic or even older), we also represent the Pre-Silurian basins, as well as the Neoproterozoic magmatic arcs. The tectonic lineaments were mainly interpreted from the gravity and magnetic maps of Fig.3.6 and they are consistent with the right-lateral kinematics along the Transbrasiliano Fault zone, also represented as a mylonitic zone in the map. In Figure 3.11b, the main features extracted from the geophysical interpretations are superimposed to the final tectonic map, as well as the location of the main profiles and wellbores. Superimposed to this map, we have also overlaid the depocenters (700m thick contour line) of the Serra Grande Group (orange in Fig.3.11b), which is the basal group of the Parnaíba basin, deposited between Late Ordovician to Lower Devonian, and of the Balsas Group (green in Fig.3.11b), representing the Upper Carboniferous to Triassic sequences of the Parnaíba basin (Daly et al., 2019).

Approximately 70% of the current surface exposures of Phanerozoic Parnaíba basin sedimentary rocks cover two basement tectonic units, the Grajaú block, part of the Amazonian-West African domain (AM-WA), and the Teresina block, part of the Northern Borborema domain (nBO). The differentiation of these blocks within the Parnaíba basement was previously proposed by Cordani et al. (2008b; purple in Fig.3.2), who named them respectively as Parnaíba and Granja basement inliers, this second one associated to the southern prolongation of the Paleoproterozoic basement of the Médio Coreaú domain. This proposal was then improved with the advances of geophysical data acquisition in the basin. De Castro et al. (2014), analyzing magnetic and gravimetric anomalies, suggested a similar division, naming them as the Parnaíba and Teresina domains (blue in Fig.3.2). Soares et al. (2018),

using seismic refraction data along the DRP, observed high velocity anomalies within the lower crust/upper mantle of the Grajaú block (HVLC in Figs. 3 and 4) and a flat and shallower Moho beneath the Teresina block. Solon et al. (2018), based on broadband magnetotelluric data along DRP, also observed a very resistive crust to the west of Barra do Corda city in contrast to a conductive crust to the east, naming them as the Western and Central blocks, respectively.

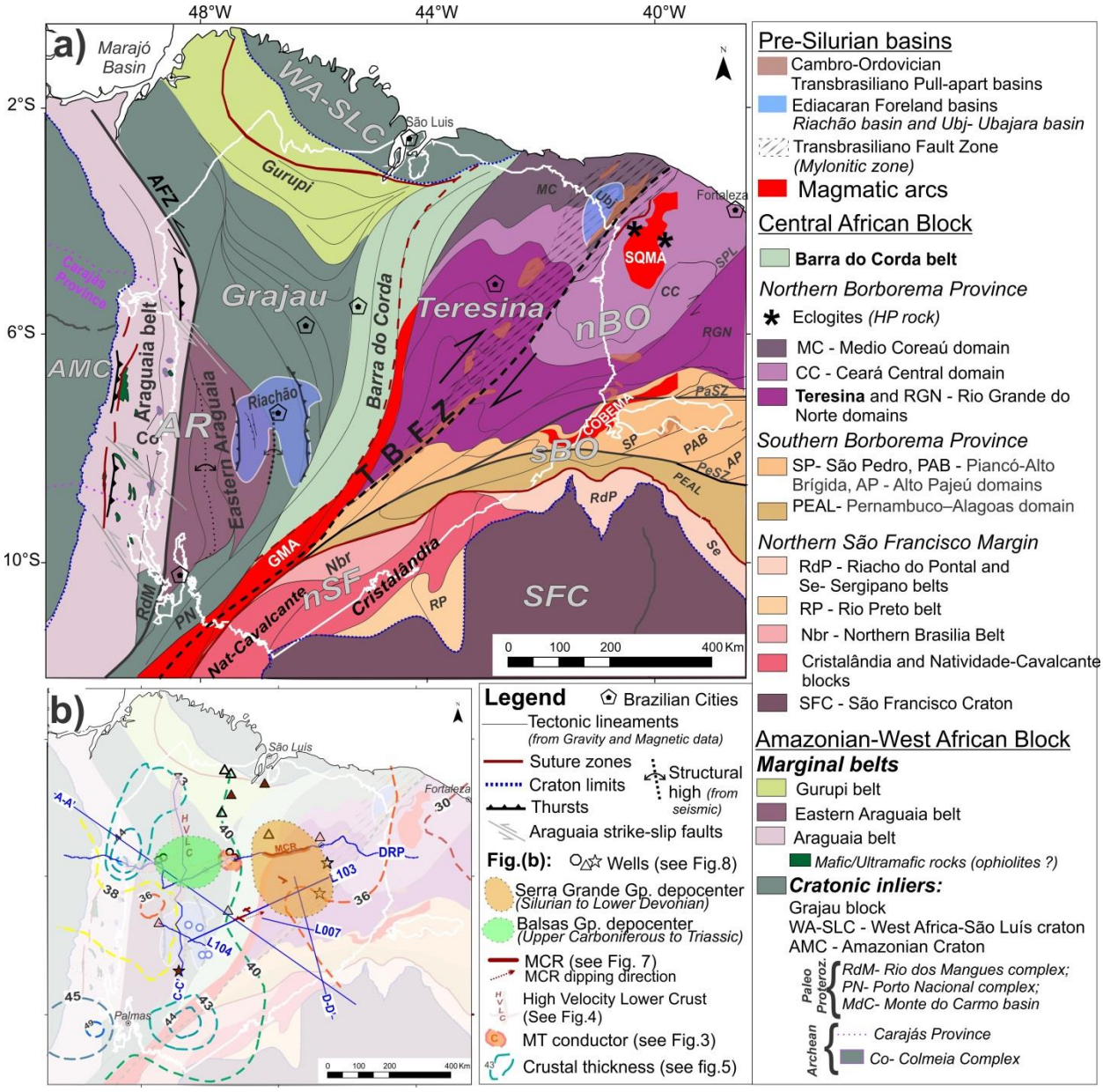

Fig.3.11 (a) Paleotectonic map of the Pre-Silurian basement of the Parnaíba basin; (b) Support map with the main features observed in the data compilation here presented, as well as the locations of the depocenter (700m thick contour line according to Daly et al., 2018) of the Serra Grande and Balsas groups, Early Paleozoic and Late Paleozoic/Early Mesozoic lithostratigraphic groups of the Parnaíba basin.

The lateral limit between these two distinctive geophysical units is here interpreted as the Barra do Corda transitional domain. The main arguments for the individualization of this domain are: (1) high Vp/Vs ratios and subtle eastward dipping anomalies within the crust between the Teresina and Grajaú domains, observed by Schiffer et al. (2021) along DRP (Fig.3.4e); (2) the presence of a crustal-scale subvertical conductor ("C" in Fig.3.3 and 3.4d) under Barra do Corda, observed by Solon et al. (2018); (3) the linear positive and negative anomalies of the residual Bouguer map (Fig.3.6c), also observed by De Castro et al. (2014); (4) the presence of the northeastwards dipping mid-crustal reflectivities observed in Fig.3.7; (6) the westwards thrusted margin of the eastern Riachão basin, proposed by Porto et al.(2018) and also here interpreted in Figs. 3.9a and 3.10d. These features, as also pointed out by some of the cited authors, correlate to deep crustal discontinuities, indicating the presence of suture zones, here interpreted as part of a Neoproterozoic mobile belt in the central Parnaíba basin basement.

This idea was tested in the model of Fig.3.10, where we interpret the external zone of metasedimentary overthrusted terranes upon the southern Grajaú block and high- grade (higher density) metamorphic rocks composing the internal zone, in the nearby Teresina block, indicating a typical reverse-metamorphic zoning observed in thrust-fold belts. We called it as the Barra do Corda belt. In the paleotectonic map (Fig.3.12a), BdC belt is represented with a sigmoidal N-S elongated shape, possibly connecting to the NE-SW Médio Coreaú domain, with related metavolcanosedimentary belts (Martinópole Group) in the NE of the Parnaíba basin and truncated by the NE-SW Transbrasiliano Lineament to the south. We also tentatively prolong the Goiás Magmatic Arc beneath central PB, observed in L103 as a low gravity anomaly, modelled as a granitic intrusion (14b in Fig.3.10c).

To the SE, we have interpreted the prolongation of the Southern Borborema Domain (sBo), integrated by Caxito et al. (2020) in the APAMCAP(AY) domain, translated as the abbreviations of Alto Pajeú-Alto Moxotó-Rio Capibaribe-Pernambuco-Alagoas-(Adamawa-Yadé) terranes (Fig.3.12). This domain is bounded by the E-W Patos and Pernambuco dextral shear zones, which according to the magnetic lineaments here observed and also noticed in De Castro et al. (2014), bend NE-SW towards the PB interior, connecting to the Transbrasiliano Fault Zone. In the MT profile of Fig.3.4g, Rocha et al. (2019) interpreted these shear zones as vertical crustal-scale conductive features (Fig.3.7d), indicating the prolongation of the

Southern Borborema structures beneath PB. In the southern part of the profile, a major suture zone is interpreted separating the “sBo” and the basement units of the Northern São Francisco margin domain (“nSF” in Fig.3.11). The “nSF” is represented by the Natividade-Cavalcante and Cristalândia blocks (Fuck et al. 2017; Caxito et al. 2020; Barros et al., 2020) and the adjacent Neoproterozoic belts (Northern Brasília, Rio Preto and Riacho do Pontal), with remarkable NE-SW oriented magnetic and gravimetric signatures, as discussed in Fig.3.6.

The northern and the western portions of the Grajaú block are characterized by WNW-ESE and N-S lineaments, representing the reworked margins parallel to the Gurupi and Araguaia belts, respectively. To the NW, where the Marajó basin (Mesozoic and Cenozoic cover) is located, due to the lack of geophysical data and some indications of thick crust (Fig.3.5), we have interpreted the NW prolongation of the Grajaú block, separating both Gurupi and Araguaia belts. This was also proposed by Daly et al. (2014; green in Fig.3.2) and suggests a possible connection of this block with the northern portion of the Amazonian craton.

We propose the differentiation of the Eastern Araguaia belt subdomain due to its distinctive thin lithosphere and thin crust (Figs.4d and 5) and to the presence of a highly reflective upper crust, with indications of eastwards verging thrust faults in the western margin of the Riachão basin (Figs. 8 and 9a; Porto et al., 2018; Miranda, 2017). The opposite tectonic transport is observed to the west, where the western portion of the Araguaia belt crops out, and to the north, along the DRP, in the deep seismic interpretation of Daly et al. (2014; Fig.3.4d). It is worth pointing out that the same pattern of thinned crust within the “eAr” was observed westwards by Albuquerque et al. (2017) beneath the adjacent Carajás Province (Archean), which is part of the Amazonian Craton. More studies are required in order to investigate the tectonic significance of this coincidence.

To the SW of PB, Cordani et al. (2008b) interpreted the Monte Alegre de Goiás-Conceição do Tocantins massif (MAC in Fig.3.2), referring to the prolongation of the Early Paleoproterozic medium- to high-grade metamorphic rocks exposed in the southern margin of PB, to the west of the TBFZ and Goiás Magmatic Arc. The increasing geochronological knowledge in this area (Gorayeb et al., 2013; Arcanjo et al., 2013; Assis et al. 2021) allowed here the subdivision of such units into Rio dos Mangues Complex (“RdM” in Figs. 8 and 11a), to the west, and the slightly older

Porto Nacional high-grade terrain (PN in Figs.8 and 11a), to the east. According to Assis et al. (2021), both units could constitute part of the Amazonian Craton since the Rhyacian, forming distinct crustal blocks during the Neoproterozoic, composing part of the Araguaia and Northern Brasília belts basement units.

Finally, the NE-SW Transbrasiliano Fault Zone, that crosses 1100km of the eastern PB, is here interpreted as a relevant tectonic feature, documented along the different analyzed geophysical datasets as a crustal-scale discontinuity or, more precisely, a zone of crustal-scale discontinuities. These observations agree with the proposal previously discussed here of the Transbrasiliano-Kandi tectonic corridor, along which shear zones and suture zones were formed during the Neoproterozoic Brasiliano Orogeny in western Gondwana (Cordani et al., 2013a, 2013b; Brito Neves et al., 2014; Caxito et al., 2020, 2021; Ganade de Araujo et al., 2014). One evidence for this interpretation is the presence of HP-UHP rocks in the Northern Borborema domain (Ganade de Araujo et al., 2014), such as the Forquilha eclogite (Fig.3.11a), in the limit between the Médio Coreaú and the Ceará Central domains. Added to this, the presence of mylonitic rocks of possibly Late Neoproterozoic age in the basement, recovered from wellbores (Fig.3.8, Cordani et al., 2008a) reinforces the interpretation of late-stage dextral strike-slip and transpressional deformation in this region, justifying the northeastwards offset of the Teresina block in relation to the Ceará Central and Rio Grande do Norte domains, interpreted in the map of Fig.3.11a.

Post-orogenic brittle strike-slip reactivations within the TBFZ are also recognized (Brito Neves et al., 1984; Cordani et al, 2008a), exposed in the Cambro-Ordovician Jaibaras trough (Oliveira and Mohriak, 2003), and interpreted in the subsurface as narrow elongated grabens (Fig.3.9b, Morais-Neto et al., 2013; Daly et al., 2014; Assis et al., 2019; Schuback, 2019), forming an Early Paleozoic system of pull-apart basins along the Transbrasiliano (TBPAB, Fig.3.11a). Ediacaran-Early Paleozoic sequences are also observed in the vicinities of the Parnaíba basin, confined along other Brasiliano shear-zones: such as the Cococi-Rio Jucá and Catolé-São Julião groups (Machado, 2006), along the E-W Borborema shear zones, and the Piriá Formation, within the NW-SE Gurupi belt, interpreted as a post-orogenic rift by Klein et al. (2017). These observations raise the possibility of the presence of other Early Paleozoic graben-like structures beneath the Parnaíba basin, as a result of post-orogenic relaxation and transtensional reactivations along Neoproterozoic shear zones (such as the ones within the proposed Barra do Corda

belt.) In this context, the shallow chaotic pattern observed in the central Parnaíba basin, here interpreted as the “Undifferentiated Metasedimentary cover” (15 in Fig.3.10), could represent this type of post-orogenic sedimentation.

Regarding to the implications of the basement configuration for the tectono-sedimentary evolution of the Phanerozoic Parnaíba basin, it is interesting to note in Fig.3.11b the migration of the depocenters from the Early Paleozoic to the Early Mesozoic in relation to the position of the tectonic domains proposed here. According to the isopach maps based on well data published by Daly et al. (2019), the 700m thick contour line of the Serra Grande Group (Silurian to Early Devonian; orange in Fig.3.11b) is located upon the Teresina domain, in the same location where the MCR-DRP was interpreted. In contrast, the thickening of the Balsas Group (Upper Carboniferous to Triassic; green in Fig.3.11b) is shifted to the west, upon the northern Grajaú subdomain, where Soares et al. (2018) and Queiroz (2019) interpreted magmatic underplating, due to the high velocity anomaly in the lower crust (HVLC). The depocenter migration of PB might suggest an inheritance of the basement crustal blocks heterogeneities in controlling the basin subsidence through time. According to very recent thermo-mechanical models in North African intracratonic basins (Perron et al., 2021), the stored gravitational potential energy inherited from density and rheological heterogeneities of accretionary continental lithosphere is the main explanation for the slow long-term subsidence of such basins, as well as for the rise of intrabasinal arches. For these authors, thermal anomalies, sediment supply rates or external far-field stresses, alone, does not account for the 1st order subsidence pattern, although these factors can temporarily change the subsidence rates.

Last but not least, it is very important to emphasize that most of the assumptions proposed here are mainly based on geophysical surveys and therefore there are multiple possible interpretations for the variety of anomalies here compiled. One example, already highlighted by Soares et al. (2018) when analyzing the WARR-DRP (Figs.3 and 4), is that younger tectonic processes might be superimposed to the Pre-Cambrian basement, such as the intense Mesozoic Magmatism (Mosquito and Sardinha formations) observed in the entire extension of the Parnaíba basin, also possibly intruding portions of the crust and causing some of the seismic anomalies discussed here. This is the reason why, for the understanding of such complex collisional system, it is essential to acquire new geochemical and

geochronological information from wellbore rock samples and to revise the few available data under the light of modern techniques (SHRIMP and LA-IPC-MS U-Pb dating, trace elements, etc.).

Implications for Neoproterozoic West Gondwana amalgamation

The evolution and amalgamation of the previously described large tectonic domains, since the Tonian until the end of Ediacaran Period, in the Neoproterozoic Era, are presented in the sketches of Fig.3.12. This evolution is based on the proposal of Caxito et al. (2020, 2021) and supported by the new geochemical and geochronological discoveries of Hodel et al. (2019) and Assis et al. (2021) for the Araguaia belt, as well as by the new geological report of Klein et al. (2017) for the Gurupi belt, previously discussed in the text (item 3.2.2).

The new assumptions we make here, modifying the sketches of Caxito et al. (2020, 2021), are related to the Parnaíba basin area and they are listed below:

- To the NW of the large Goiás-Pharusian oceanic domain (GPhO), a distentional triple junction divided the Amazonian, West African and Grajaú blocks during the Tonian (ca. 900-800 Ma), maybe reactivating some Paleoproterozoic sutures, such as described by Klein et al. (2017) along the Gurupi belt.
- Meanwhile, island arcs along the GPhO occur to the western margin of the North Borborema/Benino-Nigerian block (nBo-BeNi in Fig.3.12; called as NOBO-BENI by Caxito et al., 2020), in which we have included the Teresina domain. This is also observed in the western margin of São Francisco block, including the Cristalândia, Cavalcante-Natividade and Crixás domains and forming the juvenille magmatic rocks of the Goiás arc. In between, the Southern Borborema domain (sBo, named as APAMCAPAY in Caxito et al., 2020) is separated by N-S rifting from “nBo-BeNi” and northern SFC, with development of the E-W trending Transnordestino-Central African Ocean (ca. 700-800Ma). According to Caxito et al. (2020) and Ganade et al. (2021), this region of the CAB went through a decratonization process, resulting on weakened lithosphere and narrow oceanic domains, later involved in a transpressional orogeny

marked by intense shearing deformation, now observed in the Borborema Province. One of the constraints for this interpretation presented herein Fig.3.4d, is the presence of anomalous thinned continental lithosphere in this region.

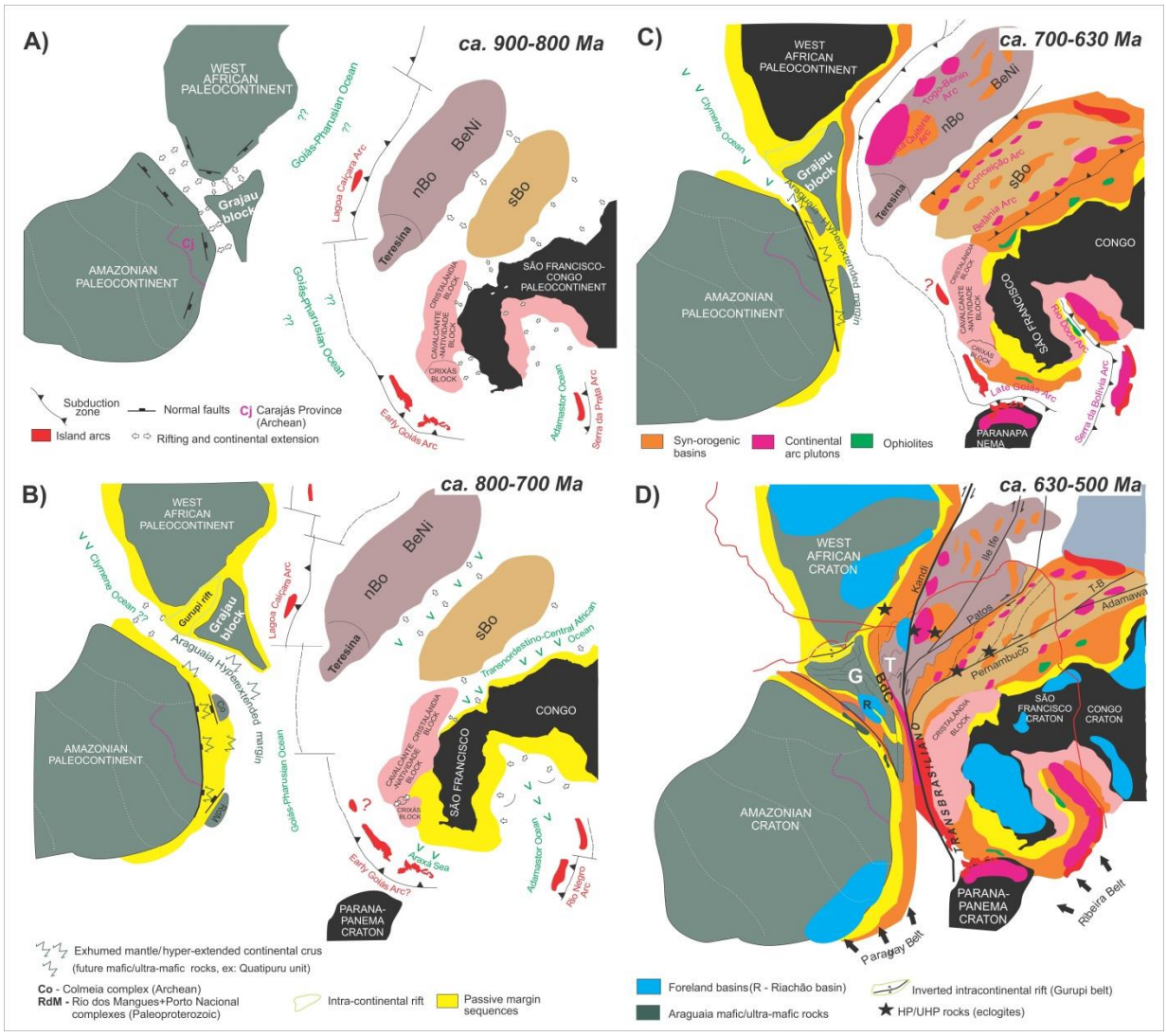

Fig.3.12 Tectonic sketches of the western Gondwana amalgamation in the vicinities of the Parnaíba basin (NE of Brazil) during the Neoproterozoic, based on the interpretations presented here and also in the last studies of Caxito et al. (2020 and 2021).

- The Tonian extensional efforts in the AM-WA domain, accelerated due to the subduction processes in the opposite eastern portion of GPhO, leads to the formation of the intracontinental Gurupi rift (e.g. Klein et al., 2017) and the Araguaia proto-ocean (part of the Clymene ocean to the north?), with zones of hyper-extended continental crust (e.g. Hodel et al., 2019), mantle exhumation and associated volcanism. In this process (ca. 700-800Ma,

Fig.3.12b), parts of the Amazonian Craton (or even from the Grajaú block?) were detached and hyper-extended, such as the Archean Colmeia Complex, close to the Carajás Province, and the Paleoproterozoic Rio dos Mangues and Porto Nacional complexes, to the south (e.g. Assis et al., 2021).

- Simultaneously, the NE GPhO was being consumed, marked by the developing of the Lagoa Caiçara arc complex, continued to ca. 650 Ma (Caxito et al., 2020), approximating the Teresina domain (in the "nBo" block) to the western passive margin of the Grajaú and West African blocks, that soon (ca.700-630 Ma) was turned into an active margin. In orange, the syn-orogenic basins of Fig.3.12c, along the eastern Grajaú block, represent the prolongation of the Neoproterozoic metasedimentary rocks of the Médio Coreaú domain (Martinópole Group) towards the proposed here Barra do Corda belt.
- The terminal stages of oblique continental collision of the West-African-Grajaú blocks with the "nBo-BeNi" in the western margin of the Grajaú block, followed by the inversion of the Araguaia hyper-extended margin and of the Gurupi rift (ca. 630 to 500 Ma). Synchronous to these continental collisions, Ediacaran forelands were formed, such as the Riachão basin, upon the southern Grajaú block, and the Ubajara basin, upon the Médio Coreaú domain.

The geophysical expression of thinned lithosphere and thinned crust observed in the Borborema Province is also observed within the eastern Araguaia belt (Figs. 4d and 5; e.g. Feng et al.,2007; Agurto-Detzel et al.,2017; Mckenzie and Tribaldos, 2018), indicating the imprints of this hyper-extended margin between the Amazonian Craton and the Grajaú block and a possible delamination of the weakened lithosphere in the later Neoproterozoic orogenic cycle, similar to what is proposed by Ganade et al.(2021) for the Borborema. To the north, close to Grajaú city, the high velocity lower crust (HVLC in Fig.3.3; Soares et al., 2018; Queiroz, 2019), instead of a Mesozoic magmatic underplate, can be interpreted as a product of eclogizitation in the lower crust of the northern Grajaú block, a typical process observed in thick continental crusts during shortening processes of orogenesis (e.g. Krystopowicz and Currie, 2013). To better constrain such assumption, however, geochemical analysis

of lower crust samples, such as mafic and ultramafic xenoliths within the basement units of Parnaíba basin, are required.

In this complex context of oblique continental collisions evolving decratonized lithosphere (e.g. Caxito et al., 2020; Ganade et al., 2021) and hyper-extended/proto-oceanic margins (e.g. Hodel et al.,2019) of the Central African and Amazonian-West African blocks, respectively, the closure of the Goiás-Pharusian main external oceanic domain occurred along the co-related belts within the Transbrasiliano-Kandi corridor (Cordani et al., 2013a). One of these belts is here interpreted as the Barra do Corda belt, beneath the central portion of the Parnaíba basin. As a result of the gravitational collapse and relaxation of the orogenic plateaus of western Gondwana orogen, strike-slip reactivations have probably caused the installation of the Early Paleozoic pull-apart basins (TBPAB in Fig.3.11a).

3.2.11 Conclusions

We were able to identify several basement domains and subdomains beneath the Phanerozoic Parnaíba basin, described on the basis of different geophysical and geotectonic approaches, which include the analysis of lithospheric and crustal thickness, seismic velocity anomalies, gravity, magnetic and electrical character of the crust, seismic interpretation constrained by wellbore information of the shallow basement and an integrated two-dimensional model of central Parnaíba crust (L103). These domains are, from west to east (see Figs.5, 6, 8 and 11): the Araguaia belt domain, including the first described eastern Araguaia belt subdomain (Ar); the Grajaú domain (G), subdivided into northern and southern Grajaú subdomains (nG and sG), the second one covered by the Ediacaran Riachão basin (RB); in the center, the newly proposed Barra do Corda belt (BdC); the Teresina domain (T) and the adjacent Transbrasiliano Fault Zone (TBFZ), along which the supracrustal Transbrasiliano Pull-Apart basins (TBPAB) were installed; the Borborema domain (Bo), divided here into northern and southern subdomains (nBo and sBo), and finally, in the SE, the crustal blocks of the Northern São Francisco margin (nSF).

We then tentatively assigned these units to greater paleotectonic crustal building blocks (Figs.1, 11 and 12) involved in the western Gondwana amalgamation during the Neoproterozoic Era, following regional interpretations (Cordani et al., 2013a, 2013b; Ganade de Araujo et al., 2014; Cordani et al.,2016). In this way, we

could refine the most updated paleoreconstructions of West Gondwana (Caxito et al., 2020, 2021), that considered a major NE-SW suture zone along the Transbrasiliano-Kandi corridor crossing the Parnaíba basin and separating the Amazonian-West African and Central African crustal building blocks.

The compilation of geophysical studies (Figs. 3 and 4) shed light on the heterogeneities of the Parnaíba basin substract, not only in their margins, where it was already expected due to the surrounding complexity of Neoproterozoic structures, but mainly in its central portion, where relevant contrasts were revealed in different dataset acquisitions along the Deep Regional Profile (DRP, Fig.3.3). These studies allowed the differentiation between the Grajaú and Teresina domains, located respectively to the west and to the east of Barra do Corda city, in central PB.

The updated map of crustal thickness (Fig.3.5) in Parnaíba basin broadens the understating of these crustal heterogeneities, informing not only the differences between western and eastern Grajaú and Teresina domains, but also the presence of a thinner crust indentation observed to the southwestern portion of PB. This region was interpreted as the SE prolongation of the Neoproterozoic Araguaia Belt beneath PB, where eastwards verging thrust faults were interpreted in the seismic reflection data (Fig.3.9a), defining a zone of back-thrusts (Eastern Araguaia domain) of the Araguaia belt upon the hidden Grajaú block (pre-Brasiliano inlier; Table 3.2).

New descriptions of mid-crustal reflectivities dipping northeastwards to the south of the DRP (Fig.3.7), along the eastern margin of the Teresina domain, reinforced the interpretation, already suggested by some authors (Solon et al.,2018; Araujo, 2019; Schiffer et al., 2021), of the presence of paleosuture zones buried beneath central PB. In the seismic profile L103 (Fig.3.10), the MCR was connected to shallower thrust faults, deforming the eastern margin of the Riachão foreland basin. This basin, previously described in the literature (Porto et al., 2018; Miranda, 2018), is key to understand the complexity of the collisional setting beneath PB, involving to the west the back-thrusts of the Araguaia belt upon the southern Grajaú block, and, to the east, the thrusts of what we here defined as the Barra do Corda belt (BdC), marking the limit between the Grajaú and Teresina domains. In the Bouguer residual map (Fig.3.6c), the BdC is characterized by NNE-SSW elongated positive and negative stripes, possibly indicating the tectonic contact of low and high

grade metamorphic rocks. A similar Bouguer signature is observed to the west, in the Araguaia belt.

Finally, the presence of Neoproterozoic mylonitic rocks recovered in the wellbores (Fig.3.8), as well as the NE-SW sigmoidal gravity and magnetic lineaments (Fig.3.6) support the interpretation of the Transbrasiliano Fault Zone as a dextral shear zone that was active in the final stages of the Brasiliano orogeny, also affecting E-W shear zones within the Borborema Province (Ganade et al., 2021). The TBFZ was reactivated during the Early Paleozoic, controlling the installation of narrow pull-apart basins beneath PB, here called as the Transbrasiliano Pull-Apart Basins (TBPAB) and interpreted in L007 (Fig.3.9b). These basins are possibly coeval to the Cambro-Ordovician Jaibaras trough and to other narrow basins constrained along Neoproterozoic reactivated faults.

It is remarkable in the seismic data (Figs. 9 and 10), the erosional unconformity limiting the base of the Parnaíba basin (Pre-Silurian Unconformity), observed especially in the southwestern portion, upon the Riachão basin. According to the isopach maps of PB, based on well data (Daly et al., 2019; Fig.3.11b), the depocenter of PB migrated from east, upon the Teresina domain, to northwest, upon the Grajaú domain, during the Paleozoic. This is an indication of inherited basement control during the basin evolution, although more studies are required to establish this causative connection. The Mesozoic magmatic and extensional events that affected the PB is another theme for future studies, once such events could reactivate or even mask geophysical signatures of the pre-Silurian basement configuration proposed here.

3.3 Additional Information

3.3.1 The Continental Lithosphere beneath the Parnaíba basin

The lithosphere includes the crust and part of the upper mantle and represents the rigid outermost layer of the Earth, varying from 50 to 300 km thick (Condie, 1997). For the analysis of the continental lithosphere in the Parnaíba basin, two studies are compiled in Fig.3.13: Mckenzie and Tribaldos (2018) and Feng et al. (2007), the latter also supported by the results of Arturo et al. (2015; see Fig.3.4). These studies use surface wave tomography to estimate shear wave velocities (Vs) as a function of depth (z), based on the phase velocities of fundamental Rayleigh and Rayleigh waveforms. The Vs(z) values indirectly indicate the lithosphere thickness, once S waves are sensitive to vertical temperature gradient changes and to the constrast with the velocity attenuation zone of the asthenospheric mantle, due to partial melting (McKenzie and Priestley, 2007; Priestley and McKenzie, 2006).

High Vs(z) values normally indicate “cores” where the lithosphere is thicker and around which continental deformation takes place, sometimes coinciding with the limits of Archean or Proterozoic cratons (McKenzie and Priestley, 2007). McKenzie et al. (2015) have built a lithospheric thickness map of Pangea by paleoreconstruction of continents in the Permian. Later, McKenzie and Rodriguez Tribaldos (2018) used this data restricted to the Parnaíba basin and obtained a range of lithospheric thickness from 150 to 180 km for the basin area (Fig.3.13.a). The northern lithosphere is thicker (170-180km) and seems to connect to the Amazonian craton “core”. The southeastern part presents lower values of 160-170 km thick, along an ENE-WSW trend, which is interpreted as a prolongation of Pan-African Brasiliano belts along the Transbrasiliano-Kandi lineament in both African and South American continents. Here, we associate the northern thicker lithosphere to the Grajaú block and the NW Araguaia belt, in contrast to the slightly thinner lithosphere of the eastern Araguaia belt, TBFZ and Borborema domains.

According to the S-wave velocity map at 100km depth obtained by Feng et al. (2007) and presented in Fig.3.13b, it is possible to recognize three areas of distinct Vs anomalies within the Parnaíba basin. This pattern is also observed in the map from Agurto-Detzel et al. (2015). In the northern part, two areas of high velocities (approx. 7% above the average 4.492 km/s) are located westward and eastward of

Barra do Corda, representing the northern Grajaú and the central Teresina domains, respectively. This thick lithosphere “core” located to NW also seems to connect to the Amazonian craton and is similar to the McKenzie et al. (2015) interpretation. Feng et al. (2007) observed high S velocities down to 150 km depth beneath the northern Parnaíba basin and correlated it to a cratonic nucleus, compatible to what is also found in the Amazonian craton and beneath the Paraná and Michigan basins. To SW, close to Riachão, there is an area of average to low velocity anomaly, which coincides with the western margin of the pre-Silurian Riachão basin (Porto et al., 2018) and with the thinned crust observed in the Eastern Araguaia domain.

In both maps of Fig.3.13, the Borborema Province is a region of thin lithosphere (140-110 km) and average to low S-wave velocities at 100km depth. This region is considered by McKenzie et al. (2015) as the southern extension of the Pan-African active margin of Pangea, which is represented by a concave area of thinner lithosphere underlying what are now North Africa, Arabia and Western Europe. Agurto-Detzel et al. (2015) noticed the same lithospheric thinning towards Borborema and the NE Brazilian margin, followed by the increase of seismicity in this area. Another thin lithospheric anomaly in the eastern margin of the Parnaíba basin, located beneath the E-W trend of the Mesozoic Araripe basin, interpreted by Garcia et al. (2015), using Magnetotelluric inversion.

Geochemical isotopic analysis of magmatic rocks represents an alternative approach to understand heterogeneities within the deeper portions of the continental lithosphere. The studies of Heilbron et al.(2018) and Silva et al.(2017) analysed samples of Mesozoic magmatic rocks restricted to the NE portion of the Parnaíba basin and concluded that they derive from different mantle sources, inferring lateral geochemical heterogeneities within the subcontinental lithospheric mantle in this area. For Heilbron et al. (2018), these differences are related to the Proterozioc tectonic evolution of the Borborema province. Their results show a spatial distribution of the Low TiO2 basic rocks with possible depleted mantle source in the NE in contrast with the High TiO2 dolerites with inferred fertile mantle source to the SE, respectively above and below the E-W prolongation of the Senador Pompeu lineament (see Fig.3.13), which also separates the Ceará Central and the Rio Grande do Norte tectonic domains in the Borborema Province (defined here as the Northern Borborema subdomain).

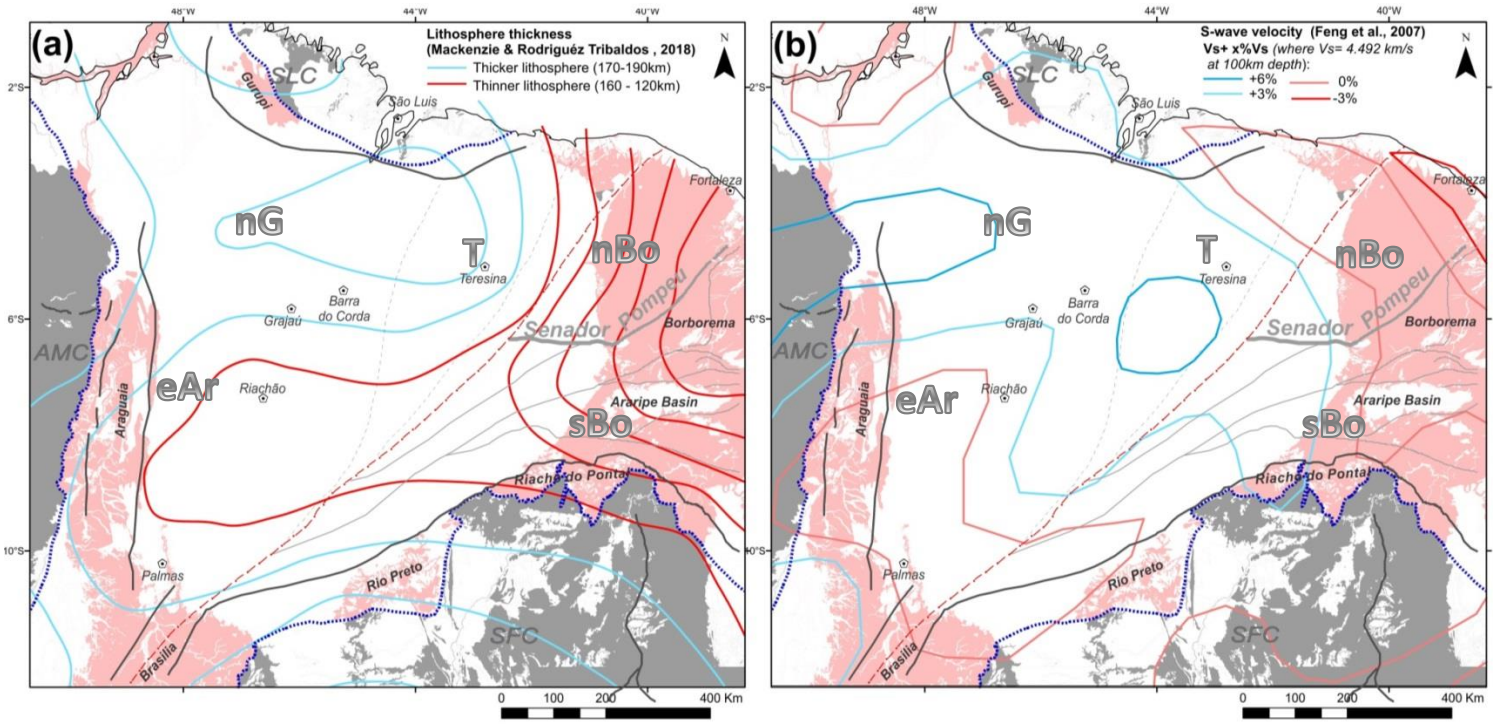

Fig.3.13: (a) Lithospheric thickness map and (b) S-wave velocity map at 100k depth slice in the Parnaíba basin and surrounding areas, modified after McKenzie and Rodriguez Tribaldos (2018) and Feng et al., (2007), respectively. “nG” stays for Norther Grajaú subdomain, “T”, Teresina domain, “eAr”, eastern Araguaia subdomain, “nBo”, northern Borborema subdomain and “sBo”, southern Borborema subdomain. Note the location of the Senador Pompeu Lineament, in gray, as a possible lithospheric limit in the Borborema Province.

3.3.2 Electrical conductivity of the crust beneath the Parnaíba basin

We compare three studies based on electromagnetic methods in order to unravel the crustal electrical conductity configuration beneath the Parnaíba basin. Arora et al. (1999) applied the GDS (geomagnetic deep sounding) methodology using an array of 29 magnetometric stations in the NW of the Parnaíba basin and surrounding areas. The result of their thin sheet model shows the conductivity distribuition within the shallow crust of PB and is presented in the map of Fig 3.14a.

Solon et al. (2018) acquired and processed approximately 1430km of broadband and long period Magnetotelluric data along the E-W DRP. Using the same type of data and processing methodology, Rocha et al. (2019) presented a NNW-SSE 470km–long profile in the SE marging of the Parnaíba basin, crossing also part of the southern Borborema Province and northern São Francisco craton. We compare the final 3D vertical inversion resistivity models of both studies, displayed in

the profiles of Figs. 3.14c and 3.14d. These profiles were also analyzed in item 3.4, but in the present topic they are shown in more detail. We also compile the horizontal depth slices of these inversions models within crustal depths of 10km, 20km and 30km, available in Solon et al. (2019) and Rocha (2019), and presented as a resistivity contour map in Fig. 3.14b.

Key observations from these literature compilations (Fig.3.14) are listed below, according to the domains suggested previously in the “Scientific Paper 1”:

- *Western Araguaia belt subdomain:* In the maps of Fig. 3.14, it is possible to observe that the northwestern portion of PB, close to the Araguaia belt, resembles a low conductive (high to moderate resistive) anomaly zone. Solon et al. (2018) noticed subvertical high resistive anomaly zones in the western stations of DRP, crossing the upper crust down to the upper mantle. They have associated them to the Quatipuru and Araguaína fault zones (Fig.3.14b), also observed by Daly et al. (2014).

- *Eastern Araguaia belt:* To the south of the western margin of PB, close to Riachão city, Arora et al. (1999) observed a subrounded low conductive anomaly. This area coincides with the observed thin crust and thin lithosphere of figures 3.5 and 3.4d, respectively, and also with the western thrusted margin of the Pre-Silurian Riachão basin (Fig.3.9a). However, this resistive anomaly might also correlate to the the surface lava flows exposures and diabase intrusions of the Juro-Triassic Mosquito Formation, defined by De Castro et al. (2018) as the Northern Mosquito Magnetic Domain, with a ENW-WSW orientation and confined to the Araguaia belt.

- *Gurupi belt/Northern Grajaú block*: In the NW Parnaíba basin, Arora et al. (1999) recognized a NW-SE-elongated high conductive anomaly, named as ‘LINK’ (Fig.3.14a), which was interpreted as a sedimentary connection between the Parnaíba Basin and the Marajó Graben (rift?), where sea transgressions have taken place during the early stages of the basin evolution. This NW-SE trend is also parallel to the main orientation of the Neoproterozoic Gurupi belt. Uchoa et al. (2020), in a NNW-SSE 180-km long MT profile crossing the northern margin of PB and adjacent Gurupi belt and São Luis

craton, also noticed highly conductive anomalies for the shallow sediments of Parnaíba and São Luis basins in contrast with highly resistive anomalies in the Gurupi belt

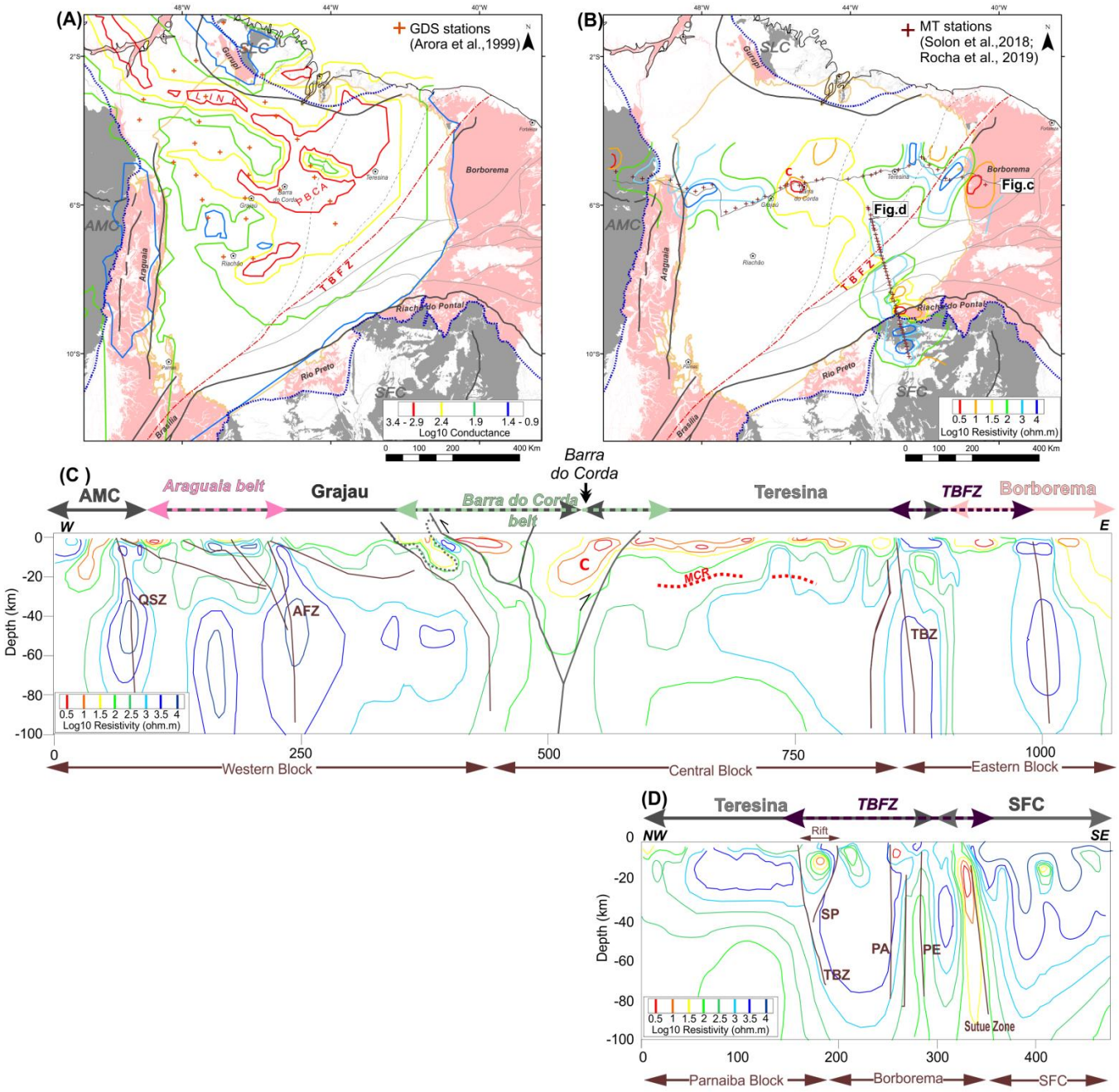

Fig. 3.14 (a) Conductance distribution map adapted from Arora et al.(1999); (b) Resistivity distribution map within crustal depths (-10 to -30 km) based on 3D inversion models from Solon et al.(2018) and Rocha (2019); and below, the vertical cross-sections of the 3D inversion models from (c)Solon et al. (2018) and (d) Rocha et al. (2019).

- *Grajaú block:* Near Grajaú city, Arora et al. (1999) and Solon et al. (2018) recovered moderate to high resistive anomalies. This is also observed in the profile of Fig.3.14c, especially at depths greater than 30km, with high resistive lower crust and upper mantle, within the entire “Western block”(brown arrows), encompassing also the Amazonian Craton, Araguaia belt and the first 200 km of the western Parnaíba Basin, within the Grajaú block. The same resistive anomaly values were observed for the São Francisco Craton, in the SE margin of PB by Rocha et al. (2019).

- *Teresina block:* In contrast, to the east, within the Teresina domain (eastern Parnaíba block), both profiles (Figs. 3.14b and 3.14c) showed moderate resistive values for the lower crust. Arora et al. (1999) described a NE-SW-elongated conductive anomaly, parallel to the TBFZ, crossed by E-W central embedded resistive anomalies, and named as the Parnaíba Basin Conductivity Anomaly (PBCA; Fig.3.14a). These authors presented two possible interpretations for the PBCA: the presence of a deep graben-like structure in the basement of the basin or carbon bearing rocks hydrothermally altered by Mesozoic magmatic activity. The resistive embedded block would be accounted for the presence of igneous sills and dykes. For us, the ‘PBCA’ (Arora et al., 1999) could correlate to the Teresina domain itself, and the WNW-ESE resistive zone, to the northern prolongation of the DRP-MCR (see Figs. 3.4 and 3.7). Southwards, close to the SW portion of L103, these authors observed a NE-SW-elongated-high-conductive anomaly. According to Solon et al. (2018) shear zones related to crustal limits might serve as paleofluid pathways preserving a high conductivity character.

- *Barra do Corda belt:* The regional contrast between the high (Grajaú or Western block) and moderate (Teresina or Central block) resistive anomalies is locally marked by a cylincrical conductor observed by Solon et al.(2018), named here as “C”, in the vicinities of Barra do Corda city. In the profile of Fig.3.14c, the “C” conductor dips westwards down to approximately 30km and it was suggested by Solon et al. (2018) as possibly caused by the presence of graphite concentrated along faults, marking a geosuture between two terranes. This supports our interpretation in the profile of crustal-scale thrust

faults arranged as a “positive flower” configuration, typical of transpressional tectonics. The seismic features, such as the high Vp/Vs ratio anomalies observed by Schiffer et al. (2021) and interpreted as a suture zone, reinforce this interpretation.

- *TBFZ/Borborema Province:* Eastwards, the trends of the contour lines of Fig.3.14b seem to align with the NE-SW strike of the TBFZ. Solon et al.(2018) observed narrow NE-SW-elongated high and low resitive zones laterally juxtaposed along the TBFZ width and called it as the Eastern block, including part of the low resistive Borborema Province (Fig.3.14c). To the SE, Rocha et al. (2019) observed the same pattern and inferred the prolongation of main suture zones of southern Borborema (Patos and PE shear faults), aligned to the conductive zones. In the profiles, the conductive and resistive zones extend from the upper crust to the upper mantle with remarkable vertical dips. In the shallow crust, a high resistive body within TBFZ was interpreted as a rift by Rocha et al. (2019). Romero et al. (2019) using broad-band MT data along the SE border of the Parnaíba, also described resistive graben-like structures, down to ~2 km, and conductive zones associated to Neoproterozoic shear zones in the upper/mid-crust.

3.3.3 The Mid-Crustal Reflectivity: further examples and forward models tests.

Table 3.3 summarizes the properties of the mid-crustal reflectivity (MCR), already described in item 3.2.7, based on seismic reflection characteristics and Bouguer gravity anomalies. We also add information of L102 and L109, where the MCR was also observed (see Fig.3.7).

Seismic Line	Lateral Extent (km)	TWT Depth (s)	Observed Bouguer Anomaly (mGal)	Comments
Deep Regional Profile (DRP)	250	8.5 to 13	-18.0 to -42.0	Curved and subhorizontal high reflective events. Moderate amplitude reflections occur beneath MCR down to 13s.
L112	28	4.8 to 7.2	-51.0 to -60.0	Two levels of parallel suborizontal high reflective events, at 4.8 and 7.2s, respectively.
L102	7	4.7 to 5.7	-50.0 to -60.0	Very short and inclined with moderated reflectivity events, at the crossing point with MCR of L112.
L109	20	5.2 to 7.1	-63.0 to -66.0	Two levels of inclined, short, high reflective events, at 5.2 and 7s, interrupted by a region of poor signal.
L117	27	5.2 to 7.0	-64.0 to -70.0	Two levels of inclined, short, high reflective events, at 5.2 and 7s, interrupted by a region of poor signal.
L108	27	4.7 to 5.7	-65.0 to -73.0	Slightly inclines short high to moderate reflective events.
L103	43 (to 70*)	4.2 to 7.0	-60.0 to -70.0	Horizontal to inclined short high relective events. *Southwestwards the MCR seems to continue for at least 70km (approx. length), reaching the shallow crust in the eastern thrusted margin of Riachão basin.

Table 3.4 Main characteristics of the Mid-Crustal Reflectivity in seismic and gravity data observed in this study and along the DRP, based on the descriptions of Daly et al. (2014); Tozer (2017) and Manenti et al. (2018).

The MCR in the Parnaíba basin is still poorly constrained in the available literature. It was first observed along the DRP by Daly et al. (2014), who did not inform any geological interpretation for the origin of this seismic anomaly. Then, in the study of Tozer (2017) the MCR was interpreted as the top of an anomalous dense lower crust of possible mafic composition beneath the entire Parnaíba block (here comprising the Grajaú and Teresina domains). This interpretation is represented in Fig.3.15, modified after Tozer (2017). The study of Manenti et al. (2018) performed some seismic processing procedures along the DRP and suggested that this layer is related to a much localized body. They suggested that the DRP-MCR could be interpreted as a magmatic intrusive subhorizontal layer confined to the middle continental crust (laccolith or sill?; Fig.3.16).

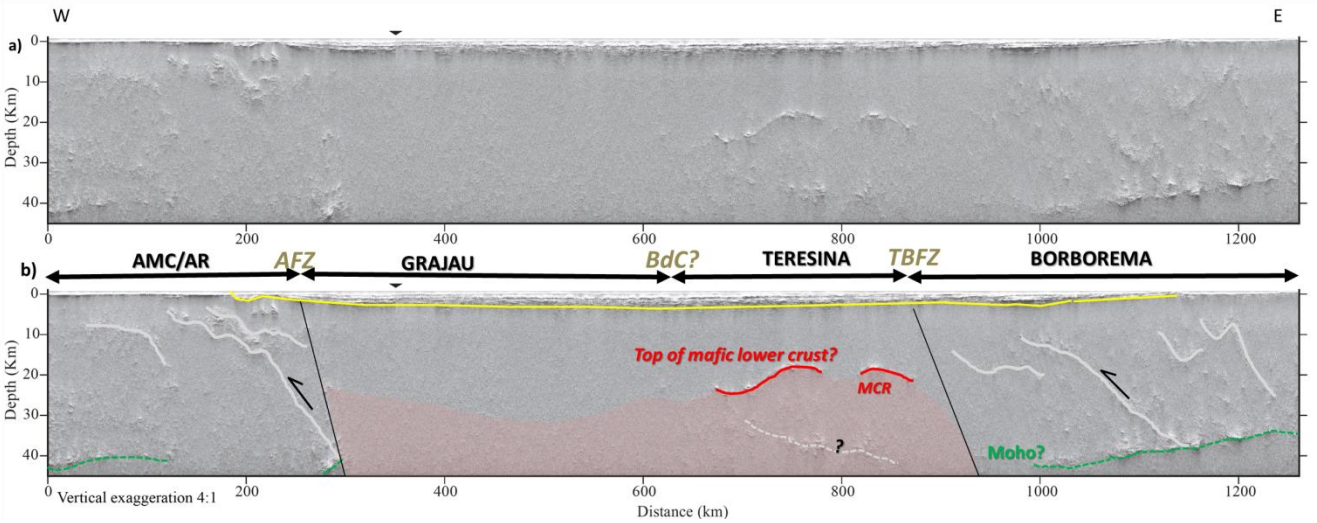

Fig.3.15 (a) Deep seismic reflection profile (DRP) in depth domain, non-interpreted version, available in Tozer (2017); (b) Interpreted DRP highlighting the main crustal discontinuities: in yellow, the base of the Parnaíba basin (PB); in green, the seismic Moho interpretation, in red, the MCR, interpreted by Tozer (2017) as the top of a mafic and dense lower crust beneath PB. The black arrows represent the tectonic domains of the basement proposed in this study, AMC stays for Amazonian Craton, AR, Araguaia belt, AFZ, Araguaína Fault Zone, BdC possible location of the Barra do Corda belt, and TBFZ, the Transbrasiliano Fault Zone.

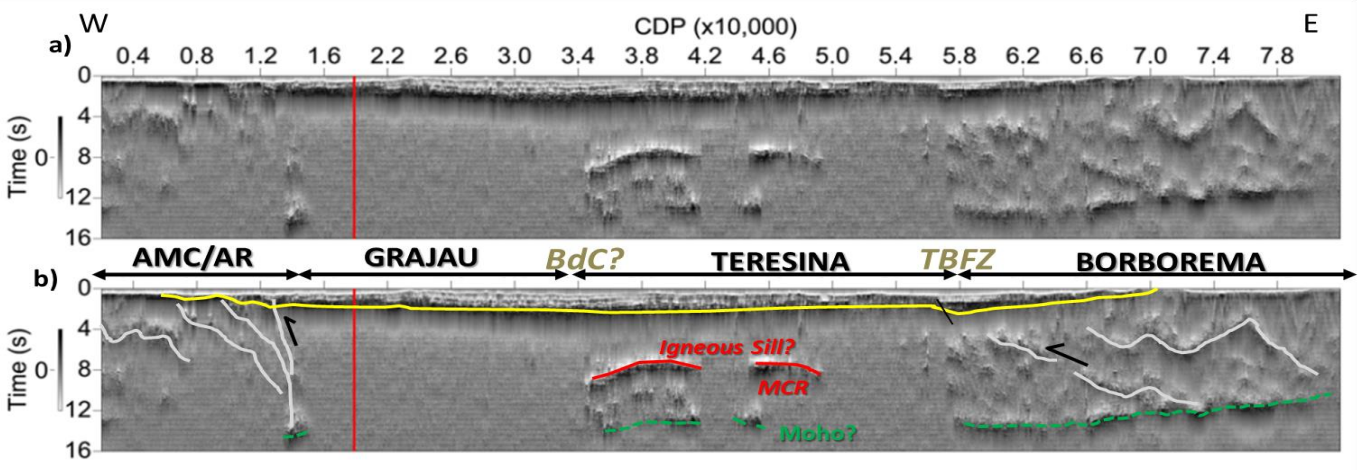

Fig.3.16 (a) Deep seismic reflection profile (DRP) in two-way time domain, non-interpreted version, available in Manenti et al. (2018); (b) Interpreted DRP highlighting the main crustal discontinuities: in yellow, the base of the Parnaíba basin (PB); in green, the seismic Moho interpretation, in red, the MCR, interpreted by Manenti et al. (2018) as an igneous intrusion within the crust. The black arrows represent the tectonic domains of the basement proposed in this study, AMC stays for Amazonian Craton, AR, Araguaia belt, AFZ, Araguaína Fault Zone, BdC possible location of the Barra do Corda belt, and TBFZ, the Transbrasiliano Fault Zone.

De Castro et al. (2018) have also observed the MCR along L103 (Fig.3.17) and interpreted it as a deep intra-basement intrusive feature, dipping northeastward from 9 to 12.5km depth, characterized by a positive long-wavelength magnetic anomaly. They correlated this region to the DRP-MCR described by Daly et al.

(2014) and Tozer et al. (2017) and interpreted these features as feeder zones for the magmatic rocks observed in the Parnaíba basin. In the TMI magnetic map of Fig. 3.17b, it is noticed that this positive magnetic anomaly in L103 occurs in other portions where the MCR is observed in the seismic, coinciding also with the western limit of the Teresina magnetic domain interpreted in De Castro et al. (2014, see Fig.3.2) and the homonymous tectonic domain interpreted in this study (see Fig.3.11). This positive magnetic lineament was regionally observed in the tectonic map of South America and coincides with the region where the Barra do Corda belt is proposed (Fig.3.11 and Fig.3.17b).

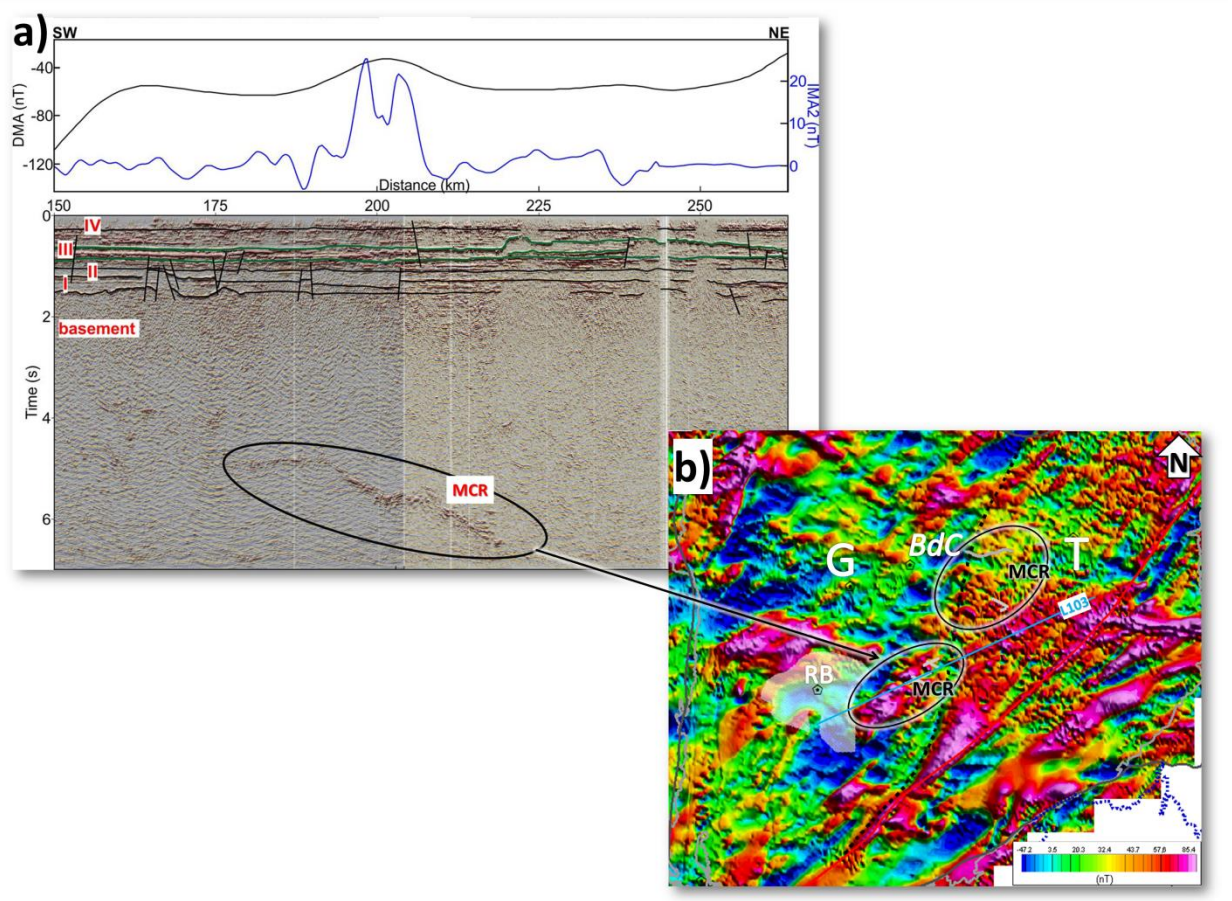

Fig.3.17 (a) Magnetic anomalies along L103; DMA refers to the deep and IMA2, to intermediate anomalies. The sedimentary sequences of the Parnaíba basin are II: Silurian–E. Devonian, III: M. Devonian–E. Carboniferous, and IV: L. Carboniferous–E. Triassic. Modified after De Castro et al. (2018); (b) Total magnetic anomaly map showing the location of the MCR observed in seismic data. The tectonic domains are: “G”: Grajaú, “T”: Teresina, “BdC”: Barra do Corda. RB stays for the pre-Silurian Riachão basin. The dashed black lines represent the regional magnetic lineament of Cordani et al.

- ***Forward Model tests of the MCR***

Two different forward models were performed along the Bouguer anomaly profile of part of L103 where the Mid-Crustal Reflectivity (MCR) was observed, presented in Figs. 3.18b and c. The main goal of these models was to test different hypothesis raised in the available literature of the Parnaíba basin about the geological origin of this seismic anomaly (Figs. 3.15 and 3.16; Tozer, 2017; Manenti et al., 2018 and De Castro et al., 2018)

First the data were compared with the regional gravity effect of the Moho relief, considering homogeneous crust and upper mantle. The fit between observed and calculated data in this specific crop of the L103 was much smaller (RMS error of 3.9 mGal; Fig.3.18a) than the one observed in the full L103 (Fig.3.9b). The Moho depth in this region presents a smooth variation from 40 to 41km depth, with the maximum value roughly positioned in the middle of the profile.

Secondly, the first test (Fig.3.18b) to model the gravity anomaly around the MCR in L103 followed the same parameters of density used by Tozer (2017), presented in Table 2.3 (see Chapter 2), considering the MCR as the top of a dense lower crust (2985 $kg.m^{-3}$). The top of the lower crust geometry was guided by the MCR reflection observed in the seismic data (Fig.3.7b). The base of the sedimentary Parnaíba basin (Pre-Silurian Unconformity) was guided by the seismic imaging (see Fig.3.9), at approximately 2.8km depth. This was estimated based on the depth converted lines available in Porto (2017), and previously described in Chapter 2.

Constant bulk density was considered for four layers, in similarity to what Tozer (2017) has applied along DRP (Table 2.3 in Chapter 2). They are, from base to top (Fig.3.18b): the mantle (3150 $kg.m^{-3}$, the same used in the model of Fig.3.9), the mafic and dense lower crust (2985 $kg.m^{-3}$), the upper crust (2810 $kg.m^{-3}$) and the Parnaíba basin sedimentary sequence (2460 $kg.m^{-3}$). The fit of the calculated anomaly for the first model in relation to the observed Bouguer data was much worse (RMS error of 10.5; Fig.3.18b) than in the model of Fig 3.18a.

In the second model (Fig 3.18c), the suggested geological interpretation for the MCR given by Manenti et al.(2018) and reinforced by De Castro et al. (2018), was tested, in which the MCR is interpreted as an ingneous intrusive layer (sill? laccolith?) within the lower crust. The following parameters were applied:

- Densities and geometries of mantle, upper crust and Parnaíba basin sedimentary layers were kept equal to the previous test (Fig.3.18b).
- Density of 2870 kg.m^{-3} for the Middle Crust (beneath the MCR), the same suggested by De Castro et al. (2014) for the Parnaíba block (see Table 2.3 in Chapter 2).
- Addition of a Lower Crust at constant 31km depth and density value of 3000 kg.m^{-3}, also assumed by Castro et al. (2014) for the Parnaíba block (see Table 2.3).
- Addition of a 1.5-2.5km thick layer of 2.985 kg.m^{-3} density (same value suggested by Tozer, 2017 for the MCR) following the same geometry of test 1, guided by the MCR observed in the seismic data.

The calculated anomaly for these above mentioned parameters presented in figure 3.18c shows a much better fit (RMS error of 4.7 mGal) with the observed data, when compared to the first model (Fig.3.18b), but a slightly worse fit when compared to the Moho relief model (Fig.3.18a).

Some conclusions are drawn from the aforementioned forward model tests. It is unlikely that the MCR is the top of a uniform dense lower crust, as suggested by Tozer (2017) and tested in Fig.3.18b. This is not only confirmed by the high RMS error of the forward model fit along L103, but also by the average Bouguer anomalies along the different regions where the MCR was observed (see Table 3.3). As presented in the Bouguer profiles of Fig.3.7, the MCR is not located essentially in a regional gravity high. Actually, the maximum values of gravity anomalies are shifted and the new observations of the MCR are located in semi-regional lows. However, residual positive gravity anomalies seem to be related to the presence of the MCR, in the order of 10-20 mgal (Fig.3.7). In the DRP the variation is greater, but the lateral length too. This implies that this layer possibly marks a dense, but localized buried body within the crust. This interpretation is reinforced by the high acoustic impedance (high amplitude) of the reflectors in the seismic reflection data, and by the positive magnetic anomalies observed in De Castro et al. (2018).

The further integrated analysis presented in the “Scientific Paper 1” (item 3.2) led to the interpretation that the MCR is related to a crustal-scale fault, separating the Grajaú and Teresina domains, within the Barra do Corda mobile belt. If so, hydrothermal fluids and metals concentrated along the fault plane could geologically

explain the observed localized high gravity and magnetic anomalies, as well as the high amplitude contrast in the seismic. Another possible explanation is the intrusion of igneous sills (testes in Fig.3.18c) along this crustal-scale discontinuity.

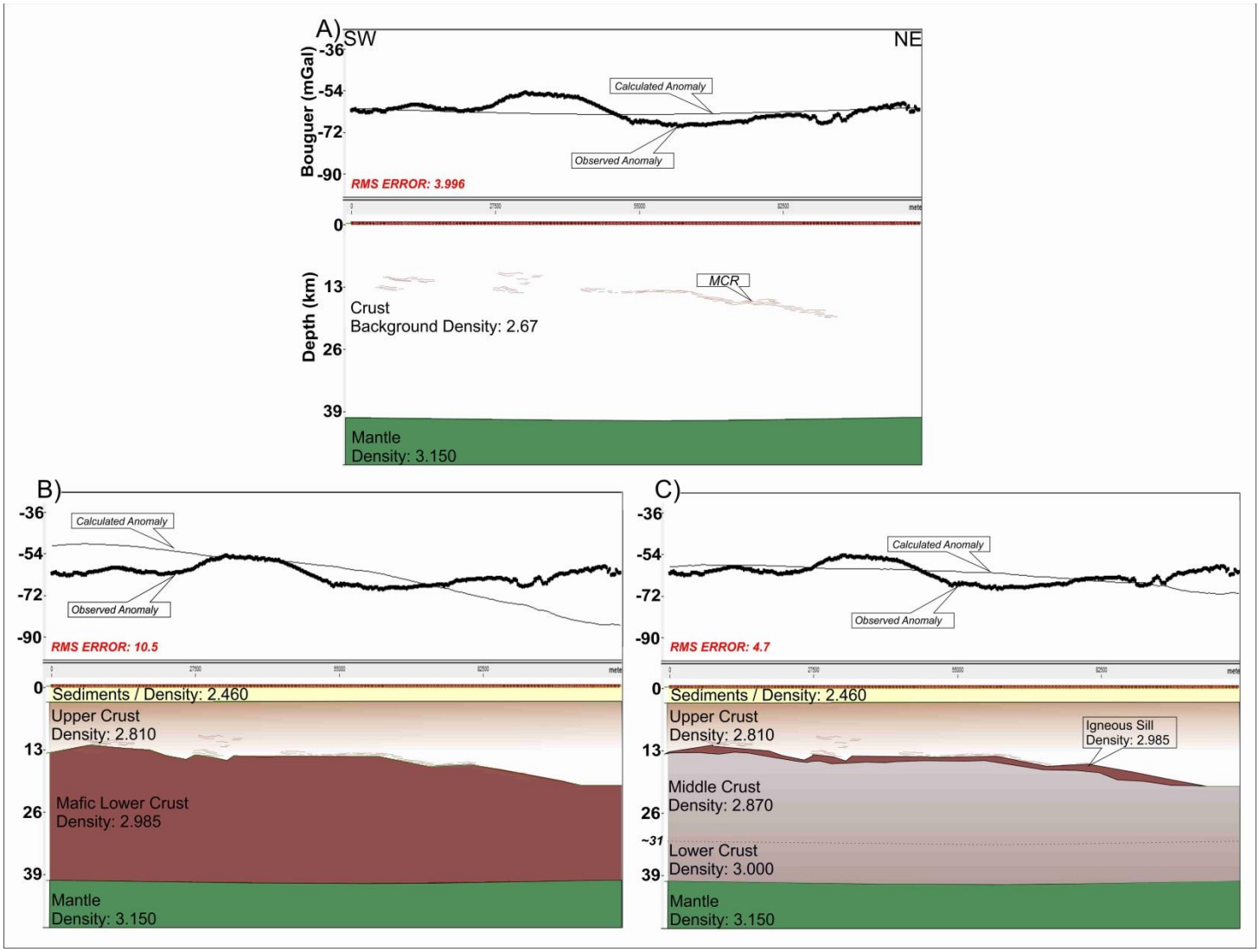

Fig. 3.18 (a) Forward model of L103 cropped to MCR region (see Fig.3.11a) and adjusted to the Moho relief. (b) Forward model (test 1) of L103 cropped to MCR region, using the same parameters of Tozer (2017) for the crustal densities (see table 2.2), where the MCR is the top of a dense lower crust. (c) Forward model (test 2) of L103 cropped to MCR region, using the same geological interpretation suggested by Manenti et al. (2018), where the MCR is a layer of magmatic intrustion.

3.4 Final Remarks

In this chapter, the Neoproterozoic/Early Paleozoic tectonic evolution of Northeast Brazil has been reviewed from the perspective of basement terranes beneath and in the vicinity of the Parnaíba basin and inside the context of recent maps of western Gondwana amalgamation.

An updated tectonic map of the basement was proposed, based on: (1) GIS compilation of geophysical datasets (seismic refraction, receiver function analysis, S-wave information of the lithosphere, magnetotelluric, gravity and magnetic anomalies, etc.); (2) updated crustal thickness map compiled from available seismological surveys; (3) reinterpretation of magnetic and gravimetric lineaments; (4) seismic interpretation of deep and shallow basement features in the central Parnaíba basin; (5) basement lithological and age information from wellbores; and (6) integrated forward models along a 500km-long NW-SE profile in the central portion of PB.

The key results of this chapter are summarized below:

- The basement of the Parnaíba basin is composed of two main pre-Brasiliano inliers (Grajaú and Teresina blocks) surrounded by Brasiliano mobile belts, assigned to two major crustal building blocks of western Gondwana: the Amazonian-West Africa (AWB; to the west/north) and the Central African blocks (CAB; to the east/northeast).
- In spite of a stable cratonic block in the center of the basin basement, a mid-crustal reflectivity was interpreted as a suture zone marking the closure of the major Goiás-Pharusian Ocean during the Neoproterozoic, along the NE-SW TranBrasiliano-Kandi corridor.
- A zone of thinned continental crust (~36km) and continental lithosphere (<160km) is observed in the southwestern portion of the Parnaíba basin, interpreted as the eastern prolongation of the Araguaia belt. Seismic data show a highly deformed shallow crust marked by back-thrusts verging eastwards.
- Two pre-Silurian basin systems were identified prior to the Parnaíba basin installation: the Ediacaran Riachão foreland basin and the Transbrasiliano pull-apart basin system.

Chapter 4

The Early Paleozoic tectonic evolution of Parnaíba Basin: links with the basement configuration.

4.1 General Outline

This chapter presents the first publication of this thesis (called here as the "Scientific Paper 2", item 4.2), entitled as: ***"The Ordovician-Silurian tectono-stratigraphic evolution and paleogeography of eastern Parnaíba Basin, NE Brazil",*** as well as some additional studies (item 4.3) related to the initial tectono-stratigraphic evolution of the Parnaíba basin during the Paleozoic and possible links with the new proposal of the basement configuration, presented in Chapter 3.

The "Scientific paper 2" aims to unravel the Ordovician-Silurian sedimentary record in the Parnaíba basin, one of the largest preserved in western Gondwana and assigned to the Serra Grande Group. Surface and subsurface data of the eastern portion of PB were used to support a depositional model for this group, including paleogeographic reconstructions of western Gondwana. The contribution of the PhD candidate for this study consisted of supporting the surface geological data sampling and analysis during the field trip (see location in Fig.2.1); interpreting and writing the topic 4 of item 4.2, called as the "Subsurface data analysis"; and helping on the final discussions, especially regarding the tectonic controls. It is worth saying that the detailed sedimentary facies analysis presented in the paper (topic 3 of item 4.2) is not deeply covered by the scope of the present Thesis.

In item 4.3, the pre-Silurian unconformity (PSU), formed prior to the Serra Grande group deposition, is presented from well, seismic and surface geological data perspectives. Its subsurface relief is compared to the final geotectonic map of the basement (Fig. 3.10). Then, the spatial distribution of the depocenters of the Parnaíba basin during the Paleozoic is briefly discussed, comparing the isopach maps of the Serra Grande, Canindé and Balsas groups with the proposed paleotectonic map of the basement.

4.2 Scientific Paper 2

[Published paper reference: "Assis, A.P., Porto, A.L., Schmitt, R.S., Linol, B., Medeiros, S.R., Correa Martins, F., Silva, D.S., 2019. The Ordovician-Silurian tectono-stratigraphic evolution and paleogeography of eastern Parnaíba Basin, NE Brazil. J. South Am. Earth Sci. 95".

Figures, tables, and topics numbering was kept as original publication. Fig.1 refers to Fig.4.1, Fig.2 to Fig.4.2, and so on. References are in the final of the thesis.]

The Ordovician-Silurian tectono-stratigraphic evolution and paleogeography of eastern Parnaiba Basin, NE Brazil

A.P. Assis[a,*], A.L. Porto[b], R.S. Schmitt[c], B. Linol[d], S.R. Medeiros[c], F. Correa Martins[e], D.S. Silva[c]

[a] Programa de Pós–graduação em Geologia, Universidade Federal Do Rio de Janeiro (PPGL/UFRJ), CEP 21941-916, Rio de Janeiro, Brazil
[b] Departamento de Geofísica, Observatório Nacional / MCTIC, CEP 20921-400, São Cristovão, Rio de Janeiro, Brazil
[c] Departamento de Geologia - IGEO, Universidade Federal Do Rio de Janeiro (UFRJ), CEP 21941-916, Rio de Janeiro, Brazil
[d] Africa Earth Observatory Network, Nelson Mandela University, Port Elizabeth, South Africa
[e] Departamento de Geociências, Universidade Federal Rural Do Rio de Janeiro (UFRRJ) CEP, 23897-000, Seropédica, Brazil

ARTICLE INFO

Keywords:
Parnaiba basin
Ordovician-silurian glaciation
Gondwana tectono-stratigraphy
Transbrasiliano lineament

ABSTRACT

The Phanerozoic Parnaiba Basin (PB) occupies 600.000 km^2 in northeastern Brazil and preserves one of the largest Ordovician-Silurian sedimentary record of western Gondwana, represented by the Serra Grande Group (SGG). This unit marks the initiation of the depositional history of Parnaiba Basin and comprises from the base to the top, the Ipu, Tianguá and Jaicós formations. Therefore the tectono-stratigraphy and paleogeography of SGG is key to unveil the genesis of PB and also the Ordovician-Silurian evolution of Gondwana. Here we present new sedimentological and tectono-stratigraphic surface and subsurface data from the eastern Parnaiba basin. Seven facies associations are described within the SGG: alluvial fan, braided river channel, outwash fan, lodgment till, shoreface, offshore and delta. They are assigned to each formation of SGG and, together with seismic and well data interpretation results, supporting a depositional model for this group. The lowermost portion of the Ipu Formation is represented by immature conglomerates in a scarp-related alluvial fan system, filling up NE-SW-elongated grabens aligned to the crustal scale Transbrasiliano Lineament. This implies that the early sedimentation of the Parnaiba Basin could relate to post-Brasiliano tectonic reactivations following the amalgamation of Gondwana. Upwards, the Ipu Formation grades to a braided river system. Its uppermost portion contains a glacial deposit, here named as the Ipueiras tillite and discontinuously preserved across the basin. This glacial record might be correlated to the Hirnantian Glaciation, a global episode of about 2 m.y. during the Ordovician-Silurian transition (c.a. 443.8 Ma), well documented in other Gondwanan basins from Africa (e.g. the Taoudeni and the Tindouf basins) and South America (e.g. the Amazonas and the Paraná basins). Above it, a 15 m thick layer of marine black shales represent the base of the Tianguá Formation and is interpreted as the maximum flooding event of Serra Grande Group. To the top and laterally, this unit grades to shoreface and deltaic facies associations and is coeval to the global deglaciation transgressive event of Early Silurian. Finally, the overlying Jaicós Formation is composed by braided river deposits in a regressive cycle, possibly related to isostatic rebound, closing the deposition of the Serra Grande Group. Regarding the paleocurrent pattern of this unit, the main northwestwards direction suggests a paleotopographic high in the central portion of western Gondwana.

1. Introduction

The Ordovician-Silurian Serra Grande Group (SGG) is the lowermost sequence of the Phanerozoic Parnaiba Basin (PB; Vaz et al., 2007; Carozzi et al., 1975: Kegel, 1953; Carozzi et al., 1975; Caputo, 1984), overlaying a major unconformity across the Precambrian metamorphic basement and Cambro-Ordovician sedimentary rocks (Daly et al., 2014). It crops out over 500 km along the eastern border of the basin, comprising one of the largest exposures of the Ordovician-Silurian sedimentary record of western Gondwana (Fig. 1). The SGG is approximately 900 m thick and is divided into three formations (Carozzi et al., 1975): Ipu, Tianguá and Jaicós, from base to top. According to Vaz et al. (2007), SGG was first deposited under continental conditions, migrating upwards to marine and then continental environments, represented by a complete 1st order transgressive-regressive cycle. Although the tectonic evolution and the hydrocarbon exploratory

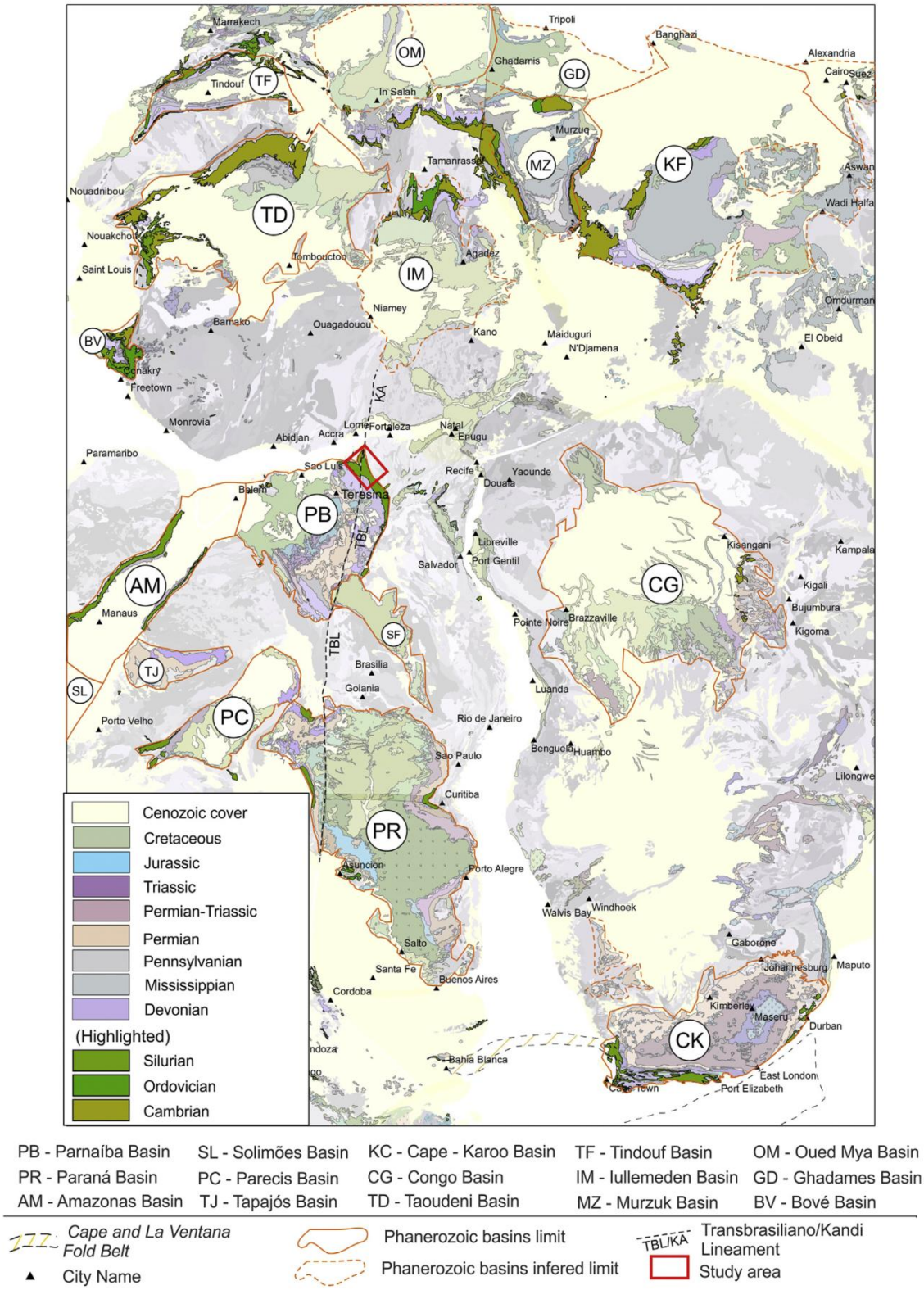

Fig. 1. Map of Central-West Gondwana reconstruction using rotated GIS data on GPlates (Gondwana Project Map, Schmitt et al.,2016) with main Phanerozoic Basins delimitated and Ordovician to Devonian deposits highlighted.

potential of the SGG have been recently discussed in national and international publications (Abelha et al., 2018; Cruz, 2016; Lima and De Sá, 2017; Metelo, 1999), many uncertainties remain to be understood, such as (1) the age of the SGG basal formation, (2) its tectonic significance and (3) the paleogeographic implications of its continental scale equivalents.

The best age for the Serra Grande Group is based on palynomorphs and the *Climacograptus cf. scalaris scalaris* graptolite zone of the Tianguá Formation, positioned at the Middle-Llandovery stage, Early Silurian (Caputo and Lima, 1984; Grahn et al., 2005; Grahn and Caputo, 1992;

Le Hérissé et al., 2001). The underlying Ipu Formation presents only ichnofossils in which the time span ranges from the Ordovician to Devonian periods, therefore its age is uncertain. Reworked glacial deposits occur in this formation, as first described by Caputo (1984) and Caputo and Lima (1984), who observed striated and flatiron shaped clasts in basal conglomerates and beds of tillite on the top. Therefore Ipu Formation might be correlated to the Late Ordovician glacial sequences of South America and northern Africa interior basins (Assine et al., 1998; Caputo and Lima, 1984; Ghienne, 2003; Hambrey, 1985; Villeneuve, 2005). Grahn et al. (2005) proposed that these tillites are lateral equivalents of the lowermost Tianguá Formation, being thus of Llandoverian age. Even though, it does not exclude the possibility that the lower layers of the Ipu Formation are Ordovician in age. Grahn et al. (2005) also proposed a long period (~40 m.y.) of sedimentation for the upper Jaicós Formation (Llandovery to Early Emsian), using palynological data, concluding that there are intraformational hiatuses within this formation.

There is a general consensus that Pre-Silurian sedimentary record of the Parnaiba Basin is controlled by inherited basement structures (Brito Neves et al., 1984; Oliveira and Mohriak, 2003). Our study area is located in its northeastern edge, where the NE-SW crustal scale fault zone Transbrasiliano Lineament (TBL) is partially covered by Pre-Silurian and SGG sedimentary layers (Figs. 1–3). This structure is correlated to the Kandi Lineament in northwestern Africa (Brito Neves et al., 1984; Góes et al., 1990, Fig. 1), and at least two sedimentary sequences related to the late-kinematics of the Brasiliano tectonic events are recognized: the Late Neoproterozoic Ubajara Group and the Cambrian-Ordovician Jaibaras Group, both of them exposed in the study area along NE-SW structures (Cordani et al., 2009a; De Castro et al., 2016, 2014). The overlying SGG in the PB is then interpreted to be the result of a sag phase of subsidence following stabilization of the Pan African-Brasiliano orogenic cycle (650-500 Ma; Brito Neves et al., 1984).

The Serra Grande Group equivalent sequences are preserved in many other interior basins of western Gondwana, such as the Amazonas and the Paraná basins, in South America; the Cape-Karoo Basin of Southern Africa; and the Taoudeni, Adraar, Tindouf and Chad basins in northern Africa; with the only exception of the Congo Basin (Central Africa) (Caputo, 1984; Linol et al., 2016a, Fig. 1). Although Gondwana paleogeographic maps of these basins have been widely debated in recent years (Schmitt et al., 2018; Scotese et al., 1999; Torsvik and Cocks, 2013), few studies provide correlation data between their Lower Paleozoic record (Caputo, 1984; Linol et al., 2015; Milani and De Wit, 2008). These basal sequences as well as the basement framework are key elements for understanding the initiation and evolution of the intracontinental syneclises across Gondwana.

This study presents new sedimentological and tectono-stratigraphic data from the Ordovician-Silurian Serra Grande Group along the northeast margin of the Parnaiba Basin. The facies analysis and geological mapping (Fig. 3) resulted in the recognition of seven facies associations and has also improved the boundaries between the three formations of SGG. For the first time, the glacial deposits of the Ipu Formation are described in detail (1:50 log), well as the outlier deposit of Santana do Acaraú (Ceará State; Fig. 3), and included in the depositional model proposed for the SGG. We have also integrated the interpretation of four seismic reflection profiles, constrained by two boreholes, in the mid-eastern region of PB, along the southwards prolongation of the Transbrasiliano Lineament, in a similar geological context of the field area. Finally, the three SGG formations are here characterized as (1) scarp-related alluvial fans, fluvio-glacial and proglacial systems (Ipu Formation); (2) a shallow marine platform and river dominated deltaic system (Tianguá Formation) and (3) a braided river depositional system (Jaicós Formation). This detailed interpretation also allowed us to refine regional correlations of SGG in the context of western Gondwana.

2. Geological setting

The Phanerozoic Parnaiba Basin deposits cover an area of about 600,000 km^2 in north and northeast regions of Brazil with a maximum thickness of 3.5 km (Fig. 2; Daly et al., 2014; Vaz et al., 2007). It is generally classified as a cratonic basin type, with low and localized subsidence rate and a long depositional history, which is initiated after the formation of supercontinents by orogenic cycles and is not related to tectonic plate boundaries (Daly et al., 2018). The Paleozoic sedimentation of PB is thought to be initiated in an Ordovician depression due to isostatic adjustments and cooling after the Gondwana amalgamation (Brito Neves et al., 1984; De Castro et al., 2014). The PB sedimentary units cover a major erosion surface named the Pre-Silurian Unconformity (PSU), which crosses the Precambrian metamorphic basement and remaining portions of the Cambro-Ordovician and Ediacaran sequences (Daly et al., 2014; Porto et al., 2018; Tozer et al., 2017; Vaz et al., 2007). According to Vaz et al. (2007), the sedimentary stack of the PB is divided into five depositional sequences, Silurian (Serra Grande Group), Middle Devonian - Lower Carboniferous (Canindé Group), Carboniferous – Lower Triassic (Balsas Group), Jurassic (Pastos Bons Formation) and Cretaceous (Corda, Grajaú, Codó and Itapecuru Formations), separated by regional, basin-scale unconformities (Fig. 2). Recently, Tozer et al. (2017) suggested a polyphase sedimentary evolution for the PB, encompassing five different tectono-stratigraphic (TS) units, also separated by basin-wide unconformities. Differently from the previous authors, they included the pre-Silurian sedimentary sequences in this classification: the Riachão (TS-1, Neoproterozoic-Cambrian - De Castro et al., 2016; Porto et al., 2018, 2018), the Jaibaras (TS-2, Cambrian-Early Ordovician – Oliveira and Mohriak, 2003; Milani and Zalan, 1999), the Parnaiba (TS-3, Late Ordovician-Early Triassic-sag phase - Serra Grande, Canindé and Balsas groups from Vaz et al., 2007), the Mearim (TS-4, Late Jurassic, post Mosquito Magmatic unit - Góes and Feijó, 1994) and the Grajaú (TS-5, Cretaceous - Rossetti et al., 2004; Góes and Feijó, 1994).

The Precambrian basement of Parnaiba Basin comprises the Borborema Neoproterozoic tectonic province to the east; the Tocantins Neoproterozoic tectonic province (Brasilia and Araguaia belts) to the west and to the south; and the Neoproterozoic Gurupi belt and Archean São Luis Craton to the north (Fig. 2). The basement in the center of basin is interpreted as a craton named the Parnaiba block (Brito Neves et al., 1984; Daly et al., 2014). Pre-Silurian sequences occur in different localities underneath PB and in its surrounding areas. Two main sequences have been described to be related to the late-kinematics of the Brasiliano orogenic events (Brito Neves et al., 1984; Cordani et al., 2009b; De Castro et al., 2016; Tozer et al., 2017). The first one is interpreted to be of Ediacaran age (Late Neoproterozoic). In subsurface, it has been described filling up a north-south elongated foreland basin beneath the mid-western portion of Parnaiba Basin, called Riachão Basin, with approximately 4.5 km of maximum thickness (Porto et al., 2018). At the surface, located in the NE border of Parnaiba basin, it is represented by the Ubajara Group, with a general NE-SW trend (Figs. 2 and 3). The second sequence is the Cambrian-Ordovician Jaibaras Group (Oliveira and Mohriak, 2003), filling up graben-like elongated troughs, interpreted as failed rifts arms controlled by normal and strike-slip reactivations of the NE-SW Transbrasiliano Lineament (Abelha et al., 2018; De Castro et al., 2016; Morais Neto et al., 2013).

The study area is positioned where the NE-SW crustal scale fault zone Transbrasiliano Lineament (TBL) crops out and continues southwards, covered by the Parnaiba Basin (Fig. 2). This structure is correlated to the Kandi Lineament in northwestern Africa and is interpreted as a mega-suture zone, active during Gondwana amalgamation (Fig. 1; Brito Neves and Fuck, 2014). The Late Neoproterozoic low-grade metasedimentary rocks of the Ubajara Group are exposed in the study area (Fig. 3), bounded by thrust faults parallel to the TBL and truncated by the Café-Ipueiras fault to the east (Silva Junior et al., 2014). This group is interpreted as shallow platform sediments deposited in a

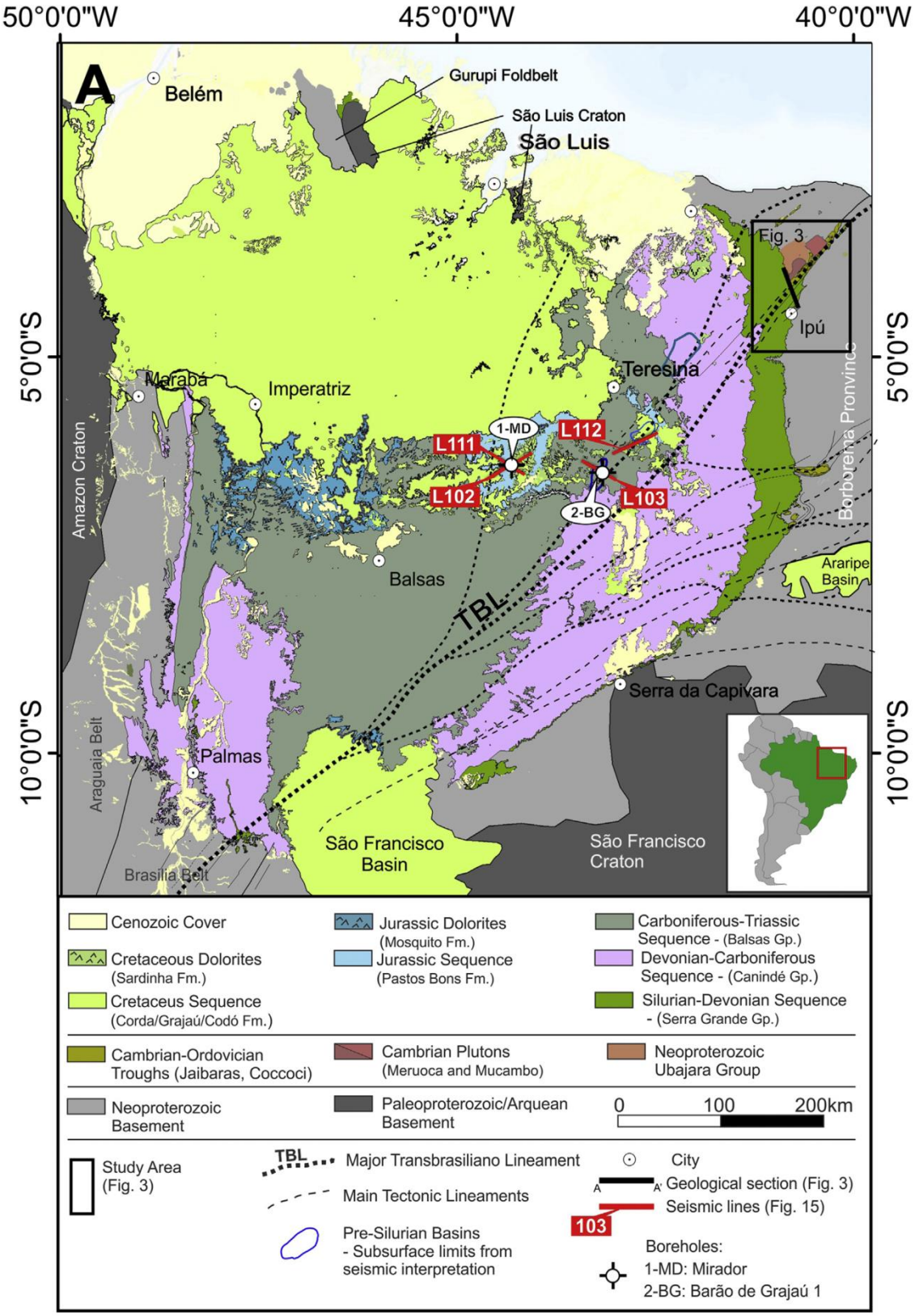

Fig. 2. Parnaiba Basin Geological Map (modified from 1:1M geological maps of the Geological Survey of Brasil - CPRM, 2004). The main tectonic lineaments related to the Transbrasiliano Lineament and to the Borborema Province were proposed by Cordani et al. (2016). Black rectangle and black line show the location of the study area (ca. 20.000 km^2) and the geological section, presented in Fig. 3. The red lines represent the location of the interpreted seismic profiles and the white dots, the location of the related boreholes. (For interpretation of the references to color in this figure legend, the reader is referred to the Web version of this article.)

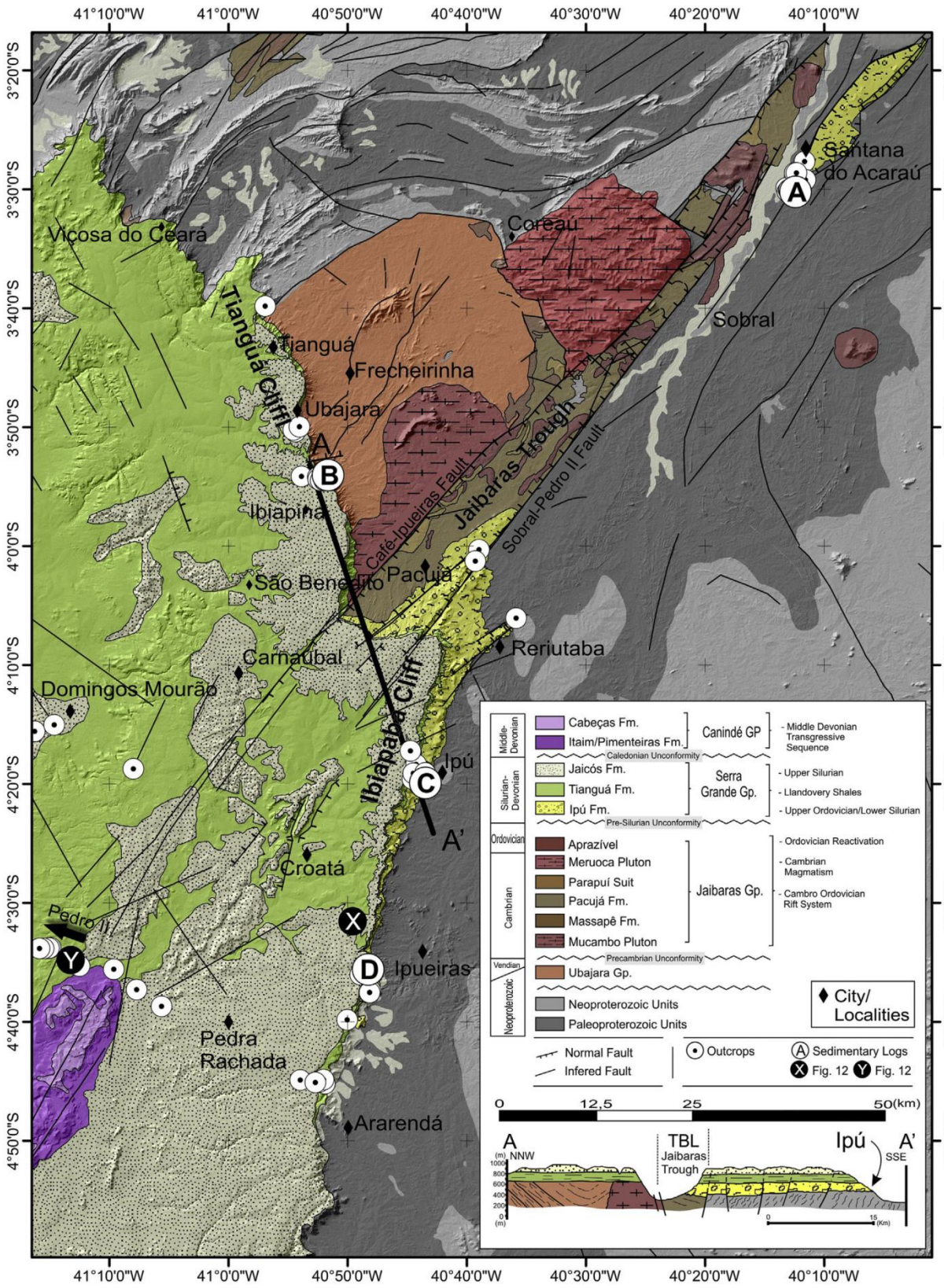

Fig. 3. Geological map of the study area along the eastern border of Parnaiba Basin and NNW-SSE cross-section (A-A'), showing Neoproterozoic Ubajara Group and Cambro-Ordovician Rift Sequences of Jaibaras Group covered by the Silurian Sequence (Serra Grande Group) and the Devonian Carboníferous Sequence (Canindé Group). White circles with dots represent visited outcrops, circles with letters A, B, C and D are outcrop logs, shown in Fig. 4. Black circles with letters X and Y represent outcrops shown in Figs. 12 and 13. Some outcrops shown along the text are referred on the map by the City/Localities names.

transpressional setting related to the Brasiliano tectonic events (Oliveira and Mohriak, 2003).

The Cambro-Ordovician Jaibaras Group (JG) (Fig. 3; Oliveira and Mohriak, 2003) is the main graben exposed in the NE margin of the Parnaiba Basin (Morais Neto et al., 2013; Oliveira and Mohriak, 2003; Quadros, 1996). Other similar grabens of the same age are identified in the eastern PB: Jaguarapi (NE-SW), Cococi (E-W) and São Julião (E-W) (Fig. 3). According to Oliveira and Mohriak (2003), the JG consists of continental immature siliciclastic sediments deposited in areas of unstable relief, with upwards decrease in tectonic activity. It is divided into three units. The basal Massapê Formation is characterized by fan polymictic clast-supported conglomerates, with basement angular fragments (including the Ubajara Group) and coarse-grained sandstone with debris and mud flows deposits. The distal portion of such alluvial fan is represented by reddish brown sandstones, siltstones and shales of the Pacujá Formation. The uppermost Aprazível Formation is composed by polymictic conglomerates with clasts of Cambrian plutonic rocks, interpreted as a sin-tectonic sequence, deposited during sinistral strike-slip reactivations of Café-Ipueiras Fault (Fig. 3) in the Lower Ordovician (Oliveira and Mohriak, 2003). Coeval to the JG deposition, there are at least four magmatic events of Cambro-Ordovician age (Coreaú Dike Swarm, Mucambo and Meruoca plutons and the mafic Parapuí Suite), suggesting a continental rift basin type for the Jaibaras graben, due to the presence of bimodal magmatism (Oliveira and Mohriak, 2003).

Therefore, the faults within the Transbrasiliano Lineament such as the Café-Ipueiras and Sobral-Pedro Segundo II, observed in the study area (Fig. 3), experienced reactivation episodes since Late Neoproterozoic-Cambrian, resulting in the deposition of the two aforementioned Pre-Silurian sequences, and even later during the opening of the Equatorial Atlantic ocean (Juro-Cretaceous; De Castro et al., 2016). According to the isopachs maps from Góes and Feijó (1994) and Tozer et al. (2017), the TBL seems to have influenced the Paleozoic sedimentation of Parnaiba Basin, since the depocenters of Serra Grande and Canindé groups in the eastern part of PB are aligned to the NE-SW TBL trend. From Pennsylvanian (Carboniferous) to Jurassic, although, the PB presents a more concentric sedimentation pattern, resulting in the basin actual shape (Góes and Feijó, 1994; Vaz et al., 2007).

2.1. The Silurian Sequence (Serra Grande group)

The Ordovician-Silurian Sequence was first recognized by Small (1914), who encompassed sandstones, conglomerates, and calcareous deposits of the northeastern edge of the Parnaiba Basin in the so-called Serra Grande Series. Kegel (1953) then postulated the Serra Grande Formation and documented an angular unconformity between this thick sandstone succession and the calcareous strata, formally encompassed in the Neoproterozoic Ubajara Group. This succession was elevated to Group category by Carozzi et al. (1975). Caputo (1984) proposed an estimated thickness range between 200 and 900 m for the SGG, based on borehole data and subdivided it into three formations: Ipu, Tianguá and Jaicós, described below.

- The basal Ipu Formation covers the Precambrian basement and Cambro-Ordovician sequences. It is composed of layered sandstones, massive and bedded conglomerates rich in quartz pebbles, interpreted to be deposited in braided rivers and alluvial fans systems. The maximum thickness is 300 m, in the northeastern sector of the basin (Caputo and Lima, 1984). In addition polymictic diamictites are interpreted as proximal glacial deposits (Caputo and Lima, 1984; Metelo, 1999). These possibly relate to the Upper Ordovician glaciation observed in the northern Gondwanan basins (i.e. Tchit Group, see Villeneuve, 2005; Caputo and Lima, 1984; Grahn and Caputo, 1992; Hambrey, 1985; Torsvik and Cocks, 2011; Villeneuve, 2005) and in the Table Mountain Group of the South African Cape Basin (Rust, 1973). According to Caputo and Lima (1984), the Ipu Formation is non-fossiliferous. Great exposures of this formation is observed in Serra da Capivara, SE margin of PB (see Fig. 2). According to Hasui (2012), SGG is locally represented only by the Ipu Fm., which unconformably overlies the metamorphic basement and is covered by the Canindé Group (Devonian). It is described as a coarse-grained trough cross-stratified sandstone in the base abruptly shifting in the top to a polimythic clast-supported conglomerate with horizontal stratification (Capivara facies). This facies possibly indicates a modification in the sedimentation regime, related to syntectonic alluvial fan deposit, with some glacial influence.
- The Tianguá Formation consists of at least three members, from base to top: (1) black shales and gray silty shales; (2) fine to medium sandstones interbedded with siltstones and shales; and (3) green to light gray siltstones with shales (Caputo and Lima, 1984). In subsurface, it reaches 380 m of maximum thickness, with an average of 150 m. This formation is interpreted to be deposited in a shallow marine environment, as attested by the occurrence of acritarchs and chitinozoans (Caputo and Lima, 1984; Grahn et al., 2005; Grahn and Caputo, 1992). The palynological content, added to the graptolite biozone, constrain alone the age for the entire SGG, positioning the Tianguá Formation at the Middle-Llandovery stage, Early Silurian (Caputo and Lima, 1984; Grahn et al., 2005; Grahn and Caputo, 1992; Le Hérissé et al., 2001).
- The Jaicós Formation conformably covers the Tianguá Formation in a gradational contact. It comprises quartz rich sandstones and conglomerates, with very scarce siltstones and shales. The average thickness of Jaicós Formation is 200 m, with a maximum of 400 m, measured in subsurface (Caputo, 1984). The paleoenvironments are interpreted as braided channels, alluvial fans and deltaic systems draining toward the north (Vaz et al., 2007). Grahn et al. (2005) described palynomorphs from the latest Pragian or earliest Emsian (Lower Devonian) at the uppermost beds, proposing a long period (~40 m.y.) of sedimentation for the Jaicós Formation (Llandovery to Early Emsian). The contact between Jaicós and the overlying Itaim Formation (Canindé Group, Devonian) is marked by an Early Devonian regional unconformity, well documented in geological maps and related to the Caledonian Orogeny, according to Vaz et al. (2007).

3. Surface data analysis

The Ordovician-Silurian sequence is best exposed on the eastern border of the Parnaiba Basin (Fig. 2). In Fig. 3, we present the results of the field work near the cities of Tianguá, Ibiapaba, Ipu, Ipueiras and Santana do Acaraú (Ceará state), and Domingos Mourão and Pedra Rachada (Piauí state), where the border of Parnaiba Basin is elevated up to 900 m above the sea level, representing a cliff landform type (Fig. 6A). We have mapped the area in 1:100.00 scale, defining mainly the contact between the three lithostratigraphic formations of Serra Grande Group, which are still poorly constrained in the available maps of the Geological Survey of Brazil (CPRM; Angelim et al., 2004; Vasconcelos et al., 2004; Silva Junior et al., 2014). The outcrops locations are presented in the map, as well as in a schematic section (A-A' in Fig. 3), which will be discussed in detail in topic 5 of this paper.

The detailed description of the sedimentary facies and the facies associations observed within Serra Grande Group are presented below, followed by its lithostratigraphic analysis, and the interpretation of depositional processes. Detailed sedimentary logs were obtained at 1:50 scale from 14 profiles, however are best represented by the four profiles A, B, C and D in Fig. 4 (location in Fig. 3) that together they represent 200 m of the SGG, registered in strategic outcrops with good exposures.

3.1. Facies descriptions

The observed facies within the Serra Grande Group are presented and described in Table 1, classified according to grain size, texture and sedimentary structures, following the nomenclature of Miall (1996) and

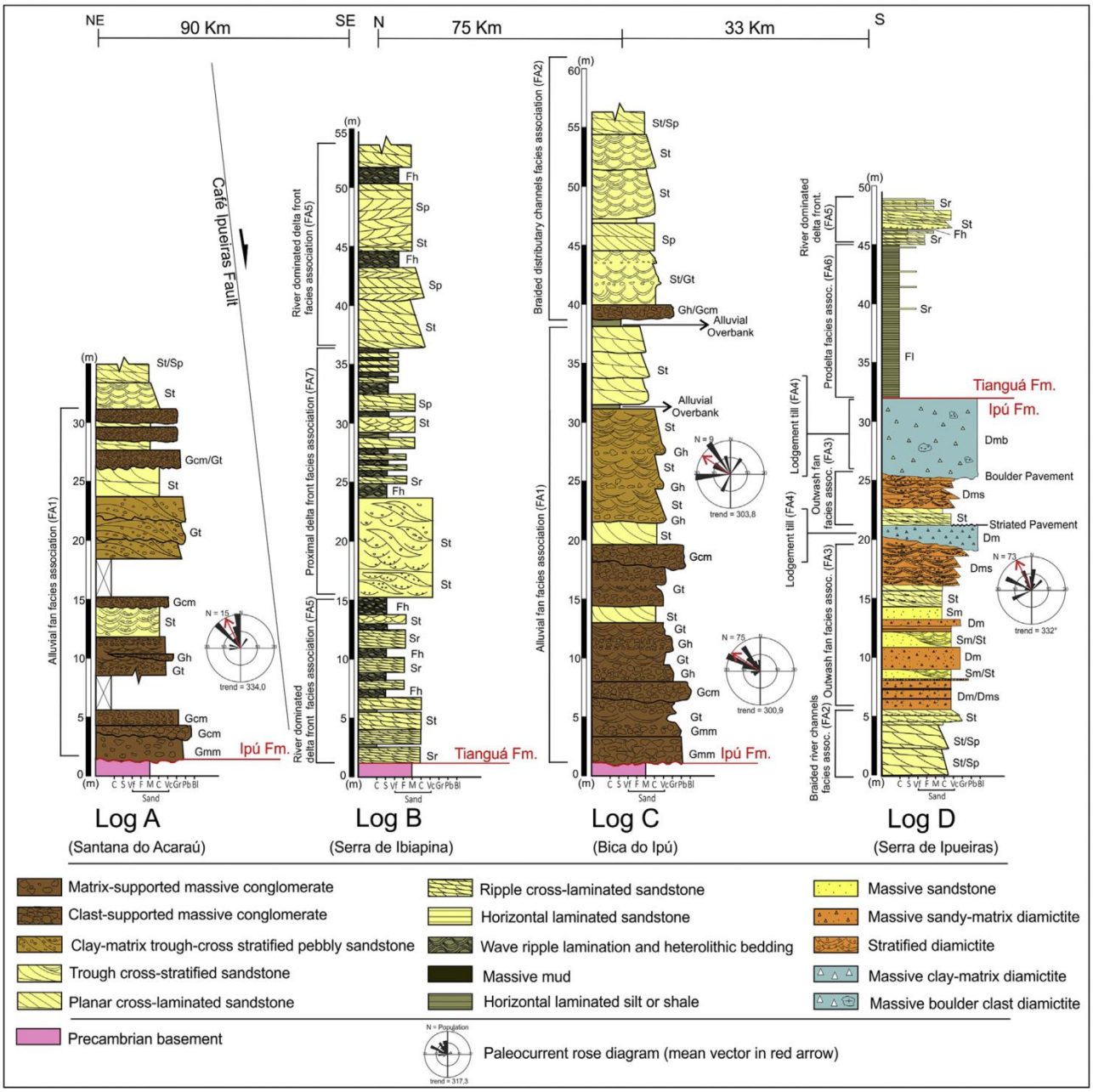

Fig. 4. Sedimentary logs and description of facies association (Fig. 3 for location). Log A: Outcrop in Santana do Acaraú location, close to CE-179 road. Note that alluvial fan facies association is above Precambrian basement. Log B: Outcrops in CE-253 road, between Caiçara (Ceará State) and Ibiapina (Ceará State). Note that shoreface facies association of the Tianguá Formation is directly above the Precambrian basement. Ipu Formation is absent in Log B, possibly because it is limited by Café Ipueiras Fault, active during deposition (see section A-A' in Fig. 3) or it is discontinuous due to paleodepressions. Log C: Outcrop in Ipu municipality (Ceará), in the Bica do Ipu waterfall; Log D: Outcrop in the road cut of CE-257 between Ipueiras (Ceará) and Croatá (Ceará). See Table 1 for facies code and explanations.

Eyles et al. (1983). The facies were then assigned to seven facies associations, corresponding to sub-environments, identified in the last column of Table 1: alluvial fans (FA1), braided river channels (FA2), outwash fans (FA3), lodgment till (FA4), prodelta (FA5), river dominated delta front (FA6) and river dominated proximal delta front (FA7).

3.2. Facies associations

3.2.1. Alluvial fans facies association (FA1)

The alluvial fans facies association (FA1) was observed in the outcrops of Santana do Acaraú (Fig. 5; Log A in Fig. 4; Fig. 3 for location), Bica do Ipu (Base of log C in Figs. 4 and 7A), Ibiapaba cliffs, and between Reriutaba and Pacujá (Fig. 3). In these locations, FA1 is directly overlying the Precambrian basement (log C, Fig. 4), representing the basal section of the Ipu Formation and it grades laterally and vertically to Braided River Channels facies association (FA2).

The basal FA1 is composed by clast and matrix-supported massive conglomerates with polymictic angular to sub-rounded clasts of pebbly size, gray coarse sandy matrix (Figs. 5A and 6B). Some of the clasts are striated and polished (Fig. 5B) and some has a flatiron shape. Above it, a group of amalgamated, irregular to tabular beds of stratified conglomerates with trough and planar cross-bedding stratification (Gt and Gp in Table 1; Fig. 5C, F and Fig. 6C), arranged in layers up to 2.0 m thick, some with lobate pinching out geometry. Thick to thin lenses (0.1–1.0 m) of coarse trough stratified sandstones, with dispersed pebbles following the trough lamination (St in Table 1) occurs interlayered

Table 1
Facies codes, description, and interpretation with respective facies association code (according to Miall, 1996 and Eyles et al., 1983).

Code	Facies	Structures	Interpretation	Facies Association
Gmm	Matrix-supported massive gravel.	Massive or weak grading.	Plastic debris flow (high-strength, viscous).	FA1
Gcm	Clast-supported massive gravel.	Massive.	Pseudoplastic debris flow (bedload, turbulent flow).	FA1, FA2
Gh	Clast-supported crudely bedded gravel.	Horizontal bedding, imbrication.	Longitudinal bedforms, lag deposits, sleeve deposits.	FA1, FA2
Gt	Gravel stratified.	Trough cross-stratifications.	Minor channel fill.	FA1, FA2
Dmb	Massive diamictites with boulders, mainly sandy matrix and deformed shearing planes.	Massive or incipient trough cross-stratifications.	Debris flow originated by meltwater plumes, in a proglacial glacier advance.	FA4, FA5
Dmm/Dmm (s)	Massive matrix-supported diamictites. (s) when sandy matrix.	Massive or incipient stratification.	Debris flow or deposition by rain-out in subaqueous bodies and meltwater plumes debris flow.	FA4, FA5
Dms	Stratified diamictites.	Trough cross- stratification and incipient planar lamination.	Debris flow, deposition of subaqueous outwash channels.	FA4
St	Sand, fine, to very coarse, may be pebbly.	Solitary or grouped trough cross-beds.	Sinuous-crested and linguoid (3-D) subaqueous dunes. ((l) subcritical flow).	FA1, FA2, FA3, FA4, FA6,
Sp	Sand, fine, to very coarse may be pebbly.	Solitary or grouped planar cross-beds.	Transverse and linguoid bedforms (2-D) subaqueous dunes.	FA1, FA2, FA3, FA4, FA6,
Sl	Sand, fine to very coarse.	Solitary or grouped low angle trough cross-bed ($< 15°$)	Scour fills, humpaback or washed-out dunes, antidunes	FA1, FA2, FA3, FA4, FA6
Sh	Sand, fine, to very coarse may be pebbly.	Horizontal lamination parting or streaming lineation	Plane-bed flow (critical flow).	FA2, FA3, FA4, FA6,
Sm	Sand, fine, to very coarse may be pebbly.	Massive or faint lamination.	Sediment-gravity flow deposits.	FA2, FA3, FA4, FA6,
Sr	Sand, very fine to coarse.	Ripple cross-lamination	Ripples migration (lower flow regime).	FA6, FA7,
Fl	Very fine sand, silt, mud and black shales.	Fine lamination or very small ripples.	Alternation between wave activity and decantation of suspensive charge in overbank or tidal influenced deposits.	FA6, FA7,
Fh	Sand and mud in heterolithic bedding.	Wavy, linsen and flaser bedding, small ripples.	Alternation between wave activity and decantation of suspensive charge.	FA6, FA7,

with conglomerates (Fig. 6 C). The middle part of FA1 is characterized by an alternation of pebbly sandstones with trough cross-bedded (St) and clast-supported conglomerates with imbricated pebbles (Gh). The sandy facies (St) present low to high angle sigmoidal bedded stratifications (Fig. 6E) and are organized in fining upwards layers ranging from 0,1 to 1 m thick, truncated by layers of massive (Gcm) or stratified (Gt) clast-supported conglomerates (Fig. 6F), and progressively thickening toward the top (up to 1,5 m thick). The middle to upper part of FA1 predominates poorly sorted coarse to granular sandstones with horizontal and trough cross stratifications (Sh and St in Table 1; Fig. 6E; Fig. 7D and E), organizes in thinning upwards sets, some with internal fining up and others with coarsening up patterns. Conglomerates tabular layers are less frequent at the middle to the top sections, and some presents thickening up pattern in the transition from sand to clast-supported conglomerates. Both of these latter facies present clay matrix and polymictic grains and clasts. To the top, layered sandstones are stacked in co-sets reach up to 5 m in thickness and are internally arranged in sets of 0.1–0.5 m thick, limited by northwestwards gently inclined to horizontal surfaces with paleocurrent pattern towards NW (see rose diagrams in log A and C on Fig. 4).

Nearby Reriutaba city, a 10-m-wide brecciated zone controlled by high angle ENE-WSW faults occurs related to FA1, as shown in Fig. 7. The sedimentological texture of FA1 is masked by the tectonic brecciated texture. There are angular clasts composed by fragments of quartz sandstones and conglomerates, still preserved, similar to the observed FA1. In Santana de Acaraú location, there is also evidence of tectonic episodes affecting the sediments of FA1. Note in Fig. 6F, the sandstone layers (St) tilted to NW.

The FA1 assemblage resembles a scarp-related alluvial fan (Allen, 1983; Barrier et al., 2010; Leleu et al., 2009 Stanistreet and McCarthy, 1993; Miall, 1996) characterized by the combination of mass gravity flow and tractive currents. The basal paraconglomerates, described in both Ipu and Santana do Acaraú localities, resemble typical facies of gravel gravity flows similar to the “fanglomerate” (steep fan deltas) exemplified by Blair and McPherson (1994). However the lack of preserved geomorphological features does not help to conclude the analogy to Blair and McPherson (1994) model of a steep fan delta. In the other hand, tabular layers of stratified amalgamated conglomerates deposited just above the latter facies, similar to GB architectural element from Miall (1996), associated laterally with lenses of coarse sandstones, in SB, CH or SG elements (Miall, 1996), suggest similarities with gravel braided channels deposits, while GB (gravel bars) were developed by migration and avulsion of gravel channels. It does explain the continuous, tabular (sometimes irregular) thick beds of conglomerates in the mentioned outcrops. Miall (1996) also describe that sandy macroforms SB and CH must occurs interbedded with gravel macroforms, representing slack-water deposits, such as abandoned channel fills within the context of braided gravel deposits, this must be the example of the intercalation of Gt, St and Gh facies shown in Fig. 6 C. Thin beds of clast-supported massive (sometimes imbricated) conglomerates (Gh) are interpreted as sheet flood deposits formed by dense hydrodynamic unconfined flows, while clast-supported layered conglomerates - braided gravel channels - are associated to confined hydrodynamic flows in distributary channels (Allen, 1983; Miall, 1996; Stanistreet and McCarthy, 1993), also described as distributary gravel channel bars in a context of an alluvial fan system by Miall (1996). Thus, the matrix-supported massive conglomerates restricted to the base of this facies association are here interpreted as proximal facies of such fans, where gravitational processes are predominant, reinforced by the nature of the clasts, followed by superimposed gravel bars and distributary braided channels within a alluvial fan.

The few layers of fine-grained sediments with horizontal laminations might be interpreted as overbank or non-channelized fine deposits (Stanistreet and McCarthy, 1993; Miall, 1996). The sandy facies that predominates in the middle and upper parts of FA1 is possibly related to the development of braided river distributary channels in distal parts of

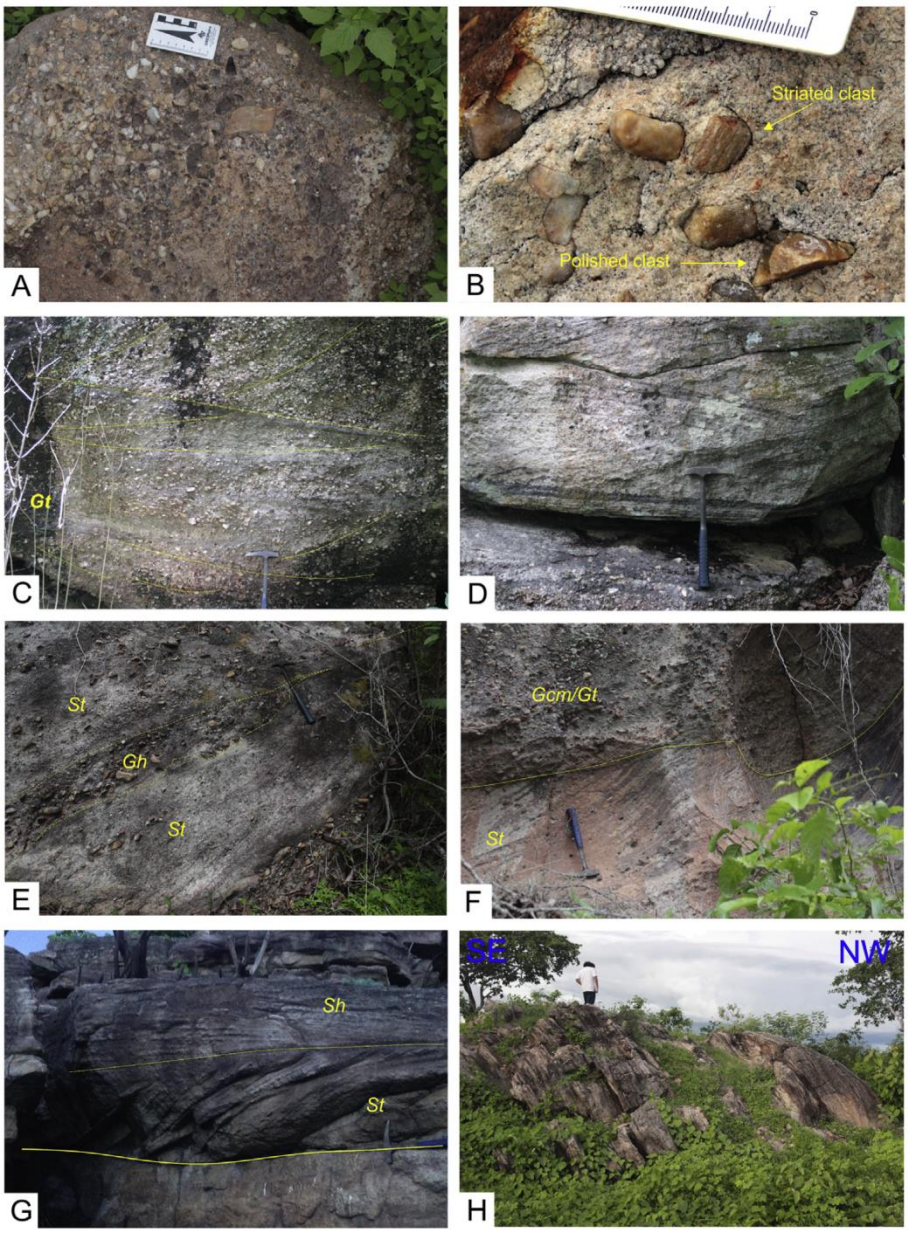

Fig. 5. (A) Paraconglomerate of the base of Log A (Fig. 4; Fig. 3 for location). Note the chaotic distribution of clasts, poorly selected, angular, faceted or well rounded. (B) Striated and flatiron shape clasts within the basal paraconglomerates of Log A. (C) Mid part of Log C, with stratified pebbly polimithic conglomerates (Gt). (D) Stratified pebbly sandsontes, organized in sets of trough cross-bedding and plane cross-bedding. Note the erosional surfaces between these sets. (E) Mid part of Log A, showing intercalations of pebbly sandstones (St) and crudely stratified conglomerates (Gh), with high angle sigmoidal cross-stratification. Both facies present erratic boulders and block size clasts. (F) Thickening upwards cycle within interleaved pebbly sandstones, (with erratic block size clasts) and crudely stratified sandstones (occasionally with well-marked cross-stratification). Note de abrupt erosional surface between the two packages (gravel bars avulsion) (G) Top of Log C, predominance of stratified sandstones, with trough cross-stratification and planar horizontal stratification. (H) Tilted sandstones close to Log A dipping at high-angle, due to faulting.

the alluvial plains (Stanistreet and McCarthy, 1993; Miall, 1996). Although the main stacking pattern of this facies association is normally thinning upwards (Logs A and C Fig. 4), coarsening and thickening upwards patterns are also recurrent in the middle portion of FA1, corroborated by the return of gravel bars (i.e. conglomerates), where some of Gt and Gh facies present matrix composed by clay and sand grains. This thickening must be related to the increase of gravel channel avulsion, due to fan lobes progradation (De Celles, 1991; Harvey et al., 2005). These authors have also emphasized that recurrent discharges of coarse sediments are intimately related to tectonic fault reactivations/episodic movements. The recurrence of polymictic clasts in the middle part of FA1 and the presence of a brecciated zone within FA1 (Fig. 7) also contribute to the interpretation of uplift pulses of the source area in a tectonic active fault scarp paleogeomorphology, reworked by episodic hydrodynamic flows and debris flows, to the top (Blair and McPherson, 1994; Stanistreet and McCarthy, 1993).

The low content of fine sediments and the fining upwards successions interrupted by immature conglomerate layers, suggest an arid to semi-arid paleoenvironment (Stanistreet and McCarthy, 1993; Harvey et al., 2005; Blair and McPherson, 1994). Finally, the presence of striated pebbles indicates either a glacial origin for FA1 or that these clasts might have been inherited from nearby melted and eroded glaciers.

3.2.2. *Braided river channels facies association (FA2)*

The braided river channels facies association (FA2) is widely recognized in the study area, composing all three formations of the SGG, particularly within the Jaicós Formation. It consists of intercalations of moderately to poorly sorted sandstone beds with dispersed pebbles and conglomeratic layers with rounded to subangular pebbles and sparse lens of fine-grained sandstones and subordinated siltstones. The sandy facies are predominant in FA2, with trough (St), planar (Sp) cross stratifications with minor horizontal (Sh) laminations. Trough and planar cross stratified sandstone bodies range from 1 to 5 m thick and are internally arranged in 0.1–1.0 m thick tabular sets, limited by planar to gently inclined and concave-up erosive surfaces (Fig. 9). There are evidence of lateral accretion packages within wide channels, with tens of meters of length (Fig. 8A) but downstream accretion bedforms are predominant mostly in medium to small size channels with

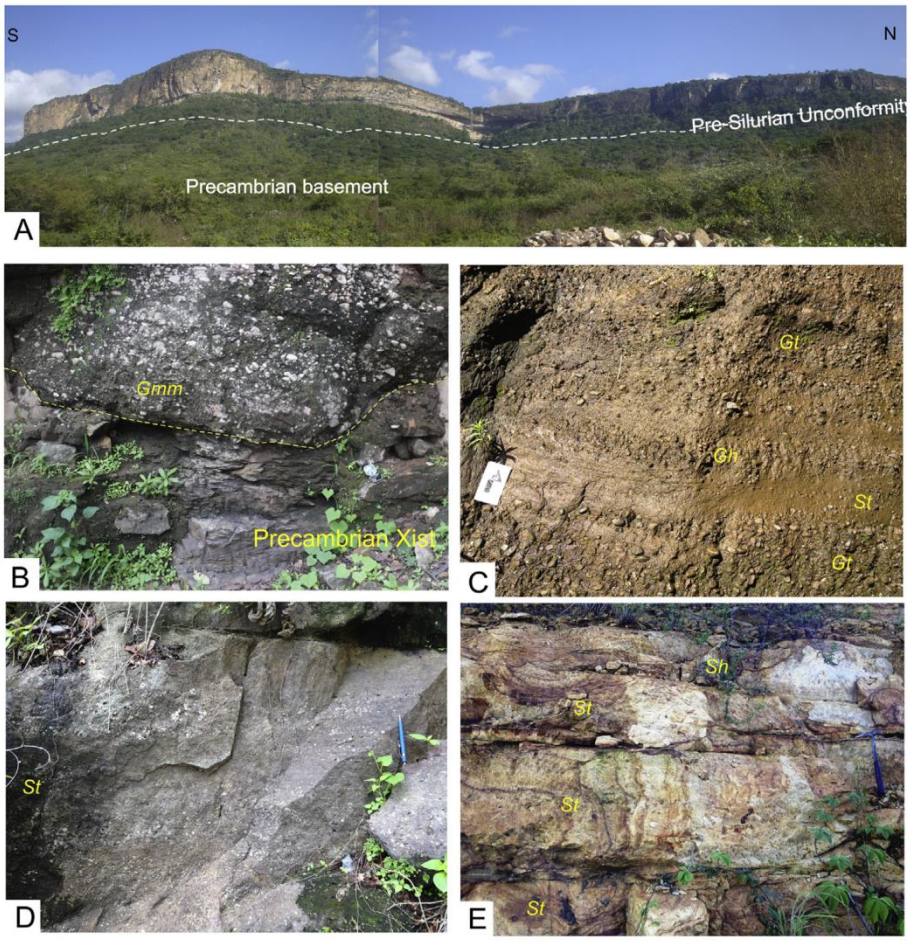

Fig. 6. (A) Sandstone cliff, c.a. 113 m of Bica do Ipu (Serra de Ibiapaba) in Ipu municipality (see Log C in Fig. 4; Fig. 3 for location). White dashed line shows the estimate Pre-Silurian unconformity. (B) Para-conglomerate covering Precambrian metamorphic unit in Bica do Ipu waterfall. C) Sedimentary stack of stratified conglomerates (Gt), crudely stratified with imbricated clasts conglomerate (Gh) and stratified pebbly sandstones. (D) Mid part of Log C, quartz rich stratified sandstones in thinning upwards cyles. (E) Top part of Log C tabular layers of stratified sand-stones, coarse to medium grain size, without any pebbles and conglomerate levels.

0.5–1.5 m width (Fig. 8B). Levels of pebbles occurs at the base of stratified sets, sometimes with clast imbrication (Fig. 8C). Paleocurrents measurements show a unimodal pattern, with a predominant north-westwards direction (diagram in Fig. 8D). Rare metric layers of massive to trough-stratified matrix-supported quartz rich conglomerates (Gmm and Gt in Table 1) and scarce silty lens with planar to very low-angle cross lamination (Fl in Table 1) are also observed.

The planar and trough-cross stratified sandstones are organized in longitudinal bars and sand bedforms. Downstream accretion (predominant), lateral accretion and channel macroforms, added to basal pebbles accumulations and very low dispersion on paleocurrent pattern indicate 2D and 3D subaqueous dunes migration within braided channels. Massive or stratified conglomerates represent gravel bars bedforms. Horizontally laminated sandstones composing sand sheet macroforms of centimetric thickness relate to upper flow-regime and vertical accretion, migration and stacking of small dunes in shallow areas of active channels (Miall, 1977). Thin layers of very fine wavy laminated sandstone and siltstone (Sr and Fl) are interpreted as overbank deposits. In sum, FA2 is similar to the deep perennial sand-bed braided river model of Miall (1996). The low dispersion of paleocurrent directions, predominance of downstream accretion macroforms (check the example of Fig. 8), lack of fine-grained sediments and the progressively upwards decrease in the size of sedimentary structures suggest a low sinuosity, braided rivers depositional system.

3.2.3. Outwash channel facies association (FA3)

The outwash channels facies association (FA3) is recognized in the outcrop of Ipueiras Hill (log D, Fig. 4; location on Fig. 3), between Ipueiras and Croatá cities (Ceará state) (Fig. 3). This facies association is constituted by alternating sandstones and stratified diamictites, grading laterally and upward into massive diamictites, as presented in the base of log D (Fig. 5). In Fig. 9A and B, we show the distribution of facies along the Ipueiras outcrop. This facies assemblage is laterally equivalent to the upper part of Ipu Formation.

These sandy (St) and conglomeratic (Gt) facies are organized in fining-up successions, ranging from 0.3 to 0.5 m thickness, grading to stratified and massive diamictites (Dms and Dmm facies in Table 1). Stratified diamictite occurs with gray to yellow clay and sandy matrix with trough cross-stratification and small-scale residual channels structures (c.a. 1.0 m wide), divided into sets of approximately 40 cm and also arranged in fining-up sequences (Fig. 9C). The clasts are mostly of pebble size, angular to rounded, composed by quartz, feldspar and lithic fragments (gneisses, granites, volcanic and sedimentary rocks - Fig. 9C). Interbedded sandstones with horizontal laminations (Sh) and low angle cross-stratifications (Sl) occur in sheets-like layers about 0.1–0.3 m thick and 1–2 m wide, sometimes with a “boudin” shape (Fig. 9D). Massive diamictite occurs in lenses up to 1.0 m thick and varying from 1.0 m up to tens of meters wide. Light gray clay matrix rich in granules and pebbles, with sparse decametric angular to sub-angular block-size clasts, composed of lithic fragments is often observed (Fig. 9E). These clasts are rarely faceted and striated. Diamictites and sandstones are interdigitated and frequently bounded by irregular surfaces composed by thin (0.05 m thick), very fine-grained, laminated sandy and silty layers. The paleocurrent measurements within the stratified diamictites are dispersed, but in general paleoflows indicate a NNW trend (Fig. 5 log D).

According to Eyles et al. (1983), this type of deposit is interpreted as sediment loads carried by channelized cohesive flows of poorly sorted sediments trapped in glaciers and episodically discharged from melting ice during the retreat phase of a glacier. The sandy sheet-like deposits

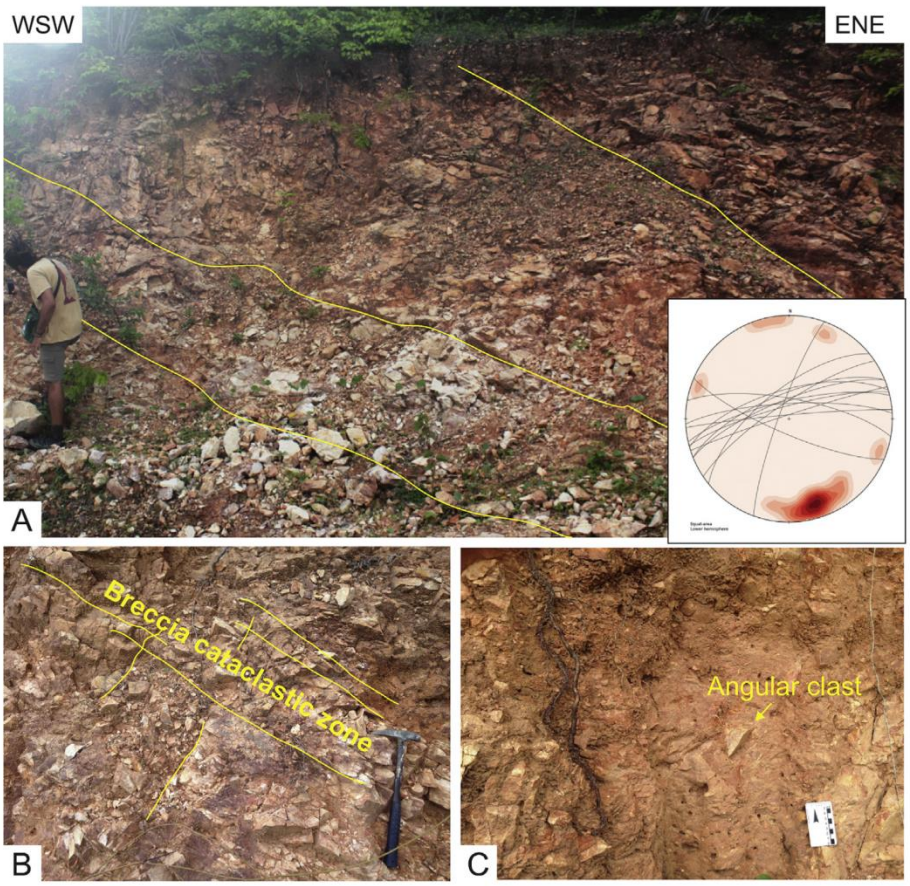

Fig. 7. (A) Brecciaed zones suggestive of scarp-related alluvial fan deposits near Reriutaba (Fig. 3 for location), stereogram shows the main ENE-WSW trend of fractures within brecciated zones, dipping at high angle to NW. (B) Breccia mainly composed by quartz sandstone fragments, yellow line shows perpendicular fracture zones within the cataclastic zone. (C) Breccia with argillaceous matrix and dispersed angular clasts, composed by fragments of quartz sandsontes. (For interpretation of the references to color in this figure legend, the reader is referred to the Web version of this article.)

can be interpreted as fluvial channels that are developed in upper flow regime to provide deposition on the defrost fronts of a glacier (Eyles et al., 1983). These deposits are covered by stratified diamictites with deformation structures in the sandy layers possibly caused by weight of the sedimentary load or shearing caused by ice slipping (Eyles et al., 1983; Eyles and Eyles, 1992). This process could also explain the appearance of boudinage in layers of sand (sand balls). Lenses of massive diamictite, bounded by irregular surfaces, can be interpreted as lodgment tills (Eyles et al., 1983). The contact between layers of stratified diamictite and sandstones is erosive and irregular, reinforcing the occurrence of cohesive flows. Thin levels with planar laminations, separating stratified diamictites, sandstones and massive diamictites can be interpreted as planar foliation generated by shearing of the superimposed sedimentary load. This indicates a glacier advance context, when melting snow comes from the glacier front during a glacier advance phase. These interbedded diamictites and sandstones are interpreted as outwash fans or outwash plains deposits (Eyles et al., 1983).

3.2.4. *Soft lodgment till facies associationl (FA4)*

Lodgment till facies association is recognized in the outcrop of Ipueiras (log D Fig. 4, location in Fig. 3). It is composed of massive diamictite rich in block-size clasts and is marked by the occurrence of boulders-size clasts (Dmb). It alternates with FA3, representing massive diamictites with lenticular and irregular layers described above, and are best represented by two thick beds of massive gray diamictites that extends throughout the Ipueiras outcrop (Dmb facies in Fig. 9A and B).

From the bottom to the top, the first thick bed (up to 4 m thick) has a lenticular geometry, with a maximum thickness of 4 m and pinching out to the west (Fig. 9A and B). It has white to gray clay rich matrix with pebbles and block-size clasts of lithic fragments of varied composition, inherited from the crystalline basement. The pebbles are angular to sub-rounded (Fig. 10A), and many show striations and faceted sides (Fig. 10B). The bounding surfaces of this first bed are irregular and erosive. The basal surface is marked by deformation plans in the overlaying layers and to the top, this massive diamictite bed is eroded by stratified diamictites (outwash channels - Fig. 10C). Only near the top of this first diamictite bed, one crudely striated pavement was identified.

The second bed (top Dmb facies in Fig. 9A and B) has tabular geometry that varies in thickness between 4 and 5 m. A boulder pavement marks the base of this upper diamictite bed, and deformed non-planar layers are also present (Fig. 10D). Its basal surface is erosive, irregular, and displace fragments of subjacent sedimentary rocks, as shown in Fig. 10E. In this upper diamictite bed, boulder size-clasts are frequent (Fig. 10E). The matrix is sandy to clay, gray in color. Striated (Fig. 10F), faceted, and polished clasts are also frequent. Laminated conglomerate lenses about 0.1 m thick, with a reddish color, occur randomly. Deformed and shear surfaces occurs within FA3 as well as foliation or irregular and discontinuous disjunctive plans, where block size clasts are accumulated (Fig. 10G). To the top, the limit is an abrupt contact with a 15 m thick unit of shale (Fig. 10E), considered as the lower part of the Tianguá Formation.

The massive diamictites with boulder size clasts are interpreted as debris flows and mass run out deposits under glacial conditions, similar to the lodgment tillites described by Eyles et al. (1983). The occurrence of boulders pavements and deformed layers reinforces the glaciogenic character of a glacier advancing till that fills the eroded relief caused by abrasion of ice, leaving rock fragments at the path and deforming subjacent non-consolidated sediments (Boulton, 1978; Carrivick and Russell, 1980; Ruszczyńska-Szenajch, 2001). Foliation and deformed surfaces, planar or non-planar, are commonly documented in glacial diamictites (Ruszczyńska-Szenajch, 2001). These structures are interpreted as the result of *glaciotectonic* activity due to "thrust" movements during a glacier advance (Eyles et al., 1983; Ruszczyńska-Szenajch,

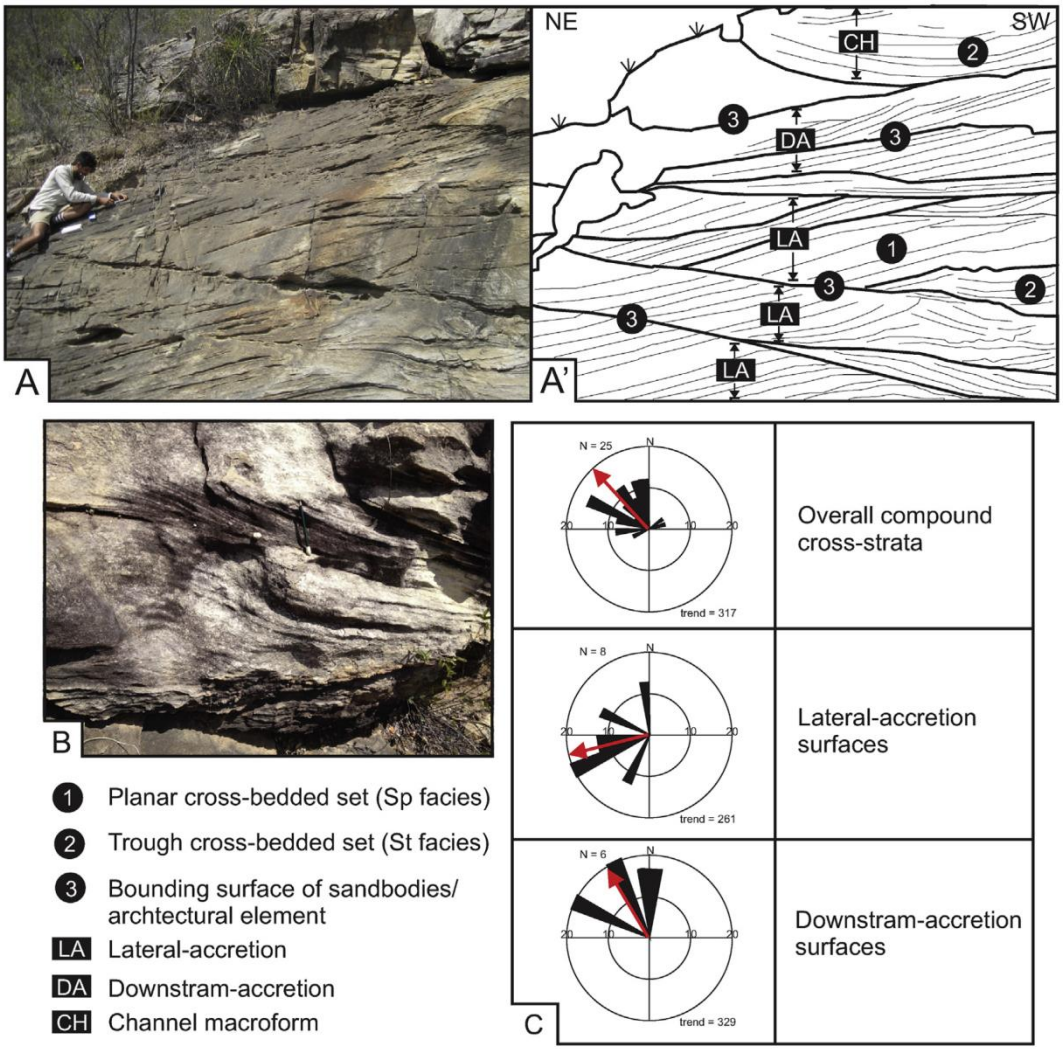

Fig. 8. Cross-bedded sandstone characteristic of the braided river channels facies association, exemple of Domingos Mourão outcrop (Fig. 3 for location) within the Jaicós Formation. (A) Planar and Trough cross-stratified sandstones organized in downstream and lateral accretion macroforms. Bounding surfaces are represented and the arrange of sandbodies are interpreted to the right. (B) Amalgamated braided channels and quartz granules accumulated in stratified lamination of St facies. (C) Rose diagrams of overall compound cross-bedded paleocurrent direction and orientation of sandbodies bounding surfaces, discriminated in Lateral-accretion surfaces and Downstream-accretion surfaces.

2001). Striated pebbles and displacement surfaces within the FA4 suggest the displacement of mass in entrapped sediments of the ice sheet. The association with outwash deposits suggests that these deposits were reworked by melting ice in glacier front (Eyles, 1993; Eyles et al., 1983). Laminated and massive lenses of reddish conglomerate can be interpreted as eskers deposits, high energy melting water that flows confined trough channels in the ice, producing deposition of sand and gravel conduits in elongated ridges (Eyles, 1993; Eyles et al., 1983).

Summarizing, taking into account the nature of clasts, the nature of matrix and the occurrence of foliation and shear plans, and also the association with outwash channels here we associated these diamictites and conglomerates to a soft lodgment till, following the nomenclature adopted by Ruszczyńska-Szenajch (2001).

3.2.5. *Prodelta facies association (FA5)*

This facies association was mapped at the top of the Ipueiras tilite (Log D, Fig. 4). The shale unit varies between 13 and 15 m in thickness, in tabular and horizontally continuous geometry (tens to hundreds of meters in length). The contact with the underlying tillites is sharp (Fig. 11A).

This facies association consists essentially of greenish gray to dark gray shales, with flat horizontal laminations (Fl) (Fig. 11C) and few millimetric levels of very fine-grained sandstone with ripple (Sr) and laminated siltstones. The shale has grains of sand dispersed in the matrix. To the top, shales grade upward into 0.1–0.3 m thick layers of fine-grained sandstones with ripples (Sr facies) (Fig. 11D) and some with sporadically bioturbation levels (Fig. 11B), grading progressively to heterolithic facies (Fh). At least two thickening up succession can be observed (Fig. 11A). The first shows the transition of dark shale grading upward into reddish and light gray very fine-grained sandstones. The second one is predominantly composed by siltstones interbedded with very fine-grained sandstones with low angle cross stratification (Sl) and ripple cross stratifications (Sr). This facies assemblage grades upward into thickening up beds to delta front facies association (described in next item).

This facies association is interpreted here as belonging to the lower portion of Tianguá Formation and was recognized superimposed on the proglacial deposits of upper Ipu Formation, in the outcrop of the Ipueiras Hill (Figs. 9–11; Fig. 3 to locate city of Ipueiras). The thick layer of dark shale indicates deposition of fine-grained sediments suspended in the distal areas of the platform and no evidence of waves or storm currents were documented, instead of, unidirectional structures

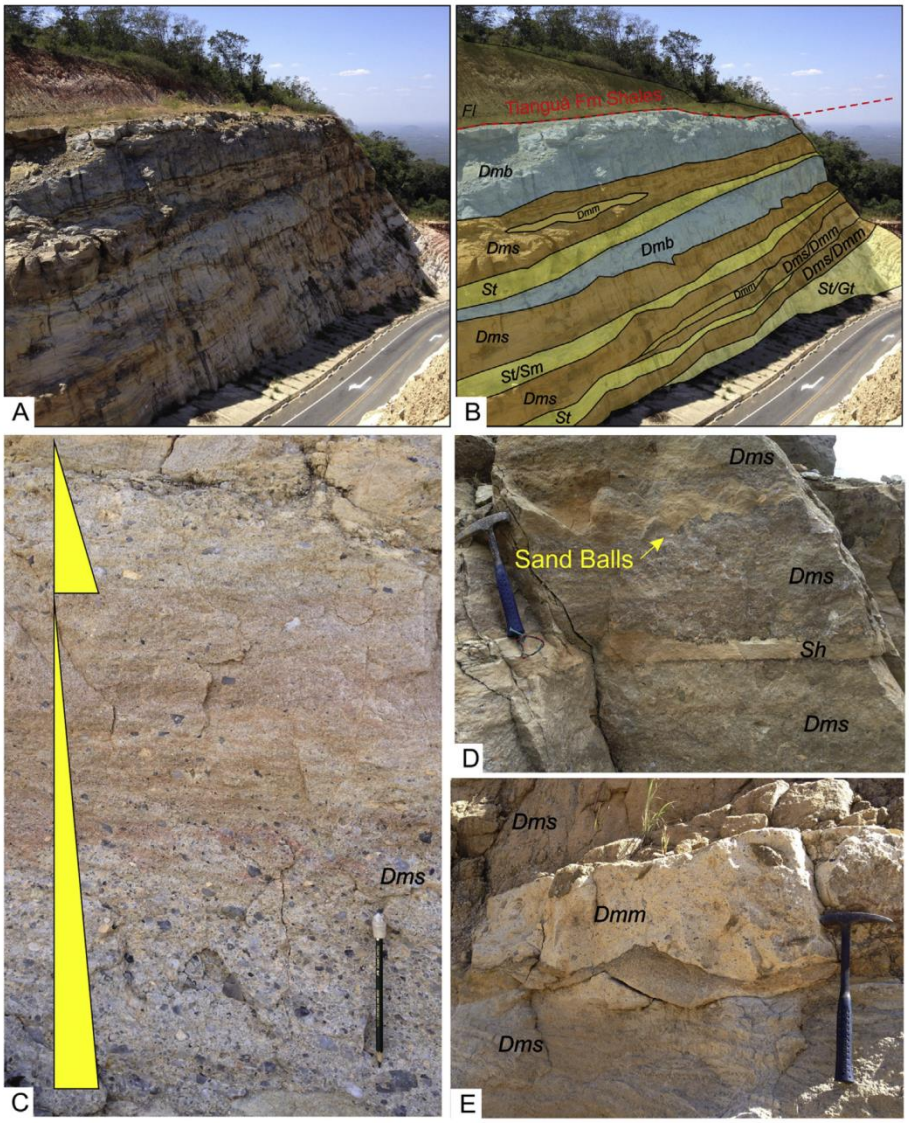

Fig. 9. (A) View of outcrop in CE-257 road cut (Log D in Fig.4; see Fig. 3 for location). (B) Interpretation of facies with pinching out geometry for the sandstones and the stratified and massive diamictites (St/Sm, Dms and Dmm). (C) Stratified diamictite with fining-up cycles as shown by yellow triangles. (D) Low angle/horizontal stratified sandstone (Sh) levels interleaved with stratified diamictites. Note the sand bolls geometry caused by deformation during deposition of Dms facies, due to sedimentary load and glacier advance. (E) Massive diamictite (Dmm) lenses within stratified diamictites. (For interpretation of the references to color in this figure legend, the reader is referred to the Web version of this article.)

are present in the sandy levels from the upper part, suggesting that these facies association can be interpreted as the distal portion of a fluvial dominated deltaic system (Bhattacharya, 2010). Layers of fine sandstones and siltstones can be interpreted as coastline sediments, brought by currents of distributary mouth bars. The upward thickening up bed pattern, reinforces the characteristic of a deltaic environment. The relationship with glacial deposits may explain the presence of grains of sand dispersed in the muddy matrix, since they may have been carried by fragments of ice floating above the water. However, no pebbly or block size dropstones were identified within the Tianguá Formation shale in a whole, which lead us to suppose that it was deposited during postglacial transgression. But considering the sharp and unconformable contact between the diamictites (Ipu Formation) and the basal shales (Tianguá Formation) the contact between this two units, in this outcrop, seems to be an unconformity.

3.2.6. River dominated delta front facies association (FA6)

The delta front facies association (FA6) is mainly observed in outcrops along the roadscuts of the Ibiapaba and Tianguá cliffs, represented in Log B (Fig. 4). It is also present in the road cut of CE-257, between Ipueiras and Croatá cities (Fig. 12, location in Fig. 3). The outcrop show in Fig. 12 is here considered as part of Tianguá Formation, that in association with proximal delta front and prodelta facies association, comprises a deltaic depositional system. For the northern portion of the study area, sandy facies with subordinated siltstones and shales are predominant and shaly facies of prodelta (FA6, described above) weren't recognized (Fig. 4).

FA6 is mainly composed by the intercalation of tabular layers of reddish to white fine-grained sandstones, laminated to massive siltstones and shales (Fig. 12A), frequently showing undulating laminations and heterolithic bedding, with overall thickness ranging from 5 to 15 m, and internally composed by 0.1–5 m thick layers, with wide lateral continuity of hundreds of meters. The sandy facies are mainly composed by well sorted quartz sandstones and preserves trough cross stratifications (St facies), mostly with low angle (Sl), horizontal and ripple cross laminations (Sh and Sr) (Fig. 12A and B). Intercalations of siltstones and shales occur in lenses of 0,01 to 0,1 m thickness, continuous for a few meters (Fig. 12C) or truncated by sandstones beds. Sandstones with trough and low angle trough cross-stratifications occur in sets and layers, ranging from 0.1 to 1.5 m with tabular to pinching-out geometry that extend laterally for a tens of meters (Fig. 12C), frequently with low angle cross bedding (Fig. 12C). In stratified sandstones the paleocurrent measurements are dispersed, but with a main (azimuth) vector to S-SE (see rose diagram in Fig. 12A). These sets of sandstones with trough and low-angle trough cross-stratification pass upward to horizontal stratified sandstones, arranged in a maximum of

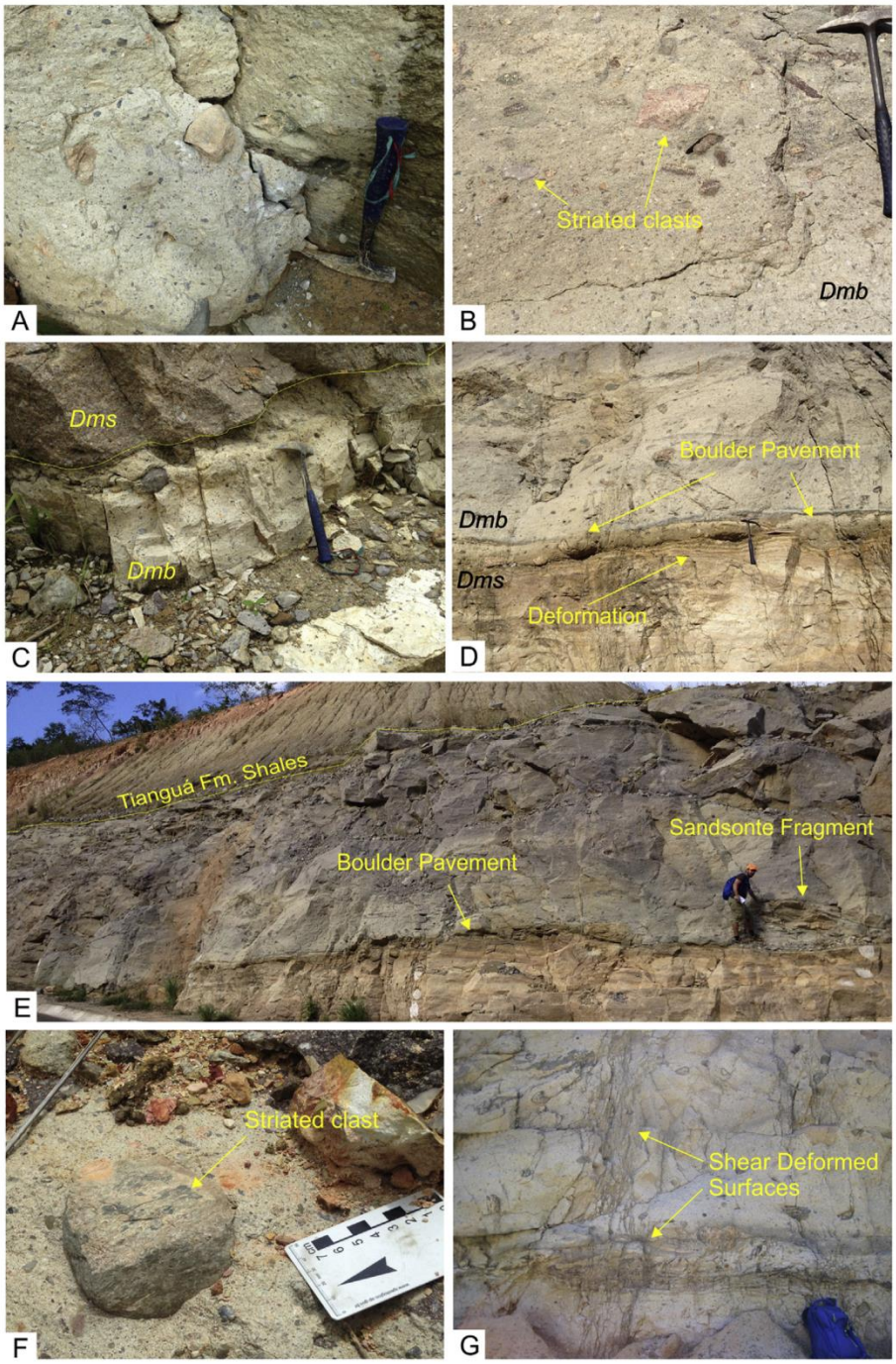

Fig. 10. (A) White clay/sandy matrix diamictite with block (sometimes boulders) clasts (Dmb). (B) Massive diamictite (Dm) with striated pavement and striated clasts. (C) Yellow line marks erosional contact between massive diamictite (bottom - Dmb) and stratified diamictite (top - Dms). (D) Contact between stratified diamictite (Dms) and massive diamictite with boulder clasts (Dmb). Note the deformed layers in Dms facies and boulder pavement in the contact. (E) Tabular bed of massive diamictite with boulder clast, note deformed layers in the underneath Dms facies, boulder pavement at the contact and to the left there is a boulder fragment of sandstone, possible of the Ipu Formation. (F) Striated gneiss clast in Dmb facies. (G) Shear deformed surfaces within the Dmb facies, indicating deformation during glacial advance. Note that in the bottom surface there is another boulder pavement. (For interpretation of the references to color in this figure legend, the reader is referred to the Web version of this article.)

0.3 m thickness and tabular geometry, bounded by flat and continuous surfaces. The beds of fine-grained sediments are predominantly composed of laminated siltstones, some with inverse grading and massive mudstones, interlayered with thin lenses of sandstones that forms wavy surfaces (Fig. 12B, C, D). Some cross-laminated sandstones beds (0.08–0.15 m in thickness) occur with load-clast structures, in concave up and down geometries (Fig. 12C). Load-casts are also present in minor scale lenses of reddish siltstones, interlayered with massive mudstones (left part of Fig. 12C).

Sandstones with trough cross-stratifications, tabular medium to thick layered (c.a. 1, 5 m), are interpreted as 3D dune migration due to the predominance of unidirectional flows possibly related to mouth bar current discharges (Bhattacharya, 2010). Low-angle cross-stratified to ripple cross lens-shaped thin layers of sandstones, with dispersive paleocurrent pattern, suggest deposition in shallow water radial mouth bars or distributary channels (Ahmed et al., 2014). Interlayered laminated inverse graded siltstones indicate an acceleration of sediments carried by hyperpycnal plumes during the river mouth flooding, followed by deceleration, depositing massive mudstones (Bhattacharya, 2010). The predominance of asymmetrical ripples in the thin lenses of sandstones suggests deposition in subcritical upper flow regime, whereas horizontal stratified tabular flat layers suggest deposition in upper flow high energy regime, both of these are related to unidirectional currents. The heterolithic intercalation between siltstones, mudstones and thin lenticular layers of fine sandstones can be interpreted as the combination increase and decrease of water discharge at the mouth bar. Soft sediment structures, as well as load-clasts, are commonly documented in river dominated deltas. It is caused by the

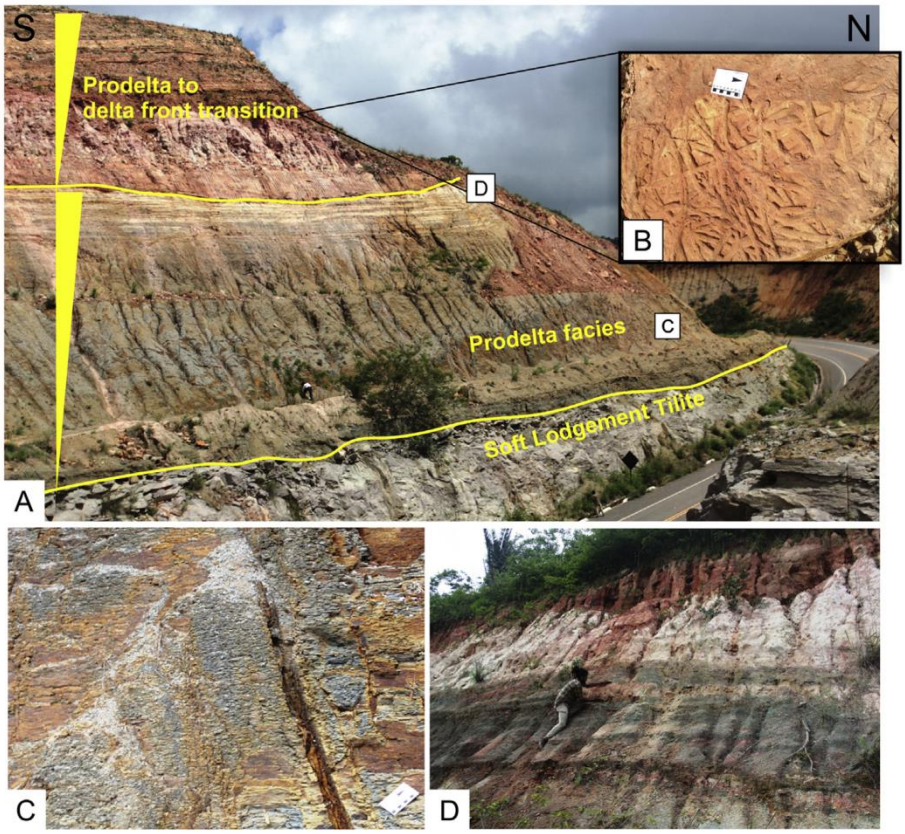

Fig. 11. Prodelta facies association in road cut CE-257 in Ipueiras Municipality (Fig. 3 for location, Log D). (A) Overall view of the dark green to gray shales in coarsening up cycles, grading to a delta front distributary channels of mouth bars deposits. The abrupt contact is shown in the bottom yellow line, between Ipueiras tillite and Tianguá black shales (c.a. 15 m thick). (B) Dark green shale, facies aspect. (C) Black shale grading to very fine sandstone (white layer), upper portion of prodelta facies association. The upper yellow line shows the transition of prodelta to river dominated delta front facies association. (For interpretation of the references to color in this figure legend, the reader is referred to the Web version of this article.)

deposition of overlaying heavier sand over mud not yet consolidated (Bhattacharya, 2010). Thefore, the interbedding and heterolithic nature, the predominance of unidirectional structures, the occurrence of radial mouth bars/distributary channels and the occurrence of load-clasts of this facies association, support the interpretation of a river dominated delta (Bhattacharya, 2010; Ahmed et al., 2014).

3.2.7. River dominated proximal delta front facies association (FA7)

This facies association occurs in outcrops along the road BR-404, near the border between the states of Piauí and Ceará, in the municipality of Pedro II (Fig. 13, and Fig. 3 for location) and near the Tianguá Cliff (middle portion of Log B in Fig. 4). The panel shown in Fig. 13 is the best representation of FA7.

This facies association consists of medium to fine-grained, moderately to well sorted sandstones in packages of up to 6 m thickness that overlaps layers of heterolithic facies (Fig. 13A and B). From the bottom to the top, this facies succession is represented by very fine-grained sandstones alternating with siltstones of light gray color. These fine sediments are organized in heterolithic beds with undulating bounding surfaces, whereas sandstone layers show asymmetrical ripples (Sr) and low angle (Sl) structures (Fig. 13C), and the siltstones have mainly horizontal to undulating laminations. Above it, in a sharp contact (Fig. 13B), there are sandstones with sigmoidal bedforms – this is observed in Tianguá Cliff and in Pedro II outcrop (Fig. 4 for Tianguá Cliff log and Fig. 13A outcrop, respectively) - in trough (St), low angle (Sl) and planar (Sp) cross stratifications, with less horizontal stratified (Sh) and climbing ripples (Sr) strata. (Fig. 13A and B). In the outcrop of Pedro II, three bounding surfaces were recognized (red lines in Fig. 13A). The bottom one separates the heterolithic facies from the stratified sandstone sets with that occurs in lobate geometry with thicknesses up to 3 m and high angle sigmoidal cross-bed. The middle surface is separating these last ones from a co-set of amalgamated low angle trough cross-stratified sandstones (Sl) organized in sets of 0.3–1 m thick laterally continuous for tens of meters that forms shallow channels structures, similar to distributary channels described in delta front facies association. To the top, a third bounding surface separates these last sets from sets of fine to very fine planar cross stratified sandstones. To the top of this succession, heterolithic facies occurs again, interbedded with dark gray siltstones and shale.

Sandy facies with lobate geometry are interpreted as mouth bars deposits in a context of a delta front. Paleocurrent directions are disperse and distinct for each macroform, indicating channels migration during deposition of successive deltaic lobes (Bhattacharya, 2010; Walker and Plint, 1992). The succession shows the repetition of an overall coarsening and thickening upward trend characteristic of progradation in which river mouth deposits prevail in sigmoidal shape macroforms geometry, overlaying a low energy system, represented by heterolithic siltstones sandstones. This high angle sigmoidal-shape macroform shown in Fig. 12A (left) can be interpreted as the collapse of the mouth bar, due to soft sediment deformation, commonly observed in river dominated deltas, in this case, covering heterolithic facies of the delta front (Mutti et al., 2000). Overlaying strata represent an upward shallowing sequence, exposing the sedimentary system to the wave and longshore currents action. Heterolithic facies occurs on top of this whole system, suggesting the repetition of flooding episodes through time.

3.3. Lithostratigraphic descriptions

The general field observations of the Silurian sequence of the Parnaiba basin, as well as the facies and facies associations classification, are assigned below to the three lithostratigraphic formations of the Serra Grande Group, organized in the schematic column of Fig. 14A.

3.3.1. Ipu Formation

The Ipu Formation crops out well at the base of the northern Ibiapaba cliff and is best represented by the Bica do Ipu profile (Log C in Fig. 4), where it reaches approximately 130 m of thickness. North to the

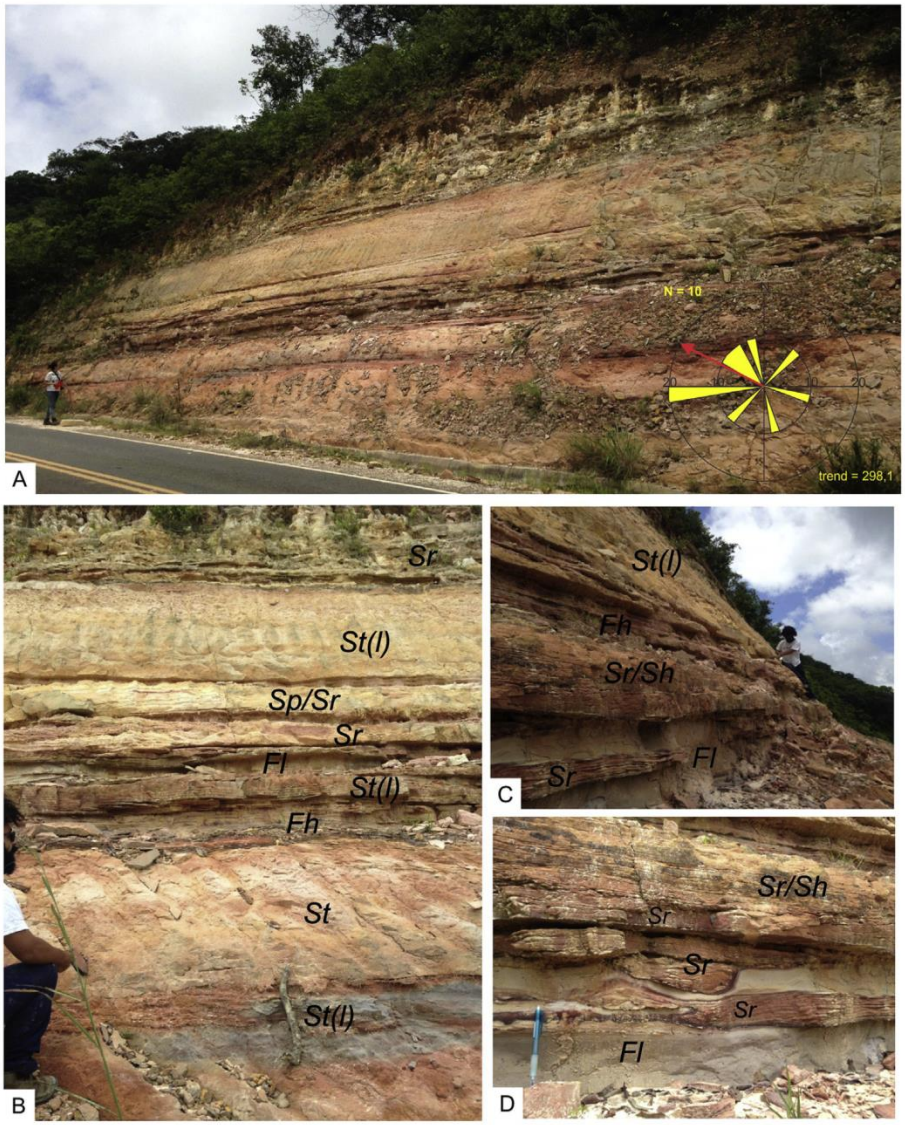

Fig. 12. Shoreface facies association within the Tianguá Formation, in the road cut of CE-257, close to Croatá district (site X in Fig. 3). (A) General view of outcrop showing the flat tabular layers. Cross bedded sandstones are predominant near the base, grading upward into heterolithic facies and ripple cross-laminated sandstones. Rose diagram in (A) represents the paleocurrent measurements from cross bedded sandstones. (B) and (C) show detail heterolithic beds with interleaved fine sandstone levels with asymmetric ripples, organized in lenticular layers with pinching out geometry. (D) Sin-depositional deformation structures due to (Sr facies) sedimentary load. Note the load cast structure in the center of the picture.

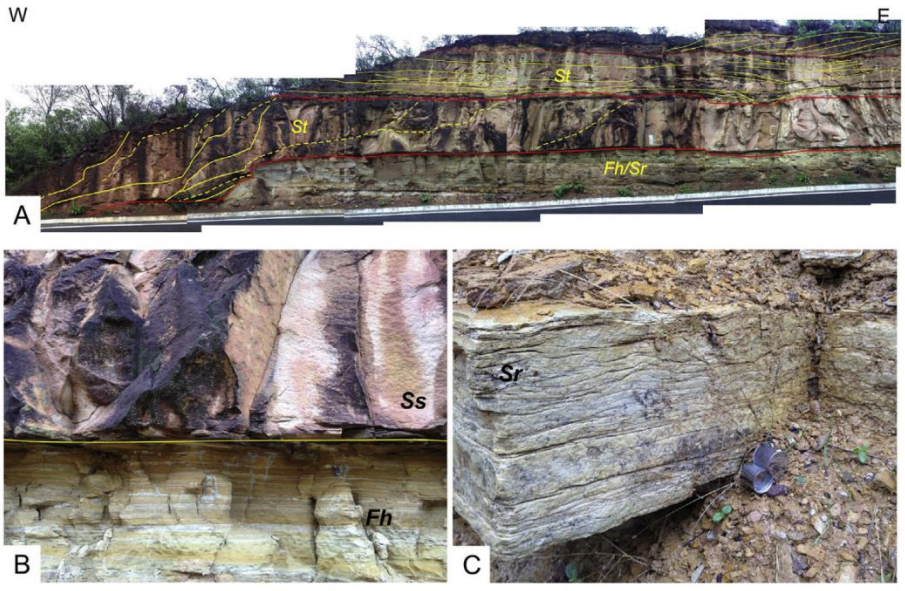

Fig. 13. (A) Stratigraphic mosaic panel located near the site Y in Fig. 3. It shows lobate geometry of sandstone bodies overlapping heterolithic beds of Tianguá Formation's deltaic facies association. The sandstones bodies represent the river mouth bars covering a deltaic plain. Sigmoidal clinoforms with trough and planar cross-bedding co-sets fill in the entire lobate geometry bed macroform. (B) Sandstone bodies are tabular with gently concave up bottom surface, overlapping heterolithic facies, with predominance of siltstone. (C) Siltstone with ripple crosslamination.

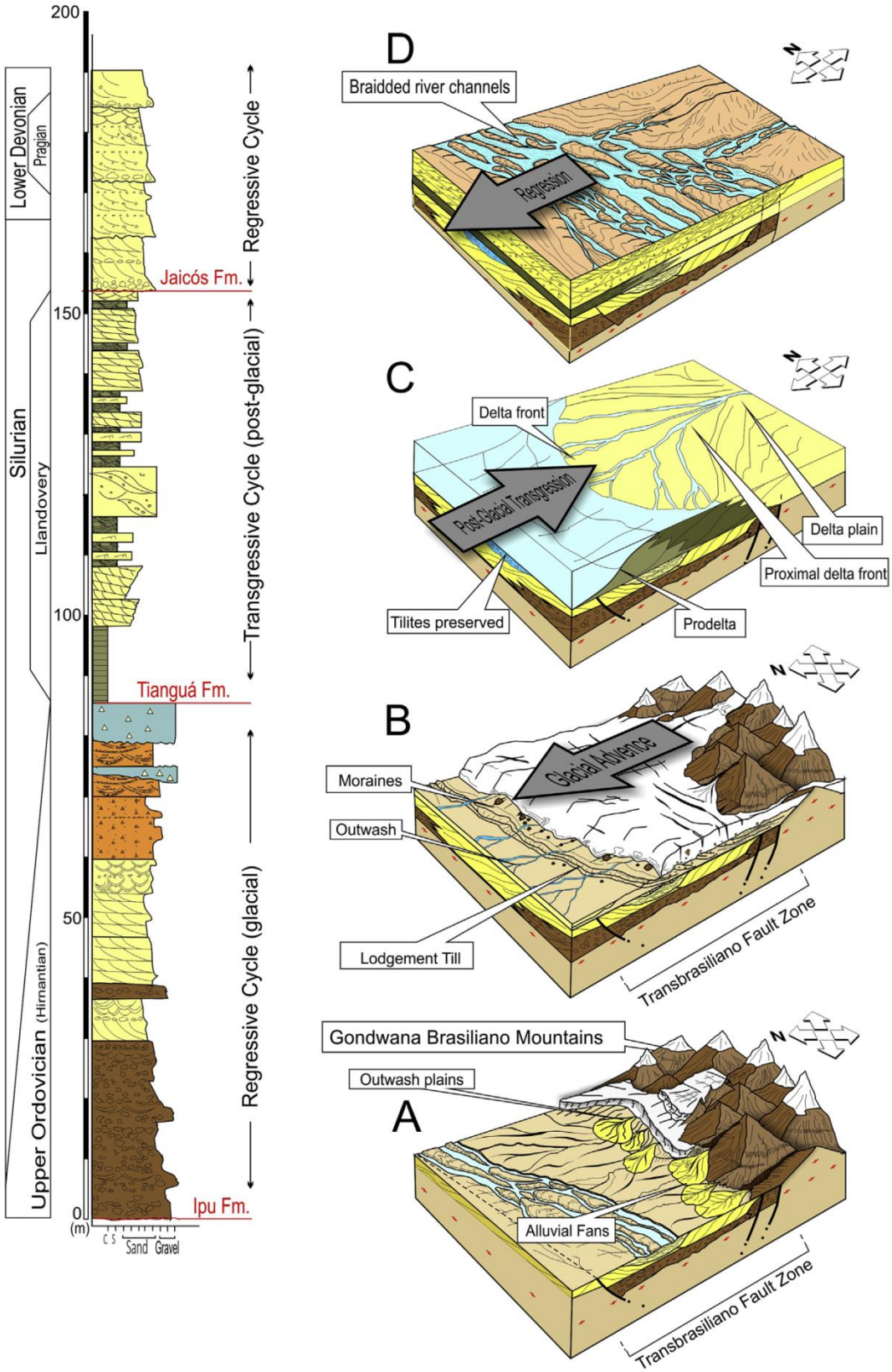

Fig. 14. Proposed model for the depositional evolution of the Serra Grande Group in the study area. (A) Schematic stratigraphic column of SGG with main transgressive/regressive (T/R) cycles. The contact between Ipu and Tianguá formations represents the maximum glacial episode, consequently the maximum regression; (B) Alluvial fan scarp-related alluvial fan conglomerates, originated by reactivations of Café-Ipueiras and Sobral-Pedro II faults during Ordovician-Silurian. The striated clasts of the basal paraconglomerates might indicate reworked fragments inherited from distal glaciers probably coming from northern/western Africa, where the South Pole was located (See also Fig. 17). (C) At the initiation of the sag phase, the stabilization of the platform is covered by a continental dry ice sheet in Lower Silurian. (D) Transgression took place during the Landovery stage and might be related to global melting water from glaciers (Tianguá Formation). (E) With the decreasing of the ice weight above the land, the platform was uplifted, resulting in isostatic post-glacial rebound, causing regression, controlling the depositional regime until the establishment of many braided shallow channels with very big amount of reworked sediments (Jaicós Formation).

Café-Ipueiras fault, in the Tianguá cliff, this formation was not observed and southwards to the Ibiapaba Cliff it gets progressively thinner, disappearing to the south of Ipueiras city (section A-A′ in Fig. 3 and location of cities).

The Ipu Formation comprises facies association FA1, FA2, FA3 and FA4, as schematically presented in Fig. 14. The entire package of this unit presents an overall bedding sense to NW, ranging from 5° to 25° of dip, in exception for the Santana do Acaraú area, in which the Ipu Formation sometimes dips at high angle (see bedding arrows in map of Fig. 3). The base of Ipu Formation comprises FA1 (alluvial fan facies association) and lies unconformable over the Precambrian basement. The total thickness of these alluvial fan conglomerates varies - in Log C (Fig. 4) it presents about 40 m of thickness, getting thicker northwards at the Ibiapaba cliff, close to the NE-SW limits of Café-Ipueiras and Sobral-Pedro II faults (Fig. 3). This feature, added to the sedimentological aspects (poor sorted subangular clasts, basement fragments, breccia texture zone), reinforces the hypothesis of a scarp-related alluvial fan for the initial deposition of the Ipu Formation. The presence of angular, faced and striated clasts inside the paraconglomerates of FA1 (Fig. 6B and C) suggest the influence of glaciers, or reworked debris coming from glaciers.

Upwards (southwards to the center of Parnaiba basin) the Ipu Formation grades to braided rivers channels (FA2), possibly related to the distal portions of such alluvial fan, in which predominates sandstones rich in quartz and sub-rounded clasts, that may suggest reworked and more mature deposits. Near the top of the Ipu Formation, fine-grained sediments are interlayered with cross-stratified sandstones (Fig. 6E) and the contact with the fluvial dominated deltaic facies associations (FA6 and FA7) seems to be conformable.

Only in one location, between the cities of Ipueiras and Croatá, c.a. 30 km south to the Bica do Ipu profile, FA3 and FA4 have been observed, composing approximately 25 m of glacial related deposits at the top of the Ipu Formation. Stratified diamictites are interpreted as outwash fans facies association (FA3), possibly related to reworked frontal glaciers areas (Eyles et al., 1983; Eyles and Eyles, 1992). Above and interfingered with outwash facies, massive diamictites with shear defomation structures (FA4) occur, representing a soft lodgment tillite (FA4) (Ruszczyńska-Szenajch, 2001). The top of this tillite is marked by a sharp contact with black shales (Fig. 11A) of the Tianguá Formation. These glacial beds dip at low angle to west, whereas the overlaying shales of Tianguá Formation are flat and, in this region, it may represent an angular unconformity. These tillites (FA3 and FA4) correlate laterally to the braided channels (FA2) observed in other sites of the study area, and are here interpreted as a datum for the transition from continental (Ipu Formation) to deltaic (Tianguá Formation) paleoenvironments within the SGG.

The Ipu Formation was also observed as an outlier outside of the Parnaiba basin limits, in Santana do Acaraú area, 70 km away from the northeast margin of the basin (Figs. 4 and 6). It is a relict mountain NE-SW elongated with FA1 and FA2, surrounded by Precambrian and Cambro-Ordovician basement. It is a graben like structure and bounded by NE-SW faults parallel to the Sobral-Pedro II lineament, to the west. The conglomerate and sandstone layers are tilted, dipping c.a. 80° to SE near the fault becoming subhorizontal towards the center of the graben. Other authors also considered this outlier to be part of the Ipu Formation, and emphasize its syntectonic nature due to reactivation of the NE-SW Sobral-Pedro II fault (Fig. 3) (Carvalho and Lins, 2002; Galvão, 2002). In both localities where FA1 are described in this work, the gravel bars stacking preserves an overall thinning upwards pattern until the middle portion, and followed by an increase in reworked clasts, evidenced by the predominance of quartz rich and rounded to sub-rounded clasts (see FA1 description and logs A and C in Fig. 4). To the middle to upper portion of FA1, polymicthic and mud matrix sandstones occurs over again, suggesting a rejuvenation of the source area, that can be associated to episodically uplifts of the basement. Besides that, close to Ipueiras (Fig. 3 to locate city of Ipueiras), the glacial deposits – top of Ipu Formation – contains abundant basement fragments, suggesting that the bottom of this unit wasn't continuous outside the eastern PB actual limits.

3.3.2. *Tianguá Formation*

The Tianguá Formation, in the vertical succession of the Tianguá Cliff in Ubajara National Park area, has at least 100 m of thickness, unconformably overlying the Late Neoproterozoic Ubajara Group as it is represented in the geological section A-A' (Fig. 3). Towards the south, in the Ibiapaba plateau, it is normally covered by vegetation and exposed along river or road cuts.

The Tianguá Formation is here interpreted as sand rich platform sediments deposited in a river dominated delta, with prodelta (FA5), delta front (FA6) and proximal delta (FA7) sub-environments. Its depositional system represents the transgression within the SGG (Fig. 14C). In the Ipueiras region, a 15 m thick black shale unit (FA5; Fig. 11) covers the Ipueiras tillites, top of Ipu Formation, and is here interpreted as datum for base of Tianguá Formation, also confirmed in subsurface data (Caputo and Lima, 1984). The basal shale of Tianguá Formation is not continuous and laterally grades to sandy facies (Caputo and Lima, 1984). This is typically expressed in the mapped area, in which the Tianguá Formation is much sandier than it is described in boreholes (personal observations). Therefore, where shale layers of FA5 is not present, the transition between braided river systems of the Ipu Formation to the delta front facies assemblages of Tianguá Formation is generally differentiated by the decrease of sand/mud ratio, and are very difficult to follow in the field.

If the uppermost Ipu Formation's tilite and the Tianguá shale layer there is no major hiatus, the abrupt change of proglacial facies to marine prodelta facies suggests a rapid retreat of the glacier, due to isostatic rebound following deglaciation and accumulation of fines in periglacial areas (Eyles et al., 1983). But in exception of scattered sand grains in the lowermost Tianguá shales, no glacial evidence was observed within the Tianguá Formation, so in this region, this contact is not transitional. The approximately 20° dipping basinwards pattern of Ipu Formation is also contrasting with the flat pattern of Tianguá layers, suggesting an angular unconformity.

In general, there is a thickening upwards array associated to the Tianguá Formation. The occurrence of fluvial dominated deltaic facies associations in two different places along the basin margin (Log B, Fig. 4; B in the map of Fig. 3) and inside the basin (Fig. 13; Y in the map of Fig. 3) at the same stratigraphic position suggests a NE-SW paleocoastline, in which mouth bars show paleocurrent sense to SE. Finally, in the top of Tianguá Formation, above deltaic facies, shallow marine related deposits were again observed near the city of Pedro II. That may represent alternation between intervals of flooding and discharge of mouth bars within the shoreline.

3.3.3. *Jaicós Formation*

The Jaicós Formation lies near the top of Tianguá and Ibiapaba cliffs (Fig. 3). It consists of thick layers of white sandstones with subordinate conglomerates and very few lenses of siltstones (Fig. 8), forming tabular ridges that overlap Tiangua Formation and delineate a plateau landform. The visited outcrops are located in the interior of the Parnaiba Basin, in Domingos Mourão city (Fig. 3; Fig. 8) and near Pedro II city, in Piauí state, where the Jaicós Formation is characterized by the braided river facies association (FA2; Fig. 8). The main paleocurrent direction is to NW, as showed in Fig. 8D. The transition from shallow marine deposits of top Tianguá Formation to fluvial deposits of Jaicós Formation represents the last regression of the SGG (Fig. 17).

4. Subsurface data analysis

For better understanding of the Ordovician-Silurian depositional aspects in subsurface of the Parnaiba Basin, four 2D seismic reflection profiles (L102, L111, L103 and L112 in Figs. 2 and 15), located in

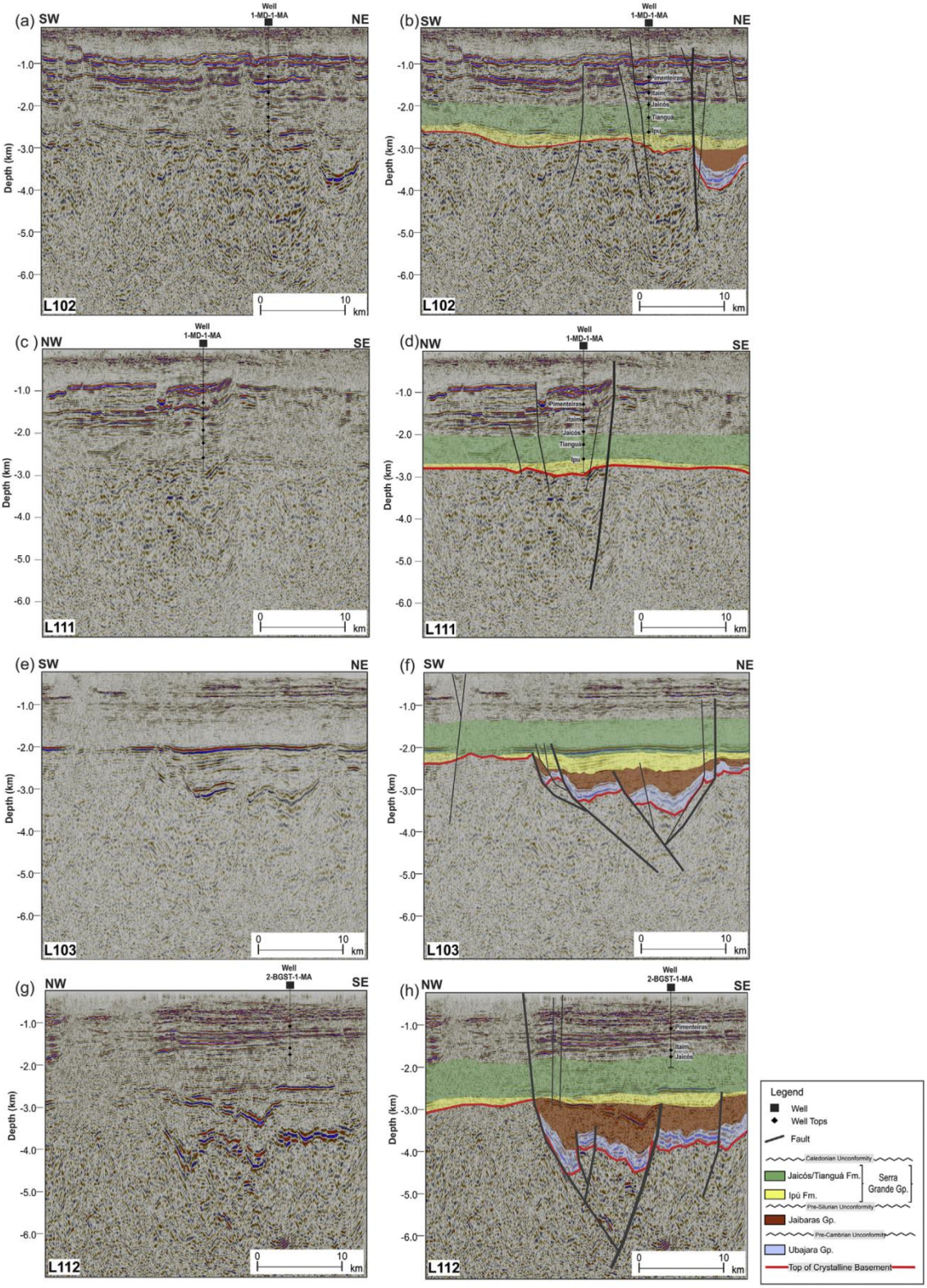

Fig. 15. Seismic interpretation of lines L102, L111, L103 and L112 in the central-eastern portion of Parnaiba basin (See Fig.2 for location). (A) (C), (E) and (G) present the uninterpreted versions of the seismic lines; (B),(D), (F) and (H) present the interpretation from base to top, of the Ubajara Group (in blue), the Jaibaras Group (in brown), the Ipu Formation (in yellow), and the Upper Serra Grande Group, represented by Tianguá and Jaicós formations (in green). In lines L102 and L111, the well 1-MD-1-MA (2820 m) has penetrated 630 m of the Tianguá and Jaicós Fm. and 277 m of conglomerate sandstones of the Ipu Fm. and did not reach the basement. In L112, the 2-BGst-1-MA well has reached 2020m of total depth within the Jaicós formation. In the map of Fig.2, it is possible to notice close to the seismic lines regional NNE-SSW and NE-SW lineaments related to the Transbrasiliano Lineament and interpreted by Cordani et al. (2016). These regional structures might correlate to the main faults interpreted here. (For interpretation of the references to color in this figure legend, the reader is referred to the Web version of this article.)

central-eastern PB, approximately 300 km southwestern to the field area, are here interpreted. The seismic lines have been acquired and granted by ANP (National Agency of Petroleum, Natural Gas and Biofuels) for academic purpose, and converted to depth using available well data and seismic-to-well tie processes (e.g. 1-MD-1-MA well tied to L102 and L111 and 1-BGst-2-MA well tied to L112, in Fig. 15; see also Porto, 2014, 2017).

These profiles have been chosen mainly because of their location, close to the southwards prolongation of the NE-SW Transbrasiliano Lineament, towards the interior of PB, which implies in a geological analogue setting for the visited field area, as well as a good subsurface imaging of the contact between Serra Grande Group and the sedimentary pre-Silurian basement units (e.g. Jaibaras and Ubajara groups). Besides that, the profiles L102 and L111 are tied to the 1-MD-1-MA well, which has penetrated the entire Serra Grande Group and also recovered polimythic conglomeratic sandstones in the base of the Ipu Formation (called as Mirador Fm. before the update from Caputo and Lima, 1984), reinforcing the similarity with the field area. Therefore, the analysis of these two perpendicular seismic lines tied to this well allowed us to have a broader interpretation of SGG along the trend of TBL.

In Fig. 15, we present L102, L111, L103 and L112 lines, not interpreted (Fig. 15A, C, E and G) and interpreted (Fig. 15B, D, F, H). Four seismic sequences, limited by three unconformities, were inferred and they are all related to the Serra Grande Group (Silurian) and to the pre-Silurian basement units. Besides well data constrain, the main criteria for seismic interpretation were the internal amplitude and continuity of the seismic reflectors, as well as their overall geometry (reflectors terminations and dip angles). We have also used available seismic analogues of this region (Oliveira and Mohriak, 2003; Morais Neto et al., 2013; Porto, 2014; Daly et al. 2014; Porto, 2017; Porto et al., 2018; Abelha et al., 2018), as well as the surface geological analysis from the field, to support a coherent regional interpretation.

In all profiles, we observe the horizontal reflectors of Parnaiba basin, reaching approximately 2.5–3 km in depth. In lines L102, L103 and L112 these layers covers graben-like shape packages, approximately 25 km wide, reaching up to 4 km depth and bounded by vertical to subvertical faults. The basal seismic sequence (blue in Fig. 15) of these grabens is characterized by strong amplitude and internally continuous reflectors, deformed in some areas (folded and faulted), with a regular thickness of approximately 350 m. This sequence was also described by Oliveira and Mohriak (2003) and Porto et al. (2018), identified as pre-Silurian sequences, correlated to the Ubajara Group (Late Neoproterozoic), composed by deformed low-grade metasedimentary rocks. At the base, it is limited by a regional unconformity (red line in Fig. 15) marked at the top of a low amplitude seismic pattern, which is here interpreted as an undifferentiated metamorphic or igneous basement.

Above the Ubajara Group, there is a sequence of low amplitude character and poorly continuous reflectors (brown in Fig. 15), with variable thickness, reaching up to 1 km of maximum thickness in L112 line. Following the publications of Oliveira and Mohriak (2003), Morais Neto et al. (2013) and Abelha et al. (2018), we attributed this sequence to the Jaibaras Group, a syn-depositional unit within the graben formation. Its base is marked by the Precambrian unconformity (top of Ubajara Group) and its top is represented by erosive truncations of dipping reflectors against a flat positive reflector, here interpreted as the angular Pre-Silurian unconformity (PSU), already identified in the literature by Daly et al. (2014) and Porto et al. (2018).

We have separated the SGG into two seismic sequences. The basal one is interpreted as the Ipu Formation (yellow in Fig. 15), with some continuous dipping reflectors of medium amplitude value and a maximum thickness of about 400 m within the graben areas. The well 1-MD-1-MA, tied to L102 and L111, did not reach the basement rocks, but has penetrated 278 m (from 2550 m to 2828 m measured depth) of the Ipu Formation. It is composed in the base by conglomeratic sandstones, with sub-angular and sub-rounded quartz and feldspar grains and granitic clasts, thick bedded to massive, showing some cross-bedding, changing upwards to argillaceous fine to medium grained sandstones and again covered by very coarse to conglomeratic sandstones. In the composite log from 1-MD-1-MA, the lowermost cored sequence is called by the name of Mirador Formation, representing the conglomeratic facies, here interpreted as the Ipu Formation and called as Serra Grande Group in the original well report. This facies was also observed in the basal conglomerates of Serra da Capivara (see location in Fig. 2) outcrop, described in the book from Hasui (2012) as part of the lowermost Ipu Formation and named as Capivara facies.

In the seismic lines (Fig. 15), it is clear to observe vertical discontinuities, interpreted as vertical fault planes, that sometimes cross the entire sedimentary package of Parnaiba basin and are rooted in the basement. One of these fault planes is located very close to the 1-MD-1-MA well location (see L102 and L111; Fig. 15b and d) and seems to limit to the west a paleodepression where the Ipu Fm. is thicker. In L103 and L112, although not constrained by well data (2-BGst-1-MA reaches up to the top of Jaicós Fm.; Fig. 15h), the Ipu Fm. depocenter was interpreted above the limits of the pre-Silurian graben. Outside the limit of these faults, the Ipu Fm. gets thinner or even disappears. This interpretation was guided also by the geological section of the Ibiapaba cliff (A-A' in Fig. 3), where there is an erosive or non-depositional hiatus of Ipu Fm. to the northwestern of the NE-SW Café-Ipueiras fault. This hiatus was also observed in Log B of Fig. 4, in contrast with the other logs to the SE of Café-Ipueiras fault. It is relevant to highlight in the map of Fig. 2 the presence of regional lineaments interpreted by Cordani et al. (2016) crossing the seismic lines. These local interpreted pre-Silurian grabens and adjacent faults have been thus possibly controlled by tectonic reactivation of basement inherited structures, related to these continental scale lineaments, such as the Transbrasiliano Lineament.

The base of Ipu Formation, or the Pre-Silurian Unconformity, appears to be irregular in the vicinities of fault planes and related pre-Silurian grabens. The top of Ipu Formation, however, is horizontal. In the well 1-MD-1-MA, the contact between Ipu and Tianguá formations is marked by a 260 m-thick diabase sill, at approximately 2500 m depth. These sills are represented by high amplitude continuous reflectors within the fine grained sediments of Tianguá Formation (see also Porto, 2014). The upper SGG seismic sequence (in green; Fig. 15) is composed by the Tianguá (base) and Jaicós (top) formations, not separated here due to the poor seismic imaging. This sequence presents an overall tabular shape with internal parallel and horizontal reflectors and an average thickness of 800 m. In L103, the reflectors of Ipu Formation are gently dipping to SW and in L112, to SE, and in both profiles, they are truncating the horizontal high amplitude reflectors of the Tianguá Formation. This probably defines an angular unconformity in the top of the Ipu Formation. Comparing to the field observations, this unconformity marks the contact between the tillites (FA4) of top of the Ipu Formation with the deglaciation black shales (FA5) of base of the Tianguá Formation in the Ipueiras outcrop (Fig. 11). This unconformity inside SGG, although, needs to be further understood in terms of Parnaiba basin regional scale, since it was not observed in the available literature yet and might be confined to local faulted areas.

The pre-Silurian sequences recognized in these seismic lines, here correlated to Ubajara and Jaibaras groups, are intensively affected by normal faults, configuring rotated blocks, horst and grabens, in a typical rift system, with the main fault localized NW of L102 and NE and SW of L103 and L112, respectively. In the location map of Fig. 2, we present the subsurface limits of pre-Silurian basins already described in the literature (Abelha et al., 2018; Daly et al., 2014; De Castro et al., 2016; Morais Neto et al., 2013) and also regional scale lineaments mapped by Cordani et al. (2016). These pre-Silurian basins are aligned along the NE-SW faults of the TBL and they crop out also in the studied field area (Jaibaras and Jaguaripe basins; Figs. 2 and 3).

In this Cambro-Ordovician continental rift context, the Ubajara

Group would represent a pre-rift deposit, due to its constant overall thickness, while the Jaibaras Group represents the syn-rift phase, thickening towards the main rift faults. Then, Ipu Formation was first deposited in the depleted areas of the vicinities of the TBL-aligned graben system (Fig. 15). This idea is corroborated by field observations (section A-A'; Fig. 3) and by the alluvial fan system described in the stratigraphic analysis (FA1). As suggested by Oliveira and Mohriak (2003), and recently corroborated by Abelha et al. (2018), a later pulse of transtensional reactivation of the Cambro-Ordovician graben faults might have controlled the initial deposition of Serra Grande Group during Ordovician-Silurian. Also in the Serra da Capivara, along the SE margin of PB, where the pre-Silurian graben of São Raimundo Nonato has been mapped by airborne surveys, Metelo (1999) and Hasui (2012) described the Ipu Formation as syntectonic scarp-related alluvial fan deposit, filling up paleodepressions of the metamorphic basement. The upper SGG sequence, seismically represented by horizontal continuous reflectors, was then deposited in a different sedimentary regime, what reinforces the idea of an unconformity within the SGG. Finally, vertical basement inherited faults cross cut the entire sedimentary package of Parnaiba Basin in all four profiles, L102, L111, L103 and L112, suggesting also later (post-Paleozoic) tectonic reactivation episodes in this area.

5. Discussions

5.1. Paleogeographic and tectono-stratigraphic evolution of the Serra Grande group

The integration of surface geological mapping, facies analysis and seismic interpretation led us to establish a paleogeographic and tectono-stratigraphic evolution model for the Ordovician-Silurian Sequence of the Parnaiba Basin. Stratigraphic sequences related to sedimentary textural variation trends, thickening and thinning upwards (regarding strata thickness pattern) and fining and coarsening upwards (regarding strata grain-size pattern) cycles, are here encompassed in the schematic stratigraphic column of Fig. 14. These observations, together with the tectonic and paleogeographic considerations, are then summed up in the block diagrams of Fig. 14.

The basal sedimentary successions of the SGG is represented by scarp-related alluvial fans grading upward and laterally to braided river channel deposits (Fig. 14B), forming a fining upwards sequence, comprising the base of Ipu Formation. A proglacial sub-enviroment is proposed for the transition between this first continental succession and the subsequent marine transgression (basal Tianguá Formation), recorded by outwash fans and lodgment till facies association (Fig. 14C). Above, there are offshore black shales, here interpreted as the Maximum Flooding Surface of the SGG (Fig. 14A), and lateral equivalents of shoreface sandstones facies association (Fig. 14D). A progressively shallowing upward trend culminated in the deposition of a deltaic subenvironment within this marine system (coarsening and thickening upwards) (Fig. 14D). The transition from marine to continental environment, is represented by a thick succession of amalgamated channels, with little or no marine influence (Fig. 14E) and organized in aggradational finning up successions (Jaicós Formation). This marks the major regression of the Silurian Sequence and is possibly related to the post-glacial isostatic rebound (Fig. 14).

The SGG is usually interpreted to be deposited in a sag phase (e.g. Brito Neves et al., 1984; Daly et al. 2014), limited by a peneplained surface, the Pre-Silurian Unconformity (PSU). In the study area, as well as in the seismic interpretation, however, we have noticed that this horizontal and continuous sag character of SGG does not define the lowermost conglomerates (FA1) of the Ipu Formation. In the field area, these layers are not continuous, distributed only southwards to the Café-Ipueiras and the Sobral-Pedro II faults (Fig. 3). Both faults are related to the crustal scale Transbrasiliano Lineament and have controlled the evolution of the Cambro-Ordovician Jaibaras trough, as presented in section A-A′ (Fig. 3) and interpreted by Oliveira and Mohriak (2003).

These alluvial fan deposits (FA1) are also preserved in Santana do Acaraú locality (Fig. 3 and Log A in Fig. 4), separated c.a. 70 km from the NE Parnaiba basin margin. This outcrop is interpreted by different authors (Destro et al., 1994; Carvalho and Lins, 2002; Morais Neto et al., 2013) as an outlier of the base of Serra Grande Group (Ipu Formation), mainly due to the sedimentological similarities and ichnofossil content (Viana et al., 2010). Destro et al. (1994) have considered that the Ediacaran-Cambrian extensional normal faults of the Jaibaras basin might have also affected the deposition of these Ordovician-Silurian siliciclastic deposits, and were later reactivated by different deformational events, possibly in the Mesozoic or even later. Oliveira and Mohriak (2003) have also identified a transcurrent reactivation along the major boundary faults of Jaibaras trough, before or simultaneously to the Silurian deposition of PB. The subsurface data interpreted by Morais Neto et al. (2013) and Abelha et al. (2018), located southwards to the seismic lines L103 and L112 location, along the TBL strike, shows the maximum thickness of the Ipu Formation inside the Jaibaras correlated graben structure. Old and recent isopach maps of the SGG based on well data (Tozer et al., 2017) also shows the highest thickness values for Ipu, Tianguá and Jaicós formations aligned to the NE-SW TBL and to the NW-SE Picos-Santa Ines Lineament (north of Parnaiba Basin). These features reinforces the idea of tectonic influence during deposition of the hole SGG. However, the Ipu Formation is the only that preserves features of a syn-sedimentary faulting deformation. Lima and De Sá (2017), Metelo (1999) and Kegel (1953) also described the Lower Ipu Formation as a syntectonic sedimentation in outcrops localized respectively in Santana do Acaraú, São Raimundo Nonato (Serra da Capivara) and Ibiapaba Cliff (see Fig. 2). Metelo (1999) has mapped alluvial conglomerates affected by reactivated faults from the basement in Serra da Capivara as the type-section of Ipu Formation in SE of Parnaíba Basin.

These literature data corroborate to the surface and subsurface data analysis here presented. In all areas with Ipu Formation's alluvial fan facies, i.e. Ipu (Ceará State), Santana do Acaraú (Ceará State) and Serra da Capivara (South of Piauí State; Metelo, 1999; Lima and De Sá, 2017; Hasui, 2012), it looks like it is deposited restricted and along tectonically depleted areas or irregular paleotopography, clearly related to major Brasiliano Neoproterozoic faults reactivated. The age of this Ipu Formation related tectonic pulse, although, is not yet constrained in the literature and is here interpreted as of Upper Ordovician age, due to its close relationship with the Jaibaras basin evolution (Cambrian to Early Ordovician) and the documented uppermost Ipu's glacial layer (Ipueiras Tilite; Figs. 9 and 10), probably of Hirnantian Age. For this reason, in contrast to what was recently suggested by Daly et al. (2018) and Tozer et al. (2017), it is not discarded here the influence of an initial extensional setting followed by flexural subsidence for the origin of Parnaíba basin, or at least for the SGG depositional mechanism in the eastern part of the basin.

The Ipu Formation is characterized by glacial influence from the base to the top. This is evidenced, at the base, by reworked clasts coming from glaciers (periglacial) and at the top by proglacial deposits, in which the main paleocurrent direction indicate the sedimentary source located to the southeast (Fig. 17). Assuming the glacial related sedimentary cycles proposed by Boulton (1990), the Serra Grande Group fit in the model of an advancing ice sheet. Whereas the initial phase is marked by regression and intense erosion, corroborated by the preservation of the basal Ipu Formation exclusively in paleodepressions related to tectonic activity or remnant paleotopography (Fig. 14A). The following subsequent fluvial systems, culminated in the proglacial deposits, suggest that the regression, as well as the glacial system, have reached their maximum stages (Fig. 14B).

For Boulton (1990) the advancing ice sheet on the continental platform produces intense crustal depression, caused by the ice sheet weight. It is possible that this must have influenced the subsidence at

the PB, resulting in the deposition of Tianguá Formation marine successions, overlapping the continental fluvial-glacial systems of Ipu Formation (FIg. 14D). Therefore the Tianguá Formation represents the deglaciation transgression, due to the equilibrium between subsidence caused by an ice sheet weight of Boulton's model and the maximum marine flooding for the Silurian sequence. The deglaciation and the deposition of Tianguá Formation are coeval to a worldwide sea level rise of Llandovery age (Caputo and Lima, 1984; Grahn et al., 2005; Grahn and Caputo, 1992). If the Tianguá Formation is the result of a isostatic rebound, i.e. the ice sheet weight no longer existing, also documented in the Paraná Basins and northern Africa basins, it also reinforces the unconformity observed between Ipu and Tianguá formations. Therefore the deposition of Tianguá Formation is coeval to the initiation of the sag phase in PB and also coeval to a worldwide documented unconformity between Ordovician and Silurian, due to the post Hinantian Glaciation. This transition would also mark a change in the tectono-stratigraphic regime within the Lower SGG, from the tectonic related continental deposits of the basal Ipu Formation to the quiet sag phase during Tianguá Formation deposition. In the observed seismic data, this transition could be interpreted as an angular unconformity (L103 and L112 in Fig. 15), and in the surface, in the vicinities of PB NE margin faults, this is represented by a non-depositional/erosive unconformity (A-A' in Fig. 3 and Log B in Fig. 4). The subsequent succession, Jaicós Formation, is represented by extensive braided river system (Fig. 14D), probably related to a regression cycle due to the sea level fall as a result of subsequent uplift of the platform, probably still due to isostatic rebound (Assine et al., 1998; Boulton, 1990). In contrast with Cruz (2016); Caputo and Lima (1984); Góes and Feijó (1994); Vaz et al. (2007), we support that the Silurian Sequence was deposited first at a regressive cycle with a maximum glacial represented by glacier advance facies, followed by transgression and regression. Therefore the variations in eustasy and isostasy was controlled mainly by the advance and retreat of an ice sheet at least for the beginning of SGG sedimentation.

5.2. Regional correlations in Western Gondwana

Western Gondwana major intracratonic basins (Fig. 1) record both global climate and geodynamic evolution during the Phanerozoic: in Brazil, the Parnaiba Basin (Northeast Brazil, the Amazonas Basin (North Brazil), and the Paraná Basin (Central-South Brazil); and, in Africa: the Cape-Karoo Basin (South Africa), the Congo Basin (Central Africa) and the Taoudeni Basin (North Africa). The correlation of their main stratigraphic charts (Fig. 16) shows a similar Lower Paleozoic record, associated to the end of the Late Neoproterozoic-Cambrian Brasiliano-Pan African tectonic events that culminated with Gondwana amalgamation (Schmitt et al., 2018; De Wit et al., 2008; Linol et al., 2016a,b). An extensive mountain system in Central Gondwana, have provided the sediment sources for many of these basins (Linol et al., 2016a,b). At the South American Platform, Late Neoproterozoic and Cambrian-Ordovician sedimentary sequences are coeval with the two last thermal pulses of the Brasiliano orogenies, restricted to grabens and troughs within the Precambrian basement. Whereas in South America cratonic basins were attributed to the Late Ordovician (Brito Neves, 2002; Brito Neves et al., 1984), in northern Africa, this Ordovician unconformity is not well developed (Villeneuve, 2005). Instead the Neoproterozoic, Cambrian, and Early Ordovician sequences, are expressive in thickness and continuous geographically and stratigraphically throughout the Sahara and Greater Chad areas (Villeneuve, 2005). In Southern Africa, the Ordovician sequences of the Cape Basin were deposited in a context of a passive margin basin, straight above Neoproterozoic metamorphic belts, but graben-like structures within Cambro-Ordovician sedimentary rocks are also locally preserved (Rust, 1973), while in Congo Basin the Ordovician to Devonian sequences are apparently absent, suggesting a hiatus of ca. 150 m.y. (Fig. 1 - Linol et al., 2016a,b).

The origin and evolution of these large intracratonic basins are ruled by three main factors: climate (oscillation of glacial and warm periods), tectonics (basement faulting and tectonic events) and transgressions (Hambrey, 1985; Villeneuve, 2005). Therefore the sedimentary record of SGG, in particular its glacial marker (Ipueiras tilite) between Ipu and Tianguá formations, is important for paleogeographical and paleoclimatological reconstructions (Fig. 16).

The Ordovician-Silurian glacial period of western Gondwana persisted for almost 35 m.y. and is widely preserved in the northern Africa basins (g.e. Taoudeni, Tindouf, Illizi) including Saudi Arabia and in South America and South Africa. Fig. 16 shows a correlation the Lower Paleozoic main units and glacial record ages among the Parnaiba, Amazonas, Taoudeni, Tindouf, Paraná and Cape basins. In northern Africa, the Ordovician-Silurian glacial record can be grouped within, or are equivalents to the Tichit Group (Villeneuve, 2005; Deynoux, 1985) from the Taoudeni Basin (Mauritania). In South America, Ordovician-Silurian glaciation units are also present at the top of the Nhamundá Formation – Trombetas Group in Amazonas Basin (Caputo and Lima, 1984), at the Iapó and Vila Maria formations – Rio Ivaí Group in Paraná Basin (Assine et al., 1998) and in Argentina (Zapla and Mecoyita formations), Peru (San Gaban Formation), and Bolivia (Cancañiri Formation - Díaz-Martínez and Grahn, 2007; Assine et al., 1998). In southern Africa, glacial deposits are represented by the Pakhuis and the Cedarbeg formations of Table Mountain Group in Cape Basin (Deynoux, 1985). These glacial records have a time span that goes from the Ashgilian (Late Ordovician) to the Llandovery (Early Silurian). These indicate that an ice sheet covered western Gondwana during the transition between the Ordovician and the Silurian (Caputo and Crowell, 1985; Ghienne, 2003; Hambrey, 1985- Fig. 17).

Northern Africa glacial deposits preserve Late Ordovician graphitolites and brachiopod fossils, whereas in South America, glacial deposits are considered to be from the Early Silurian (Caputo and Crowell, 1985; Caputo and Lima, 1984) based on chitinozoans, acritarchs and graphitolites. In northern Africa, deformed sand bodies - interpreted as outwash fans, plus massive tillites, that grades laterally and upwards to varve like clays with dropstones, are interpreted as glaciomarine deposits, dated as Hirmantian (Late Ordovician) in the Taoudeni, Tindouf and Illizi basins (Ghienne, 2003). In South America and southern Africa, the glacial record is mainly in association with marine deposits, in exception in Parnaiba Basin, that is glacio-fluvial (Assine et al., 1998; Rust, 1973; Grahn and Caputo, 1992; Caputo and Lima, 1984), dated from the Early Silurian (Grahn and Caputo, 1992). In the Congo Basin (Central Africa) no Silurian sequences are present, due to a 150 m.y. hiatus/erosion (Caputo, 1984; Linol et al., 2016a, Fig 1; Fig. 16).

There is a relative consensus, based on paleomagnetic data, that Gondwana was localized nearby the South Pole from 445 to 410 Ma (Fig. 17; Torsvik and Cocks, 2013). At ca. 445 Ma, Hirnantian age (Late Ordovician), the South Pole was localized near northern Africa, at the West African Craton (Torsvik and Cocks, 2013). In a period no longer than 5 m.y., the South Pole was migrating from northern Africa towards northeast Brazil, which resulted in many glacial deposits, subglacial erosion and striated pavements documented by northward paleocurrent towards the northern platform of Gondwana (Le Heron and Howard, 2010) (Fig. 17A). At ca. 440 Ma, Early Silurian, the South Pole was positioned somewhere around north Brazil (Fig. 17B), below the Amazonas Craton. In Amazonas and Paraná basins, these glacial deposits grade to fossiliferous marine subglacial facies of the Pitinga Formation. But the equivalent Tianguá Formation of the Parnaíba Basin, suggests a deglaciation marine flooding, or simply different ages for each formation (Fig. 16).

Indeed, more than one single glacier advance must have occurred during this period (Grahn and Caputo, 1992). Another particularity of the Ordovician and Silurian glacial deposits, is the large quantity of sand in the tillites matrix, compared to other stratigraphic correlates (e.g. Neoproterozoic and Permo-Carboniferous - Huuse et al., 2012). This can be explained in a simplistic way, by the peneplanization of the mountain belts after the Gondwana amalgamation, producing a large

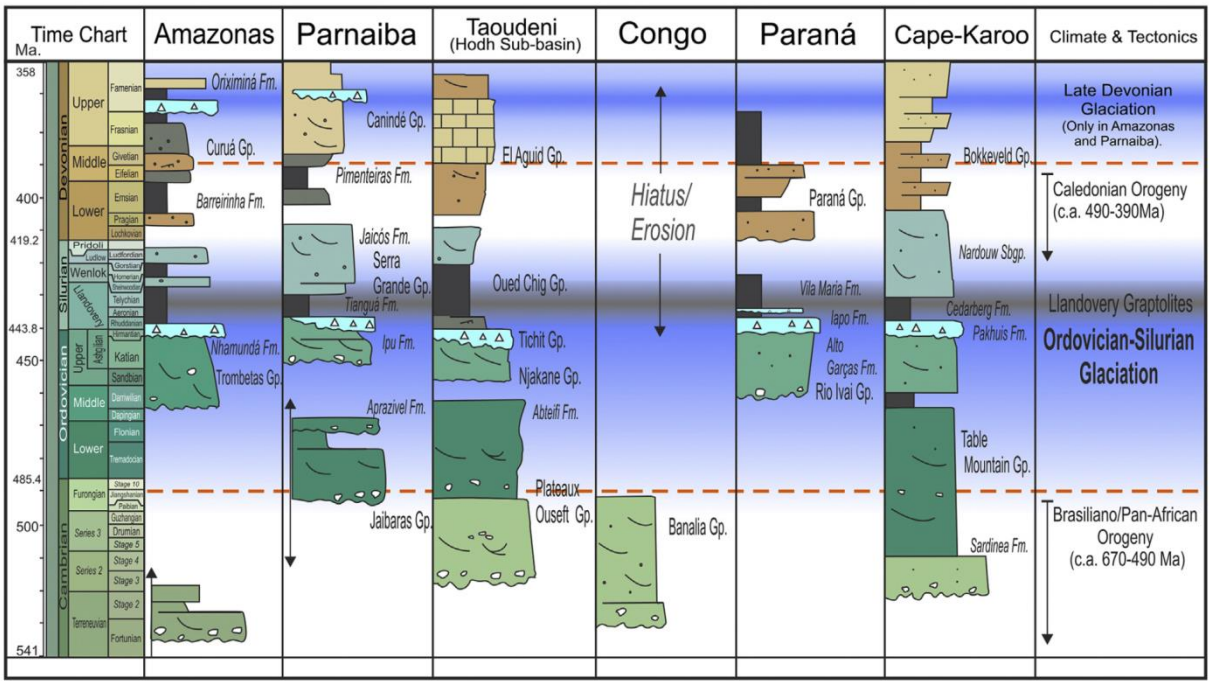

Fig. 16. Summary of the Lower Paleozoic stratigraphic columns of the major western Gondwana basins, highlighting the correlation between the estimated ages for glacial deposits in Amazonas, Parnaiba, Taoudeni, Paraná and Cape-Karoo basins, and the correspondent hiatus in Congo Basin. The dark gray tide is the Llandovery *Climacograptus Scalaris Scalaris* cf. graptolite zone. The blue areas shows the two peak of glaciation in Lower Paleozoic, the bottom one, is the Hirnantian Glaciation and the upper blue area is the Late Devonian glaciation registered in Parnaíba and Amazonas basins (Caputo and Crowell, 1985). The light blue sequence within the stratigrapgic columns represent glacial deposits. This diagram is adapted from Linol et al., 2016a,b integrating with data from Boulton and Deynoux (1981), Caputo and Crowell (1985), Caputo and Lima (1984), Deynoux (1985), Grahn and Caputo (1992), Le Hérissé et al. (2001), Rincón Cuervo et al. (2018), Rust (1973), Assine et al. (1998) and Villeneuve (2005). (For interpretation of the references to color in this figure legend, the reader is referred to the Web version of this article.)

amount of reworked sediments (Hambrey, 1985; Le Heron et al., 2010). The rapid migration of Gondwana towards south in South America must have influenced in the melting of ice sheet and culminated in a global scale transgression (Torsvik and Cocks, 2013), evidenced by black shales rich in organic matter, including the Tianguá Formation in the Parnaiba Basin (Fig. 17B). This transgression is well documented in all of these major basins, and is a good datum for correlation due to it typical fossil assemblage and palynomorths, coeval to the *Climacograptus* cf. *scalaris scalaris* graptolite biozone (Llandovery – Early Silurian) (Grahn et al., 2005; Grahn and Caputo, 1992) (Fig. 16). The stratigraphic equivalents of the Tianguá formation are (Fig. 16): the Pitinga Formation (Trombetas Group - Amazonas Basin), the Vila Maria Formation (Rio Ivaí Group - Paraná Basin), the Cederberg Formation (Table Mountain Group - Cape Basin) and graptolitic shales of the Oued Chig Group (Taoudeni Basin). The post-glacial "hot" shales represent the main source rock for hydrocarbon in northern Africa, and Middle East, being the world's largest area of hydrocarbon source rocks worldwide (Abelha et al., 2018; Huuse et al., 2012; Torsvik and Cocks, 2013). The rapid transgression and consequently removal of the weight of the Gondwana ice sheet, induced uplift by isostatic rebound and a worldwide regression event (Hambrey, 1985). Following this, the Jaicós Formation was deposited, interpreted in this paper as mainly fluvial deposits, but evidence of shallow platform, deltaic and submarine fans are also noticed, in surface and subsurface (Fig. 16 - Caputo and Lima, 1984). Indeed, the Jaicós Formation is mainly composed by coarse sediments, including conglomerates, and few fine sediments at the bottom, confirming a continuous sedimentation between Tianguá and Jaicós formations. However, for Grahn et al. (2005) the Jaicós Formation ranges from the Upper Llandovery to the Lower Emsian (Devonian), but, based on its palynological content, one or more hiatuses are present. This worldwide regression pattern is also supported by coastline migration from the south of Algeria towards the north of Morocco recorded by shallow marine facies (Berry and Boucot, 1973; Caputo and Lima, 1984). The Jaicós Formation equivalents are: the Manacapuru (Trombetas Group), the base of Furnas (Paraná Group - Paraná Basin), the Nardouw (Table Mountain Group) and the Atafaitafa (Algerian Sahara) formations.

6. Conclusions

The Serra Grande Group (SGG) records deposition in continental and marine paleo-environments during the Late Ordovician (lower Ipu Formation), Silurian (Ipu, Tianguá and Jaicós formations) and Early Devonian (uppermost part of Jaicós Formation) within the Parnaiba Basin (PB). This sequence comprises at least seven facies associations, described in the eastern portion of PB (Figs. 2 and 3): alluvial fans (FA1), braided river channels (FA2), outwash fans (FA3), lodgment till (FA4), prodelta (FA5), river dominated delta front (FA6) and river dominates proximal delta front (FA7).

The basal layers of the Ipu Formation represent scarp-related alluvial fan facies vertically grading to deposits of braided river channels, discontinuously covered by a glacial deposits, here named as the Ipueiras Tillite. Different aspects of the lowermost Ipu Formation, corroborated by literature data (Abelha et al., 2018; Hasui (2012); Metelo, 1999), suggest that this unit was deposited in an active intracontinental tectonic context possibly related to fault reactivations along the NE-SW Transbrasiliano Lineament, such as the Cambro-Ordovician normal faults of the Jaibaras graben. Those aspects include: (1) the occurrence of faults, tilted and brecciated layers (Figs. 5H and 7), (2) typical scarp-related alluvial fan facies association (logs A and C in Fig. 4) in this unit, (3) the hiatus of the Ipu Formation observed in field mapping (section A-A' in Fig. 3; Log B in Fig. 4). Also in subsurface seismic imaging (Fig. 15), the thickening of SGG group in the vicinities of the pre-Silurian graben area and the angular possible unconformity on the top of Ipu Formation reinforce this idea. Therefore, we propose here that the Ipu Formation must be related to a pre-sag phase,

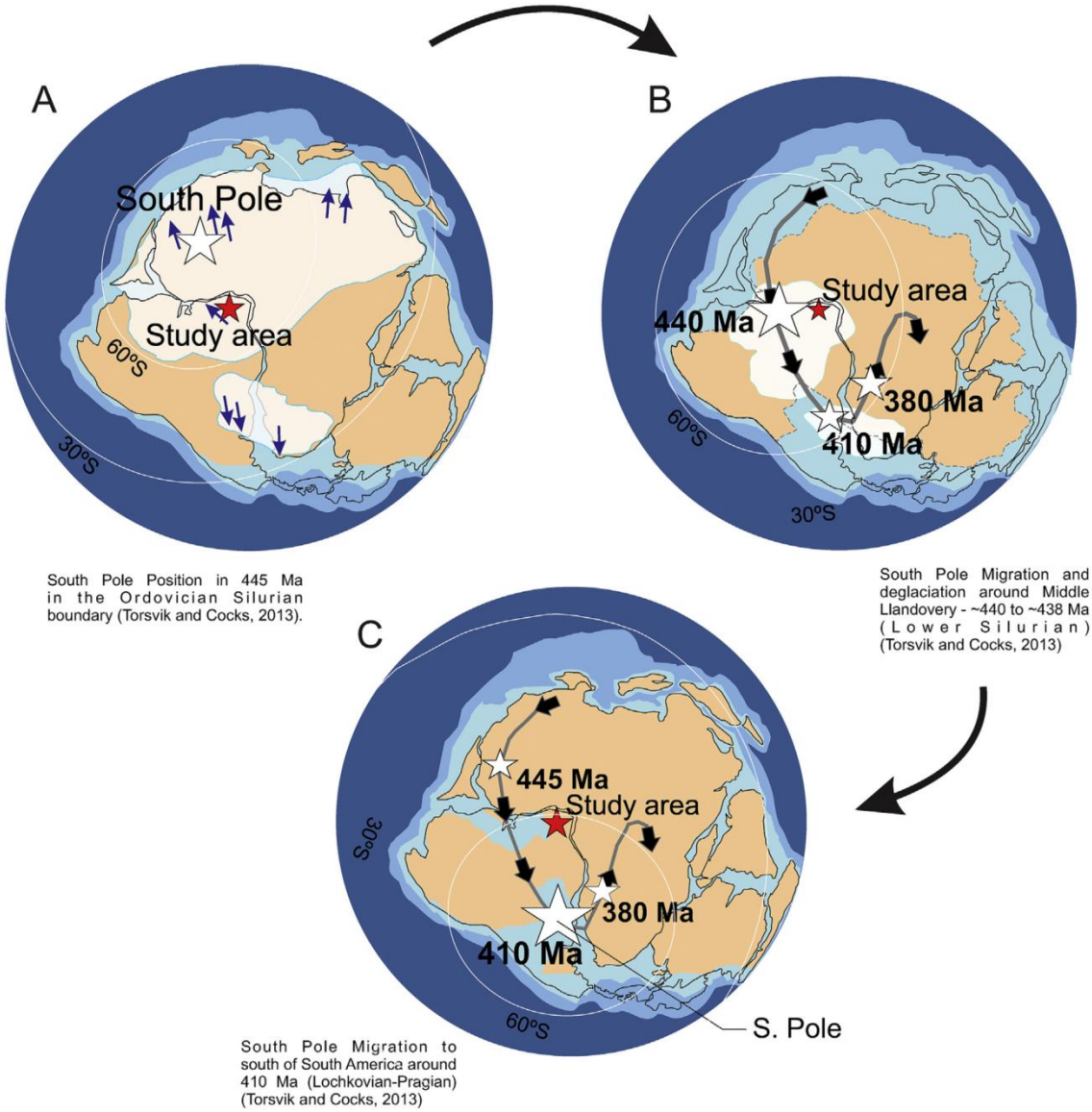

Fig. 17. Evolution scheme of South Pole migration and paleogeographic evolution model for the transition between (A) Ordovician (Lowermost Ipu Formation), (B) Lower Silurian (Ipu, Tianguá and lowermost Jaicós Formation) and (C) Early Devonian (uppermost Jaicós Formation). South Pole position is based on paleomagnetic data from Torsvik and Cocks (2013).

following reactivations of regional faults. A regional unconformity within the Serra Grande Group is then expected in the transition from the Ipu Formation to the Tianguá Formation. Although this unconformity was observed in mapping and seismic scales, and in the particular case of Ipueiras outcrop, this is not clearly observed everywhere, for instance in the Ibiapaba cliff, where both Ipu and Tianguá formations are composed mainly by sandy facies, leaving limitations to this interpretation and requiring further investigations.

The glacial deposits within the top of Ipu Formation were described in detail (Log D, Fig. 4), separated into two glacial related facies association (Outwash Fans and Lodgment Till). This glacial influence was observed also in the base of Ipu Formation (striated and faced pebbles of Fig. 5B). These evidence suggest that the base of the SGG (Ipu Formation) is represented by a glacial influenced regressive sequence, which culminates in the maximum glacial stage (ice sheet advance deformation; Fig. 10D, E and G), registered by the Ipueiras tillite. The sharp contact of this tillite with the marine prodelta shally facies grading upwards to delta-front/shoreface, proximal delta-front and fluvial systems, respectively, added to the absence of any glacial evidence, suggest that Tianguá and Jaicós formations were deposited in a transgressive-regressive cycle, controlled first by the deglaciation of Hirnantian glacial period and then by its isostatic rebound.

The Ipueiras tillite within the uppermost part of Ipu Formtation might correlate with the global episode of glaciation at the Ordovician-Silurian boundary, equivalent with Iapó (Paraná), Pakhuis (Cape-Karoo, South Africa), Nhamundá (Amazonas), Tchit Group (Taoudeni basin, Mauritania) formations. The NW pattern of paleocurrent measurements within the Serra Grande Group differ to those of the Paraná and Cape-Karoo basins (SE trend), but is consistent with the trend of the northern African basins (e.g. Taoudeni). This suggests a regional paleotopographic high in the central portion of western Gondwana, corroborated by the absence of Silurian-Devonian sequences preserved in the Congo Basin (central Gondwana).

Acknowledgements

This paper is a contribution to the IGCP-628 "The Gondwana geological Map and its tectonic evolution". The fieldwork was supported by

4.3 Additional Information

4.3.1 The Pre-Silurian Unconformity

Widely observed in the literature of the Parnaíba basin (e.g. Góes and Feijo, 1994; Vaz et al.,2007), the pre-Silurian unconformity (PSU) was recently described in the seismic data and named as so after the studies of Daly *et al.* (2014) and Porto *et al.* (2018), respectively. The PSU represents the basal horizon of the Parnaíba basin, characterized as a regional erosive unconformity upon the pre-Silurian basement that sometimes also occurs as an angular unconformity. This unconformity was formed prior to the Ipu Formation deposition (basal lithostratigraphic formation of the Serra Grande Group, Ordovician/Silurian), and therefore it is certainly older than 443.8 M.y. According to Daly et al. (2014), PSU represents a peneplain that postdates the Brasiliano orogeny, sealing the complex structures underlying the basin and implying that its initial deposition was not controlled by the major discontinuities observed in the basement, but possibly due to thermal driven subsidence mechanisms.

The following topics present the analysis of the Pre-Silurian Unconformity, based on three different data analysis approaches. First, a regional subsurface structural map of the PSU in depth is displayed, based on information of 20 wells that reached the pre-Silurian basement (see Appendix II). This map is compared to the tectonic domains described in Chapter 3. Secondly, seismic examples and a structural map in depth of the seismic PSU horizon in the mid-southern portion of PB are analyzed, bringing more details to the previous map. Finally, images of outcrops in the NE portion of the Parnaíba basin exemplify the surface exposures of the PSU.

- ***PSU from well data analysis***

To build the map of Figure 4.18, the Inverse distance weighted (IDW) interpolation algorithm available in ArcMap software was used. This methodology is suitable for sparse and irregular datasets and calculates the weights proportional to the inverse of the distance between the observed data point and the predicted location. The rate of decrease in the weights is dependent on a power value ‘p’, which, in this case, was equal 2 (inverse distance squared weighted interpolation). In sum, the practical meaning of this interpolation method is that the reliability of the calculated basin thickness values is greater the closer it is from the observed data (the depth of the PSU from wells).

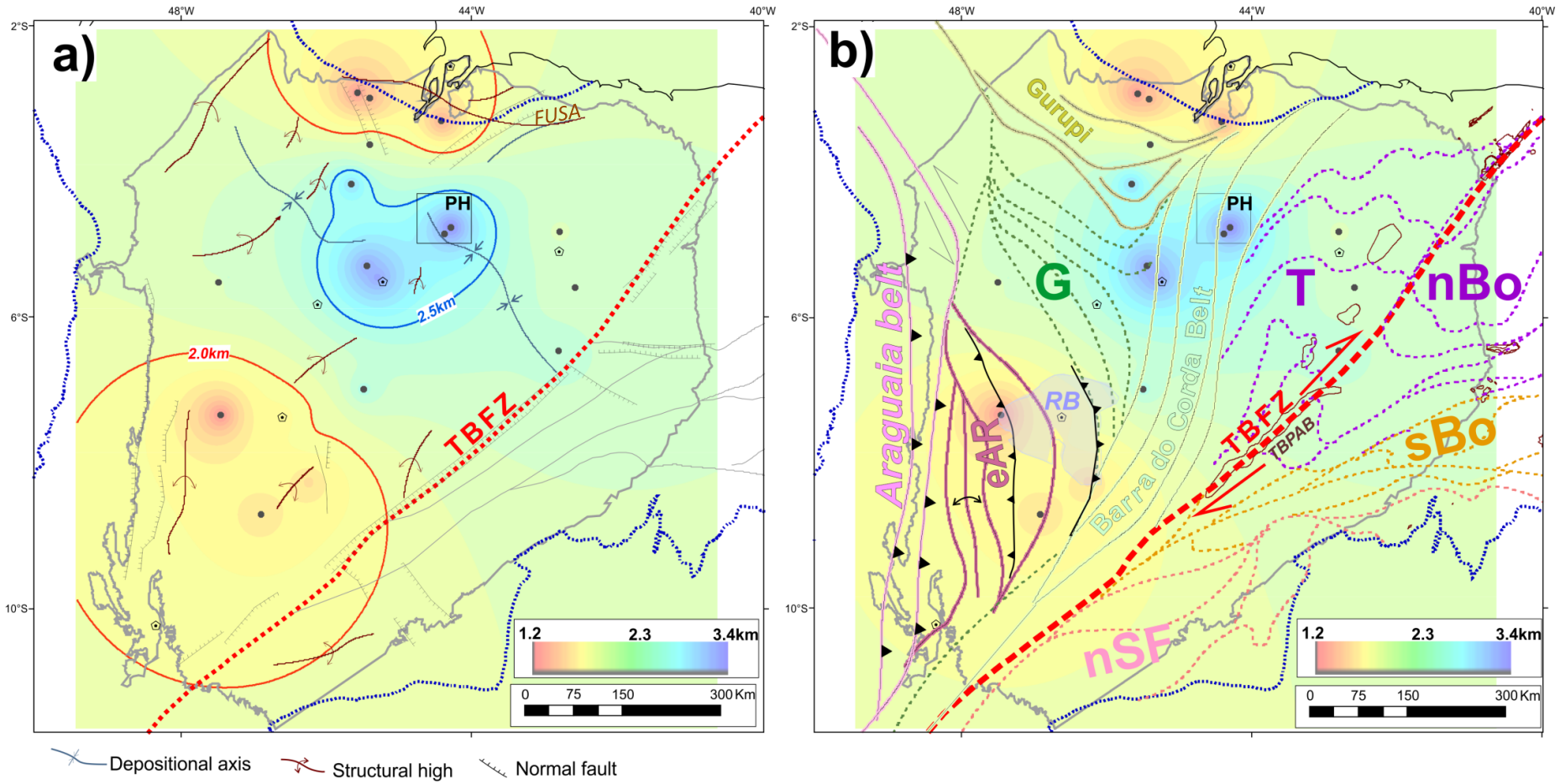

Fig. 4.18 (a) Structural map in depth of the PSU relief in subsurface based on wellbore information (grey dots); the depositional axis, structural highs and normal faults are from Miranda et al. (2018), as well as the “Hawks Park” location (PH), where the gas field of the Parnaíba basin are located. (b) Tectonic lineaments and domains of the basement of the Parnaíba basin (see Fig.3.11) superimposed to the map of (a). The Brasiliano belts are: “AR”: Araguaia belt, “eAr”: eastern Araguaia belt subdomain, Gurupi belt, and Barra do Corda belt. “G” stays for the Grajaú and “T” for the Teresina domains. To the south of Transbrasiliano Fault Zone (TBFZ), “nSF" refers to the northern margin of the São Francisco craton, and “nBo” and “sBo” are the northern and southern domains of the Borborema Province.The pre-Silurian basins are: “RB”: Riachão and “TBPAB”: Transbrasiliano pull-part basins.

The map of Fig.4.18a shows the present location of the depocenter and structural high portions of the basin, it means, where the PSU, and consequently the Parnaíba basin, gets deeper. When compared to the map of Fig.4.18b, some preliminary observations can be drawn:

- The location of the maximum depths of PSU (>2.5km) is centered to the mid-northern portion of PB, close to the vicinities of Barra do Corda city. This coincides to where the Barra do Corda belt (Fig.4.18b) was here defined and where Solon et al. (2018) observed the “C” conductor, down to 10-40km depth (sees Figs. 3.4 and 3.14).
- The PSU gets shallow coincidently upon the western portion of the Riachão basin, where the Eastern Araguaia belt subdomain was defined (Fig.4.18b). A N-S-oriented structural high was observed by Miranda et al. (2018), parallel to the limit between the “eAr” and “Ar”, roughly where an anticline was interpreted in the basement map (Fig.4.18b).
- To the north, where the Gurupi belt is located, the PSU is also shallow, possibly due to the presence of the Ferrer-Urbano Santos Arch, formed in the Mesozoic, during the Gondwana break-up. Although representing a high for the entire Parnaíba basin, this region is the local depocenter of the Cretaceous sequence of PB (see Fig.4 of Appendix III; Lima et al., 2020), which lies unconformably upon the offlaps of the Paleozoic sequences of PB.
- The gas fields located in the “Hawks Park” (PH in Fig.4.18. a) are shifted to the northeastern portion of the depocenter of PB (isoline of 2.5 km) upon the northern portion of the interpreted Barra do Corda belt. The generation, trap and seal of the petroleum system of the basin are conditioned by the presence of igneous sills of Mesozoic age (Porto,2014; Cunha et al., 2012; Miranda et al., 2018). According to the thickness maps of Lima et al. (2020; Fig.5 of Appendix III), and Daly et al. (2014), this region also coincides with great volumes of these diabase sills in the subsurface. Another spatial correlation is the presence of the MCR observed in the DRP, located between Teresina and “PH”.

- ***PSU from seismic data***

The interpretation of the PSU horizon in the seismic lines converted to depth, available in 295 and 317 surveys (see Fig.2.1 and Fig.2.3) is presented in the contour map of Fig.4.19. This grid covers an area to the SW of the main depocenter where there is a lack of wellbores. This way, this map brings more details for the understanding of the PSU relief.

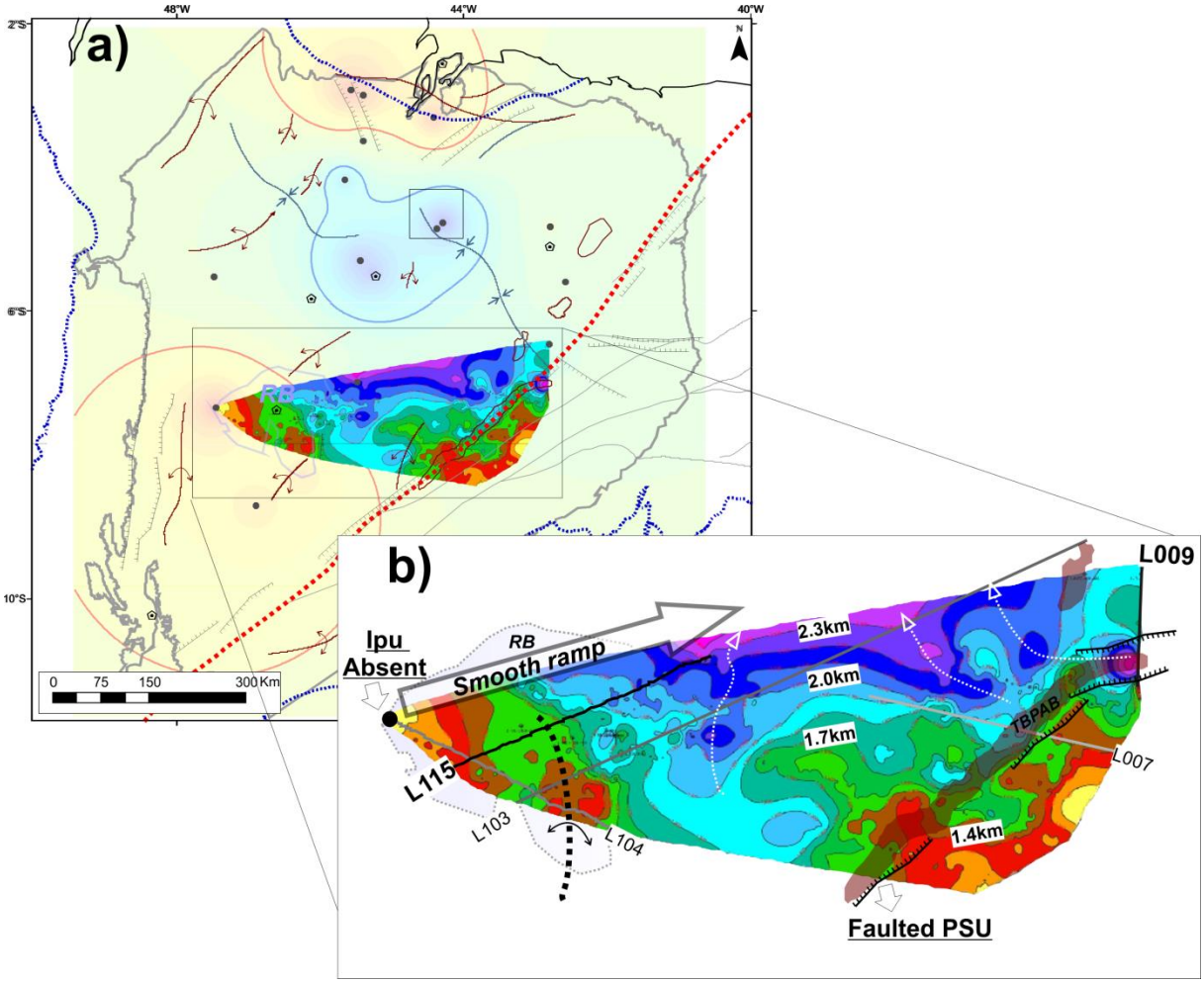

Fig. 4.19 (a) Contour map of the PSU seismic horizon in depth superimposed to the structural map of the PSU from wellbores available in Fig.4.18a. (b) Zoom of the contour map of the PSU seismic horizon in depth. The grey lines represent the seismic lines presented in Chapter 3 (L104, L007, L103), the black lines are the seismic lines L115 and L009, presented in the following figures. The white dashed arrows indicate local paleodepressions in the relief of the PSU, further discussed in the text.

The PSU analyzed from the seismic data varies from 1.3km (to the SE of the Transbrasiliano Fault Zone and towards the Eastern Araguaia belt), down to 2.3km northwards, where the basin depocenters based on wellbores was also observed. In the SW portion of the Parnaíba basin, upon the pre-Silurian Riachão basin, the PSU

is characterized as a smooth ramp, dipping to the north. In L115 (Fig.4.20), this ramp is exemplified as a remarkable erosive angular unconformity, truncating some NE-dipping events of the Riachão basin (Riachão III sequence; Fig.4.20c). This is also clearly shown in L104 (see Fig.3.9). Another interesting feature in this region is the smooth anticline (dashed black line in the map of Fig.4.19b) deforming the PSU and observed in L103 (Fig.3.10c between traces 801-2401). These shallower values of the PSU are centered upon the eastern depocenter of the basin (depocenter of the Riachão III sequence). In L104, to the SW, the lower portion of the Serra Grande Group (Ipu and Tianguá formations) is absent, as testified by the Carolina well (1-CL-1-MA), which sampled clastic sediments of the Jaicós Formation unconformably overlying a Neoproterozoic diorite gneiss (see Figs. 3.8 and 3.9 and Appendix II).

In sum, the characteristics observed in the seismic data in this region (equivalent to the eastern Araguaia and southern Grajaú basement domains; Fig. 4.18b) indicate a tectonic inversion of the Ediacaran (Porto et al., 2018) Riachão basin prior to the initiation of the Parnaíba basin sedimentation. It is also possible that this area was a high during Ordovician-Silurian times, when the lower Serra Grande Group sedimentation has occurred, due to the presence of a non-depositional unconformity (erosive?) in well data.

Near the Transbrasiliano Fault Zone, however, the seismic data show different features for the PSU. As already suggested in Assis et al. (2019; “Scientific paper 2”) in Fig.4.15, the Ordovician-Silurian sequence of the Parnaíba basin, more specifically, the Ipu Formation, seems to get thicker along pre-Silurian graben structures, here associated to the Cambro-Ordovician Transbrasiliano Pull-Apart Basins (TBPAB in Fig.4.19). This is represented, therefore, by localized paleodepressions in the relief of the PSU (Fig.4.19b). In the L009 profile (Fig.4.21), the graben structure observed to the south is connected to the graben of L007 (Fig. 3.9b; TBPAB). It is noticed that the PSU is faulted in this region of L009. There are subvertical faults affecting the basin that seem to be reactivated from rooted basement faults (e.g. Morais-Neto et al., 2013). To the north of L009, the PSU marks the unconformity between sandstones of the Ipu Formation and a Neoproterozoic mylonitic rock reached by the Floriano well (1-FL-1-PI; see Appendix II), possibly formed by dextral-shear deformations of the TBFZ during the Brasiliano orogeny (e.g. Caxito et al.,2020).

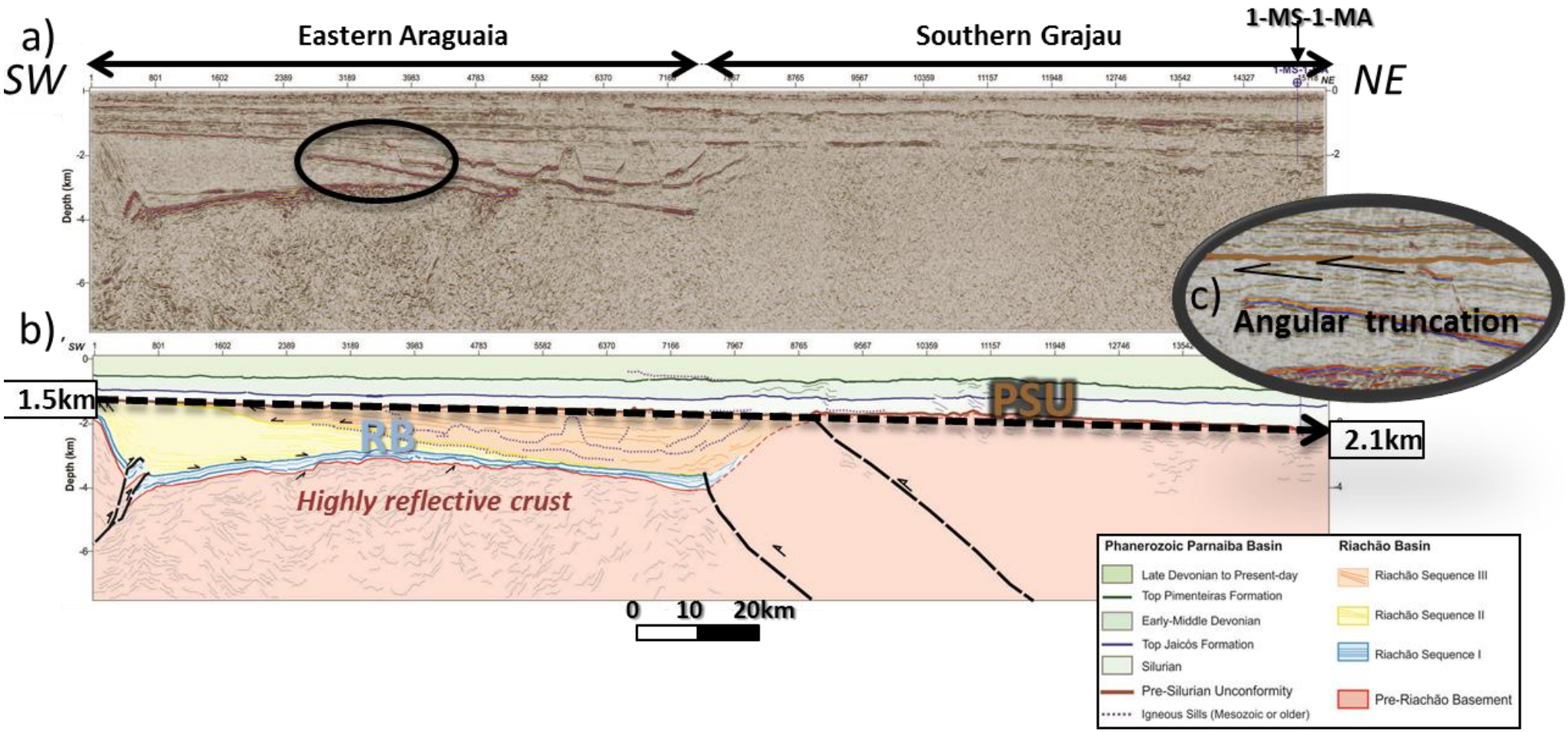

Fig.4.20 (a) raw and (b) interpreted seismic line L115, located in the SW of the Parnaíba basin, upon the Riachão basin (RB). The dashed black arrow along PSU highlights the smooth erosive ramp that characterizes the PSU in this region, also highlighted in the map of Fig.19b. In (c) a zoom of the erosive angular truncations of the Riachão basin sediments against the PSU is shown. The basement domains here interpreted are indicated in the upper part of the profile (a) by the black arrows. Modified after Porto (2017).

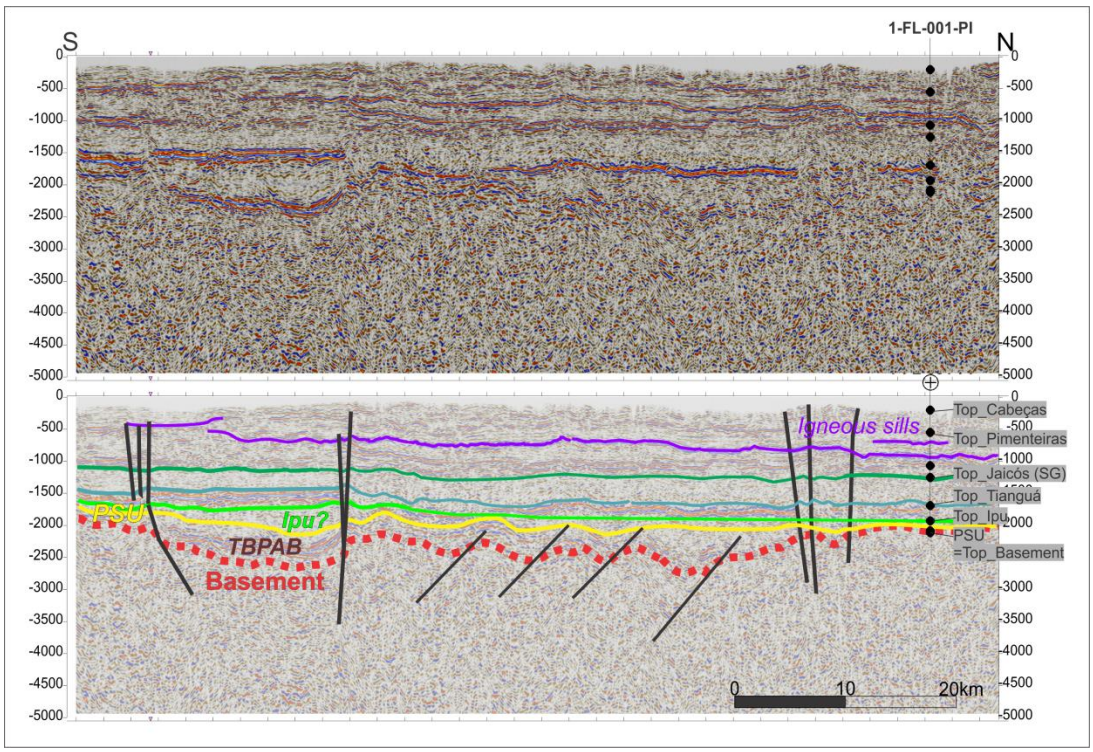

Fig.4.21 Seismic reflection L009 in depth, located in the vicinities of the Transbrasiliano Fault Zone, showing the location of the Floriano well in the northern portion, which penetrated a Neoproterozoic mylonitic rock (see Appendix II) and a graben structure to the south, in the prolongation of the TBPAB interpreted in L007 (see Fig.3.9b). A thickening of the Ipu Formation (top represented by the green horizon) upon this graben is interpreted, filling up a paleodepression of the PSU (in yellow).

- ***Recognizing the PSU in the field (NE Parnaíba basin)***

The field trip to the NE of the Parnaíba basin (see Fig.2.1 and the location maps of item 4.2) recognized the basal sedimentation of the Parnaíba basin in the Ibiapaba cliff, in Ceará state. This cliff is characterized by the uplifted border of the Parnaíba basin, preserving the most expressive outcrops of Ordovician-Silurian rocks in the NE of Brazil. The off-lap pattern of uplifted Paleozoic sequences in the eastern margin of the Parnaíba basin was observed along the DRP profile in Daly et al. (2014) and Tozer (2017). The figure 4.22 below illustrates this relationship between seismic data and the geomorphology of the surface relief.

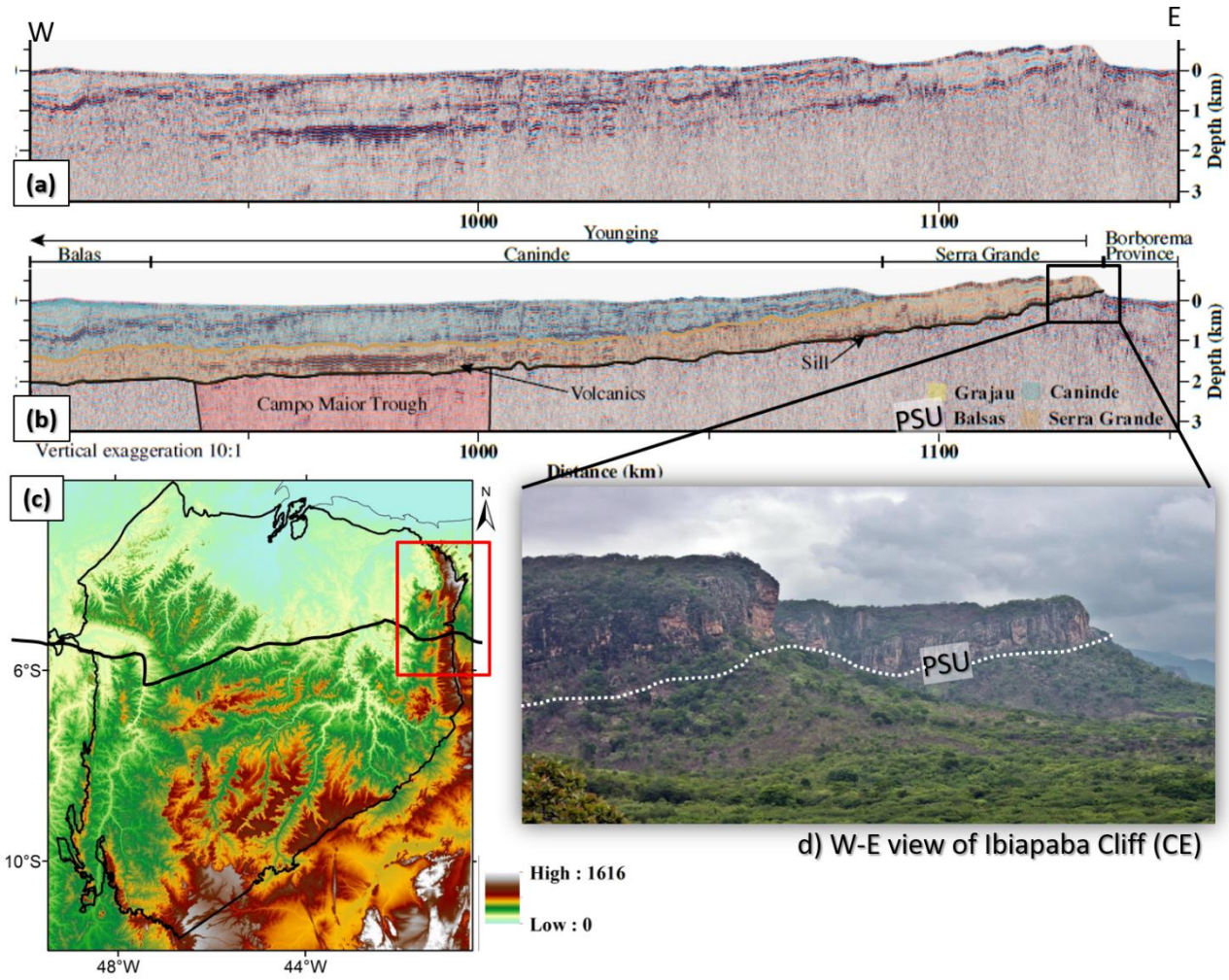

Fig. 4.22 (a) Eastern portion of the Deep seismic reflection profile (DRP) available in Tozer (2017), with the respective interpretation (b) showing the off-lap pattern of the uplifted margin of the Parnaíba basin; (c) the elevation map of the Parnaíba basin based on SRTM data, showing the location of the DRP(black line) and the Cliff alon the NE margin of the Parnaíba basin (red inset), ~1000-1500m above the sea; (c) an W-E view of the Ibiabapa cliff in Ceará state, showing the Serra Grande Group overlying the pre-Silurian basement.

Further examples of the outcropping PSU are shown in Figs. 4.23 and 4.24. The first pictures of Fig. 4.23 were taken in the National Ubajara Park (Ceará state) and show the geological unconformity between the Serra Grande Group (Ordovician-Silurian) and the sequences of the Late Neoproterozoic Ubajara basin, interpreted as a foreland basin located in the limit between the Médio Coreaú and Ceará Central domains of Northern Borborema Province (see Fig. 310; Caxito et al., 2020). In Figs. 4.23(b) and (c), the Serra Grande Group lies upon the folded carbonatic rocks of the Frecheirinha Formation and the PSU is recognized as an erosive angular unconformity. According to Chiglino et al. (2015), the deposition of the Frecheirinha Formation occurred between 635 and ca. 580 Ma, in the Ediacaran, along the continental margin of the Goiás-Pharusian ocean. Porto et al. (2018) compared these

carbonates as coeval to the basal Riachão I sequence in the Riachão basin (see Figs. 3.9a and 4.20). In Fig. 4.24, the conglomeratic facies of the lower Ipu Formation (see item 4.2 for more details) unconfomably overlies Paleoproterozoic metamorphic units of the Médio Coreaú domain (Granja Complex), which is also the basement of the Ubajara basin.

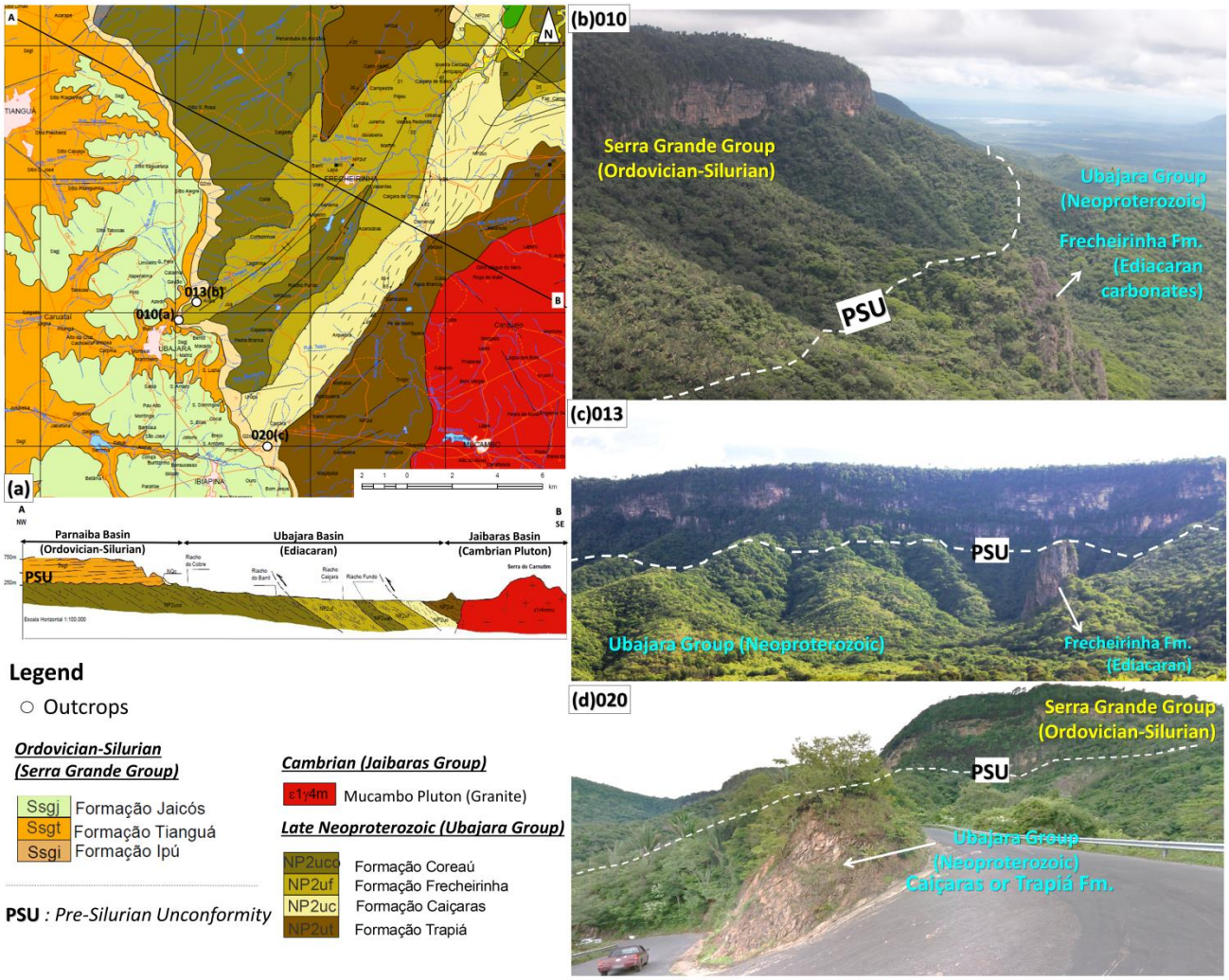

Fig. 4. 23 **Field examples of the PSU in the region of Ibiapaba cliff, Ceará state. (a) Geological map available in the Frecheirinha chart (SA.24-Y-C-VI; scale 1:100.000; Silva Junior et al., 2014) of the Geological Survey of Brazil (CPRM), with the location of the outcrops and schematic NW-SE geological section (A-A'). (b) , (c) and (d) show the Serra Grande group overlying the Ubajara Group.**

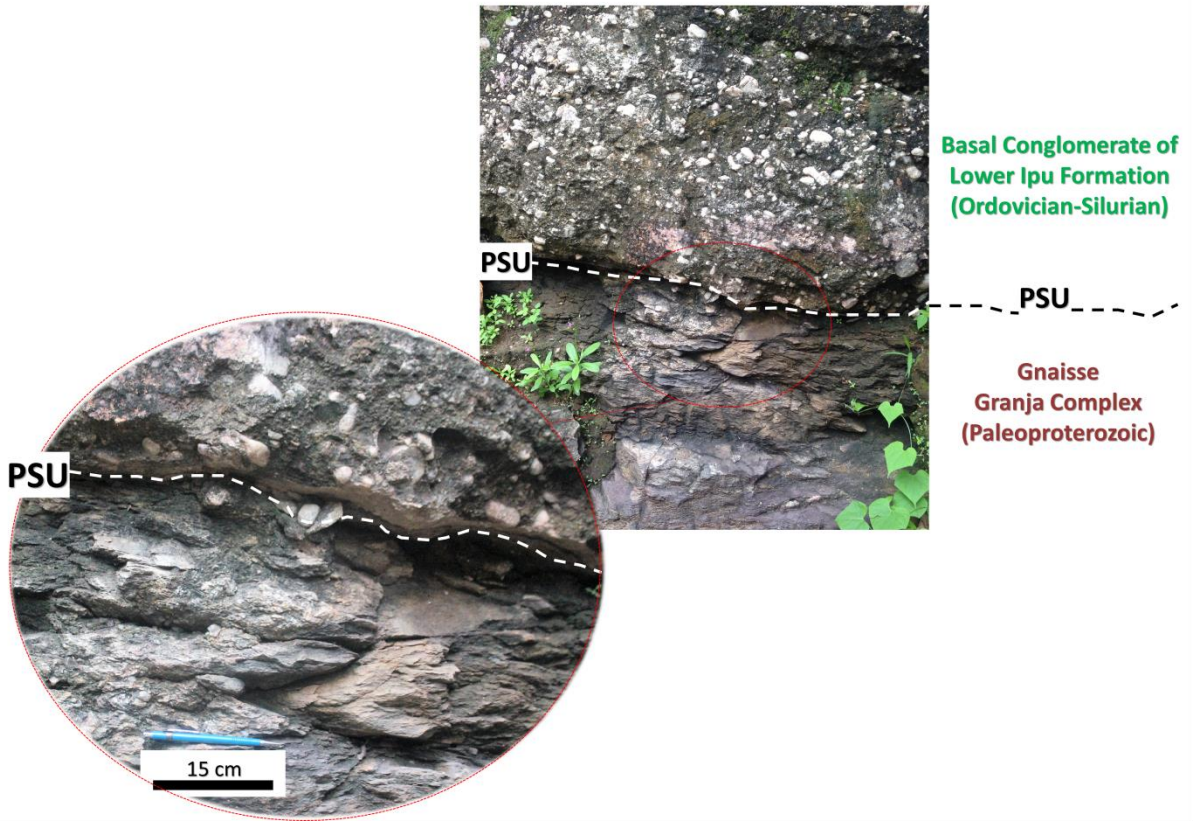

Fig. 4. 24 Detail of the pre-Silurian unconformity (PSU) marking the contact between conglomerates of the lower Ipu Formation and the Paleoproterozoic gneiss of the Granja Complex (Médio Coreaú Domain). The detailed description of these conglomerates is available in item 4.2. Location of the photo: Bica do Ipu, Ceará state.

4.3.2 Paleozoic evolution of the Parnaíba basin: depocenter migration and the basement configuration.

The change of the depocenter location during the Phanerozoic evolution of the Parnaíba Basin as well as the presence of active internal arches and regional unconformities have been widely observed since the first studies in the basin (Mesner & Wooldridge, 1964; Cunha, 1985; Góes and Feijó, 1994; Vaz et al., 2007). In Appendix III (Lima et al. 2020), E-W and N-S cross sections based on well data exemplify this situation.

The following isopach maps of Fig.4.25 illustrate this change in the depocenter during the Paleozoic-Early Mesozoic evolution of the Parnaíba basin. The methodology used for the interpolation is the same previously described in item 4.3.1 and the input data are shown in the list of wells available in Appendix II. The main basement tectonic domains defined in Chapter 3 (Fig. 3.11) are then superimposed to each of the isopach maps and the observations about this comparison are presented in the next paragraphs. Three sedimentary lithostratigraphic groups, associated to three main sequences of the Parnaíba basin, are represented, following the stratigraphic chart of Vaz et al. (2007), they are: Serra Grande (Late Ordovician-Silurian), Canindé (Middle Devonian-Early Carboniferous) and Balsas groups (Carboniferous-Early Triassic).

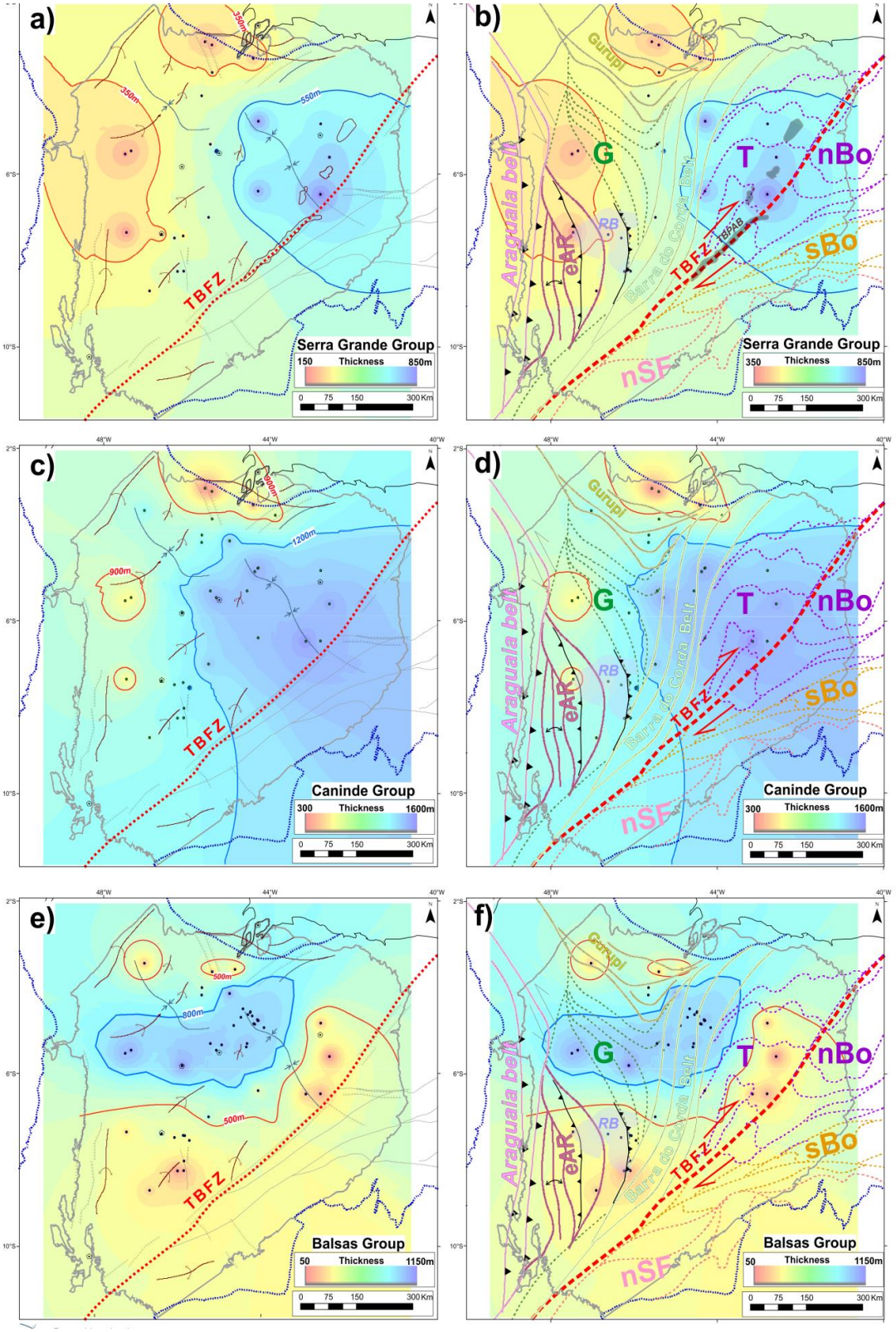

Fig. 4.25 (a), (c) and (e) are the isopach maps of the three main lithostratigraphic groups of the Parnaíba basin, Serra Grande (Late Ordovician-Silurian), Canindé (Middle Devonian-Early Carboniferous) and Balsas groups (Carboniferous-Early Triassic). The depositional axis, structural highs and normal faults are from Miranda et al. (2018). In (b), (d) and (f), the main contours of the basement tectonic units of the Parnaíba basin area superimposed to the respective isopach maps. The Brasiliano belts are: “eAr”: eastern Araguaia belt subdomain, Gurupi belt, and Barra do Corda belt. “G” stays for the Grajaú and “T” for Teresina domains.To the south of the Transbrasiliano Fault Zone (TBFZ), “nSF" refers to the northern margin of the São Francisco craton, and “nBo” and “sBo”

are the northern and southern domains of the Borborema Province.The pre-Silurian basins are: “RB”: Riachão and “TBPAB”: Transbrasiliano pull-part basins.

The most remarkable observation of these maps is that the maximum thickness values of the Serra Grande (>550m) and Canindé groups (>1200m), first Paleozoic sequences of the Parnaíba basin, are located upon the NE of the Teresina domain, while for the Balsas group (Late Paleozoic-Early Mesozoic), the depocenter (>800m thick) is shifted to the west, upon the Grajaú block. The three sequences are preserved with moderate thicknesses upon the northern portion of the Barra do Corda belt, in the central Parnaíba.

Another interesting observation is that the area defined as the Eastern Araguaia belt domain, where the Ediacaran Riachão foreland basin is described (Porto et al., 2018; Miranda, 2017), was possibly a paleo high during the Paleozoic and Early Mesozoic evolution of the Parnaíba basin. The signs of tectonic inversion in this area are prior to the PSU formation, due to the presence of evident erosive truncations in the top of the Riachão basin (Figs. 3.9, 3.10, 4.20).

In the maps of the Serra Grande Group (SGG; Figs. 4.25a and b), the grabens mapped in subsurface and associated to the Transbrasiliano Pull-Apart basins system are displayed. It is possible to notice the thickening of the SGG coincident to this region, especially to the NE.

4.4 Final Remarks

In Chapter 4, the Ordovician-Silurian tectono-sedimentary evolution of the Parnaíba basin has been presented based mainly on facies analysis of field observations in the NE of the Parnaíba basin and some seismic interpretations. Then, the Pre-Silurian Unconformity, prior to the deposition of the Serra Grande Group, was characterized in different examples. Finally, as well as the PSU contour map, the thickness maps of the Paleozoic sequences were compared to the main tectonic contours of the pre-Silurian basement, derived from the results of Chapter 3.

Some key results of Chapter 4 are listed below:

- The lowermost Ipu Formation (base of the Serra Grande Group) located in the NE of the Parnaíba basin is characterized by immature conglomerates in a scarp-related alluvial fan system, deposited in an active intracontinental tectonic context possibly related to fault reactivations along the NE-SW TBFZ or filling up paleo depressions constrained to the Cambro-Ordovician TBPAB.
- The Ipueiras tillite was first described, composing the uppermost portion of the Ipu Formation. It is a glacial deposit correlated to the Hirnantian Glaciation during the Ordovician-Silurian transition, well documented in other Gondwanan basins. Unconformably upon it, the Tianguá and Jaicós formations were deposited in a transgressive-regressive cycle, controlled first by the deglaciation and then by isostatic rebound.
- The pre-Silurian unconformity (PSU) described in the seismic data is characterized as a planar erosive unconformity upon most of the basin area, especially to the SW of the basin, where the remnant Ediacaran Riachão basin is located. However, to the NE, some localized faults and depressions are observed affecting the PSU, possibly related to Early Paleozoic reactivations along the TBFZ.
- The maximum depth of the Parnaíba basin (~3.5km) coincides with the location of the northern portion of the Neoproterozoic Barra do Corda belt, between the Grajaú, Teresina and Gurupi domains. However, when observing the evolution of the thickness maps during the Paleozoic, the first depocenter was located upon the Teresina domain, in the northern Borborema Province, and later, shifted to the west, upon the northern Grajaú block.

Chapter 5

Discussions, conclusions and future work

The giant Phanerozoic Parnaíba basin, in the NE of Brazil, hides a complex orogenic system marked by diachronic and oblique collisional fronts involving major and minor continental masses and the consumption of distinct oceanic realms, of different ages, scales and paleogeography (Cordani et al., 2013a, b; Schmitt et al., 2018;Caxito et al., 2020). This is not a surprise given the very complex Neoproterozoic Brasiliano-Pan African configuration of the outcropping domains along the edges of the basin, including the Borborema Province, Araguaia belt, Gurupi belt, the northern Brasília belt and associated Goiás magmatic arc, as well as the minor belts in the northern margin of the São Francisco Craton.

In subsurface, the first records of the basement from wellbores already indicated the continuity of Neoproterozoic metamorphic terranes and the prolongation of four distinct basement inliers beneath the basin (Cordani et al., 2008a, b). The compilation presented in Chapter 3 of very recent geophysical datasets of the shallow and deep crusts and of the lithosphere beneath the Parnaíba basin shed light on the expected complex configuration of this hidden portion of the Precambrian evolution of the NE of Brazil.

A simplified sketch (Fig. 5.1) presents a summary of the tectonic model proposed in this thesis for the Neoproterozoic basement of the Parnaíba basin, prior to its Late Ordovician-Silurian installation, complementing the previously presented maps and sketches of Chapter 3 (Fig. 3.10, 3.11, 3.12.). This model builds on several previous works, broadly speaking, assuming that the western Gondwana amalgamation involved two larger crustal building blocks: the Amazonian-West Africa and the Central African blocks, separated by a major oceanic domain, called the Goiás-Pharusian Ocean, amalgamated along the Transbrasiliano-Kandi corridor (Cordani et al 2013a, b; Ganade de Araujo et al., 2014; Caxito et al., 2020). Indeed, the interpretation presented here also takes into account recent tectonic studies of the Borborema Domain (e.g. Caxito et al., 2020; Ganade et al., 2021); Gurupi (e.g. Klein et al., 2017) and Araguaia (e.g. Hodel et al., 2019) domains.

Two main contributions are envisaged by the herein proposed tectonic model. The first one is to shed light on the internal structure of the Parnaíba block, as defined by Daly et al (2014; 2018; 2019) along the Deep Regional Profile. As illustrated in Figure 5.1, instead of a stable cratonic block, the so-called “Parnaíba block” is actually made of different crustal domains, separated by a thrust belt (or at least by a paleosuture zone?), here called as the Barra do Corda belt, and located in the central Parnaíba basin. The geophysical evidences to support such interpretations include: (1) the presence of the northeastwards dipping mid-crustal reflectivity (MCR; see items 3.2.7 and 3.3.3) in the central Parnaíba basin; (2) the presence of crustal-scale sub vertical MT conductor under Barra do Corda city (Solon et al., 2018); (3) crustal thickness (see item 3.2.5) and seismological (ex. Vp/Vs ratios; Schiffer et al.,2020) heterogeneities between the western and eastern portion of the Parnaíba basin; (4) high velocity lower crust beneath the NW of PB, but not in the eastern portion (Soares et al., 2018; Queiroz, 2019); (5) linear positive and negative anomalies in Bouguer map associated to a thrust belt in central PB.

A second contribution is the definition of the eastern Araguaia belt domain, beneath the SW Parnaíba basin, configuring a zone of back thrusts upon the so-called Grajaú block. This is evidenced mainly by: (6) a region of thinned crust and thinned lithosphere (see item 3.3.1) in SW of PB; (7) the thrusted margins and highly deformed crust (highly reflective crust) observed in the western portion of the remnant Ediacaran Riachão basin (see item 3.2.8; Porto et al., 2018).

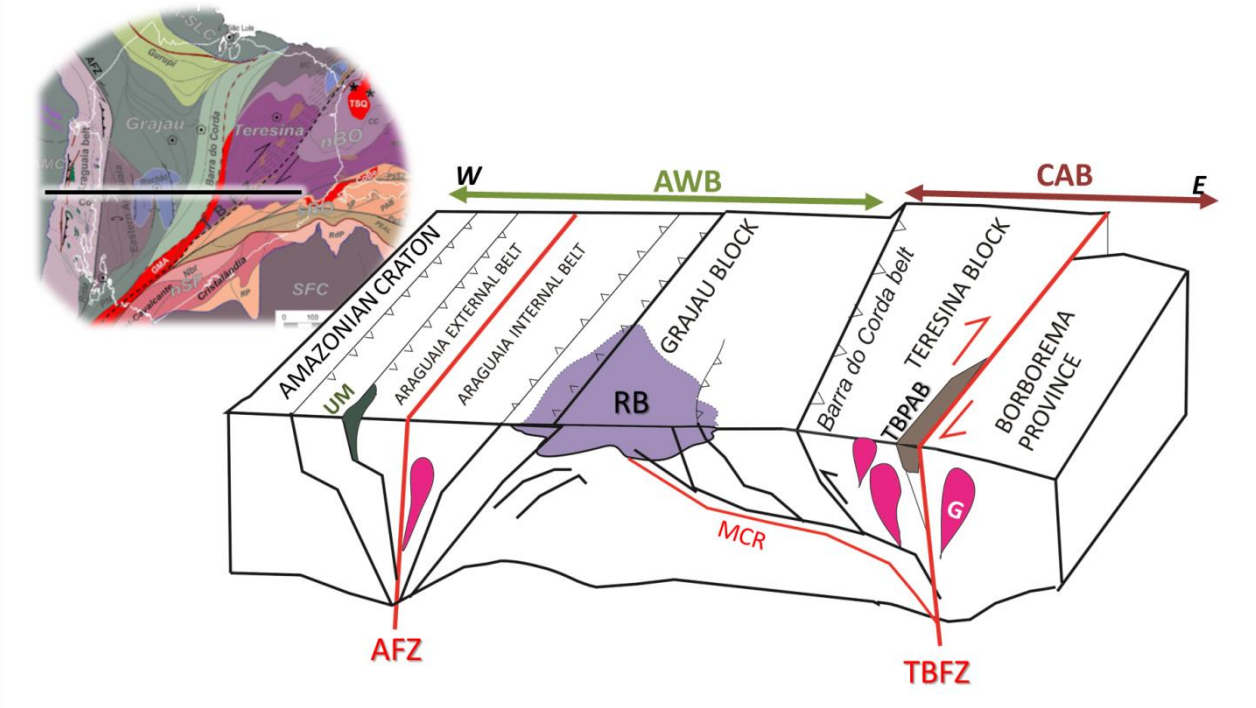

Fig.5.1 Simplified W-E sketch illustrating the tectonic relationships between the domains of the Neoproterozoic basement of the Parnaíba basin presented in Fig.3.10 (auxiliary map) and discussed in Chapter 3. “AFZ” stays for Araguaína Fault Zone, “UM”, ultramafic rocks, “G” granitoids; “RB”, Riachão basin, “MCR”, mid-crustal reflectivity, “TBFZ”, Transbrasiliano Fault Zone and TBPAB, Transbrasiliano pull-apart basins. The main crustal building blocks: Amazonian-West Africa (AWB) and the Central African (CAB).

In Chapter 4, the paleotectonic and paleogeographic conditions for the development of the Ordovician-Silurian sedimentation in the Parnaíba basin upon the regional erosive Pre-Silurian unconformity (PSU) were analyzed. Surface and subsurface observations indicate that the initial sedimentation of PB, marked by scarp-related alluvial-fan conglomerates in its eastern portion, seems to be constrained along paleo-valleys embedded within reactivated Neoproterozoic crustal-scale faults of the Transbrasiliano-Kandi corridor (Assis et al., 2019; item 4.2). The glacial conditions observed in outcrops of the Ipu Formation correlates to other Gondwanan basin records and possibly played an important role for the further stratigraphic (transgressive-regressive cycle) and subsidence (isostatic rebound?) controls of the younger sequences of the Serra Grande Group (Tianguá and Jaicós).

Regarding the implications of the basement configuration for the tectono-sedimentary evolution of the Phanerozoic Parnaíba basin, it is interesting to note the migration of the depocenters from the Early Paleozoic to the Early Mesozoic in relation to the position of the tectonic domains proposed here. The thickening of the

Serra Grande Group (Late Ordovician-Silurian) is located upon the Teresina domain, close to where the MCR-DRP was interpreted (see item 3.3.3 and Daly et al., 2014). In contrast, the thickening of the Balsas Group (Upper Carboniferous to Triassic) is shifted to the west, upon the northern Grajaú subdomain, where Soares et al. (2018) and Queiroz (2019) interpreted magmatic underplating, due to the high velocity anomaly in the lower crust (HVLC). This suggests an inheritance of the basement crustal blocks heterogeneities in controlling the basin subsidence through time.

The recent study investigating cratonic basins formation in the Wilson Cycle, published in Daly et al. (2019) reinforced the idea that most of such tectonic settings were formed after long orogenic cycles associated with supercontinent assembly. This seems to be the case of Parnaíba basin, possibly formed and initiated upon a thickened Brasiliano-Pan African orogenic plateau formed after the Goiás-Pharusian ocean consumption along the Transbrasiliano-Kandi corridor.

In terms of the theories regarding the subsidence driving mechanisms of cratonic basins, more investigations are required, once the complexity of the basement of such massive areas is being constantly unraveled and updated with the advances of geophysical studies, such as the ones compiled here (see item 3.2.4).

Daly et al. (2019) proposed that the subsidence of the Parnaíba basin could have been driven by the presence of a dense lower crust and or upper mantle – which could formed through magmatic or metamorphic processes – through viscoelastic relaxation and thermal contraction after plume activity beneath the large continental land mass. Following these authors, the presence of such a dense lower crust and upper mantle is coincident with the area of mid-crustal seismic reflectivity along DRP and to the presence of a relative gravity anomaly high over the centre of the Parnaíba basin. However, recent geophysical studies (Solon et al., 2018; Coelho et al., 2018; Soares et al., 2018; Lima et al.,2019; Schiffer et al., 2021; etc.) did not support the interpretation that a denser lower crust is found in the area of the MCR (see item 3.2.4). Indeed, in this thesis an alternative interpretation for this reflectivity is proposed, as a crustal-scale fault limiting two different domains. Moreover, the crustal thickness map herein produced put into evidence a Moho geometry by far more complex than the one pointed out along the DRP (Daly et al. 2014), indicating crustal heterogeneities within the basin area (see item 3.2.5).

A very recent thermo-mechanical model in North African intracratonic basins (Perron et al., 2021) showed that the stored gravitational potential energy inherited from density and rheological heterogeneities of accretionary continental lithosphere is the main explanation for the slow long-term subsidence of such basins, as well as for the rising of intrabasinal arches. For these authors, thermal anomalies, sediment supply rates or external far-field stresses, alone, do not account for the 1st order subsidence pattern, although these factors can temporarily change the subsidence rates. Obviously, this type of model needs to be tested and validated in other areas, such as the Parnaíba basin, but a further investigation in future works seems to be an interesting study once the complex orogenic setting hidden beneath PB is known.

Last but not least, it is very important to emphasize that most of the assumptions proposed here are mainly based on geophysical surveys and therefore there is an inherent ambiguity for the interpretations. This thesis did not cover, for example, an important player for the Parnaíba basin evolution: the Mesozoic Magmatism prior to the Gondwana break-up, widely observed in most of seismic and well data along the basin area. This and even younger tectonic processes might be superimposed to the Precambrian basement structures, masking some of the geophysical anomalies compiled here. It is also essential to integrate to this model direct information of the basement, such as the basement rock samples from wellbores, that need to be revised under the light of modern geochemical and geochronological techniques.

References

Abelha, M., Petersohn, E., Bastos, G., Araújo, D., 2018. New insights into the Parnaíba Basin: Results of investments by the Brazilian National Petroleum Agency. Geol. Soc. Spec. Publ. 472, 361–366. https://doi.org/10.1144/SP472.13

Agurto-Detzel, H., Assumpção, M., Bianchi, M., Pirchiner, M., 2017. Intraplate seismicity in mid-plate South America: Correlations with geophysical lithospheric parameters. Geol. Soc. Spec. Publ. 432, 73–90. https://doi.org/10.1144/SP432.5

Albuquerque, D.F., França, G.S., Moreira, L.P., Assumpção, M., Bianchi, M., Barros, L.V., Quispe, C.C., Oliveira, M.E., 2017. Crustal structure of the Amazonian Craton and adjacent provinces in Brazil. J. South Am. Earth Sci. 79, 431–442. https://doi.org/10.1016/j.jsames.2017.08.019

Allen, J.R.L., 1983. Studies in fluviatile sedimentation: Bars, bar-complexes and sandstone sheets (low-sinuosity braided streams) in the brownstones (L. devonian), welsh borders. Sedimentary Geology. 33, 237–293. https://doi.org/10.1016/0037-0738(83)90076-3

Allen, P.A., Armitage, J.J. 2012. Cratonic basins. In: Busby, C., Azor, A. (eds), Tectonics of Sedimentary Basins: Recent Advances. Blackwell Publishing Ltd., Oxford, United Kingdom, Ch. 30, 602-620.

Almeida, FFM de; Carneiro, C. Del Ré. Inundações marinhas fanerozóicas no Brasil e recursos minerais associados. *Mantesso Neto, V.; Bartorelli, A.; Carneiro, CDR*, 2004, 43-60.

Araújo, V.C.M., 2019. Imageamento sísmico da litosfera sob a Bacia do Parnaíba : Estudo de refração profunda e função do receptor com estações de período curto. PhD Thesis. Universidade de Brasília, Brasília.

Arcanjo, S.H.D.S., Abreu, F.A.M., Moura, C.A.V., 2013. Evolução geológica das sequências do embasamento do Cinturão Araguaia na região de Paraíso do Tocantins (TO), Brasil. Brazilian J. Geol. 43, 501–514. https://doi.org/10.5327/Z2317-48892013000300007

Arora, B.R., Padilha, A.L., Vitorello, Í., Trivedi, N.B., Fontes, S.L., Rigoti, A., Chamalaun, F.H., 1999. 2-D geoelectrical model for the Parnaiba Basin conductivity anomaly of northeast Brazil and tectonic implications. Tectonophysics 302, 57–69. https://doi.org/10.1016/S0040-1951(98)00272-8

Assine, M.L., Alvarenga, C.J.S., Perinotto, J.A.J., 1998. Formação Iapó: Glaciação Continental No Limite Ordoviciano/Siluriano Da Bacia Do Paraná. Revista Brasileira de Geociencias. 28, 51–60.

Assis, A.P., Porto, A.L., Schmitt, R.S., Linol, B., Medeiros, S.R., Correa Martins, F., Silva, D.S., 2019. The Ordovician-Silurian tectono-stratigraphic evolution and paleogeography of eastern Parnaíba Basin, NE Brazil. J. South Am. Earth Sci. 95, 102241. https://doi.org/10.1016/j.jsames.2019.102241

Assis, C.R.F., Moura, C.A.V., Milhomem Neto, J.M., Gorayeb, P.S.S., Dias, A.N.C., 2021. Zircon U-Pb geochronology and Lu-Hf isotope systematics of the Araguaia Belt basement Rocks: Evidence of links with the southeastern Amazonian Craton, Brazil. Precambrian Res. 356. https://doi.org/10.1016/j.precamres.2020.106090

Assumpção, M., Bianchi, M., Julià, J., Dias, F.L., Sand França, G., Nascimento, R., Drouet, S., Pavão, C.G., Albuquerque, D.F., Lopes, A.E.V., 2013. Crustal thickness map of Brazil: Data compilation and main features. J. South Am. Earth Sci. 43, 74–85. https://doi.org/10.1016/j.jsames.2012.12.009

Barrier, L., Proust, J. N., Nalpas, T., Robin, C., & Guillocheau, F. (2010). Control of alluvial sedimentation at foreland-basin active margins: a case study from the northeastern Ebro Basin (southeastern Pyrenees, Spain). *Journal of Sedimentary Research*, *80*(8), 728-749. https://doi.org/10.2110/jsr.2010.069

Barros, R. de A., Caxito, F. de A., Egydio-Silva, M., Dantas, E.L., Pinheiro, M.A.P., Rodrigues, J.B., Basei, M.A.S., Virgens-Neto, J. das, Freitas, M. de S., 2020. Archean and Paleoproterozoic crustal evolution and evidence for cryptic Paleoarchean-Hadean sources of the NW São Francisco Craton, Brazil: Lithochemistry, geochronology, and isotope systematics of the Cristalândia do Piauí Block. Gondwana Res. 88, 268–295. https://doi.org/10.1016/j.gr.2020.07.004

Beltrao, J.F., Silva, J.B.C., Costa, J.C., 1991. Robust polynomial fitting method for regional gravity estimation. Geophysics 56, 80–89. https://doi.org/10.1190/1.1442960

Berry, W.B.N., Boucot, A.J., 1973. Glacio-Eustatic control of late Ordovician-Early Silurian platform sedimentation and faunal changes. *Geological Society of America Bulletin*, *84*(1), 275-284.. https://doi.org/10.1130/0016-7606

Bhattacharya, J.P., 1992. Deltas, Facies models: Response to sea level change. Geological Association of Canada. 157-177.

Blair, T.C.; McPherson, J. G. 1994. Alluvial fans and their natural distinction from rivers based on morphology, hydraulic processes, sedimentary processes, and facies assemblages. Journal of sedimentary research, 64(3a), pp. 450-489.. https://doi.org/10.1306/D4267DDE-2B26-11D7-8648000102C1865D

Blair, T.C., 2000. Sedimentology and progressive tectonic unconformities of the sheetflood-dominated Hell's Gate alluvial fan, Death Valley, California. Sedimentary. Geology. 132, 233–262. https://doi.org/10.1016/S0037-0738(00)00010-5

Boulton, G.S., 1978. Boulder shapes and grain-size distributions of debris as indicators of transport paths through a glacier and till genesis. Sedimentology. 25(6), 773-799. https://doi.org/10.1111/j.1365-3091.1978.tb00329.x

Boulton, G.S., 1990. Sedimentary and sea level changes during glacial cycles and their control on glacimarine facies architecture. Geological Society of London, Special Publication. 53, 15–52.

Boulton, G.S., Deynoux, M., 1981. Sedimentation in glacial environments and the identification of tills and tillites in ancient sedimentary sequences. Precambrian Research. 15, 397–422. https://doi.org/10.1016/0301-9268(81)90059-0

Brito Neves, B.B., Fuck, R.A., Pimentel, M.M., 2014. The Brasiliano collage in South America: A review. Brazilian J. Geol. 44, 493–518. https://doi.org/10.5327/Z2317-4889201400030010

Brito Neves, B.B. de, Fuck, R.A., 2014. The basement of the South American platform: Half Laurentian (N-NW)+half Gondwanan (E-SE) domains. Precambrian Research. 244, 75–86. https://doi.org/10.1016/j.precamres.2013.09.020

Brito Neves, B., 2002. Main Stages of the Development of the Sedimentary Basins of South America and their Relationship with the Tectonics of Supercontinents. Gondwana Research. 5, 175–196. https://doi.org/10.1016/S1342-937X(05)70901-1

Brito Neves, B.B., Fuck, R.A., Cordani, U.G., Thomaz F, A., 1984. Influence of basement structures on the evolution of the major sedimentary basins of Brazil: A case of tectonic heritage. Journal of Geodynamics. 1, 495–510. https://doi.org/10.1016/0264-3707(84)90021-8

Caputo, M. V., & Crowell, J. C., 1985. Migration of glacial centers across Gondwana during Paleozoic Era. *Geological Society of America Bulletin*, *96*(8), 1020-1036. https://doi.org/10.1130/0016-7606.96

Caputo, M. V., Lima, E.C., 1984. Estratigrafia, idade e correlação do Grupo Serra Grande-Bacia do Parnaíba. Anais do XXXIII Congresso Brasilero de Geologia. pp. 228–241.

Caputo, M.V., 1984. Stratigraphy, Tectonics, Paleoclimatology and Paleogeography of Northern Basins of Brazil 583.

Carozzi, A. V., Falkenhein, F. V. H., Carneiro, R. G., Esteves, F. R., and Contreiras, C. J. A., 1975, Análise Ambiental e Evoluçao Tectônica sinsedimentar da Seção Siluro-Eocarbonífera da Bacia do Maranhão: Ciência-Técnica-Petróleo, Seção Exploração de Petróleo, Publicação no. 7, p. 89.

Carrivick, J.L., Russell, A.J., 1980. Glacifluvial Landforms of Deposition Introduction: Glacifluvial Systems. Sedimentol. J. Glaciol. J. Geol. https://doi.org/10.1016/B978-0-444-53643-3.00083-2

Carvalho, M.J., Lins, F. a. P.L., 2002. Estruturação da Formação Serra Grande na Região de Santana do Acaraú (CE) e a Reativação do Lineamento Sobral-

Pedro II: Integração com Dados Geofísicos. II Work. Avaliação Anual dos PRH's-ANP da Universidade Federal do Rio Grande do. N 1–4.

Caxito, F. de A., De Lira Santos, L.C.M., Ganade, C.E., Bendaoud, A., Fettous, E.H., Bouyo, M.H., 2020. Toward an integrated model of geological evolution for NE Brazil-NW Africa: The Borborema Province and its connections to the Trans-Saharan (Benino-Nigerian and Tuareg shields) and Central African orogens, Brazilian Journal of Geology. https://doi.org/10.1590/2317-4889202020190122

Caxito, F.A., Basto, C.F., Santos, L.C.M. de L., Dantas, E.L., Medeiros, V.C. de, Dias, T.G., Barrote, V., Hagemann, S., Alkmim, A.R., Lana, C., 2021. Neoproterozoic magmatic arc volcanism in the Borborema Province, NE Brazil: possible flare-ups and lulls and implications for western Gondwana assembly. Gondwana Res. 92, 1–25. https://doi.org/10.1016/j.gr.2020.11.015

Chulick, G.S., Detweiler, S., Mooney, W.D., 2013. Seismic structure of the crust and uppermost mantle of South America and surrounding oceanic basins. J. South Am. Earth Sci. 42, 260–276. https://doi.org/10.1016/j.jsames.2012.06.002

Coelho, D.L.O., Julià, J., Rodríguez-Tribaldos, V., White, N., 2018. Deep crustal architecture of the Parnaíba basin of NE Brazil from receiver function analysis: Implications for basin subsidence. Geol. Soc. Spec. Publ. 472, 83–99. https://doi.org/10.1144/SP472.8

Cordani, U.G., Brito Neves, B. B., & Thomaz Filho, A. 2009a. Estudo preliminar de integração do Pré-Cambriano com os eventos tectônicos das bacias sedimentares brasileiras (Atualização). Boletim Geociências da Petrobras, Rio de Janeiro, 17(1), pp. 205-219.

Cordani, U.G., Brito Neves, B.B., Fuck, R.A., Porto, R., Filho, A.T., Bezerra Da Cunha, F.M., 2008a. Estudo preliminar de integração do Pré-Cambriano com os eventos tectônicos das bacias sedimentares brasileiras (Republicação). Bol. Geociencias da Petrobras 17, 137–204.

Cordani, U.G., De Neves, B.B.B., Filho, A.T., 2008b. Estudo preliminar de integração do Pré-Cambriano com os eventos tectônicos das bacias sedimentares brasileiras (Atualização). Bol. Geociencias da Petrobras 17, 205–219.

Cordani, U.G., Pimentel, M.M., Araújo, C.E.G. De, Fuck, R.A., 2013a. The significance of the Transbrasiliano-Kandi tectonic corridor for the amalgamation of West Gondwana. Brazilian J. Geol. 43, 583–597. https://doi.org/10.5327/Z2317-48892013000300012

Cordani, U.G., Pimentel, M.M., De Araujo, C.E.G., Basei, M.A.S., Fuck, R.A., Girardi, V.A.V., 2013b. Was there an ediacaran clymene ocean in central south America? American journal of science. Am. J. Sci. 313, 517–539. https://doi.org/10.2475/06.2013.01

Cordani, U.G., Ramos, V.A., Fraga, L.M., Cegarra, M., Delgado, I., Souza, K.G. de, Gomes, F.E.M., Schobbenhaus, C., 2016. Tectonic map of South America: scale 1:5000000. Explanatory notes. 12. https://doi.org/10.14682/2016TEMSA

Cordani, U.G., Teixeira, W., D'Agrella-Filho, M.S., Trindade, R.I., 2009b. The position of the Amazonian Craton in supercontinents. *Gondwana Research*, *15*(3-4), pp. 396-407. https://doi.org/10.1016/j.gr.2008.12.005

Cruz, E. M. A. 2016. *Análise estratigráfica da Sequência Siluriana da Bacia do Parnaíba, NE do Brasil*. Universidade Federal do Rio Grande do Norte. Natal - Rio Grande do Norte, Brasil. Master's thesis, p. 62.

Cunha, F.M.B. da, 1986. Evolução paleozóica da Bacia do Parnaíba e seu arcabouço tectônico. Universidade Federal do Rio de Janeiro, Rio Janeiro, Brazil. Master Thesis, p. 107.

CUNHA, P.R.C. et al. Parnaíba Basin - The Awakening of a Giant. In: 11th Simposio Bolivariano Exploracion Petrolera en las Cuencas Subandinas, 2012, Cartagena de indias. Extended abstract. Cartagena de Indias: Asociación Colombiana de Geólogos y Geofísicos del Petróleo, 2012.

Daly, M.C., Andrade, V., Barousse, C.A., Costa, R., McDowell, K., Piggott, N., Poole, A.J., 2014. Brasiliano crustal structure and the tectonic setting of the Parnaíba basin of NE Brazil: Results of a deep seismic reflection profile. Tectonics. *33*, pp. 2102-2120 https://doi.org/10.1002/2014TC003632

Daly, M.C., Fuck, R.A., Julià, J., Macdonald, D.I.M., Watts, A.B., 2018. Cratonic basin formation: A case study of the Parnaíba Basin of Brazil. Geol. Soc. Spec. Publ. 472, 1–15. https://doi.org/10.1144/SP472.20

Daly, M.C., Tozer, B., Watts, A.B., 2019. Cratonic basins and the Wilson cycle: A perspective from the Parnaíba basin, Brazil. Geol. Soc. Spec. Publ. 470, 463–477. https://doi.org/10.1144/SP470.13

De Castro, D.L., Fuck, R.A., Phillips, J.D., Vidotti, R.M., Bezerra, F.H.R., Dantas, E.L., 2014. Crustal structure beneath the Paleozoic Parnaíba Basin revealed by airborne gravity and magnetic data, Brazil. Tectonophysics 614, pp. 128-145. https://doi.org/10.1016/j.tecto.2013.12.009

De Castro, D.L., Hilario Bezerra, F., Adolfo Fuck, R., Mary Vidotti, R., 2016. Geophysical evidence of pre-sag rifting and post-rifting fault reactivation in the Parnaíba basin, Brazil. Solid Earth 7, pp. 529–548. https://doi.org/10.5194/se-7-529-2016

De Castro, D.L., Oliveira, D.C., Hollanda, M.H.B.M., 2018. Geostatistical Interplay Between Geophysical and Geochemical Data: Mapping Litho-Structural Assemblages of Mesozoic Igneous Activities in the Parnaíba Basin (NE Brazil). Surv. Geophys. 39, 683–713. https://doi.org/10.1007/s10712-018-9463-5

De Lima, M.V.A.G., Stephenson, R.A., Soares, J.E.P., Fuck, R.A., De Araújo, V.C.M., Lima, F.T., Rocha, F.A.S., 2019. Characterization of crustal structure by comparing reflectivity patterns of wide-angle and near vertical seismic data from the Parnaíba Basin, Brazil. Geophys. J. Int. 218, 1652–1664. https://doi.org/10.1093/gji/ggz227

De Wit, M. J., Stankiewicz, J., & Reeves, C. (2008). Restoring Pan-African-Brasiliano connections: more Gondwana control, less trans-Atlantic corruption. Geological Society, London, Special Publications. In: Pre-Cenozoic Correlations Across the South Atlantic Region. 294, pp. 399-412.

Della Fávera, J. C. 1990. Tempestitos da bacia do Parnaíba. Universidade Federal do Rio Grande do SUl. Porto Alegre, Rio Grande do Sul, Brazil. Ph. D. thesis, p. 400.

Destro, N., Szatmari, P., Ladeira, E.A. 1994. Post-Devonian transpressional reactivation of a Proterozoic ductile shear zone in Ceará, NE Brazil. Journal of Structural Geology. 16, pp. 35-45. DOI: 10.1016/0191-8141(94)90016-7.

Deynoux, M. 1985. Terrestrial or waterlain glacial diamictites? Three case studies from the Late Precambrian and Late Ordovician glacial drifts in West Africa. Palaeogeogr. Palaeoclimatol. Palaeoecol. 51, pp. 97–141.

Deynoux, M., 1980. Les formations glaciaires du Précambrian terminal et de la fin de 1'Ordovicien en Afrique de l'Ouest; deux exemples de glaciation d'inlandsis sur une plate-forme stable. Trav. Lab. Sci. Terre, St. Jerôme, Marseille, (B), 17, p. 554.

Díaz-Martínez, E., Grahn, Y., 2007. Early Silurian glaciation along the western margin of Gondwana (Peru, Bolivia and northern Argentina): Palaeogeographic and geodynamic setting. Palaeogeogr. Palaeoclimatol. Palaeoecol. https://doi.org/10.1016/j.palaeo.2006.02.018

Dreimanis, A., 1989. Tills, their genetic terminology and classification. In: Goldthwait, R.P., Matsch, C.L. (Eds.), Genetic Classification of Glacienic Deposits. Balkema, Rotterdam, pp. 17–84.

Dumas, S., Arnott, R.W.C., 2006. Origin of hummocky and swaley cross-stratification - The controlling influence of unidirectional current strength and aggradation rate. Geology. 34, pp. 1073-1076. https://doi.org/10.1130/G22930A.1

Eyles, N., & Eyles, C. H. (1992). Glacial depositional systems. Facies models: Response to sea level change, pp. 73-100.

Eyles, N., 1993. Earth's glacial record and its tectonic setting. Earth Science Review. 35, p 248. https://doi.org/10.1016/0012-8252(93)90002-O

Eyles, N., Eyles, C.H., Miall, A.D., 1983. Lithofacies types and vertical profile models; an alternative approach to the description and environmental interpretation of glacial diamict and diamictite sequences. Sedimentology. 30, pp. 393-410. https://doi.org/10.1111/j.1365-3091.1983.tb00679.x

Feng, M., van der Lee, S., Assumpção, M., 2007. Upper mantle structure of South America from joint inversion of waveforms and fundamental mode group velocities of Rayleigh waves. J. Geophys. Res. Solid Earth 112, 1–16. https://doi.org/10.1029/2006JB004449

Ganade De Araujo, C.E., Rubatto, D., Hermann, J., Cordani, U.G., Caby, R., Basei, M.A.S., 2014. Ediacaran 2,500-km-long synchronous deep continental subduction in the West Gondwana Orogen. Nat. Commun. 5. https://doi.org/10.1038/ncomms6198

Ganade, C.E., Weinberg, R.F., Caxito, F.A., Lopes, L.B.L., Tesser, L.R., Costa, I.S., 2021. Decratonization by rifting enables orogenic reworking and transcurrent dispersal of old terranes in NE Brazil. Sci. Rep. 11, 1–13. https://doi.org/10.1038/s41598-021-84703-x

Garcia, X., Julià, J., Nemocón, A.M., Neukirch, M., 2019. Lithospheric thinning under the Araripe Basin (NE Brazil) from a long-period magnetotelluric survey: Constraints for tectonic inversion. Gondwana Res. 68, 174–184. https://doi.org/10.1016/j.gr.2018.11.013

Ghienne, J.F., 2003. Late Ordovician sedimentary environments, glacial cycles, and post-glacial transgression in the Taoudeni Basin, West Africa. Palaeogeogr. Palaeoclimatol. Palaeoecol. 189, pp. 117–145. https://doi.org/10.1016/S0031-0182(02)00635-1

Góes, A.M.O., Feijó, F.J., 1994. Bacia do Paranáiba. Bol. Geociencias da Petrobrás. 8, pp. 57-67.

Góes, A.M.O., Souza, J.M.P., Teixeira, L.B., 1990. Estágio Exploratório e Perspectivas Petrolíferas da Bacia do Parnaíba. Bol. Geociências da Petrobras 4, 55–64.

Gorayeb, P.S.S., Chaves, C.L., Moura, C.A.V., Da Silva Lobo, L.R., 2013. Neoproterozoic granites of the Lajeado intrusive suite, north-center Brazil: A late Ediacaran remelting of a Paleoproterozoic crust. J. South Am. Earth Sci. 45, 278–292. https://doi.org/10.1016/j.jsames.2013.04.001

Grahn, Y., Caputo, M. V., 1992. Early Silurian glaciations in Brazil. Palaeogeography Palaeoclimatology Palaeoecology. 99, pp. 9–15. https://doi.org/10.1016/0031-0182(92)90003-N

Grahn, Y., De Melo, J.H.G., Steemans, A.P., 2005. Integrated Chitinozoan and Miospore Zonation of the Serra Grande Group (Silurian-Lower Devonian),

Parnaíba Basin, Northeast Brazil. Revista Española de Micropaleontologia. 37, pp. 183–204.

Hambrey, M.J., 1985. The late Ordovician-Early Silurian glacial period. Palaeogeography Palaeoclimatology Palaeoecology. 51, pp. 273–289. https://doi.org/10.1016/0031-0182(85)90089-6

Harvey, A. M., Mather, A. E., & Stokes, M. (2005). Alluvial fans: geomorphology, sedimentology, dynamics—introduction. A review of alluvial-fan research. Geological Society of London, Special Publications, 251, pp. 1-7. https://doi.org/10.1144/GSL.SP.2005.251.01.01

Hasui, Y., Abreu, F.D.A.M. de, Silva, J.M.R. da, 1977. Estratigrafia da faixa de dobramentos Paraguai-Araguaia no centro-norte do Brasil. Bol. IG 8, 107. https://doi.org/10.11606/issn.2316-8978.v8i0p107-117

Heilbron, M., Guedes, E., & Mane, M. (2018). Geochemical and temporal provinciality of the magmatism of the eastern Parnaíba Basin. In *Cratonic Basin Formation: A Case Study of the Parnaíba Basin of Brazi*.*l* London: Geological Society.~

Heilbron, M., Cordani, U., Alkmim, F.F.. (Org.). São Francisco Craton, Eastern Brazil Tectonic Genealogy of a Miniature Continent. 1ed.Cham, Switzerland: Springer, 2017, v. 1.

Herz, N., Hasui, Y., Costa, J.B.S., Matta, M.A.D.S., 1989. The Araguaia fold belt, Brazil: A reactivated Brasiliano-Pan-African cycle (550 Ma) geosuture. Precambrian Res. 42, 371–386. https://doi.org/10.1016/0301-9268(89)90020-X

Hodel, F., Trindade, R.I.F., Macouin, M., Meira, V.T., Dantas, E.L., Paixão, M.A.P., Rospabé, M., Castro, M.P., Queiroga, G.N., Alkmim, A.R., Lana, C.C., 2019. A Neoproterozoic hyper-extended margin associated with Rodinia's demise and Gondwana's build-up: The Araguaia Belt, central Brazil. Gondwana Res. 66, 43–62. https://doi.org/10.1016/j.gr.2018.08.010

Huuse, M., Le Heron, D.P., Dixon, R., Redfern, J., Moscariello, A., Craig, J., 2012. Glaciogenic reservoirs and hydrocarbon systems: an introduction. Geological

Society of London, Special Publications. 368, 1–28. https://doi.org/10.1144/SP368.19

Kegel, W., 1953, Contribuição para o estudo do Devoniano da Bacia do Parnaíba:

Klein, E.L., Lopes, E.C. dos S., Tavares, F.M., Campos, L.D., Souza-Gaia, S.M. de, Neves, M.P., Perrotta, M.M., 2017. Área de relevante interesse mineral: cinturão do Gurupi.

Kotschoubey, B., Hieronymus, B., de Albuquerque, C.A.R., 2005. Disrupted peridotites and basalts from the Neoproterozoic Araguaia belt (northern Brazil): Remnants of a poorly evolved oceanic crust? J. South Am. Earth Sci. 20, 211–230. https://doi.org/10.1016/j.jsames.2005.05.007

Krystopowicz, N.J., Currie, C.A., 2013. Crustal eclogitization and lithosphere delamination in orogens. Earth Planet. Sci. Lett. 361, 195–207. https://doi.org/10.1016/j.epsl.2012.09.056

Le Hérissé, A., De Melo, J.H.G., Quadros, L.P., Grahn, Y., Steemans, P., 2001. Palynological characterization and dating of the Tianguá Formation, Serra Grande Group, northern Brazil. Correlaçâo De Seqüências Paleozóicas Sul-Americanas. 20, pp. 25–41.

Le Heron, D.P., Armstrong, H.A., Wilson, C., Howard, J.P., Gindre, L., 2010. Glaciation and deglaciation of the Libyan Desert: The Late Ordovician record. Sedimentary Geology. 223, pp. 100–125. https://doi.org/10.1016/j.sedgeo.2009.11.002

Le Heron, D.P., Howard, J., 2010. Evidence for Late Ordovician glaciation of Al Kufrah Basin, Libya. Journal of African Earth Science. 58, pp. 354–364. https://doi.org/10.1016/j.jafrearsci.2010.04.001

Leleu, S., Ghienne, J.F., Manatschal, G., 2009. Alluvial fan development and morpho-tectonic evolution in response to contractional fault reactivation (Late Cretaceous - Palaeocene), Provence, France. Basin Research. 21, pp. 157–187. https://doi.org/10.1111/j.1365-2117.2008.00378.x

Lima, F.G.F., De Sá, E.F.J., 2017. Controle estrutural da borda sudeste da Bacia do Parnaíba, Nordeste do Brasil: relação com eventos geodinâmicos no

Gondwana. Geologia USP. Série Científica. 17, pp. 3-21. https://doi.org/10.11606/issn.2316-9095.v17-125909

Linol, B., de Wit, M.J., Barton, E., de Wit, M.M.J.C., Guillocheau, F., 2016a. U-Pb detrital zircon dates and source provenance analysis of Phanerozoic sequences of the Congo Basin, central Gondwana. Gondwana Research. 29, pp. 208–219. https://doi.org/10.1016/j.gr.2014.11.009

Linol, B., De Wit, M.J., Milani, E.J., Guillocheau, F., Scherer, C., 2015. New regional correlations between the Congo, Paraná and Cape-Karoo basins of Southwest Gondwana, in: Geology and Resource Potential of the Congo Basin. https://doi.org/10.1007/978-3-642-29482-2_13

Linol, B., Wit, M.J. De, Kasanzu, C.H., Schmitt, S., Corrêa-martins, F.J., Assis, A. P. 2016b. Origin and Evolution of the Cape Mountains and Karoo Basin. Springer, pp. 183-192 https://doi.org/10.1007/978-3-319-40859-0

Lloyd, S., Van Der Lee, S., França, G.S., Assumpção, M., Feng, M., 2010. Moho map of South America from receiver functions and surface waves. J. Geophys. Res. Solid Earth 115, 1–12. https://doi.org/10.1029/2009JB006829

Luz, R.M.N., Julià, J., Do Nascimento, A.F., 2015. Crustal structure of the eastern Borborema Province, NE Brazil, from the joint inversion of receiver functions and surface wave dispersion: Implications for plateau uplift. J. Geophys. Res. Solid Earth 120, 3848–3869. https://doi.org/10.1002/2015JB011872

Machado, M. A., 2006. Caracterização descritiva e genética de ocorrências cupro-hematíticas no setor sudoeste do sistema Orós-Jaguaribe, Província Borborema. MSc thesis. Universidade de Brasília, Brasília.

Manenti, R.R., Souza, W.E., Porsani, M.J., 2018. Reprocessing and interpretation of deep structures in a regional transect of the Parnaíba Basin, Brazil. Geol. Soc. Spec. Publ. 472, 101–107. https://doi.org/10.1144/SP472.17

McKenzie, D., Priestley, K., 2008. The influence of lithospheric thickness variations on continental evolution. Lithos 102, 1–11.

Mckenzie, D., Daly, M.C. & Priestley, K. 2015. The lithospheric structure of Pangea. Geology, 43, 783–786.

Mckenzie, D., Tribaldos, V.R., 2018. Lithospheric heating by crustal thickening: A possible origin of the Parnaíba Basin. Geol. Soc. Spec. Publ. 472, 37–44. https://doi.org/10.1144/SP472.5

Mesner, J. C. & Wooldridge, L. C. P. (1964) – Estratigrafia das bacias paleozoica e cretácea do Maranhão. Rio de Janeiro, Boletim Técnico Petrobras 7, p. 137-164.

Metelo, C.M.S., 1999. Caracterização estratigráfica do Grupo Serra Grande (Siluriano) na borda sudeste da Bacia do Parnaíba. Universidade Federal do Rio de Janeiro. Rio Janeiro, Brasil. Master thesis, p. 102.

Miall, A. D. (1977). A review of the braided-river depositional environment. Earth-Science Reviews, 13, 1-62. https://doi.org/10.1016/0012-8252(77)90055-1

Miall, A. D., 1996., The Geology of Fluvial Deposits - Sedimentary Facies, Basin Analysis, and Petroleum Geology. Springer, Verlag Berlin Heidelber. https://doi.org/10.1007/978-3-662-03237-4

Milani, E.J., De Wit, M.J., 2008. Correlations between the classic Paraná and Cape–Karoo sequences of South America and southern Africa and their basin infills flanking the Gondwanides: du Toit revisited. Geological Society of London, Special Publications. 294, pp. 319-342. https://doi.org/10.1144/SP294.17

Miranda, V. N., 2017. Bacia pré-siluriana na porção centro-oeste da Provincia Parnaíba, NE do Brasil. MSc thesis. Universidade Federal do Rio Grande do Norte, Natal.

Mocitaiba, L.S.R., De Castro, D.L., De Oliveira, D.C., 2017. Cartografia geofísica regional do magmatismo mesozoico na Bacia do Parnaíba. Geol. USP - Ser. Cient. 17, 169–192. https://doi.org/10.11606/issn.2316-9095.v17-455

Morais Neto, J.M. de, Jr., I.T., Santos, S.F., Vasconcelos, C.S., Menezes, J.R.C. de, Ribas, M. de P., Iwata, S.A., 2013. Expressão Sísmica Das Reativações Tectônicas Do Lineamento Transbrasiliano Na Bacia Do Parnaíba. XIV Simpósio Nac. Estud. Tectônicos - VIII Int. Symp. Tectonics, Chapada dos Guimarães, Bras. Vol. An. (CD), ST4.

Morais Neto, J.M., Trosdtorf Jr, I., Santos, S.F., Vasconcelos, C.S., Menezes, J.R.C., Ribas, M.P., Iwata, S.A., 2013. Expressão sísmica das reativações tectônicas do Lineamento Transbrasiliano na bacia do Parnaíba, in: Proceeds of the VIII International Symposium on Tectonics, Chapada Dos Guimarães, Brazil, Extended Abstract.

Mutti, E., Tinterri, R., Biase, D. D., Fava, L., Mavilla, N., Angella, S., & Calabrese, L. 2000. Delta-from facies associations of ancient flood-dominated fluvio-deltaic systems. Revista de la Sociedad Geológica de España, 13(2), pp. 165-190.

Oliveira, D.C., Mohriak, W.U., 2003. Jaibaras trough: An important element in the early tectonic evolution of the Parnaíba interior sag basin, Northern Brazil. Mar. Pet. Geol. 20, pp. 351–383.

Paixão, M.A.P., Nilson, A.A., Dantas, E.L., 2008. The neoproterozoic quatipuru ophiolite and the Araguaia fold belt, central-northern Brazil, compared with correlatives in NW Africa. Geol. Soc. Spec. Publ. 294, 297–318. https://doi.org/10.1144/SP294.16

Pedrosa, Jr., N.C., Vidotti, R.M., Fuck, R.A., Leopoldino, K.M., Castelo, R.M.G., 2014. Journal of South American Earth Sciences Structural framework of the Jaibaras Rift , Brazil , based on geophysical data 1–17. http://dx.doi.org/10.1016/j.jsames.2014.07.005

Perron, P., Le Pourhiet, L., Guiraud, M., Vennin, E., Moretti, I., Portier, É., Konaté, M., 2021. Control of inherited accreted lithospheric heterogeneity on the architecture and the low, long-term subsidence rate of intracratonic basins. BSGF - Earth Sci. Bull. 192. https://doi.org/10.1051/bsgf/2020038

Porto, A., Daly, M.C., La Terra, E., Fontes, S., 2018. The pre-Silurian Riachão basin: A new perspective on the basement of the Parnaíba basin, NE Brazil. Geol. Soc. Spec. Publ. 472, 127–145. https://doi.org/10.1144/SP472.2

Porto, A.L., 2017. The pre-Silurian Riachão basin, a new perspective into the basement configuration of the cratonic Parnaíba basin, NE Brazil. MSc thesis. Observatório Nacional, Rio de Janeiro.

Porto, A.L., 2014. Mapeamento Sísmico de Intrusões Ígneas na Porção Sudeste da Bacia do Parnaíba e suas Implicações para um modelo de sistema Petrolífero

Não Convencional. Undergraduate thesis. Universidade do Estado do Rio de Janeiro, Rio de Janeiro.

Priestley, K., McKenzie, D., 2006. The thermal structure of the lithosphere from shear wave velocities. Earth and Planetary Science Letters 244, 97–112.

Quadros, M.L.E.S., 1996, Estudo tectono-sedimentar da Bacia de Jaibaras, na regia˜o entre as cidades de Pacujá e Jaibaras, noroeste do Estado do Ceará. Universidade Federal do Pará. Belém, Pará. Masters thesis, p. 134.

Queiroz, D.S. De, 2019. Transecta sísmica N-S através do depocentro da Bacia do Parnaíba : Aproximação por função do receptor e CCP. MSc Thesis. Universidade de Brasília, Brasília.

Rincón Cuervo, H.D., Soares, E.A.A., Caputo, M.V., Dino, R., 2018. Sedimentology and stratigraphy of new outcrops of Silurian glaciomarine strata in the Presidente Figueiredo region, northwestern margin of the Amazonianas Basin. Journal of South America Earth Science. 85, pp. 43–56. https://doi.org/10.1016/j.jsames.2018.04.023

Rocha, N.S., Fontes, S.L., La Terra, E.F., Fuck, R.A., 2019. Lithosphere structures of the Parnaíba Basin and adjacent provinces revealed by deep magnetotelluric imaging. J. South Am. Earth Sci. 92, 1–11. https://doi.org/10.1016/j.jsames.2019.02.020

Romero, G., La Terra, E.F., Panetto, L.P., Fontes, S.L., 2019. Upper crustal structures of the southeast edge of Parnaíba basin using 3D magnetotelluric data imaging. J. South Am. Earth Sci. 96. https://doi.org/10.1016/j.jsames.2019.102392

Rust, I. C. (1973). The evolution of the Paleozoic Cape Basin, southern margin of Africa. In The South Atlantic. Springer, Boston, MA, pp. 247-276.

Saltus, R.W., Blakely, R.J., 2011. Unique geologic insights from “non-unique” gravity and magnetic interpretation. GSA Today 21, 4–11. https://doi.org/10.1130/G136A.1

Schiffer, C., de Lima, M.V.A.G., Soares, J.E.P., Stephenson, R., de Araújo, V.C.M., Lima, F.T., Rocha, F.A.S., Trindade, C.R., Fuck, R.A., 2021. Vp/Vs ratios in the Parnaíba Basin from joint active-passive seismic analysis – Implications for

continental amalgamation and basin formation. Tectonophysics 801. https://doi.org/10.1016/j.tecto.2020.228715

Schmitt, R.S., Silva, E.A., Collins, A.S., Reeves, C., Fragoso, R.A., Richetti, P.C., Fernandes, G.L. de F., Benedek, M.R., Costa, R.L., Assis, A.P., 2016. Gondwana tectonic evolution recounted through the Gondwana map—IGCP-628. In: Abstracts of 35th International Geological Con- Gress, Cape Town, South Africa.

Schmitt, R. da S., de Araújo Fragoso, R., Collins, A.S., 2018. Suturing Gondwana in the Cambrian: The Orogenic Events of the Final Amalgamation, in: Geology of Southwest Gondwana. Springer, pp. 411–432. https://doi.org/10.1007/978-3-319-68920-3_15

Schuback, V. H. T., 2019. Interpretação Sísmica e Modelagem gravimétrica 2D do Paleozoico inferior na porção Sudeste da bacia do Parnaíba. MSc thesis. Universidade do Estado do Rio de Janeiro, Rio de Janeiro.

Scotese, C.R., Boucot, A.J., McKerrow, W.S., 1999. Gondwanan palaeogeography and palıoclimatology. Jounal of African Earth Science. 28, pp. 99-114. https://doi.org/10.1016/S0899-5362(98)00084-0

Silva Junior, O.G. da, Santos, M.V. dos, Moura, C.A.V., Nascimento, R. da S., Vilas, R.N.N., 2014. Carta geológica: folha Frecheirinha-SA. 24-YC-VI. CPRM, Serviço Geológico do Brasil.

Sloss, L.L., 1990. Epilog, in: Interior Cratonic Basins. The American Association of Petroleum Geologists Tulsa, pp. 799–805.

Small, H. L., 1914, Geologia e suprimento d'água subterrânea no Piauí e parte do Ceará, Brasil: Instituto e Obras Contra Secas, Série I.D. Rio de Janeiro, piblic. 32, p. 146.

Soares, J.E.P., Stephenson, R., Fuck, R.A., Lima, M.V.A.G.D.E., Araújo, V.C.M.D.E., Lima, T., Rocha, F.A.S., Trindade, C.R.D.A., Geociências, I. De, Ribeiro, C.D., Brasília, U. De, Rs, S., 2018. Structure of the crust and upper mantle beneath the Parnaíba Basin , Brazil , from wide-angle re fl ection – refraction data Tectonic setting The Parnaíba Basin is a sag basin occupying an area. Geol. Soc. London 472, 67–82.

Solon, F.F., Fontes, S.L., La Terra, E.F., 2018. Electrical conductivity structure across the Parnaíba Basin, NE Brazil. Geol. Soc. Spec. Publ. 472, 109–126. https://doi.org/10.1144/SP472.19

Tohver E., Cawood P.A., Rossello E.A., Jourdan F., 201. Closure of the Clymene Ocean and formation of West Gondwana in the Cambrian: evidence from the Sierras Australes of the southernmost Rio de la Plata craton, Argentina. Gondwana Res 21:394–405.

Torsvik, T.H., Cocks, L.R.M., 2011. The Palaeozoic palaeogeography of central Gondwana. Geological Society of London, Special Publications. 357, pp. 137–166. https://doi.org/10.1144/SP357.8

Torsvik, T.H., Cocks, L.R.M., 2013. Gondwana from top to base in space and time. Gondwana Research 24, pp. 999–1030. https://doi.org/10.1016/j.gr.2013.06.012

Tozer, B., 2017. Crustal structure, gravity anomalies and subsidence history of the Parnaíba cratonic basin, Northeast Brazil. PhD Thesis. Univerisity of Oxford, Oxford.

Tozer, B., Watts, A.B., Daly, M.C., 2017. Crustal structure, gravity anomalies, and subsidence history of the Parnaíba cratonic basin, Northeast Brazil. Journal of Geophysical Researsch Solid Earth. 122, pp. 5591–5621. https://doi.org/10.1002/2017JB014348

Trindade, C.R., 2014. Espessura Crustal e Razão de Poisson do Brasil Central: Uma Aproximação por Função do Receptor. MSc Thesis. Universidade de Brasília, Brasília.

Uieda, L., Barbosa, V.C.F., 2017. Fast nonlinear gravity inversion in spherical coordinates with application to the South AmericanMoho. Geophys. J. Int. 208, 162–176. https://doi.org/10.1093/gji/ggw390

Van der Meijde, M., Julià, J., Assumpção, M., 2013. Gravity derived Moho for South America. Tectonophysics 609, 456–467. https://doi.org/10.1016/j.tecto.2013.03.023

Vaz, P.T., Rezende, N.G.A.M., Wanderley Filho, J.R., Silva Travassos, W.A., 2007. Bacia do Parnaíba. Bol. Geociencias da Petrobras 15, pp. 253–263.

Viana, M.S.S., Oliveira, P. V., Sousa, M.J.G., Baroso, F.R.G., Vasconcelos, V.A., Melo, R.M., Lima, T.A., Oliveira, G.C., Chaves, A.P.P., 2010. Ocorrências Icnofossilíferas do Grupo Serra Grande (Siluriano da Bacia do Parnaíba), Noroeste de Estado de Ceará. Revista Geologia - Universidade Federal do Ceará. 23, p. 13.

Villeneuve, M., 2005. Paleozoic basins in West Africa and the Mauritanide thrust belt. Journal of African Earth Science. 43, pp. 166–195.

Walker, R.G., Plint, A.G., 1992. Wave-and storm-dominated shallow marine systems. Facies Models-response to sea level change, pp. 219-238.

Zhu, L., Kanamori, H., 2000. Moho depth variation in southern California from teleseismic receiver functions. Journal of Geophysical Research 105 (B2), 2969–2980.

Appendix I

"Seismographic Stations Information"

(Table and Auxiliary Map)
Equivalent to "SUPPLEMENTRAY MATERIAL 1"
of "Scientific Paper 1"

Station	X(Long)	Y (Lat)	H (km)	Source *(See references)*
PEXB	-48.3006	-12.1056	37,8 ± 1.2	Assumpção et al.,2013
BESB	-43.5774	-6.67307	35.6 ± 1.4	Assumpção et al.,2013
CS6B	-38.6995	-5.51904	30.4 ± 2.5	Assumpção et al.,2013
LJDO	-48.29	-9.77	42.9 ± 0.4	Trindade, 2014
SAMA	-47.59	-8.86	44.1 ± 0.7	Trindade, 2014
NOAC	-47.63	-9.99	44.8 ± 0.9	Trindade, 2014
MOCA	-47.83	-10.63	43.9 ± 0.6	Trindade, 2014
PATO	-47.31	-10.64	44.7 ± 2.7	Trindade, 2014
SFTO	-46.64	-10.18	46.7 ± 14	Trindade, 2014
PIUM	-49.18	-10.44	53 ± 2.3	Trindade, 2014
RET1	-48.55	-10.67	41.3 ± 1.3	Trindade, 2014
NBPS	-41.446	-4.394	39.7 ± 1.1	Luz et al.,2015
NBMO	-40.041	-3.311	34.4 ± 0.3	Luz et al.,2015
NBPB	-39.584	-5.543	36.9 ± 0.6	Luz et al.,2015
SBBR	-40.371	-3.74518	35.5 ± 1.0	Luz et al.,2015
LP02	-39.635	-4.513	30.9 ± 0.6	Luz et al.,2015
TUC4	-49.5499	-4.25792	41.8 ± 2.0	Albuquerque et al.,2017
LAJE	-48.3483	-9.98052	41.7 ± 3.6	Albuquerque et al.,2017
SMTB	-47.6106	-8.86218	36.9 ± 0.4	Albuquerque et al.,2017
PAL1	-47.5868	-6.64928	31.4 ± 2.2	Albuquerque et al.,2017
PAL2	-47.3132	-6.74446	35.4 ± 1.5	Albuquerque et al.,2017
BPPF	-47.2775	-6.29236	45.8 ± 0.2	Coelho et al.,2018
STSN	-46.6113	-6.1258	42.2 ± 0.7	Coelho et al.,2018
GRJU	-46.0878	-5.89975	43.6 ± 0.7	Coelho et al.,2018
GENI	-45.5524	-5.53093	45.1 ± 0.8	Coelho et al.,2018
BDCO	-45.0289	-5.51904	43.7 ± 0.5	Coelho et al.,2018
PRDT	-44.3984	-5.37627	41.1 ± 1.9	Coelho et al.,2018
STSR	-43.8273	-5.32868	40.0 ± 0.4	Coelho et al.,2018
BUCO	-43.2205	-5.19781	39.3 ± 0.5	Coelho et al.,2018
TRZN	-42.6495	-5.13832	40.3 ± 1.1	Coelho et al.,2018
BP_00	-50.20351	-5.51903	37 ± 2.1	Araujo, 2019
BP_01	-49.94781	-5.42512	37.8 ± 3.8	Araujo, 2019
BP_02	-49.67061	-5.44005	38.3 ± 2.1	Araujo, 2019
BP_03	-49.39870	-5.44102	38.1 ± 2.5	Araujo, 2019
BP_04	-49.07796	-5.42786	40.5 ± 3.1	Araujo, 2019
BP_05	-48.86055	-5.47653	49.7 ± 4.6	Araujo, 2019
BP_06	-48.57927	-5.53693	49.5 ± 3.7	Araujo, 2019
BP_07	-48.36077	-5.69813	49.9 ± 2.3	Araujo, 2019
BP_08	-48.10600	-5.73157	44.2 ± 2.5	Araujo, 2019
BP_09	-47.84593	-5.65297	43.4 ± 4.3	Araujo, 2019
BP_10	-47.58424	-5.55614	42.1 ± 2.7	Araujo, 2019
BP_11	-47.30866	-5.56494	41.5 ± 2.8	Araujo, 2019
BP_12	-47.03419	-5.59780	41.2 ± 1.7	Araujo, 2019

BP_13	-46.78689	-5.58506	41.4 ± 4.9	Araujo, 2019
BP_141	-46.47201	-5.68900	41.6 ± 1.1	Araujo, 2019
BP_15	-46.04532	-5.75632	42.7 ± 4.0	Araujo, 2019
BP_16	-45.80336	-5.64585	41.6 ± 2.7	Araujo, 2019
BP_171	-45.20704	-5.41478	42.3 ± 3.6	Araujo, 2019
BP_172	-44.91978	-5.36669	40.7 ± 2.0	Araujo, 2019
BP_173	-44.64743	-5.32479	41.2 ± 3.6	Araujo, 2019
BP_18	-44.39504	-5.29963	38.6 ± 2.0	Araujo, 2019
BP_19	-44.13615	-5.36015	37.4 ± 2.4	Araujo, 2019
BP_20	-44.13615	-5.27665	37.2 ± 3.1	Araujo, 2019
BP_21	-43.61212	-5.23745	37.7 ± 0.2	Araujo, 2019
BP_22	-43.33032	-5.19278	37.7 ± 0.1	Araujo, 2019
BP_23	-43.06687	-5.10947	38.7 ± 1.9	Araujo, 2019
BP_24	-42.83722	-5.15004	38.8 ± 1.7	Araujo, 2019
BP_25	-42.59166	-5.05624	39.2 ± 2.2	Araujo, 2019
BP_26	-42.39786	-5.12597	38.3 ± 1.3	Araujo, 2019
BP_27	-42.09840	-5.26398	40 ± 2.2	Araujo, 2019
BP_28	-41.89689	-5.29237	40.7 ± 0.7	Araujo, 2019
BP_29	-41.54291	-5.32641	38.3 ± 1.9	Araujo, 2019
BP_30	-41.28563	-5.33823	37.4 ± 0.6	Araujo, 2019
BP_31	-40.99248	-5.27260	37.9 ± 0.1	Araujo, 2019
BP_32	-40.99248	-5.17623	37.3 ± 0.4	Araujo, 2019
BP_33	-40.49734	-5.29115	36 ± 0.6	Araujo, 2019
BP_34	-40.27947	-5.43164	35.3 ± 2.3	Araujo, 2019
BP_35	-40.00283	-5.43617	35.4 ± 2.6	Araujo, 2019
ST_02	-46.8764	-8.7728	40.6 ± 3.5	Queiroz, 2019
ST_03	-46.8004	-8.4923	42.4 ± 3.2	Queiroz, 2019
ST_04	-46.9219	-8.2735	41.4 ± 1.1	Queiroz, 2019
ST_05	-46.8428	-8.0603	43.9 ± 0.9	Queiroz, 2019
ST_06	-46.9015	-7.822	40.7 ± 1.7	Queiroz, 2019
ST_07	-46.8863	-7.5988	41.5 ± 0.5	Queiroz, 2019
ST_08	-47.0169	-7.3694	41 ± 2.5	Queiroz, 2019
ST_09	-46.8401	-7.1139	41.9 ± 0.8	Queiroz, 2019
ST_10	-46.8433	-6.8503	43.4 ± 1.7	Queiroz, 2019
ST_11	-47.0096	-6.611	41 ± 1.2	Queiroz, 2019
ST_12	-46.8636	-6.3734	41.7 ± 1.5	Queiroz, 2019
ST_13	-46.8601	-6.1136	39.8 ± 2.3	Queiroz, 2019
ST_14	-46.7658	-5.9016	40.5 ± 2.0	Queiroz, 2019
ST_15	-46.7244	-5.7636	40.6 ± 2.3	Queiroz, 2019
ST_16	-46.8213	-5.6016	43.2 ± 2.2	Queiroz, 2019
ST_18	-46.7975	-5.0212	42.2 ± 2.3	Queiroz, 2019
ST_19	-46.7872	-4.7644	42.3 ± 2.1	Queiroz, 2019
ST_20	-46.857	-4.5081	40.2 ± 5.9	Queiroz, 2019
ST_23	-47.0393	-3.9144	45.3 ± 1.9	Queiroz, 2019
ST_24	-47.0728	-3.4955	45.5 ± 2.8	Queiroz, 2019
ST_25	-46.9542	-3.1543	43.7 ± 4.4	Queiroz, 2019

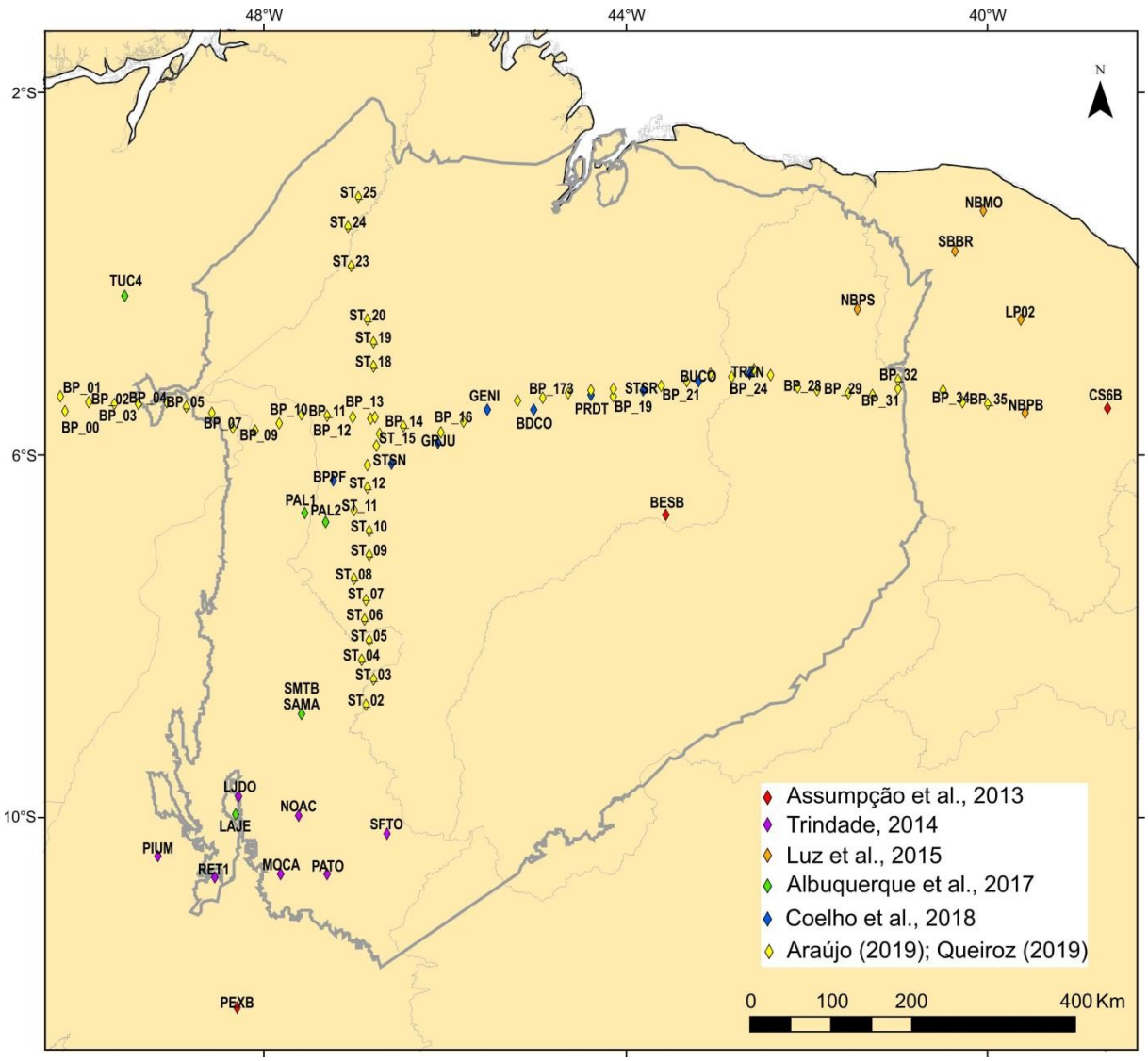

AUXILIARY MAP WITH SEISMOGRAPHIC STATIONS LOCATION

Appendix II

“Well data information”

(Table 1 – Well tops
Table 2 – Basement information and Auxiliary Map;
equivalent to “SUPPLEMENTRAY MATERIAL 2” in “Scientific Paper 1”)

POÇO	Prof. Final	Embasamento	Ipu	Tianguá	Jaicos	Itaim	Pimenteiras	Cabeças	Longá	Poti	Piaui	Pedra de Fogo	Motuca	Sambaíba	Pastos Bons	Grajaú	Codó	Itapecurú
1AT 0001 MA	1200	1176	1145	1047	955	855	695	NP	NP	NP	NP	NP	NP	NP	NP	665	518	4
1CA 0001 MA	1936	NP	NP	1837	1609	1409	1013	790	655	397	103	3	NP	NP	NP	NP	NP	NP
1CI 0001 MA	1442	1430	1413	1305	1210	1100	909	NP	NP	NP	NP	NP	NP	NP	NP	882	729	NP
1CL 0001 MA	1170	1160	NP		1016	856	683	620	490	315	139	4	NP	NP	NP	NP	NP	NP
1FL 0001 PI	2405	2374	2220	1983	1544	1361	840	493	387	110	3	NP	NP	NP	NP	NP	NP	NP
1FM 0001 MA	1821	1800 R	1683	1564	1287	1110	668	556	434	132	3	NP	NP	NP	NP	NP	NP	NP
1FO 0001 MA	1644	1630 R	1555	1433	1170	1000	580	465	335	38	3	NP	NP	NP	NP	NP	NP	NP
1GI 0001 PA	2359	NP	2313	2170	1905	1753	1203	1084	923	784	547	NP	NP	NP	NP	NP	NP	6
1IZ 0002 MA	2335	2308 R	2302	2246	2099	1960	1780	1663	1521	1392	1148	968	758	354	NP	NP	35	5
1MA 0001 PI	2178	2175	2104	1828	1534	1387	1118	545	423	200	3	NP	NP	NP	NP	NP	NP	NP
1MD 0001 MA	2828	2667 M	2550	2162	1920	1764	1238	1048	910	520	174	66	27	NP	NP	3 C	NP	NP
1MS 0001 MA	2555	2460	2302	2186	1980	1785	1196	1032	949	632	306	165	3	NP	NP	NP	NP	NP
1-OGX-101-MA	1952	NP	NP	NP	NP	NP	1822	1669	1598	1017	852	558	357	203	173	147 C	31	0
1-OGX-102-MA	2235	NP	NP	NP	NP	NP	2197	1814	1618	1120	914	714	447	230	216	205 C	18	0
1-OGX-107-MA	1627	NP	NP	NP	NP	NP	NP	NP	1607	1125	950	891	391	269	242	211 C	72	0
1-OGX-110-MA	1906	NP	NP	NP	NP	NP	1844	1684	1580	1129	948	927	369	278	217	186 C	63	0
1-OGX-16-MA	3168	3408	3050	2848	2613	2476	2006	1666	1382	1168	908	696	402	231	154	110 C	35	0
1-OGX-22-MA	3144	3275	2855	2720	2602	2456	2005	1655	1515	1165	905	708	441	231	154	110 C	35	0
1-OGX-34-MA	2577	NP	NP	NP	NP	NP	2155	1900	1790	1180	920	735	435	265	165	125 C	45	0
1-OGX-59-MA	2621	NP	NP	NP	NP	NP	1794	1624	1519	1119	944	674	464	284	224	164 C	34	0
1-OGX-77-MA	2471	NP	NP	NP	NP	NP	1822	1552	1452	962	722	477	362	122	82	42 C	6	NP
1-OGX-92-MA	2110	NP	NP	NP	NP	NP	1962	1752	1488	1130	909	563	423	220	181	143 C	0	NP
1-OGX-93-MA	3322	3264	3025	2916	2703	2558	1790	1703	1523	1207	1000	658	534	346	291	118 C	30	0
1PA 0001 MA	2865	2845	2686	2555	2397	2247	1721	1627	1542	1273	984	780	560	NP	504	413	318	6
1PD 0001 MA	2844	NP	NP	2745	2515	2366	1919	1645	1380	1157	865	647	440	190	153	115 C	3	NP
1RB 0001 MA	1837	NP	NP	1758	1515	1294	890	810	618	345	65	3	NP	NP	NP	NP	NP	NP
1TB 0001 MA	2128	2076 R	2026	1896	1695	1486	948	833	728	495	192	40	3	NP	NP	NP	NP	NP
1TB 0002 MA	1603	NP	NP	NP	NP	1428	928	813	704	463	152	5	4	NP	NP	NP	NP	NP
1TM 0001 MA	1688	1685	1600	1500	1312	1140	771	639	522	273	25	4		NP	NP	NP	NP	NP
1VG 0001 MA	1029	NP	NP	NP	NP	NP	NP	NP	NP	549	270	122	3	NP	NP	NP	NP	NP
1VG 0001R MA	2887	1802 R	1768	1670	1502	1302	1053	920	775	549	265	122	3	NP	NP	NP	NP	NP
2BAC 0001 MA	3252	3229	3101	2967	2748	2561	1912	1794	1583	1348	1040	808	580	383	347	277 C	102	5
2BGST0001 MA	2020	NP	NP		1775	1615	1109	800	450	211	3	NP	NP	NP	NP	NP	NP	NP
2CP 0001 MA	3423	3408	3055	2848	2613	2476	2006	1666	1382	1168	908	696	402	231	154	110 C	35	5
2IZST0001 MA	2177	2150	NP	2094	1971	1835	1654	1565	1434	1282	1065	895	705	273	NP	NP	27	3
2NGST0001 MA	2573	NP	NP	2557	2372	2235	1702	1612	1470	1267	976	781	552	159	NP	14	14 C	NP
2NLST0001 PI	2275	2210	2002	1793	1503	1338	1034	548	433	20	4	NP	NP	NP	NP	NP	NP	NP
2PMST0001 MA	2164	2128	2045	1920	1789	1650	1325	1139	1050	853	645	NP	NP	NP	NP	587	435	3
2SLST0001 MA	2495	NP	2485	2355	2200	2048	1582	1476	1309	1095	805	577	498	NP	NP	483	350	4
2VBST0001 MA	1941	1925 R	1815	1710	1502	1304	935	800	623	400	105	4	NP	NP	NP	NP	NP	NP
2VGST0001 MA	1647	NP	1492	1357	1220	1080	748	415	NP	NP	NP	NP	NP	NP	NP	385	270	4
3-OGX-38-MA	1960	NP	NP	NP	NP	NP	1950	1777	1691	1176	966	965	464	278	164	112	19	0
3-OGX-46D-MA	2215	NP	NP	NP	NP	NP	2092	1711	1445	1235	994	742	456	299	214	178 C	91	0
3-OGX-88-MA	1733	NP	NP	NP	NP	NP	1843	1685	1576	1095	958	641	424	247	197	136 C	14	6
9PAF 0001 MA	832	NP	NP	NP	NP	NP	NP	NP	NP	794	550	NP	NP	NP	NP	NP	425	2
9PAF 0002 MA	819	NP	NP	NP	NP	NP	NP	NP	709	678	NP	NP	NP	NP	NP	660	533	2
9PAF 0003 MA	867	NP	NP	NP	NP	NP	NP	NP	814	780	NP	NP	NP	NP	NP	757	602	2
9PAF 0004R MA	785	NP	NP	NP	NP	NP	NP	NP	749	720	NP	NP	NP	NP	NP	697	555	2
9PAF 0007 MA	1384	1353	1323	1208	1100	992	661	NP	NP	NP	NP	NP	NP	NP	NP	650	562	3

Well Name	Code in Fig.3.8	X (LONG)	Y (LAT)	Elevation (meters)	Top of Pre-Silurian Basement (MD in meters)	Basement Lithology Description	Basement Age (Ma), including method and material	Source of Age Information (See paper references)	Comments
1-AT-1-MA	1	-45.576306	-2.922800	30.0	1176.0	Mica-schist/ Quartzite	N/A		
1-CI-1-MA	2	-45.408567	-2.998393	58.0	1430.0	Chlorite-biotite quartz schist	N/A		
9-PAF-7-MA	3	-44.417043	-3.308735	27.0	1353.0	Micaceous quartzite with scattered pyrite. Dip angle 35-40º.	504 ±15 (K-Ar); biotite	Cordani et al., 2008a	Possibly correlated to the schist in 1-PMst well. No information about the correlation with the Quartz Syenite, outcropping 60km apart, in Rosario city, to the north.
2-PMST-1-MA	4	-45.400423	-3.633740	41.1	2128.0	Quartz Clorita Xisto com clivagem mergulhando 70o e fraturas subverticais preenchidas com calcita.	520 (Rb-Sr); total rock	Cordani et al., 2008a	
1-PA-1-MA	5	-45.655671	-4.174342	99.0	2845.0	Green undifferentiated metamorphic rock, with Chlorite and Actinolite	N/A		At 2736, depth. Chert texture in Sandstones in Ipu or Mirador Fm.
2-CP-1-MA	6	-44.297368	-4.764227	112.0	3408.0	Schist, light to dark green, very micaceous.	N/A		
1-MA-1-PI	7	-42.799426	-4.827626	119.0	2175.0	Muscovite-microcline-pagioclase gneiss, very altered with hydrothermal calcite veins	670 (Rb-Sr); total rock	Cordani et al., 2008a	Alternative age of 775 +/- 35 (??)
2-BAC-1-MA	8	-45.445076	-5.300276	217.0	3229.0	Undifferentiated rock with variegated texture, altered basalt or polymictic conglomerateconglomerate(?). Classified as a Pre-Silurian sedimentary sequence	N/A		Classified as a Pre-Silurian sedimentary sequence
1-OGX-93-MA	9	-45.3	-5.453899	206.0	3264.0	Intercalations of grey sandstones, greywackes and greyish to greenish shales.	N/A		
1-IZ-2-MA	10	-47.351136	-5.450673	148.5	2308.0	Quartz trachyte above volcanic tuff or Ignimbrite			Ipu Fm. at 2302m and absent or eroded in the neighbour well 2IZST
2-IZST-1-MA	11	-47.490799	-5.527375	119.0	2150.0	Volcanic Tuff with dip angle of 40º described from core sample. In the cuttings: Brwon to reddish shale, with quartz veins and pyrite. Interprete as Riachão Fm., Tocantins Group (Pre-Cambrian).	N/A		At 2095 m (equivalent to Fm.Tiangua in Composite Log ??), a pre-Silurian quartzite was sampled, also observed in 1-TB well, but absent in 1-VG well.
2-NLST-1-PI	12	-42.586284	-5.600918	164.0	2210.0	Propilitized mylonite, possibly andesitic protolith (?). Dark grey metamorphosed shale intercalated with quartzite and a Diabase sill intrustion.	N/A		Two faults, similar to diabase dykes are observed in the surface of the well location. The well is localized upon a Carboniferous horst, indicating a reactivation of the TBFZ.
1-FL-1-PI	13	-42.804133	-6.458594	290.0	2374.0	Talc-quartz schist or Philonite	670 (Rb-Sr); total rock	Cordani et al., 2008a	
1-MS-1-MA	14	-45.491185	-6.992030	251.0	2460.0	Quartz mica schist	1420 (Rb-Sr) ; total rock	Cordani et al., 2008a	
1-CL-1-MA	15	-47.460090	-7.344732	176.5	1160.0	Quartz diorite gneiss	608 ± 21 (K-Ar); biotite	Cordani et al., 2008a	
1-VG-1R-MA	16	-46.624106	-7.396301	388.1	1802.0	Riachão Fm. (arcosean sandstone, shale, siltstone, diabase intrusion)	N/A		
2-VBST-1-MA	17	-46.309924	-7.471304	392.0	1925.0	Riachão Fm. (arcosean sandstone)	N/A		
1-FO-1-MA	18	-46.236608	-8.260194	400.0	1630.0	Riachão Fm. (greywacke)	N/A		
1-FM-1-MA	19	-46.088548	-8.252971	488.0	1800.0	Riachão Fm. (sandstone, siltstone, brown conglomerate)	N/A		
1-TM-1-MA	20	-46.907187	-8.708809	634.0	1685.0	Mylonitic Syenite	469 ± 11 (K/Ar)	Well folder	

Appendix III

"Conference Paper"

Rio Oil & Gas Expo and Conference 2020

ISSN 2525-7579

Conference Proceedings homepage: www.ibp.org.br/biblioteca/riooilegas

PERSPECTIVAS EXPLORATÓRIAS PARA A BACIA DO PARNAÍBA

EXPLORATORY PERSPECTIVES FOR THE PARNAIBA BASIN

Claudio Coelho de Lima (https://orcid.org/0000-0002-6476-2253)[1];**Mathieu Moriss** (https://orcid.org/0000-0003-4398-4575)[2];**Victor Matheus Joaquim Salgado Campos**[3];**Amanda Lira Porto** (0000-0002-6204-0599)[4];**Ana Maria Góes**[5].

1. LIMAGEO, INDEPENDENTE, . RIO DE JANEIRO - RJ - BRASIL, claudiolimageologist@icloud.com 2. EMERSON, ENGENHEIRO, . RIO DE JANEIRO - RJ - BRASIL, mathieu.moriss@emerson.com 3. UFRJ, DOUTORANDO, . RIO DE JANEIRO - RJ - BRASIL, victorsalgadocampos@hotmail.com 4. OBSERVATORIO NACIONAL, DOUTORANDO, . RIO DE JANEIRO - RJ - BRASIL, amandaliraporto@gmail.com 5. USP, PROFESSORA, . SãO PAULO - SP - BRASIL, anamgoes@gmail.com

Resumo

Diante da forte demanda por gás para uso em usinas termoelétricas e dado que poços exploratórios recentemente perfurados nas bordas da bacia foram secos, três questões se colocam para a exploração na Bacia do Parnaíba. 1) Acumulações comerciais de hidrocarbonetos existiriam apenas na parte central da bacia? 2) As bordas estariam definitivamente condenadas? 3) Haveria ainda outas situações favoráveis, ainda não testadas? Um modelo geológico regional foi construído, com base na análise de visualizações integradas de dados, informações e conhecimento, provenientes de diferentes fontes: geologia de superfície e subsuperfície, topografia, geologia do petróleo, magnetometria, gravimetria, tectônica de placas, geometria da Moho, sismicidade, tensões atuais regionais, localização dos campos produtores, produção acumulada e reservas provadas. O modelo geológico propõe que três grandes regimes de esforços foram os responsáveis pela arquitetura final da bacia. 1) Eojurássico/Eocretáceo, pré-Breakup do Gondwana, eventos magmáticos e reativações de grandes falhas regionais – responsáveis pelas acumulações -foram controlados por compressão EW e extensão NS. 2) Eocretáceo/Mioceno, durante o desenvolvimento da Margem Equatorial da Placa Sul-Americana, instalou-se um regime de esforços caracterizado por compressão NS e extensão EW, responsável pelo soerguimento das bordas da bacia (basement uplift), deixando aproximadamente na sua posição original uma depressão alongada na direção WNW-ESSE. 3) O regime atual de esforços caracteriza-se por compressão NW-SE e extensão NE-SW e é responsável pela sismicidade observada ao longo das bordas da bacia. A evolução dos regimes de esforços favorece a preservação de acumulações na parte profunda da bacia e atribui maior risco a estruturas localizadas nas bordas.

Palavras-chave: Bacia do Parnaíba. exloração. regime de esforços. soerguimento. embasamento

Abstract

To cope with the strong demand for gas from thermoelectric power plants and given that recently drilled wells on the basin´s borders were dry, ongoing exploration in the Parnaiba basin faces three questions. 1) Could commercial gas fields only be found in the central deeper portion of the basin? 2) Basin´s borders are definitely condemned? 3) Are there non-tested areas to be explored? A regional geological model was built on the basis of the analysis of integrated visualizations of data, information and knowledge from different sources: surface and subsurface geology, topography, petroleum geology, gravity, magnetics, plate tectonics, Moho geometry, seismicity, present day regional stresses, gas field locations, cumulative gas production and proven reserves. The model states that three major stress regimes have been responsible for the final basin architecture. 1. Early Jurassic /Early Cretaceous, before Gondwana breakup, magmatism and regional fault reactivation - responsible for the gas accumulations- were controlled by EW compressional / NS extensional stresses. 2. Late Cretaceous/Miocene, during the development of the Equatorial Margin of the South America Plate, NS compressional / EW extensional stresses were responsible for basement uplift affecting the borders of the basin, resulting an elongated WNW-ESE depression that roughly remained in its original position. 3. Present day NW-SE compressional / NE-SW extensional stresses are responsible for the seismicity observed along the basin´s borders. The regional stresses' evolution favours preservation of gas accumulations within the deeper part of the basin whereas imposes risk to structures located on the uplift borders.

Keywords: Parnaíba Basin. exploration. stress regime. uplift. basement

Received: 13/02/2020 | **Accepted:** 21/04/2020 | **Available online:**
Article Code: IBP0045_20
Cite as: Proceedings of the Rio Oil & Gas Expo and Conference, Rio de Janeiro, RJ, Brazil, 2020.
DOI:

1. Introdução

A Bacia do Parnaíba é uma grande bacia sedimentar cratônica brasileira que se estende por aproximadamente 600000 km^2 (Fig.1). As acumulações de gás desta bacia são formadas por um sistema petrolífero definido por Miranda et al. (2018) como "atípico", constituído por rochas ígneas e sedimentares. O efeito térmico de soleiras de diabásio de idade mesozoica, intrudidas em folhelhos devonianos da Fm. Pimenteiras, ricos em orgânica, causaram a maturação da matéria orgânica, o que gerou principalmente gás. O gás gerado foi aprisionado em trapas com fechamento quaquaversal, formadas também por soleiras margeadas por falhas, intrudidas nos reservatórios – principalmente arenitos carboníferos da Fm. Poti e arenitos devonianos da Fm. Cabeças.

Figura 1 - Visualização integrada das estruturas regionais, da geometria do embasamento, do topo da Fm. Pimenteiras, dos campos produtores (Parque dos Gaviões) e das áreas com declaração de comercialidade (Gavião Carijó e Gavião Tesoura). Contornos do embasamento extraídos de Miranda et al. (2018). Topografia das áreas onde a aflora a Fm. Pimenteiras extraída do SRTM – Shutlle Radar Topographic Mission, topografia digital adquirida e disponibilizada pela NASA, em resolução de 30m, https://www2.jpl.nasa.gov/srtm/. Perfis no topo da Fm Pimenteiras AA' e BB', obtidos a partir de poços. Também mostrada na figura a localização das seções geológicas CC' e DD', apresentadas nas Figuras 3 e 4.

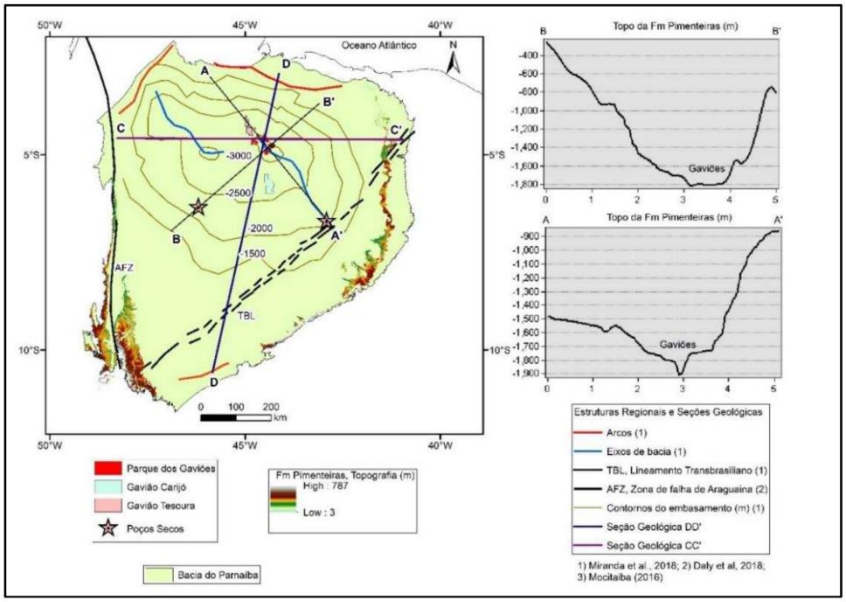

Fonte: Figura produzida pelos autores a partir de dados disponíveis na base de dados da Ouro Preto Petróleo e Gás – OPOG. O Lineamento Transbrasiliano (TBL) e Zona de Falha de Araguaína (AFZ) são estruturas regionais herdadas do Ciclo Brasiliano (Daly et al., 2014). Os arcos, que delimitam a configuração atual da bacia e os eixos de bacia foram extraídos de Miranda et al. (2018).

A partir da nona Rodada de Licitações da ANP em 2008, o esforço exploratório implicou a descoberta de 7 campos comerciais de gás (Parque dos Gaviões; Miranda et al., 2018). Tais campos localizam-se na parte central da bacia, onde o embasamento encontra-se a aproximadamente - 3000 m e o topo da Fm. Pimenteiras a aproximadamente -1800 m (Fig. 1). Declarações de comercialidade mais recentes (Gavião Tesoura e Gavião Carijó; ENEVA, 2020), encontram-se em situações estruturalmente mais altas, mas ainda próximas da parte central da bacia, com o embasamento ocorrendo em profundidades em torno de -2500 m (Fig.1). Por outro

lado, os dois poços exploratórios recentemente perfurados em situações estruturais mais altas, mais próximas das bordas da bacia foram classificados como secos (Fig. 1). Diante da forte demanda por gás para uso em usinas termoelétricas, três questões se colocam para o estágio exploratório atual da Bacia do Parnaíba. 1) Acumulações comerciais de hidrocarbonetos existiriam apenas na parte central, mais profunda da bacia? 2) As bordas da bacia estariam definitivamente condenadas quanto à perspectiva de sucesso exploratório, sobretudo em função da ruptura do selo? 3) Haveria ainda outras situações favoráveis, ainda não perfuradas para a exploração na bacia? Este trabalho tenta propor respostas às duas primeiras questões formuladas, enquanto um outro trabalho de Lima et al. (2020, neste evento) tenta propor uma resposta à terceira questão.

2. Metodologia

Um modelo geológico regional conceitual foi construído na perspectiva da busca de respostas às questões acima formuladas. O modelo baseou-se na análise de visualizações georeferenciadas integradas de dados, informações e conhecimento, provenientes de diferentes fontes: geologia de superfície e subsuperfície, topografia, geologia do petróleo, magnetometria, gravimetria, tectônica de placas, geometria da Moho, sismicidade, tensões atuais regionais e localização dos campos produtores. Um modelo geológico 3D foi construído para a Bacia do Parnaíba, com base nos marcadores de horizontes encontrados em 56 poços, disponíveis na base de dados da Ouro Preto Óleo e Gás – OPOG, topografia digital e no mapa geológico de superfície feito pela CPRM (Schobbenhaus et al., 2004). Para a construção das superfícies que representam os horizontes modelados (topografia, topos de formações e discordâncias), o algoritmo utilizado (Mallet, 2002), honra a topografia e os marcadores em todos os poços e também os afloramentos dos respectivos horizontes no mapa geológico.

3. Resultados

3.1. A configuração atual da bacia é o resultado do soerguimento de blocos do embasamento (basement uplift) produzido por inversões tectônicas

Rodrigues (1995) identificou três níveis na Fm. Pimenteiras onde ocorrem as maiores concentrações de carbono orgânico, associados a altos valores de raios gama (RG) e de resistividade e a baixos valores de densidade, denominados por ele como "Folhelhos Radioativos" A, B e C, depositados respectivamente na base, na porção intermediária e no topo desta formação. Ainda segundo Rodrigues (1995), os Folhelhos C foram depositados durante a inundação máxima do Devoniano e por esta razão foram considerados neste trabalho como um bom datum, cuja geometria deposicional foi assumida como aproximadamente horizontal.

Na Figura 1, observa-se que o topo da Fm. Pimenteiras encontra-se na sua posição mais baixa a aproximadamente -1800m, na área do Parque dos Gaviões e a partir desta área, em cotas cada vez mais altas em direção às bordas da bacia. Ainda na Figura 1, observa-se que na área aflorante desta formação, a topografia atinge a quase 800m, implicando que o topo da Fm. Pimenteiras hoje apresente um desnível estrutural da ordem de no mínimo 2.5km, entre a borda leste e o centro da Bacia do Parnaíba.

O Grupo Canindé engloba as Fms. Itaim, Pimenteiras, Cabeças, Longá e Poti, que se depositaram entre as Discordâncias Eodevoniana e Mesocarbonífera (Vaz et al., 2007). A comparação entre o mapa de isópacas e o mapa de contornos estruturais deste grupo mostra que

o máximo de isópacas encontra-se na área do Lineamento Transbrasiliano, numa área onde hoje o topo do Grupo encontra-se estruturalmente alto (Fig. 2).

Figura 2 - Isópacas e contornos estruturais do topo do Grupo Canindé, Eodevoniano-Mesocarbonífero (Vaz et al., 2007). Legenda complementar na Figura 1

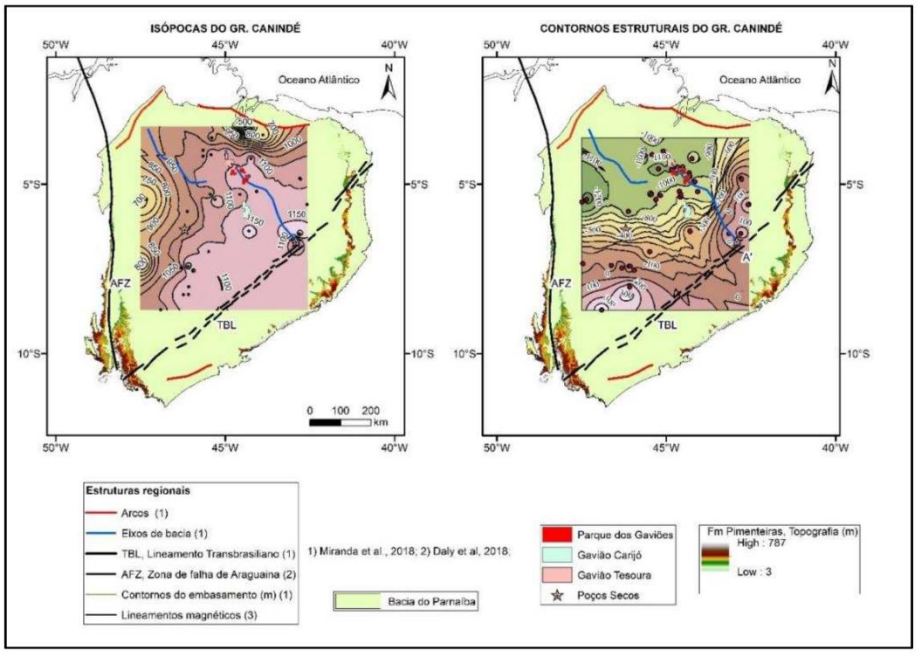

Fonte: Mapas construídos a partir de dados de poços da base de dados da OPOG.

O Grupo Serra Grande, subjacente ao Grupo Canindé, depositado principalmente durante o Siluriano, é composto pelas Fms. Ipu, Tianguá e Jaicós (Vaz et al., 2007). A Fm. Tianguá é formada principalmente por folhelhos depositados em plataforma rasa e por esta razão foi considerada no presente trabalho como um datum regional. Num padrão semelhante ao apontado para os folhelhos da Fm. Pimenteiras na Figura 1, os folhelhos marinhos da Fm. Tianguá são encontrados em profundidades em torno de -2600 m na área do Parque do Gaviões e, a partir desta área, são encontrados em cotas cada vez mais altas em direção às bordas da bacia. Na borda leste, os afloramentos do Grupo Serra Grande formam escarpas recuantes com cotas que chegam a +995 m, acima do nível do mar.

Estas observações implicam que os depocentros dos Grupos Canindé e Serra Grande foram fortemente soerguidos na borda leste da bacia, em resposta ao soerguimento de blocos do embasamento subjacente (basement uplift). Interpreta-se aqui que este soerguimento foi induzido por compressão tectônica, num contexto similar ao que foi identificado em restaurações estruturais na borda oeste da bacia, conduzidas Daly et al (2014). Os resultados destas restaurações mostraram que a configuração atual desta borda é o resultado de uma complexa evolução estrutural, que compreende eventos de inversão tectônica posteriores ao Permiano e anteriores ao Albiano. Tais eventos reativaram a zona de falha de Araguaína, induzindo soerguimentos da ordem de 2km, da mesma ordem de grandeza dos soerguimentos identificados neste trabalho para a borda leste, acima mencionados. Os resultados ainda mostram que no final da inversão tectônica ocorreu um colapso gravitacional de idade pré-albiana, cujo espaço foi preenchido por sedimentos do Cretáceo Superior (Fm. Itapecuru).

Nas figuras 3 e 4, cuja localização é mostrada na Figura 1, mostram-se seções geológicas extraídas do modelo geológico 3D da Bacia do Parnaíba, construído nesta investigação. A

extremidade leste da seção CC' (Fig. 3) coincide com o Lineamento Transbrasiliano, uma das estruturas regionais mais importantes da bacia, herdadas do Ciclo Brasiliano (Daly et al., 2014). Notar na figura o forte soerguimento do embasamento e toda a coluna sedimentar, junto à borda leste. A partir do Parque dos Gaviões, a erosão expõe rochas cada vez mais velhas para leste. Na extremidade da seção, sobre o Lineamento Transbrasiliano, afloram os sedimentos do Grupo Serra Grande– de idade siluriana, em cotas topográficas da ordem de 500m. Notar que o soerguimento a leste do Parque dos Gaviões afeta a Discordância Pré Cretácea, o que implica que pelo menos parte do soerguimento do embasamento (basement uplift) foi posterior ao Cretáceo.

Figura 3 - Seção geológica extraída do modelo geológico 3D da Bacia do Parnaíba a partir de dados de poços, topografia digital e mapa geológico de superfície da CPRM (Schobbenhaus et al., 2004). Escalas horizontal e vertical em metros, exagero vertical de 100x.

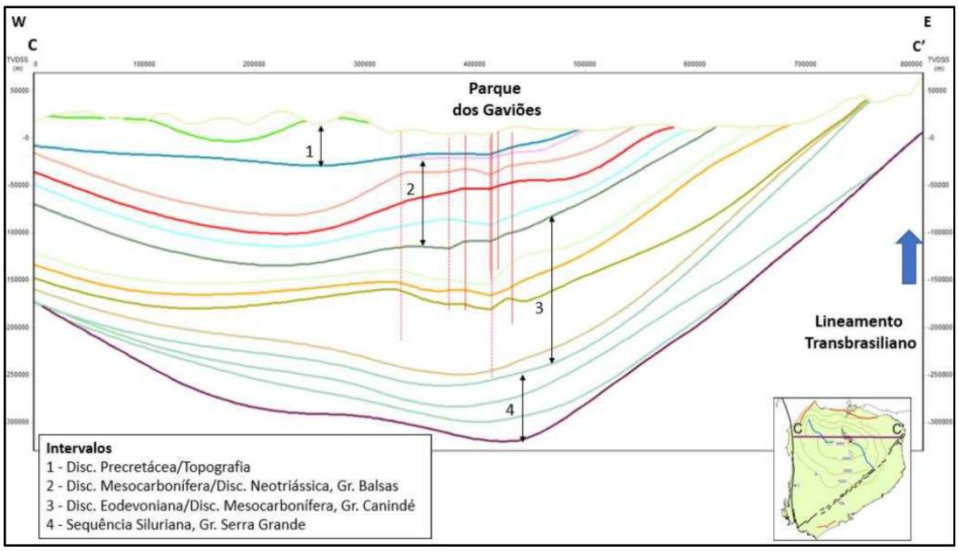

Fonte: A imagem foi produzida pelos autores, sendo o mapa geológico de superfície extraído da CPRM (Schobbenhaus et al., 2004).

Outras feições-chave para um entendimento da configuração atual da bacia podem ser observadas na seção geológica DD' (Fig. 4). Na extremidade norte da seção, observa-se o Arco Ferrer-Urbano Santos, uma estrutura regional cujo soerguimento começou no Paleozoico, mas que foi parcialmente erodida pela Discordância Precretácea. Sobre esta discordância e hoje ocorre uma espessa coluna de sedimentos cretáceos, um cenário consistente com os resultados das restaurações estruturais conduzidas por Daly et al. (2014) para a borda oeste da bacia.

A Discordância Precretácea, na porção norte da seção mergulha para norte, em direção ao Arco Ferrer -Urbano Santos. A partir do ponto onde a discordância aparece em superfície (~400 km a partir da origem), afloram unidades cada vez mais velhas em direção a sul, até a região onde a seção cruza o Lineamento Transbrasiliano. Nesta região afloram os sedimentos mais antigos, que marcam o topo do intervalo Eodevoniano/Mesocarbonífero. A partir do Lineamento Transbrasiliano, em direção a sul afloram unidades cada vez mais novas mergulhando para o sul, o que inclui a Discordância Pré-Cretácea. O padrão de afloramentos descrito caracteriza a ocorrência de uma grande antiforma -um anticlinal-, cujo topo está sendo erodido, em resposta a soerguimentos do embasamento (basement uplift). Dado que o soerguimento afetou a Discordância Precretácea, pelo menos parte do soerguimento foi posterior ao Cretáceo, a exemplo do foi mostrado acima para a seção CC'.

Figura 4 - Seção geológica extraída do modelo geológico 3D da Bacia do Parnaíba a partir de dados de poços, topografia digital e mapa geológico de superfície da CPRM (Schobbenhaus et al., 2004). Escalas horizontal e vertical em metros, exagero vertical de 100x.

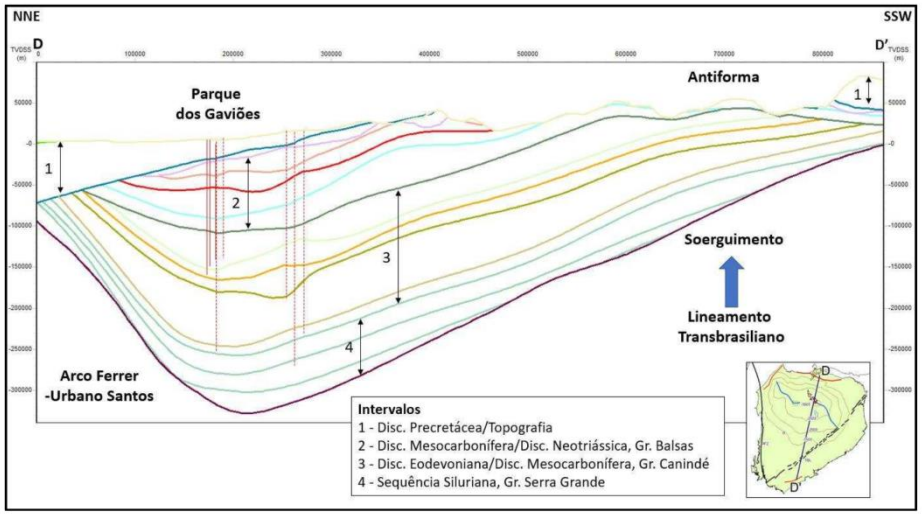

Fonte: A imagem foi produzida pelos autores, sendo o mapa geológico de superfície extraído da CPRM (Schobbenhaus et al., 2004).

O conjunto das informações expostas e discutidas acima colocam em evidência que a configuração atual da Bacia do Parnaíba é o resultado de deformações estruturais que implicaram movimentos verticais da ordem de no mínimo 2.5 km, assumindo-se como datum o topo da Fm. Pimenteiras. Em outras palavras, a configuração atual da Bacia do Parnaíba é o resultado de soerguimentos de blocos do embasamento (basement uplift), que são, pelo menos em parte, posteriores ao Cretáceo. Em direção às bordas soerguidas, afloram unidades cada vez mais antigas até que aflore o embasamento, frequentemente em cotas mais baixas do que os sedimentos, que formam assim uma escarpa recuante.

3.2. Compressão EW/Extensão NS: o regime de esforços durante o Eojurássico/Eocretáceo

Dois pulsos magmáticos principais foram identificados na Bacia do Parnaíba (Vaz et al., 2007): i) Fm Mosquito, idade média 178 ma, Eojurássico; ii) Fm Sardinha, idade média 124 Ma, Eocretáceo (Fig. 5). Datações das soleiras associadas às acumulações, se existirem, não foram encontradas na literatura pelos autores do presente trabalho.

Klöcking et al. (2018), com base na modelagem de elementos raros, concluíram que ambos os pulsos de magmatismo resultaram de descompressão do manto litosférico subcontinental. Tais autores e Heilbron et al. (2018) também correlacionaram o evento Mosquito com as primeiras manifestações do breakup do Gondwana e o evento Sardinha ao rifteamento entre a América do sul e África e à formação da província magmática Paraná-Etendeka. Daly et al. (2014) reconheceram que os eventos magmáticos são importantes componentes da evolução da bacia, da sua história termal e do seu contexto tectônico, indicando que diques e soleiras são feições dominantes no perfil sísmico de reflexão profunda (DSRP), que afetam o imageamento da bacia, explorando falhas e acamamentos durante a intrusão. Tais autores sugeriram correlação entre os eventos de inversão tectônica identificados nas restaurações e os pulsos magmáticos Mosquito (Eojurássico) e Sardinha (Eocretáceo). Esta sugestão é consistente com a boa correlação espacial observada entre o Lineamento Transbrasiliano, o Lineamento Picos-Santa Inês de Cunha (1986) e várias manifestações de

]

magmatismo, o que inclui afloramentos do evento Sardinha, diques de diabásio, kimberlitos; isólitas totais de diabásio (Fig. 5).

Figura 5 - Magmatismo, isólitas de diabásio, estruturas regionais e modelo conceitual do regime de esforços tectônicos proposto para o Eojurássico/Eocretáceo. Legenda complementar na Fig. 1.

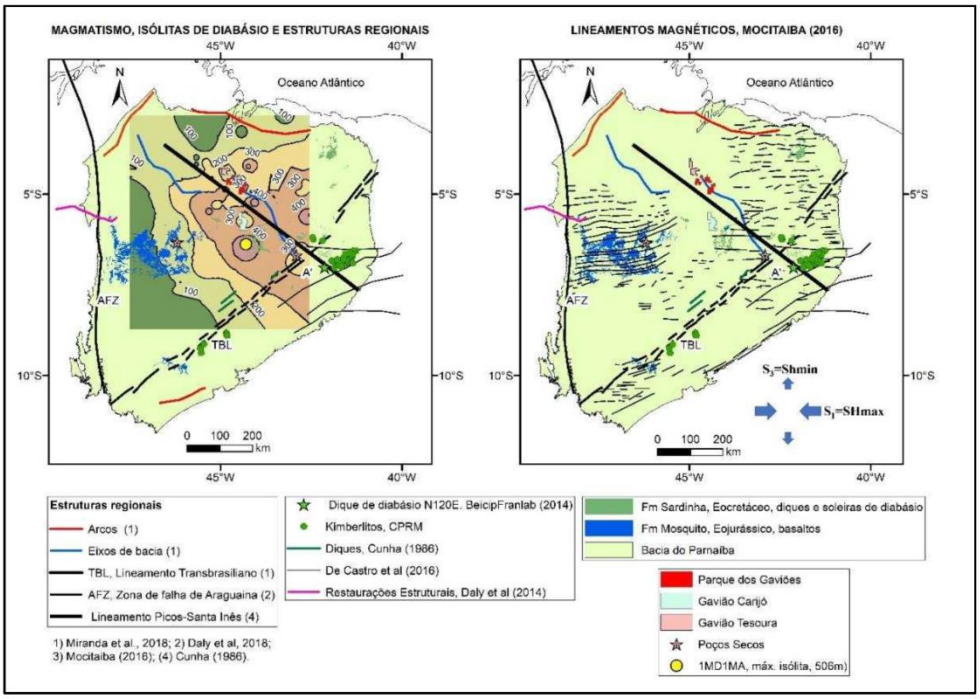

Fonte: Mapas construídos a partir de dados da base de dos da OPOG. Afloramentos dos pulsos Mosquito (Eojurássico) e Sardinha (Eocretáceo) foram extraídos do mapa geológico de superfície da CPRM (Schobbenhaus et al., 2004).

Mocitaiba (2016) produziu uma cartografia do magmatismo na bacia do Paranaíba a partir de dados aeromagnéticos e de uma técnica de mapeamento semiautomático (SOM, Self Organizing Maps), obtendo assim o Campo Magnético Anômalo (CMA). Através da utilização de filtros, este autor decompôs o CMA em três componentes: Campo Magnético Profundo (CMP); Campo Magnético Raso (CMR); e, Campo Magnético Intermediário (CMI), que captura principalmente fontes magnéticas da crosta superior – incluindo a bacia. Para refinar a cartografia, Mocitaiba (2016) aplicou ao CMI duas filtragens espectrais, Amplitude do Sinal Analítico e Derivada Vertical. A amplitude do sinal analítico é um filtro – baseado nos gradientes vertical e horizontais do campo magnético -, que amplifica os comprimentos de onda curtos e atenua os longos nas três direções ortogonais (x,y,z), realçando as bordas de anomalias induzidas por contatos e falhas, produzindo assim um máximo nos contrastes magnéticos. Com base nos resultados das filtragens espectrais e nas medidas de campo, Mocitaiba (2016) identificou vários domínios magnéticos, separou os eventos Mosquito e Sardinha e traçou lineamentos magnéticos. Tais lineamentos foram por ele interpretados como "riftes" de direções ENE-WSWS e NNE-SSW, o que confirmaria uma ideia proposta por Góes (1995), segundo a qual os sedimentos das formações Pastos Bons e Corda, associados às rochas básicas dos eventos Mosquito e Sardinha, formariam um sequência vulcano-sedimentar, depositada num rifte (a Bacia de Alpercatas). Mocitaiba (2016) ressaltou ainda o forte controle exercido por lineamentos EW (Senador Pompeu), associados ao lineamento Transbrasiliano, que teriam controlado as intrusões do magmatismo Sardinha a leste e do magmatismo Mosquito a oeste.

Em realidade os lineamentos magnéticos observados têm uma direção aproximadamente EW através de toda a área; não se identificam lineamentos magnéticos na direção NNE-SSW (Fig. 5). Em função desta constatação, neste trabalho rejeita-se a interpretação de Mocitaiba (2016) para os lineamentos identificados, mas se aceita a identificação objetiva dos mesmos feita por ele. Isto porque, dado o grande contraste de suscetibilidade magnética entre as rochas magmáticas e as encaixantes, os lineamentos identificados devem representar contrastes laterais de magnetização, ou seja, devem indicar a presença de corpos magnéticos, possivelmente diques associados aos eventos magmáticos. Em função disto, nesta investigação interpretam-se tais lineamentos como manifestações de uma extensão regional de direção aproximada NS, associada a uma compressão regional de direção aproximada EW, conforme o modelo conceitual de esforços tectônicos apresentado na Figura 5. Com base neste modelo, ambos os eventos magmáticos poderiam estar associados a reativações transtensionais de falhas regionais, em resposta ao regime de esforços proposto. Reativações destrais – ao longo de falhas NE-SW - e sinistrais ao longo de falhas NW-SE seriam esperadas. Neste modelo, trechos destas estruturas onde ocorrem variações locais de direção (dilational jogs), favoravelmente orientadas com relação às tensões tectônicas regionais, teriam funcionado como dutos para a ascensão do magma à superfície. Isto explicaria o máximo de isólitas encontrar-se na vizinhança do Lineamento Transbrasiliano e corpos kimberlíticos concentrarem-se onde as falhas tendem a orientar-se na direção EW (Fig. 5).

A Fm. Sambaíba, de idade Triássica, foi depositada num ambiente desértico, Vaz et al (2007). Consistentemente com o regime de esforços tectônico aqui proposto, o mapa de isópacas desta formação com base em poços mostra que os valores máximos ocorrem ao longo de um eixo EW, numa área adjacente aos derrames basálticos da Fm. Mosquito (Eojurássico), que se colocaram sobre a Fm Sambaíba (Fig. 6). Estas observações são consistentes com a noção de que os esforços extensionais - cuja evolução culminou nos processos associados ao breakup-, já estariam atuando no Triássico, um diagnóstico consistente com algumas das datações disponíveis do magmatismo Mosquito que fornecem idades neotriássicas, Porto (2014).

Uma outra evidência sobre a atuação de regime esforços de esforços aqui proposto - numa escala ainda mais regional-, pode ser buscado no Magmatismo Rio Ceará Mirim, Almeida et al. (1988). Este magmatismo é formado por diques de direção aproximada EW, que se estendem por 300km, desde a região costeira do RN até a região de Solonópole-Jaguaretama, a aproximadamente 200km da borda leste da Bacia do Parnaíba. As idades obtidas para dois destes diques distribuem-se entre 130 a 134 Ma (K-Ar em rocha total), e para um terceiro dique, 150 Ma. Por conseguinte, as idades são compatíveis com os pulsos magmáticos da Bacia do Parnaíba, em que pese o fato das datações deste antigo trabalho terem sido feitas pelo método de rocha total e que, portanto, mereçam ser refeitas pelos métodos hoje disponíveis.

3.3. Compressão NS/Extensão EW: regime de esforços atuante no Neocretáceo/Terciário

Reconstituições cinemáticas, Schettino e Turco (2009), mostram que o breakup e o desenvolvimento da Margem Equatorial se deram através de uma cinemática destral, associada à abertura do Atlântico Norte. Em decorrência desta cinemática, espera-se que tenha sido gerado ao longo da Margem Equatorial, um regime de esforços caracterizado por compressão NS extensão EW (Fig. 7). Lima et al. (2009) comprovaram a atuação deste regime de esforços na Bacia Potiguar, com base na análise estrutural de afloramentos e na geologia subsuperfície, demonstrando que inversões estruturais decorrentes deste regime desempenharam um importante papel na formação das trapas dos reservatórios da Fm Açu, depositada no Cretáceo Superior. Estes autores também demonstraram, através datações geocronológicas (U-Th/He), que movimentações de uma grande falha de direção NW, que limita em subsuperfície um

campo de petróleo, ocorreram entre 17 -22 Ma. Estes resultados indicam que o regime de esforços caracterizado por compressão NS e extensão EW tenha atuado desde o Cretáceo Superior até pelo menos o Mioceno, na Bacia Potiguar.

Figure 6 - Isópacas da Fm. Sambaíba.

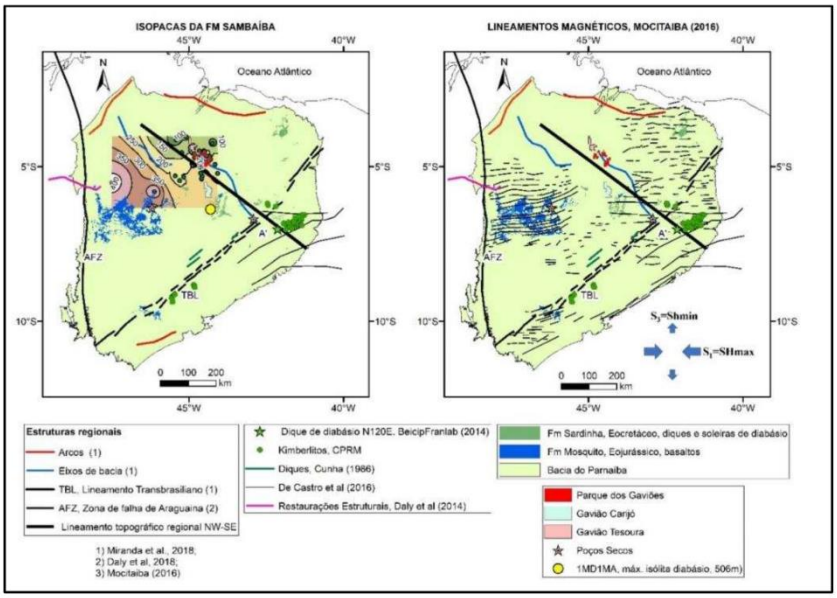

Fonte: Mapa construído a partir de dados de poços da base de dados da OPOG.

Na Figura 7 são mostradas áreas adjacentes à Bacia do Parnaíba onde são documentadas deformações neocretáceas. Zalán (1984) colocou em evidência um expressivo cinturão transpressivo de idade cenomaniana (Neocretáceo), documentado na sub-bacia do Piauí-Camocim, uma área que na nomenclatura atual da ANP localiza-se no limite entre as bacias marítimas de Barreirinhas e Ceará. O prolongamento off-shore do Lineamento Transbrasiliano é uma zona de deformação transpressiva, definida como Lineamento Transversal, que separa as sub-bacias de Acaraú (a NW) e de Mundaú (a SE), Destro et al (1994).

As seções geológicas mostradas acima (Figs. 3 e 4) demonstram a existência de importantes soerguimentos na Bacia do Parnaíba, os quais, pelo menos em parte são posteriores à Discordância Precretácea, sendo, portanto, atribuíveis, no mínimo ao Cretáceo/Terciário. Com base nestas observações, os soerguimentos de embasamento demonstrados nas seções geológicas são interpretados nesta investigação como uma resposta ao regime de esforços tectônicos decorrentes da cinemática destral que controlou o desenvolvimento da Margem Equatorial (Fig.7).

3.4. Compressão NW-SE/Extensão NE-SW, regime atual de esforços

A sismicidade observada na Bacia do Parnaíba e suas adjacências é mostrada na Figura 7. Concentrações de sismos ocorrem ao longo das grandes estruturas regionais, no embasamento adjacente, junto às bordas das bacias (Lineamento Transbrasiliano, Zona de Falha de Araguaína e Arco Ferrer Urbano Santos. Não ocorrem sismos na parte central da bacia do Parnaíba, onde por exemplo, localiza-se o Parque dos Gaviões e os sismos que ocorrem dentro dos limites da bacia localizam-se nas bordas soerguidas, onde a denudação é intensa. Estudos sismológicos mostram que o regime de esforços hoje atuante ao longo da Margem Equatorial é

predominantemente transcorrente, caracterizado por compressão paralela à costa e extensão normal à costa, Assumpção et al. (2014), é hoje observado ao longo de toda a Margem Equatorial. Esse padrão foi confirmado no estudo sismológico de um sismo de magnitude 4, que ocorreu no Arco Ferrer Urbano Santos, Dias et al. (2017): o mecanismo focal determinado indica que o regime de esforços nesta área é transcorrente, com compressão NW-SE (eixo P da sismologia) e extensão NE-SW (eixo T da sismologia).

Figure 7 - Sismicidade, regime de esforços, estruturas regionais, deformações Neocretáceas e regimes de esforços tectônicos propostos nesta investigação.

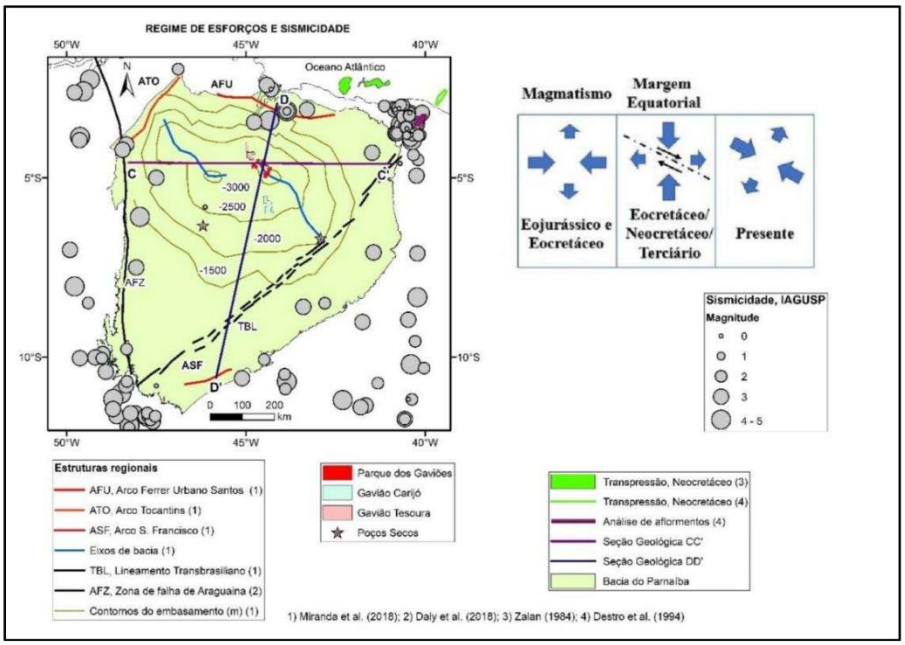

Fonte: Mapa construído a partir de dados de poços da base de dados da OPOG.

A comparação entre a sismicidade (Fig. 7) e a seção geológica CC' (Fig. 3) mostra que os sismos ocorrem nas extremidades da seção, onde os horizontes foram soerguidos. Isto é particularmente evidente na extremidade leste, onde a denudação é máxima. Nesta região, situada sobre o Lineamento Transbrasiliano, o soerguimento e a denudação fazem aflorar a base da coluna sedimentar – constituída pelo Gr. Serra Grande (Siluriano), a cotas superiores a mais +500m. Estas observações indicam que o soerguimento do embasamento da borda leste (basement uplift) – continua ocorrendo, em resposta ao regime compressivo de esforços atuais. A mesma relação entre sismicidade e soerguimento de horizontes pode ser observada através da comparação entre sismicidade e a geometria dos horizontes na seção DD' (Fig. 4). Os sismos ocorrem nas extremidades da seção, onde os horizontes foram soerguidos, principalmente na extremidade norte onde ocorre o Arco Ferrer Urbano Santos, indicando que as falhas que delimitam este alto continuam sendo reativadas.

4. Discussão

Os regimes de esforços aqui propostos para o intervalo Eojurássico-Eocretáceo e para o Presente baseiam-se em evidências visualizáveis na Bacia do Parnaíba e adjacências, enquanto que o regime proposto para o Neocretáceo-Terciário baseia-se numa reconstituição do breakup

e do desenvolvimento da Margem Equatorial (Schettino e Turco, 2009) e em estudos feitos na Bacia Potiguar (Lima et al., 2009; Bezerra et al., 2020). A inferência de que os resultados da Potiguar possam ser diretamente aplicados na Bacia do Parnaíba deve ser considerada como uma hipótese de trabalho a ser desenvolvida e testada em investigações futuras nesta bacia. Entretanto, independentemente do modelo aqui proposto, os resultados mostrados nas seções geológicas (Figs. 3 e 4) demonstram que o soerguimento das bordas da Bacia do Parnaíba ocorreu, pelo menos em parte, depois do Cretáceo.

Soerguimentos de embasamento (basement uplift) dobram a cobertura sedimentar por bending, isto é, por um dobramento produzido por forças que são normais ao acamamento subhorizontal das rochas sobrejacentes. Apesar de relativamente pouco discutido na literatura brasileira, trata-se de um mecanismo reconhecido há muito tempo, na indústria do petróleo, que tanto pode ajudar ou como pode comprometer a existência de acumulações de petróleo, a depender da relação temporal entre a formação da trapa e a migração. No campo de Ghawar – o maior campo do mundo, na Arábia Saudita, o soerguimento do embasamento foi o mecanismo responsável pela formação da trapa ARAMCO (1959). Na realidade, campos supergigantes da Arábia Saudita formaram-se por soerguimentos de blocos do embasamento "basement uplift" – uma estruturação produzida pela reativação compressiva de blocos anteriormente formados por tectônica extensional, Edgell (1992). No caso da Bacia Potiguar, as trapas formadas por inversão estrutural no Cretáceo Superior/Terciário, Lima et al. (2009), foram preenchidas por petróleo cuja migração foi necessariamente muito recente. No caso da Bacia do Parnaíba, o soerguimento das bordas durante o Cretáceo/Terciário possivelmente destruiu o selo de eventuais acumulações formadas no Eocretáceo, sobretudo nas áreas onde a denudação foi mais intensa, à medida em que se caminha para as bordas soerguidas da bacia.

5. Considerações finais

O sistema petrolífero atípico responsável pelas acumulações do Parque dos Gaviões implica que a maturação, a geração, a migração e o trapeamento tenham sido eventos simultâneos ao magmatismo e a reativações de falhas. Por conseguinte, eventos posteriores, potencialmente podem abrir as trapas e destruir acumulações eventualmente formadas. A evolução dos regimes de esforços proposta no modelo geológico conceitual favorece a preservação de acumulações na parte profunda da bacia – que, segundo o modelo conceitual permaneceu na posição original - e atribui maior risco a estruturas localizadas nas bordas, que foram e continuam sendo soerguidas, em resposta ao esforços tectônicos que operaram no Cretáceo/Terciário e que continuam operando no Presente. Este modelo geológico regional conceitual responde às duas primeiras das questões acima formuladas. A terceira questão – que indaga sobre a existência potencial de situações ainda não testadas nesta bacia – é abordada num outro trabalho Lima et al. (2020, neste evento).

6. Agradecimentos

Os autores são muito gratos à permissão da Ouro Preto Óleo e Gás para a publicação deste trabalho, feito fundamentalmente a partir da base de dados desta companhia, com o objetivo explícito de promover a circulação e discussão de ideias na indústria e na academia. Os autores agradecem também à Emerson Automation Solutions pela intensa participação na investigação.

Referências

Almeida, F. F. M., Carneiro, C. D. R., & Machado Jr., D. L. (1988). Magmatismo pós-Paleozóico no nordeste oriental do Brasi. *Revista Brasileira de Geociências*, *18*(4), 451–462.

Aramco. (1959). Ghawar Oil Field, Saudi Arabia. *AAPG Bulletin*, *43*(2), 434–454.

BeicipFranlab. (2014). *Field trip details booklet May 2014 post field trip. Relatório interno OPOG* Rio de Janeiro.

Bezerra, F. H., & De Castro, D. L. (2020). Postrift stress field inversion in the Potiguar Basin, Brazil–Implications for petroleum systems and evolution of the equatorial margin of South America. *Marine and Petroleum Geology*, *111*(1), 88–104.

Cunha, F. D. (1986). *Evolução paleozóica da Bacia do Parnaíba e seu arcabouço tectônico.*(Dissertação de Mestrado). UFRJ, Rio de Janeiro.

Daly, M. C. (2014). *Tectonics*, *33*(11), 2102–2120.

Destro, N., Szatmari, P., & Ladeira, E. A. (1994). Post-Devonian transpressional reactivation of a Proterozoic ductile shear zone in Ceará, NE Brazil. *Journal of Structural Geology*, *16*(1), 35–45.

Dias, F. L., Assumpção, M., & Bianchi, M. B. (2017). The intraplate Maranhão earthquake of 2017 January 3, northern Brazil: Evidence for uniform regional stresses along the Brazilian equatorial margin. *Geophysical Journal International*, *213*(1), 387–396.

Edgell, H. S. (1992). Basement tectonics of Saudi Arabia as related to oil field structures. In*Basement Tectonics* (pp. 169–193). Dordrecht: Springer.

ENEVA. (2020). *https://www.eneva.com.br/nossos-negocios/exploracao-e-producao*. Retrieved from https://www.eneva.com.br/nossos-negocios/exploracao-e-producao

Góes, A. (1995). *A Formação Poti (Carbonífero Superior) da Bacia do Parnaíba*. USP.

Heilbron, M., Guedes, E., & Mane, M. (2018). Geochemical and temporal provinciality of the magmatism of the eastern Parnaíba Basin. In *Cratonic Basin Formation: A Case Study of the Parnaiba Basin of Brazil* London: Geological Society.

Klöcking, M., White, N., & MacLennan, J. (2018). Role of basaltic magmatism within the Parnaíba cratonic basin, NE Brazil. In *Cratonic Basin Formation: A case Study of the Parnaíba Basin of Brazil*(Vol. 1).

Lima C.C., Pessoa, O., & Vasconcelos, P. (2009). The Role of Compressional Horizontal Stresses (σ1=SHmax) in the Evolution of the Potiguar Basin (NE Brazil) and the Age of Trap Formation for Its Main Reservoir (Açu Fm (p. 20). Presented at the AAPG INTERNATIONAL CONFERENCE & EXHIBITION, Rio de Janeiro. Retrieved from http://www.searchanddiscovery.com/abstracts/html/2009/intl/abstracts/lima2.htm?q=%2BtextStrip%3Aclaudio+textStrip%3Alima

Mallet, J.L. (2002). *Discrete Smooth Interpolation (DSI) Geomodeling*. New York: Oxford University Press.

Miranda, F. S., Vettorazzi, A. L., & Cunha, P. R C. (n.d.). Atypical igneous-sedimentary petroleum systems of the Parnaíba Basin, Brazil: seismic, well logs and cores. In *Cratonic Basin Formation: A case Study of the Parnaíba Basin of Brazil* (Vol. 1).

Porto, A. (2014). *Mapeamento sísmico de intrusões ígneas na porção sudeste da Bacia do Parnaíba e suas implicações para um modelo de sistema petrolífero não convencional* (Trabalho de Conclusão de Curso). UERJ.

Rodrigues, R. (1995). *A geoquímica orgânica na Bacia do Parnaíba* (Tese de Doutorado). UERJ, Porto Alegre.

Schettino, A., & Turco, E. (2009). Breakup of Pangaea and plate kinematics of the central Atlantic and Atlas regions. *Geophysical Journal International*, *178*(2), 1078–1097.

Schobbenhaus, C., Gonçalves, J. H., & Santos, J. O. S. (2004).*Carta Geológica do Brasil ao Milionésimo, Sistema de*

Informações Geográficas-SIG e 46 folhas na escala 1: 1.000. 000. Brasília: CPRM.

Vaz, P. T., Rezende, N. G. A. M., & Wanderley Filho, J. R. (2007). Bacia do Parnaíba.*Boletim de Geociências Da PETROBRAS*, *15*(2), 253–263.

Zalan, P.V. (1984). *Tectonics and sedimentation of the Piaui- Camocim Sub-Basin, Ceara Basin, Offshore Northeastern Brazil* (Ph.D Thesis). Colorado School of Mines.